



Tesis Doctoral

Unraveling Adipose Tissue Expandability: Molecular Mechanisms, Novel Biomarkers, and Therapeutic Targets for Liver Fat Deposition

Autor

Marta López Yus

Director/es

José Miguel Arbonés Mainar

Silvia Lorente Cebrián

UNIVERSIDAD DE ZARAGOZA

Departamento de Bioquímica y Biología Molecular y Celular

2023

Dr. José Miguel Arbonés Mainar, investigador del Instituto Aragonés de Ciencias de la Salud (IACS) y Dra. Silvia Lorente Cebrián, Investigadora de la Universidad de Zaragoza,

Certifican:

Que la tesis doctoral con el título “Unraveling Adipose Tissue Expandability: Molecular Mechanisms, Novel Biomarkers, and Therapeutic Targets for Liver Fat Deposition”, ha sido realizada en la Unidad de Investigación Traslacional del Hospital Universitario Miguel Servet, bajo su tutela y que reúne, a su juicio, las condiciones para optar al grado de doctor.

Zaragoza, diciembre 2023

José Miguel Arbonés Mainar

Silvia Lorente Cebrián

Este trabajo ha sido financiado con fondos de los proyectos de investigación PI17/02268 y PI22/01366 (Instituto de Salud Carlos III), el Fondo Europeo de Desarrollo Regional (FEDER): “Una manera de hacer Europa” y el Gobierno de Aragón (B03_23R, cofinanciado por FEDER Aragón: “Construyendo Europa desde Aragón”). La doctoranda ha sido beneficiaria de beca predoctoral de la Diputación General de Aragón y de una beca de estancia de investigación EMBO (Scientific Exchange Grant #9603) para la realización de un intercambio científico en el Karolinska Institutet (Estocolmo, Suecia).

Gracias, José Miguel, por acordarte de esa estudiante de prácticas que pasó el verano en el laboratorio hace ya años y ofrecerme la oportunidad de formar parte de este proyecto. Gracias, Silvia, por aparecer en el momento en el que más lo necesitaba.

Gracias, Raquel y Mapi, por acompañarme en todo momento durante estos años, tanto dentro como fuera del laboratorio. Por ayudarme siempre, pero sobre todo por aguantarme y consolarme cuando más lo he necesitado. Gracias a todos los miembros de Adipofat, a los que ya se han ido y a los nuevos fichajes, porque sin vosotros este trabajo no habría sido posible.

Gracias a todas las personas que han pasado por la UIT. Gracias a las Patricas, por acogerme en tantas ocasiones y hacerme sentir una más, especialmente a Pilar y Paula, por esas cervezas que tantas veces han acabado de manera inesperada. Gracias a las biobanqueras, por las risas en las comidas que me han alegrado tantos días. Ensayos, neumo, giraldos, bsicos... todos, de una manera u otra, habéis aportado vuestro granito de arena a este trabajo.

Gracias al laboratorio de Mikel y Niklas, por acogerme como una más desde el primer día. Por darme la oportunidad de aprender y disfrutar de la ciencia a ese nivel. Gracias, Scott y Danae, por compartir conmigo todo vuestro conocimiento y, por supuesto, por las cervezas de los viernes que hacían el frío de Estocolmo más llevadero.

Gracias a todos los que me han acompañado durante esta etapa. A mi Pandilla, por interesarse siempre en “mis grasitas” e intentar entender un poquito mejor mi trabajo, pero, sobre todo, por ayudarme a desconectar de él siempre que lo he necesitado. Gracias, Raquel, por aguantarme durante ya más de 25 años, por estar ahí sin excepciones y, por su puesto, por ser mi traductora personal. A mis chicas Golgi, por estar siempre tan cerca a pesar de la distancia. A mis biotechs, porque lo que unió la carrera ya es para siempre. Por entenderme y apoyarme, por los reencuentros, ya sea en un zulo, un festival improvisado o una casa rural, en los que parece que no ha pasado el tiempo, pero sobre todo, por ser tan majicos. A Sergio, gracias por estos años de convivencia intensa, los bailes salseros, las reflexiones vitales en el salón y por tener siempre el consejo adecuado para mí.

Gracias, Nacho, por aguantarme, por entenderme como nadie y por hacerme cada día más feliz.

Y gracias, papá, mamá y Blanca, por apoyarme en todas mis decisiones, por animarme a seguir en todo momento y por mostrarme siempre el lado bueno de las cosas, aunque la vida, a veces, no sea justa. Gracias yayo Simón por ser mi ejemplo a seguir.

No puedo sentirme más afortunada.

INDEX

ABSTRACT	1
RESUMEN	3
1. INTRODUCTION.....	5
1.1. Adipose tissue (AT)	7
1.1.1. Types of AT	7
1.1.2. Composition of white adipose tissue (WAT)	8
1.1.2.1. Adipose – derived mesenchymal stem cells (ADMSCs)	8
1.1.2.2. Mature adipocytes	8
1.1.2.3. Other cellular types within AT	9
1.1.3. Metabolic function of WAT	9
1.1.3.1. Lipids storage and mobilization	10
1.1.3.2. Endocrine function	10
1.2. Obesity	12
1.2.1. Etiology of obesity	13
1.2.2. Classification of obesity phenotypes	13
1.2.3. AT dysfunction in obesity	14
1.2.4. Body fat distribution in obesity: AT expandability theory	15
1.3. Comorbidities associated to obesity: Non-alcoholic fatty liver disease	16
1.3.1. Prevalence of NAFLD	16
1.3.2. Classification of NAFLD	16
1.3.3. Pathogenesis of NAFLD.....	17
1.3.3.1. Role of genetic and epigenetic factors	17
1.3.3.2. Role of AT dysfunction.....	18
1.3.3.3. Role of insulin resistance	18
1.3.3.4. Role of low-degree chronic systemic inflammation	19
1.3.3.5. Role of mitochondrial dysfunction and oxidative stress	19

1.4.	Diagnosis of obesity phenotypes and its metabolic complication	20
1.4.1.	Anthropometric parameters	20
1.4.2.	Imaging techniques.....	21
1.4.3.	Circulating biomarkers	21
1.4.3.1.	Adipokines	21
1.4.3.2.	Markers of glucose-insulin homeostasis	22
1.4.3.3.	Inflammatory biomarkers	22
1.4.4.	Omics-based biomarkers	23
1.4.4.1.	Genomics.....	23
1.4.4.2.	Transcriptomics	24
1.4.4.3.	Metabolomics	24
1.5.	Treatment of obesity and its metabolic complications: genetic modification of ADMSC as an alternative	26
1.5.1.	ADMSC-based therapy	26
1.5.2.	Genetic modification of ADMSC: CRISPR/Cas9 gene editing	27
2.	HYPOTHESIS AND OBJECTIVES	31
2.1.	Hypothesis	33
2.2.	Objectives	33
3.	MATERIALS AND METHODS	35
3.1.	Human cohort description.....	37
3.2.	Characterization of human cohort.....	37
3.2.1.	Tissue samples collection	37
3.2.2.	Plasma biochemistry.....	37
3.2.3.	Computer tomography analysis	38
3.2.4.	Histological examination	38
3.3.	Isolation of hADMSC.....	39
3.4.	Cell culture.....	39

3.4.1.	hADMSC culture and differentiation	39
3.4.2.	HepG2 culture	40
3.4.3.	HepG2-adipocytes co-culture	40
3.5.	CRISPR/Cas9 genomic modification of hADMSC	40
3.5.1.	Design and selection of a single guide RNA	40
3.5.2.	Cells transfection with sgRNAs and Cas9	41
3.6.	Assessment of genomic mutation efficiency	41
3.6.1.	Genomic DNA isolation	42
3.6.2.	PCR	42
3.6.3.	Sanger sequencing	42
3.6.4.	ICE analysis	43
3.7.	Gene expression analysis	43
3.7.1.	RNA isolation	43
3.7.2.	RNA retro-transcription	44
3.7.3.	Real-time PCR	44
3.7.4.	AmpliSeq transcriptome analysis	45
3.8.	Protein analysis	46
3.8.1.	Protein isolation	46
3.8.2.	Protein quantification	46
3.8.3.	Sodium dodecyl sulfate-polyacrylamide gel electrophoresis	47
3.8.4.	Western blot	47
3.8.5.	ELISA	48
3.9.	Cell characterization assays	49
3.9.1.	Cellular staining	49
3.9.1.1.	Oil Red O staining	49
3.9.1.2.	Fluorescent staining:	49
3.9.2.	Lipid metabolic assays	50

3.9.2.1. Lipolysis	50
3.9.2.2. De novo lipogenesis	50
3.9.2.3. Fatty acids uptake.....	51
3.10. Statistical analysis	51
3.10.1. Differential gene expression analysis	51
3.10.2. Gene ontology enrichment analysis	52
3.10.3. Construction of weighted gene co-expression networks and identification of modules	52
4. RESULTS.....	53
4.1. Chapter I	55
4.2. Chapter II	81
4.3. Chapter III.....	109
5. DISCUSSION	139
6. CONCLUSIONS	149
7. REFERENCES.....	155
8. ANNEXES	183
8.1. Annex I. <i>Review</i>	185

ABBREVIATIONS

AAA	Aromatic amino acids
ACC	Acetyl CoA carboxylase
ADMSC	Adipose derived-mesenchymal stem cells
AKT	Serine/threonine kinase 1
ALT	Alanine aminotransferase
AMP	Adenosine monophosphate
AMPK	AMP-activated protein kinase
aP2	Adipocyte fatty acid binding protein
AST	Aspartate transaminase
AT	Adipose tissue
ATGL	Adipose triglyceride lipase
BAT	Brown adipose tissue
BCAA	Branched-chain amino acids
BIA	Bioimpedance analysis
BMI	Body mass index
BMP	Bone morphogenetic protein
BP	Biological processes
BSA	Bovine serum albumin
CCDC3	Coiled-Coil Domain Containing 3
CCL2	Chemokine ligand 2
CDKN1A	Cyclin Dependent Kinase Inhibitor 1A
C/EBP α	CCAAT/enhancer-binding protein alpha
C/EBP β	CCAAT/enhancer-binding protein beta
cmiRNAs	Circulating miRNAs
CRISPR	Clustered Regularly Interspaced Short Palindromic Repeats
CRP	C-reactive protein
CT	X-ray computed tomography
CTx	Cross-linked C-terminal telopeptide of type I collagen
CTGF	Connective tissue growth factor
CVD	Cardiovascular diseases
DAG	Diacylglycerol
DEG	Differentially expressed genes

DNL	<i>De novo</i> lipogenesis
DUSP1	Dual specificity phosphatase 1
DXA	Dual-energy X-ray absorptiometry
ECM	Extracellular matrix
ELISA	Enzyme-Linked Immunosorbent Assay
EV	Extracellular vesicle
FABP-4	Fatty-acid binding protein 4
FA	Fatty acid
FAS	Fatty acid synthase
FBS	Fetal bovine serum
FDR	False discovery rate
FFA	Free fatty acid
FGF	Fibroblast growth factor
FLI	Fatty liver index
FTO	Fat Mass And Obesity Associated
GADD45B	Growth Arrest And DNA Damage Inducible Beta
gDNA	Genomic DNA
GGT	Gamma-glutamyl-transferase
GLUT4	Glucose transporter 4
GO	Gene ontology
gRNA	Guide RNA
GWAS	Genome-wide association studies
hADMSC	Human adipose-derived mesenchymal stem cells
h	Hour
HbA1c	Glycated hemoglobin
HCC	Hepatocarcinoma
H&E	Hematoxylin-eosin
HLC	Hepatocyte – like cell
HOMA	Homeostatic model assessment
HSL	Hormone-sensitive lipase
HUMS	Hospital Universitario Miguel Servet
IBMX	3-isobutyl-1-methylxanthine
ICE	Inference of CRISPR Edits
IGF	Insulin growth factor

IL-1 β	Interleukin 1 β
IL-6	Interleukin 6
IL-8	Interleukin 8
IL-10	Interleukin 10
IL-18	Interleukin 18
IPC	Insulin-producing cell
IR	Insulin resistance
IRS-1	Insulin receptor substrate 1
ISM1	Isthmin 1
JNK	Jun N-terminal kinase
KO	Knocked out
lncRNAs	Long non-coding RNAs
LDL	Low-density lipoprotein
LPL	Lipoprotein lipase
MAPK	Mitogen-activated protein kinase
MCP-1	Monocyte chemoattractant protein-1
MetS	metabolic Syndrom
MGL	Monoacylglycerol lipase
MHO	Metabolically healthy obese
min	Minuts
miRNA	Micro RNAs
MRI	Magnetic resonance imaging
mRNA	Protein-coding RNAs
MRS	Magnetic resonance spectroscopy
MSC	Mesenchymal stem cells
MUO	Metabolically unhealthy obese
NAFL	Non-alcoholic fatty liver / steatosis
NAFLD	Non-alcoholic fatty liver disease
NAS	NAFLD score
NASH	Hepatosteatosis
ncRNAs	Non-coding RNAs
NF- κ B	Nuclear factor kappa-B
NHEJ	Non-homologous end joining
NRIP1	Nuclear receptor-interacting protein 1

PCA	Principal component analysis
PCR	Polymerase chain reaction
PDGF	Platelet-derived growth factor
PFA	Paraformaldehyde
PIL	Palmitate-induced lipogenesis
PNPLA3	Patatin-like phospholipase domain-containing protein 3
PPAR γ	Peroxisome proliferator-activated receptor gamma
PVDF	Polyvinylidene difluoride membrane
RNP	Ribonucleoprotein complex
ROS	Reactive oxygen species
RPKM	Reads Per Kilobase of transcript, per Million mapped reads
r. t.	Room temperature
S100A9	S100 calcium-binding protein A9
S100A12	S100 calcium-binding protein A12
scWAT	Subcutaneous white adipose tissue
SDS-PAGE	Sodium dodecyl sulfate-polyacrylamide gel electrophoresis
SEM	Standard error of the mean
SFA	Subcutaneous fat area
sgRNA	Single guide RNAs
SIK1	Salt Inducible Kinase 1
SNP	Single nucleotide polymorphisms
SOCS3	Suppressor of cytokine signaling
SREBP-1c	Sterol regulatory element-binding protein 1c
SVF	Stromal vascular fraction
T2DM	Type 2 diabetes mellitus
T3	Triiodothyronine
TFA	Total fat area
TG	Triglyceride
TGF- β	Transforming growth factor - β
TM6SF2	Transmembrane 6 superfamily member 2
TNF- α	Tumoral necrosis factor α
UCP1	Uncoupling protein 1
VFA	Visceral fat area
visWAT	Visceral white adipose tissue

VLDL	Very-low density lipoprotein
WAT	White adipose tissue
WC	Waist circumference
WGCNA	Weighted gene co-expression networks analysis
WHO	World Health Organization
WHR	Waist to hip ratio

ABSTRACT

Accumulating evidence indicates that obesity is closely associated with an increased risk of metabolic diseases, such as insulin resistance, type 2 diabetes (T2DM), or non-alcoholic fatty liver disease (NAFLD). The development of these obesity-associated comorbidities depends largely on how functionally resilient the adipose tissue (AT) is in response to excessive nutrient supply. The subcutaneous white adipose tissue (scWAT) is the primary lipid storage organ and regulates systemic energy homeostasis by controlling metabolic flexibility and lipid fluxes to other organs. As an individual gains weight, scWAT expands to store the excess calories from the diet. Once the storage capacity is exceeded, the scWAT fails to accumulate lipids appropriately, redirecting the lipid flux to other organs. This ectopic fat accumulation occurs primarily in the visceral adipose tissue (visWAT) and liver, leading to visceral obesity and liver steatosis, respectively, and promotes comorbidities associated with obesity as T2DM or NAFLD.

This work explores the molecular mechanisms leading to the correct expansion of scWAT in patients with obesity, and its link to the development of obesity-associated comorbidities. We aim to reveal novel biomarkers or therapeutic targets for this disease, that is alarmingly increasing in our society. To this end, we performed a high throughput gene expression analysis from scWAT of patients with different degrees of adiposity and correlated the results with two metabolic indicators highly influenced by the expandability capacity of scWAT: the subcutaneous/visceral ratio and the liver steatosis.

Our results prove the importance of distinguishing AT location to classify obesity phenotypes and proposes ISM1 as a novel non-invasive biomarker to predict abdominal fat partitioning and, consequently, to evaluate obesity-related health risks.

Moreover, we identified three genes, *SOCS3*, *DUSP1*, and *SIK1*, dysregulated in AT of patients with liver steatosis. We demonstrated that they regulate multiple aspects of adipocyte function and evaluated the potential of CRISPR/Cas9 modulation of these genes to treat NAFLD.

In conclusion, our results highlight the importance of scWAT fat storage capacity. We propose some genes as key regulators of AT functionality, that could be further explored to evaluate its potential as biomarkers or therapeutic targets for obesity-associated comorbidities.

RESUMEN

Cada vez hay más evidencias de que la obesidad está estrechamente asociada a un mayor riesgo de padecer enfermedades metabólicas, como la resistencia a la insulina, la diabetes de tipo 2 (DMT2) o la enfermedad del hígado graso no alcohólico (EHGNA). El desarrollo de estas comorbilidades asociadas a la obesidad depende en gran medida de la resistencia funcional del tejido adiposo en respuesta a un aporte excesivo de nutrientes. El tejido adiposo blanco subcutáneo (TAB-Sc) es el principal órgano de almacenamiento de lípidos y regula la homeostasis energética sistémica, controlando la flexibilidad metabólica y los flujos de lípidos a otros órganos. A medida que un individuo aumenta de peso, el TAB-Sc se expande para almacenar el exceso de calorías de la dieta. Una vez superada su capacidad de almacenamiento, el TAB-Sc es incapaz de acumular lípidos adecuadamente y redirige el flujo de lípidos a otros órganos. Esta acumulación ectópica de grasa se produce principalmente en el tejido adiposo visceral (TAB-Vis) y en el hígado, lo que conduce a la obesidad visceral y a la esteatosis hepática, respectivamente, y favorece el desarrollo de comorbilidades asociadas a la obesidad como la DMT2 o la EHGNA.

Este trabajo se centra en investigar los mecanismos moleculares que regulan la expansibilidad del TAB-Sc en pacientes con obesidad, y su relación con el desarrollo de comorbilidades asociadas a la obesidad. El objetivo principal es identificar nuevos biomarcadores o dianas terapéuticas para esta enfermedad, que está aumentando de forma alarmante en nuestra sociedad. Para ello, se ha realizado un análisis de expresión génica a partir de biopsias de TAB-Sc de pacientes con diferentes grados de adiposidad y se han correlacionado los resultados con dos indicadores metabólicos muy influenciados por la capacidad de expansibilidad del TAB-Sc: el cociente de grasa subcutáneo/visceral y la esteatosis hepática.

Nuestros resultados demuestran la importancia de distinguir la localización del tejido adiposo para clasificar los fenotipos de la obesidad y proponen la *ISM1* como un nuevo biomarcador no invasivo para predecir la localización de la grasa abdominal y, en consecuencia, para evaluar los riesgos metabólicos relacionados con la obesidad.

Además, identificamos tres genes, *SOCS3*, *DUSP1* y *SIK1*, cuya expresión se encuentra alterada en el TAB-Sc de pacientes con esteatosis hepática. Demostramos que estos genes

regulan múltiples aspectos de la función del adipocito y evaluamos el potencial de la edición de estos genes con la tecnología CRISPR/Cas9 para tratar la EHGNA.

En conclusión, nuestros resultados ponen de manifiesto la importancia de almacenar correctamente la grasa excesiva en el TAB-Sc y no de manera ectópica. Proponemos algunos genes como reguladores clave de la funcionalidad del tejido adiposo, que podrían tener potencial como biomarcadores o dianas terapéuticas para las comorbilidades asociadas a la obesidad.

1. INTRODUCTION

1.1. Adipose tissue (AT)

Adipose tissue (AT) is an extraordinarily flexible and heterogeneous organ^{1,2}. While historically viewed as a passive site for energy storage, it is well known that AT regulates many aspects of whole-body physiology, including food intake, energy balance, insulin sensitivity, body temperature, and immune responses³.

1.1.1. Types of AT

In human body, there are two main types of AT with well differentiated functions: white adipose tissue (WAT) and brown adipose tissue (BAT)⁴. WAT is primarily responsible for energy storage⁵, while BAT is a thermogenic tissue that generates heat by uncoupling oxidative phosphorylation⁶. In the last decades, a third type of AT, beige or brite (brown in white) AT, has also been identified. This tissue has the ability to switch between energy storage and thermogenesis, depending on physiological demands⁷ (Figure 1).

WAT is the more abundant type of AT. The distribution of WAT in the body differs between individuals and is influenced by genetic and environmental factors. WAT stores vary in size, ranging from 5 to 60% of total body weight⁸. In general, WAT is found in subcutaneous depots (beneath the skin) and visceral depots (around organs such as the liver and intestines), although there are also smaller depots in other locations such as bone marrow and muscle tissue⁹. Subcutaneous WAT (scWAT) stores more than the 80% of total body fat, while visceral WAT (visWAT) represent 10-20% of total body fat in men and 5-10% in women¹⁰.

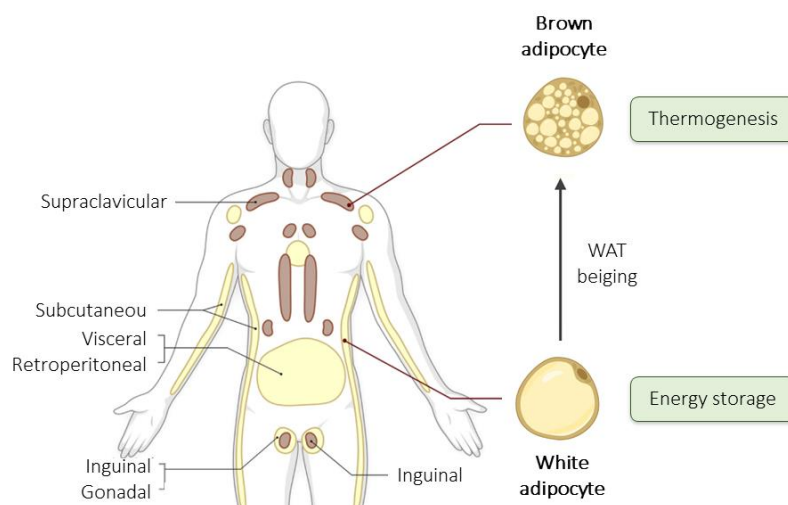


Figure 1. Adipose tissue distribution in humans. White adipose tissue (WAT), represented in yellow, is primarily responsible for energy storage; while brown adipose tissue (BAT), in brown, is a thermogenic tissue.

1.1.2. Composition of white adipose tissue (WAT)

WAT is a highly heterogeneous tissue composed by different cell types surrounded by a network of blood vessels, nerve terminals and lymph nodes, and all of them immersed in a complex collagen matrix¹.

1.1.2.1. Adipose – derived mesenchymal stem cells (ADMSCs)

Adipose – derived mesenchymal stem cells (ADMSCs) are multipotent stroma cells present in AT, characterized by the capacity to differentiate into cell types of mesodermal origin, including adipocytes, osteoblast, and chondrocytes¹¹.

ADMSCs are known to have self-renewal capacity, which is the ability to divide and differentiate into more specialized cells while maintaining their stem cell characteristics¹². ADMSCs divide mainly in the early childhood and puberty, while during adulthood, they ensure replenishment of aged non-functional adipocytes¹³.

1.1.2.2. Mature adipocytes

Mature adipocytes are functional cells of WAT responsible for energy storage. Adipogenesis is the process by which ADMSCs differentiate into adipocytes. This process is regulated by a complex interplay of transcription factors, signaling pathways, and epigenetic modifications. It involves three well-defined stages: (i) commitment of MSCs to the adipocyte lineage; (ii) mitotic clonal expansion; and (iii) terminal differentiation¹⁴ (Figure 2).

In the first step, ADMSCs undergo lineage commitment and differentiation into preadipocytes, which are precursor cells specifically restricted to the adipocyte lineage^{15,16}. This process is regulated by a complex interplay of multiple pathways including mitogen-activated protein kinase (MAPK), transforming growth factor - β (TGF- β), AMP-activated protein kinase (AMPK), bone morphogenetic proteins (BMPs), Wnt, and Hedgehog pathways¹⁷. This commitment is then followed by mitotic clonal expansion, involving replication of DNA and duplication of cells, and growth arrest¹⁸.

When the committed preadipocyte stops growing, it activates the master regulator of adipogenesis, peroxisome proliferator-activated receptor- γ (PPAR γ), and transcription co-activators CCAAT/enhancer-binding protein α and β (C/EBP α and C/EBP β). This determines a dramatic increase in lipogenic genes, such as acetyl CoA carboxylase

(ACC), fatty acid synthase (FAS), adipocyte fatty acid binding protein (aP2) and glucose transporter 4 (GLUT4)^{19,20}.

At the completion of differentiation, mature adipocytes express all the markers of early adipocyte differentiation as well as the peptide hormones adiponectin and leptin; the lipases adipose triglyceride lipase (ATGL) and hormone-sensitive lipase (HSL); and high levels of the lipid-droplet-associated protein perilipin 1, resulting in functional adipocytes able to store lipids^{21,22}.

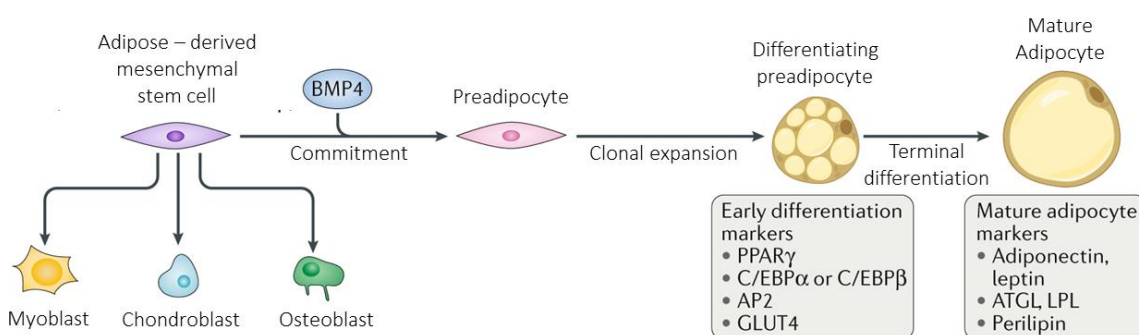


Figure 2. Adipose – derived mesenchymal stem cell (ADMSC) differentiation into mature adipocytes. The process starts with the commitment of MSCs to the adipocyte lineage, followed by mitotic clonal expansion and terminal differentiation. Modified from Ghaben et al¹⁴.

1.1.2.3. Other cellular types within AT

Mature adipocytes occupy most of the WAT size. Nevertheless, other cellular types related to vasculature and immune function are present in this tissue: endothelial cells, blood cells, fibroblasts, pericytes, macrophages, and several types of immune cells. These non-adipocyte cell types perform both physiological and pathophysiological functions by communicating with the adipocytes via secreted factors. The number and diversity of these cell types varies with developing obesity and metabolic dysfunction^{1,23}.

1.1.3. Metabolic function of WAT

The primary function of WAT is to regulate energy balance by storing and releasing fatty acids (FAs) in response to changes in energy availability. However, WAT also secretes a variety of hormones and cytokines, known as adipokines, that play important roles in the regulation of multiple physiological processes²⁴.

1.1.3.1. Lipids storage and mobilization

AT is the primary site of lipid storage in the form of triglycerides (TG), which can be released when energy demand exceeds supply. To maintain full body energy homeostasis, two main processes are highly regulated in WAT: lipogenesis and lipolysis²⁵ (Figure 3).

Lipogenesis refers to the process of synthesizing new lipids from excess glucose or FAs in the diet. This process occurs in the cytoplasm of adipocytes and is tightly regulated by numerous hormones and enzymes^{26,27}. The main hormone regulating this process is insulin, which promotes the uptake of glucose and FAs into adipocytes and stimulates the activity of key enzymes involved in lipid synthesis, such as acetyl CoA-carboxylase (ACC) and fatty acid synthase (FAS)²⁸. Other hormones, such as glucagon and cortisol, can inhibit lipogenesis by reducing insulin signaling, acting as negative regulators²⁹.

Lipolysis, on the other hand, refers to the process of breaking down stored lipids in AT to release energy to be used by peripheral organs. It is critical for maintaining energy homeostasis during periods of fasting or exercise when glucose levels are low, and the body needs to rely on stored fat for energy³⁰. Lipolysis is regulated by enzymes called lipases, which are activated by signals from the sympathetic nervous system and hormones such as glucagon, epinephrine, and norepinephrine³¹. The main lipases regulating this process are adipose triglyceride lipase (ATGL), hormone-sensitive lipase (HSL) and monoacylglycerol lipase (MGL)³².

The balance between lipogenesis and lipolysis in AT is tightly regulated to ensure that the body has a constant supply of energy to meet its metabolic needs³³.

1.1.3.2. Endocrine function

In addition to its role in energy storage, WAT also serves as an important endocrine organ, secreting a variety of adipokines that regulate metabolic, inflammatory, and immune processes throughout the body³⁴. The endocrine function of WAT is closely linked to its metabolic and storage functions, as it plays a critical role in the maintenance of glucose and lipid homeostasis³⁵ (Figure 3).

Our present knowledge of AT-secreted adipokines includes over 100 proteins exerting cross talk with other cells/tissues. Leptin and adiponectin are the most abundant and well-characterized adipokines, whereas more recently discovered molecules such as resistin, fatty-acid binding protein 4 (FABP-4), omentin, visfatin, lipocalin-2 or chemerin have

also been proposed to play important functions. Leptin was the first identified secreted adipokine and has been shown to regulate appetite and energy expenditure. It is an important feedback signal to the brain about the size and status of the AT³⁶. Adiponectin, on the other hand, enhances insulin sensitivity and FAs oxidation in skeletal muscle and liver, which helps to maintain glucose and lipid homeostasis³⁷.

Proinflammatory factors such as tumor necrosis factor- α (TNF- α), interleukin 6 (IL-6), interleukin 8 (IL-8), interleukin 18 (IL-18), interleukin 1 β (IL-1 β), or chemokine ligand 2 (CCL2) are also produced by WAT and are all increased in obesity³⁸.

Moreover, WAT secretes extracellular vesicles (EVs), which are small membrane-bound particles that contain various bioactive molecules, including microRNAs (miRNAs), proteins, and lipids^{39,40}, that also contribute to energy homeostasis at local and systemic level.

The endocrine function of WAT is regulated by various factors, including nutritional status, physical activity, hormonal levels, and environmental cues. The dysregulation of WAT function, as seen in obesity and metabolic disorders, can lead to the development of insulin resistance (IR), chronic inflammation, and other metabolic and cardiovascular complications^{41,42}.

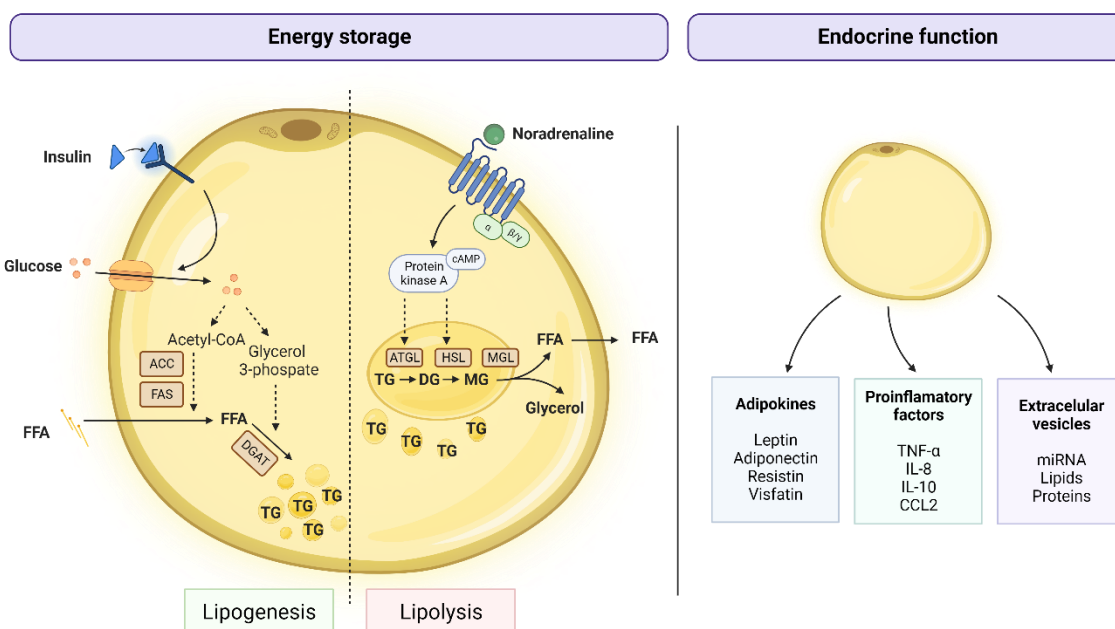


Figure 3. Functions of white adipose tissue (WAT). WAT regulates energy balance by storing (lipogenesis) and releasing (lipolysis) fatty acids (FA). WAT also secretes a variety of molecules that play important roles in the regulation of multiple physiological processes.

1.2. Obesity

According to the definition by the Obesity Medicine Association, "Obesity is chronic, relapsing, multifactorial, neurobehavioral disease, wherein an increase in body fat promotes adipose tissue dysfunction and abnormal fat mass physical forces, resulting in adverse metabolic, biomechanical, and psychosocial health consequences"^{43,44}. Therefore, it is important to consider obesity not as a condition simply caused by an excessive fat accumulation, but as a heterogeneous pathology that promotes the development of comorbidities that severely impair an individual's health.

The World Health Organization (WHO) reported that obesity has nearly tripled worldwide since 1975. In 2016, more than 1.9 billion adults were overweight and over 600 million were obese. The alarming point is that obesity spreads rapidly not only among adults, but also in children and the elderly⁴⁵. This poses a major public health issue, since obesity is a major contributor to the global burden of chronic diseases⁴⁶. In fact, obesity is associated with an increased risk of developing IR and is a major risk factor for many diseases such type 2 diabetes (T2DM)⁴⁷, non-alcoholic fatty liver disease (NAFLD)^{48,49}, cardiovascular diseases (CVD)⁵⁰, atherosclerosis⁵¹, hypertension⁵² or several types of cancer⁵³.

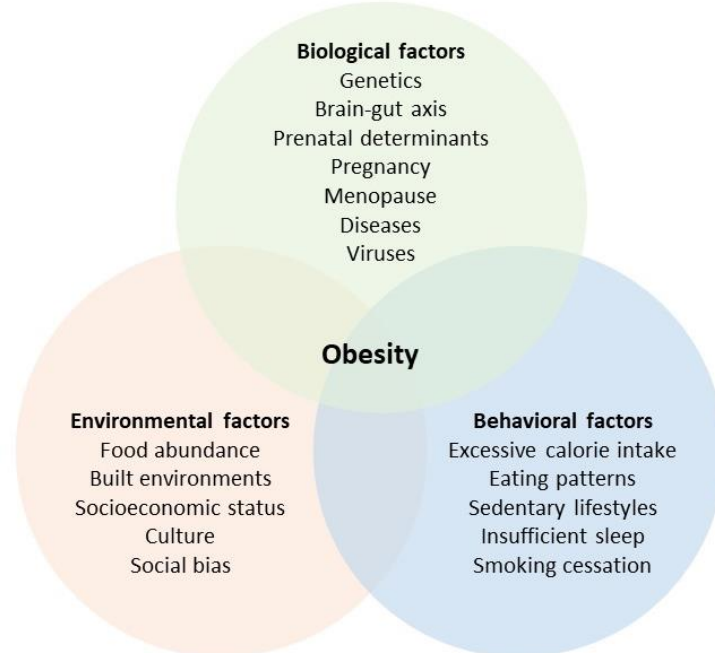


Figure 4. Etiology of obesity. Biological, environmental and behavioral factors that contribute to positive energy balance, excess weight gain and, consequently, obesity.

1.2.1. Etiology of obesity

The etiology of obesity is multifactorial and complex, involving biological, environmental, and behavioral factors⁵⁴. The key biological factors include genetics, brain-gut axis, prenatal determinants, pregnancy, menopause, neuroendocrine conditions, medications, physical disability, gut microbiome, and viruses. Propensity to develop obesity due to one or more of these elements is exacerbated by environmental and behavioral influences. Environmental factors include food abundance, built environments, socioeconomic status, culture, social bias, and environmental chemicals. Behavioral factors comprise excessive calorie intake, eating patterns, sedentary lifestyles, insufficient sleep, and smoking cessation⁵⁵ (Figure 4).

1.2.2. Classification of obesity phenotypes

The body mass index (BMI) is the anthropometric parameter traditionally used for classifying obesity. It is a surrogate marker for fat mass based on the height and the weight ($BMI = \text{weight (kg)} / [\text{height (m)}]^2$), that classifies subjects as normal weight ($BMI < 25 \text{ kg/m}^2$), overweight ($BMI 25-30 \text{ kg/m}^2$) or obese ($BMI \geq 30 \text{ kg/m}^2$)⁵⁶. However, the use of universal BMI cut-off points to classify obesity has important limitations, as BMI do not consider body composition (i.e., skeletal muscle mass) and, therefore, do not consistently reflect adiposity in a particular individual⁵⁷. Total fat mass, may be a more accurate measure of the metabolic phenotype than BMI. However, increasing evidence shows that the absolute amount of body fat does not unambiguously reflects metabolic health at an individual level. For instance, some extremely obese people are not diabetic, while other overweight people develop severe IR and diabetes. Another condition in which the association between AT mass and metabolic health might seem paradoxical is lipodystrophy. A deficiency of AT, as in patients with lipodystrophy, is also associated with metabolic complications⁵⁸. Taken together, excessive AT mass as well as a (partial) lack of AT are related to metabolic complications. This suggests that the absolute amount of fat stored may not be the most important factor determining the relationship between obesity and metabolic complications. Obesity-related adverse health consequences, therefore, appear to be related to fat distribution and AT functionality⁵⁹.

Emerging evidence suggests that these characteristics of AT (functionality and distribution) are good indicators of the patient's metabolic status, allowing to distinguish between metabolically healthy obese (MHO) and metabolically unhealthy obese

(MUO)^{60,61}. MHO individuals are characterized by a functional AT distributed mainly in the subcutaneous area, while MUO are characterized by a dysfunctional AT that leads to lower subcutaneous fat mass and ectopic fat deposition, which contribute to metabolic complications^{62,63} (Figure 5). However, the mechanisms that underlie inter-individual differences in body fat functionality and distribution are complex and not well understood⁶⁴.

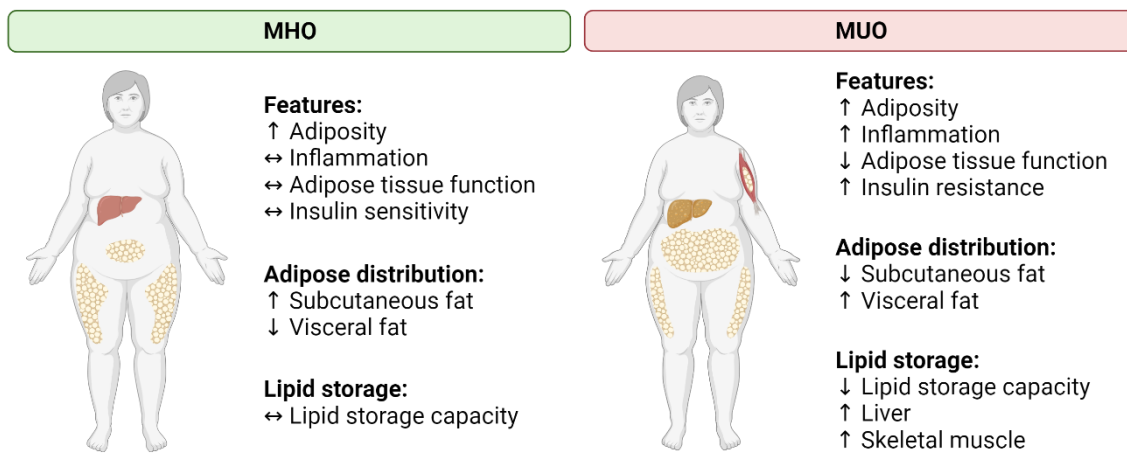


Figure 5. Obesity phenotypes. Characteristics of metabolically healthy obese (MHO) and metabolically unhealthy obese (MUO).

1.2.3. AT dysfunction in obesity

During a prolonged positive energy balance, the inability to increase AT mass through adipocyte hyperplasia (formation of new adipocytes from precursor differentiation) leads to adipocyte hypertrophy (increase in adipocyte size)⁶⁵. This is a key characteristic of AT dysfunction, as enlarged adipocytes have a reduced capacity to store dietary surplus as they are already overloaded with stored lipids^{66,67}.

As adipocytes expand in size, their mechanical stress increase because their contact with neighboring cells and extracellular matrix components increase. Adipocytes also experience hypoxia, as the hypertrophic growth of the AT is not accompanied by a similar expansion rate of angiogenesis⁶⁸. Moreover, hypertrophic adipocytes and damaged cells release proinflammatory cytokines that attract and activate immune cells. All these promote a chronic low-grade inflammation state in AT that severely alters AT functionality⁶⁹.

Furthermore, the enlarged adipocytes in obese individuals are partially resistant to antilipolytic effect of insulin. Increased lipolysis leads to increased release of free fatty acids (FFAs) into the bloodstream, resulting in the ectopic deposition of lipids causing lipotoxicity. All these disturbances may lead to the development of systemic IR, oxidative stress and contribute pathogenesis of obesity related comorbidities⁷⁰.

1.2.4. Body fat distribution in obesity: AT expandability theory

The body fat distribution, which is highly conditioned by AT functionality, is the second characteristic of AT that determines the obesity-related adverse health consequence. The excessive calories from the diet are stored primary in scWAT. When scWAT reaches its maximal storage capacity, AT fails to store lipids appropriately. The lipid flux is then redirected to other organs where it is accumulated as ectopic fat, causing insulin resistance through lipotoxic and inflammation-related mechanisms⁷¹. This ectopic accumulation occurs primarily in the visceral adipose tissue (visWAT) and liver, leading to visceral obesity and liver steatosis, respectively^{72,73} (Figure 6).

This suggests that the factor linking obesity and its associated comorbidities may not be the absolute amount of fat accumulated *per se* but the disbalance between energy excess and AT storage capacity. This storage capacity might be eventually limited, and this limit varies greatly between individuals (AT expandability hypothesis⁷¹). This limit is determined by the differential expression of genes, proteins, microRNAs, and metabolites from different cell types⁷⁴. Although many genes are well known to be involved in regulating this process, the complete molecular mechanism that determines this expandability limit still needs to be fully understood.

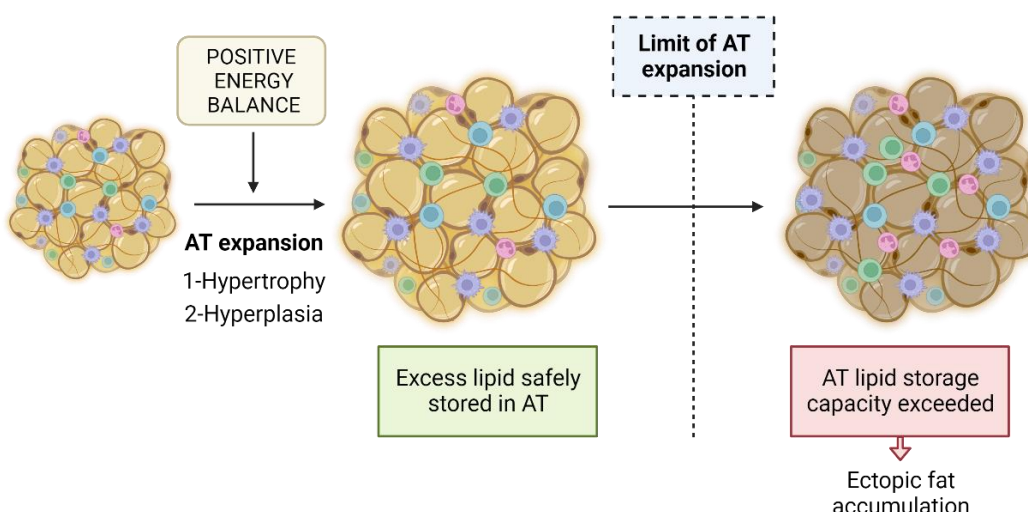


Figure 6. Adipose tissue expansion during obesity. Modified from Vidal-Puig et al.⁷⁵

All the above suggest that scWAT could be protective, while visWAT contributes to metabolic risk^{69,76}. For instance, a major deposition of fat in visWAT correlates with increased risk of T2DM and CVD, while an increase of subcutaneous fat is associated with favorable adipokine production and improved plasma lipid profiles^{62,63}.

Therefore, it is critical to distinguish between subcutaneous and visceral fat accumulation, as each fat depot might have a different metabolic function. And consequently, the sc/vis ratio could be a good indicator of the metabolic status, as it will be detailed in the following sections.

1.3. Comorbidities associated to obesity: Non-alcoholic fatty liver disease

NAFLD is one of the main comorbidities associated to obesity. It is estimated that more than 75% of patients with obesity are affected by NAFLD^{48,77}.

1.3.1. Prevalence of NAFLD

NAFLD is becoming one of the most common liver diseases in the world, reaching a global occurrence of almost 25% over the past four decades, and it is presently known to have a close, bidirectional association with obesity⁷⁸. As a result of its high prevalence, NAFLD is now the world's fastest-growing cause of liver-related mortality worldwide and is emerging as a significant cause of end-stage liver disease, primary liver cancer, and liver transplantation with a considerable health economic burden⁷⁹.

1.3.2. Classification of NAFLD

NAFLD is an umbrella term for a variety of conditions caused by excessive fat accumulation in hepatocytes in people who drink little or no alcohol. Steatosis (NAFL), defined as the presence of fat in more than 5% of hepatocytes, represents the first step of the NAFLD progression, although it is mostly benign and remains clinically silent⁸⁰. However, in many cases (10-30%) complications can lead to steatohepatitis (NASH), characterized by inflammation, fibrosis and hepatocellular injury⁸¹. These stages are reversible, but NASH may advance to cirrhosis or even hepatocarcinoma (HCC), which are irreversible conditions and liver function is severely altered⁸² (Figure 7).

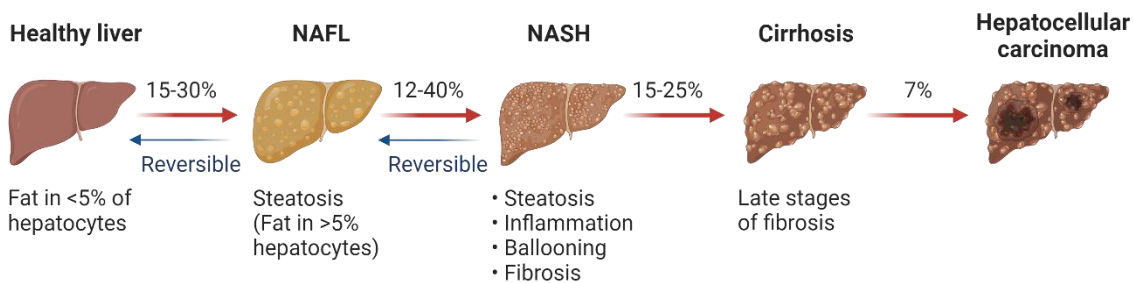


Figure 7. Spectrum of non-alcoholic fatty liver disease (NAFLD) progression. The development of NAFLD is divided into four stages: simple steatosis (NAFL), steatohepatitis (NASH), liver cirrhosis, and eventually hepatocarcinoma (HCC).

1.3.3. Pathogenesis of NAFLD

Although the pathogenesis of NAFLD and NASH is not fully understood, it is known to be complex and multifactorial, including the interplay of several genetic, metabolic, environmental, and dietary variables⁸³.

Several hypotheses have been proposed to explain the pathophysiology of NAFLD. First, a two-hit theory was presented. According to this hypothesis, the first hit is an excessive buildup of lipids in the liver, which is produced by a variety of factors such as a high-fat diet, a sedentary lifestyle, obesity, or IR. This first hit sensitizes the liver to the second hit, which is likewise produced by several metabolic insults that induce inflammation and fibrogenesis⁸⁴.

However, most recent evidence has suggested more complex mechanisms. This theory, named as the “multiple parallel hits hypothesis”, involves different elements acting together, rather than in series. According to this theory, IR, genetic and epigenetic factors, mitochondrial dysfunction, endoplasmic reticulum stress, microbiota, chronic low-grade inflammation, and dysfunction of AT all represent synchronic causes of both NAFLD development and progression⁸⁵.

1.3.3.1. Role of genetic and epigenetic factors

Several genetic variants, specially single nucleotide polymorphisms (SNP), have been associated both with the development and progression of NAFLD⁸⁶. For instance, a SNP of the patatin-like phospholipase domain-containing protein 3 (PNPLA3) has been reported to be crucial in NAFLD development⁸⁷. PNPLA3 gene encodes a protein named adiponutrin, which exerts a lipolytic activity on TG. The PNPLA3 148M allele (rs738409 C/G) is associated with a reduced *de novo* lipogenesis and a higher expression of SREBP-

$1c^{88}$. In humans, this polymorphism is further associated with an increased incidence of steatosis and a higher degree of liver fibrosis⁸⁹. Other examples is transmembrane 6 superfamily member 2 (TM6SF2) gene, that encodes a protein that promotes the secretion of very-low density lipoproteins (VLDLs)⁹⁰. Its variant rs58542926, through a loss of function, is associated with lower plasma VLDL levels and higher alanine aminotransferase (ALT) levels, that promotes hepatic steatosis⁹¹.

Beyond the role of genetic variants, some studies have been focusing on the potential impact of epigenetics on the development of NAFLD⁹². DNA methylation is among the crucial epigenetic determinants which lead to steatosis up to NASH and it is mainly affected by the dietary shortage of methyl group donors (e.g., betaine, choline, and folate)⁹³. For instance, folate levels affect the expression of genes involved in FFA synthesis and its deficiency seems to be involved in the intrahepatocyte accumulation of TG⁹⁴.

1.3.3.2. Role of AT dysfunction

Dysfunctional adipocytes can no longer accumulate fat, so the lipid flux to the liver increases, thus promoting steatosis. Moreover, mediators secreted from AT induce increased systemic FFAs, aberrant adipokines, altered exosomes (and their genetic and protein cargo), and increased proinflammatory cytokines. All these influence TG metabolism, IR, inflammation, and fibrosis in the liver, culminating in the development of NAFLD (Figure 8)^{95,96}. It has been shown that adiponectin reduces hepatic IR by inhibiting glycogenolysis and lipogenesis and increasing glucose consumption⁹⁷. It has also antifibrotic, anti-inflammatory and antioxidant properties that contribute to the genesis and progression of NAFLD and NASH^{98,99}. Leptin, on the other hand, exerts an anti-steatotic effect, decreasing lipid accumulation and lipotoxicity, and a proinflammatory effect, stimulating fibrogenesis; suggesting that the different leptin levels promote beneficial or detrimental consequences for the liver^{100–102}.

1.3.3.3. Role of insulin resistance

IR plays a key role in the development of NAFLD, as it causes an increase in hepatic lipogenesis and an inhibition of AT lipolysis, with a subsequent elevated flow of FFA in the liver¹⁰³. Fat accumulates within the hepatocytes mainly as TG deriving from the esterification of glycerol and FFAs. The hepatic accumulation of TG does not represent

itself as a hepatotoxic event, rather as a defense mechanism able to balance the excess FFAs in the plasma¹⁰⁴. However, other bioactive intermediates, such as ceramides and diacylglycerols (DAGs), can induce lipotoxicity, resulting in inflammation, necrosis, and liver fibrosis. NAFLD progresses to NASH when the mechanisms protecting hepatocytes from lipotoxicity are depleted. This induces necrosis and secondary repair phenomena mediated by hepatic stellate cells, with the deposition of scar collagen tissue, hence the development and progression of fibrosis^{105,106} (Figure 8).

1.3.3.4. Role of low-degree chronic systemic inflammation

Several mechanisms contribute to increased levels of inflammatory cytokines in NAFLD, both in the liver and at systemic level. Two main inflammatory pathways, Jun N-terminal kinase (JNK) and IKK-NF-κB, are critically involved in the development of the chronic inflammation occurring during NAFLD. JNK belongs to the family of MAPKs and is associated with the induction of apoptosis¹⁰⁷, while IKK is required for the activation of nuclear factor kappa-B (NF-κB) that induces production of inflammatory cytokines such as TNF-α and IL-6¹⁰⁸.

Hepatic exposure to increased levels of pro-inflammatory cytokines leads to histological changes characteristic of NASH, such as hepatocyte necrosis and apoptosis, neutrophil chemotaxis, activation of hepatic stellate cells, and production of Mallory bodies (aggregates of cytokeratin intermediate filaments). This plays a significant role in the disease's development from basic steatosis to NASH and fibrosis. Furthermore, persistent inflammation may promote carcinogenesis and hence contribute to the progression of the disease to HCC¹⁰⁹.

1.3.3.5. Role of mitochondrial dysfunction and oxidative stress

When the lipid flow exceeds mitochondrial and peroxisomal capacity, respiratory oxidation collapses, thus leading to impairment in lipid homeostasis, generation of harmful metabolites, and overproduction of reactive oxygen species (ROS)¹¹⁰. These molecules lead to oxidative stress and contribute to hepatic necro-inflammatory processes and further mitochondrial damage. Moreover, ROS, along with oxidized low-density lipoproteins (LDL), can activate Kupffer and hepatic stellate cells, thus resulting in collagen deposition and secondary liver fibrosis^{111,112}.

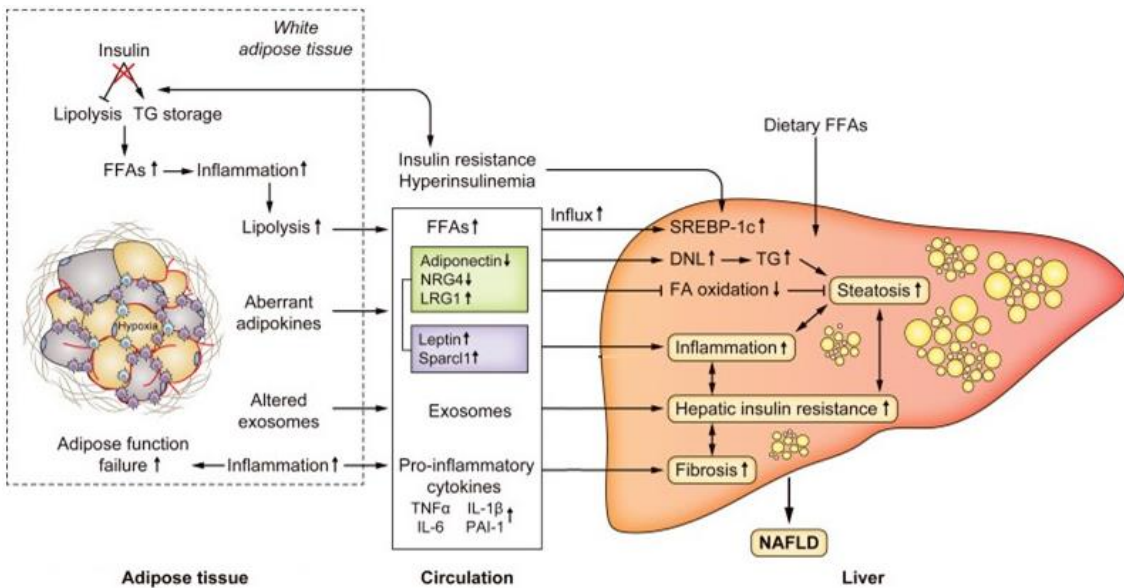


Figure 8. Adipose tissue – liver cross talk in the progression of NAFLD/NASH associated to obesity. Modified from Lee E. et al¹¹³.

1.4. Diagnosis of obesity phenotypes and its metabolic complication

The increasing prevalence of obesity worldwide confers a significant global public health burden, as it is a known risk factor for many diseases. Therefore, it is necessary to prevent, detect, and appropriately treat obesity to reduce the future health and economic costs of this problem. The first step to achieve this is to reliably diagnose individuals. In this sense, many different diagnosis methods have been proposed to classify obesity phenotypes and to predict metabolic complications associated to obesity¹¹⁴ (Table 1).

1.4.1. Anthropometric parameters

Anthropometric parameters are widely used as diagnosis methods for obesity and its metabolic complications as they are non-invasive and cost-effective tests¹¹⁵. The BMI is the most widely used method to estimate the amount of body fat¹¹⁶. However, since BMI cannot detect regional variations in fat deposition, other measures able to capture abdominal obesity, such as waist circumference (WC)¹¹⁷ or waist/hip ratio (WHR, waist circumference divided by the hip circumference)¹¹⁸ are also employed.

In general, none of these anthropometric parameters differentiate between fat and muscle mass, which have opposite health impacts, nor the contribution of subcutaneous or visceral fat^{119,120}. Therefore, other methods that consider adiposity and AT distribution are needed to properly classify obesity phenotypes.

1.4.2. Imaging techniques

Due to the above described limitations of classical obesity measures, other more complex techniques to assess body compartments have also been incorporated in obesity diagnosis; including bioimpedance analysis (BIA), dual-energy X-ray absorptiometry (DXA), computed tomography (CT) and magnetic resonance imaging (MRI) or magnetic resonance spectroscopy (MRS) scans¹²¹. They allow to quantify the volume and mass of different body areas such as AT in the subcutaneous, visceral, and coronary (fat tissue around the heart and heart vessels) compartments, and fat-free lean compartments such as bone marrow and skeletal muscle tissue¹²².

Currently, CT and MRI are the gold standard methods for the quantitative evaluation of intra-abdominal AT distribution^{123,124}. These techniques allow to distinguish between subcutaneous and visceral fat depots and, therefore, to calculate the sc/vis ratio, which has been reported to be a good indicator of the metabolic health of obese patients^{125–128}.

Imaging techniques hold great potential for obesity research as well as clinical use and risk stratification. However, they are considerably more complex and require computerized processing. Moreover, the establishment of guidelines and thresholds to determine abnormal and detrimental levels of fat mass, and whether these levels might vary according to ethnicity, age, sex, and fat-free mass, is still pending. Consequently, the current applicability of these techniques in clinical practice remains rather limited¹¹⁴.

1.4.3. Circulating biomarkers

The identification of biomarkers in human circulation that reflect the underlying biological mechanisms for the increased disease risk may be an alternative approach to characterize the relevant obesity phenotype. Several circulating molecules have been identified as obesity-associated biomarkers, that can be classified into three main groups: adipokines, markers of glucose-insulin pathway and inflammatory markers^{129–131}.

1.4.3.1. Adipokines

Adipokines have been proposed as biomarkers of obesity, as their production is often dysregulated in obese individuals and contribute to the pathogenesis of obesity-associated metabolic complications¹³². Numerous adipokines altered in the obese state have been identified in the past decades¹³³.

Higher leptin concentrations are observed in obese individuals and leptin levels have been directly correlated with the percentage of fat mass^{134,135}. Several studies have investigated associations of leptin levels with metabolic complications¹³⁶ and have shown that obesity-associated hyperleptinemia promotes hypertension¹³⁷, contributing to increase CVD risk^{138,139}. By contrast, circulating adiponectin levels are inversely related with body weight, even though adiponectin is a protein synthesized and secreted predominantly by adipocytes into the peripheral blood. This inverse association is also observed with visceral fat accumulation¹⁴⁰. The mechanism of this paradoxical relation remains unclear. Moreover, low circulating adiponectin concentrations are associated with a variety of diseases, including IR¹⁴¹, T2DM¹⁴², dyslipidemia¹⁴², metabolic syndrome (MetS)^{143,144}, NAFLD¹⁴⁵, CVD¹⁴⁶ or atherosclerosis; while hyperadiponectinemia is also associated with renal and pulmonary diseases¹⁴⁷. The role of other adipokines such as FABP-4 or visfatin in obesity-related chronic disease risk is less-well understood. For instance, a positive association between circulating FABP-4 and risk of diabetes and heart failure has been suggested¹⁴⁸, while clinical studies have proposed a role of visfatin in inflammatory and atherogenic processes in various metabolic diseases including T2DM and MetS¹⁴⁹.

1.4.3.2. Markers of glucose-insulin homeostasis

It is well known that obesity is associated with impaired glucose uptake and IR¹⁵⁰. Therefore, different biomarkers related with insulin signaling have been investigated. For instance, fasting insulin and C-peptide, which is cleaved from proinsulin, have been shown to positively correlate with BMI¹⁵¹. Higher fasting insulin concentrations were associated with higher risk of hypertension and coronary heart disease¹⁵², while C-peptide has been shown to predict total and cardiovascular mortality in non-diabetic individuals^{153,154}. Insulin metabolism is tightly linked with the insulin-like growth factors (IGF), an evolutionary conserved group of factors exerting long-term effects on growth¹⁵⁵. IGF-1 has been proposed as a diabetes risk biomarker, as some studies showed a lower risk of glucose intolerance or T2DM in individuals with high *versus* low IGF-1 concentrations^{156,157}.

1.4.3.3. Inflammatory biomarkers

Obesity is associated with chronic low-grade systemic inflammation, which has been suggested to play a key role in the pathogenesis of IR¹⁵⁸. In AT of people with obesity, the secretion of cytokines such as TNF- α and IL-6 is upregulated, which stimulates the

hepatic release of acute-phase proteins such as C-reactive protein (CRP)¹⁵⁹. Due to the availability of standardized assays and its temporal stability, CRP is the most-studied inflammatory biomarker in relation to disease risk. Higher CRP concentrations have been associated with higher risk of coronary heart disease, ischemic stroke, vascular and non-vascular mortality as well as death from several cancers. However, CRP is rather unspecific^{160,161}.

All these circulating molecules serve as biomarkers of obesity-related comorbidities and their measurement can help to evaluate the metabolic status of an individual or the effectiveness of interventions aimed to improve metabolic health. However, it is important to consider that their levels can also be influenced by other factors such as gender, age or lifestyle, and that biological pathways interact in a complex manner, which complicates the establishment of a net value for a particular biomarker. Therefore, the interpretation of these biomarkers' levels should be done in conjunction with other clinical and biochemical measurements and the identification of a complete panel of biomarkers that collectively reflect the metabolic status of each patient is still needed.

1.4.4. Omics-based biomarkers

In this context, omics approaches have shown promise in improving our understanding of obesity and its diagnosis, as they integrate several data to uncover molecular patterns linked with the disease. Intensified efforts in omics research have been invested in the identification of genes (genomics), RNA (transcriptomics) and metabolites (metabolomics) linked to obesity. Further novel omic-based biomarkers include epigenomics, proteomics, glycomics or microbiomics^{161,162}.

1.4.4.1. Genomics

Genetic susceptibility of obesity is determined by the influence of multiple genetic variants^{163,164}. Therefore, genome-wide association studies (GWAS) have become a useful tool to identify genetic variants critical in obesity that may serve as biomarkers¹⁶⁵. A recent GWAS based on 700,000 individuals identified 941 near-independent SNPs associated with BMI¹⁶⁶. Regarding body fat distribution, much fewer variants have been associated, a large meta-analysis including 224,459 individuals identified and replicated 49 loci¹⁶⁷. The strongest and most often replicated variants are located within the Fat Mass And Obesity Associated (FTO) gene^{168,169}. Some of the FTO genetic variants have been

linked to hunger regulation^{170,171}, energy expenditure^{172,173} or circadian rhythm¹⁷⁴ as well as to chronic diseases including different types of cancer¹⁷⁵, but the mechanisms underlying the FTO genetic associations with obesity have not been fully understood^{176,177}. Some of the other genetic variants that have been linked to obesity are found within the genes of biomarkers described in the previous section, such as in the leptin, leptin receptor¹⁷⁸, or adiponectin¹⁷⁹.

1.4.4.2. Transcriptomics

The transcriptome of adipocytes, from both subcutaneous and visceral WAT, has revealed more than a thousand genes whose expression is altered in obese as compared to lean individuals, as well as genes whose expression is correlated with the development or progression of metabolic complications^{180,181}. However, the limited availability of AT biopsies, makes difficult to use adipocyte transcriptome as biomarker of metabolic status in the clinical practice. As an alternative, peripheral blood transcriptome has also been studied to find biomarkers in obesity¹⁸². Some studies have correlated whole-blood mRNA levels with BMI and the gene expression signatures pointed to key metabolic pathways involved in protein synthesis, enhanced cell death from proinflammatory or lipotoxic stimuli, enhanced insulin signaling, and reduced defense control against ROS¹⁸³.

Transcriptomic biomarkers include not only protein coding RNAs (mRNAs), that represent less than 2% of the total genomic sequence, but also non-coding RNAs (ncRNAs) such as miRNAs and long ncRNAs (lncRNAs)¹⁸⁴. miRNAs have emerged as promising biomarkers in obesity as they have shown to exert important regulatory roles in adipocytes^{185,186} and some of them are released into the bloodstream [circulating miRNAs (cmiRNAs)] and, therefore, can be detected by minimal invasive methods. Several cmiRNAs with dysregulated expression in plasma of people with obesity compared to lean have been identified, but further validation is needed to confirm their potential as biomarkers^{187,188}.

1.4.4.3. Metabolomics

Alterations in many metabolites have been found to be associated with obesity, including higher plasma levels of branched-chain amino acids (BCAA) and aromatic amino acids (AAA) as well as lower plasma levels of glycine^{189–191}. Interestingly, these biomarkers have also been linked to IR and a higher risk of T2DM^{192,193}. An important branch of

metabolomics with special relevance in obesity research is lipidomics, as plasma lipids are mediators of metabolic dysfunction and obesity-related chronic diseases^{194,195}. For decades, simple lipid profile analysis has been a fundamental tool in clinical practice to assess dyslipidemia^{196,197}. Moreover, lipidomic studies identified higher levels of FFA as well as short- and medium-chain acylcarnitines in obese compared to lean subjects. Indeed, many of these markers were associated with T2DM risk independently of BMI and WC, suggesting that they may improve the prediction of the disease^{198–200}.

These omic-based biomarkers can provide new insights into pathophysiologic pathways, improve the clinical identification of patient at increased risk for disease, facilitate monitoring of disease progression and prognosis, represent targets for therapy, and allow more personalized treatment decisions for individual patients. However, the precise roles and relevance of most of them remain uncertain and it is needed to validate their reproducibility before they can be applied in clinics. Indeed, the clinical diagnosis of obesity is currently widely restricted to the measurement of BMI and more complex tests are rarely performed in clinical medicine.

Table 1. Overview of diagnosis methods for obesity and its metabolic complications.

Category		Pros	Cons
Anthropometric parameters	BMI WC WHR	<ul style="list-style-type: none"> • Non-invasive • Cost-effective tests 	<ul style="list-style-type: none"> • Do not consider adiposity and AT distribution
Imaging techniques	BIA DXA CT MRI	<ul style="list-style-type: none"> • Allow to quantify the fat volume and distribution • High accuracy and reproducibility 	<ul style="list-style-type: none"> • Complex, require computerized processing • Lack of guidelines and thresholds
Circulating biomarkers	Adipokines Insulin pathway Inflammatory markers	<ul style="list-style-type: none"> • Non-invasive • Cost-effective tests 	<ul style="list-style-type: none"> • Levels influenced by multiple factors • Lack of guidelines and thresholds
Omics-based biomarkers	Genomics Transcriptomics Metabolomics Lipidomics	<ul style="list-style-type: none"> • Integrate several data • Allow more personalized diagnosis 	<ul style="list-style-type: none"> • Complex, require computerized processing • Validation of its reproducibility is needed

1.5. Treatment of obesity and its metabolic complications: genetic modification of ADMSC as an alternative

Lifestyle modifications such as diet and exercise remain the cornerstone of obesity treatment. However, in many cases, it is not sufficient to reduce body weight to stop the progression of comorbidities associated with obesity. Currently, bariatric surgery remains the most effective and cost-saving intervention for obesity, although, because of its complexity, it seems unaffordable to reduce the obesity pandemic expansion²⁰¹. On the other hand, some pharmacological strategies targeting the energy balance regulatory system are now reaching clinically relevant reductions in body weight^{202,203}.

In this context, the appearance of new tools and techniques of genetic engineering as well as advances in understanding the molecular basis of obesity have given rise to new precision medicine approaches targeting the AT²⁰⁴. These innovative approaches include ADMSC-based therapy and gene therapy for obesity²⁰⁵.

1.5.1. ADMSC-based therapy

Transplantation of MSCs obtained from AT (ADMSCs) have been proposed as an alternative therapeutic strategy for obesity and its metabolic complications^{11,206,207}. ADMSC can migrate to a wide range of tissues, specialty inflammatory and pathological sites and possess immunomodulatory properties²⁰⁸. It has been reported that ADMSC transplantation improves AT inflammation by reducing pro-inflammatory cytokines as interleukin 1β (IL-1β), IL-6 or TNF-α secretion^{209–211}. It also restores glucose homeostasis by improving insulin sensitivity, as it contributes to the activation of insulin receptor substrate 1 (IRS-1) - serine/threonine kinase 1 (AKT) - GLUT4 pathway^{212,213}. Moreover, ADMSC can differentiate into multiple lineages after transplantation. They are able to differentiate into insulin-producing cells (IPCs) and contribute to insulin production^{214,215}, as well as into hepatocyte like cells (HLCs) and contribute to restore liver function^{210,216}. All these contribute to restore the metabolic balance altered in obesity (Figure 9).

The results obtained in animal models have confirmed the effects of ADMSC therapy on weight loss, changes in AT composition, and improvement of related comorbidities such as diabetes or NAFLD²¹⁷.

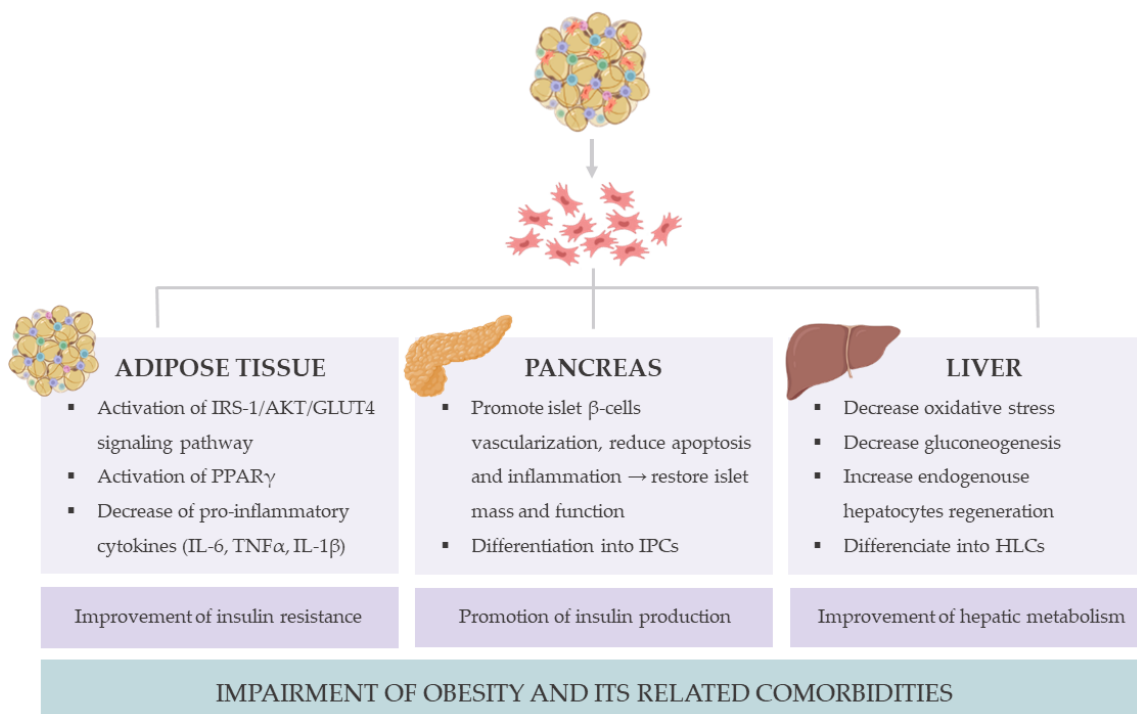


Figure 9. Mechanisms of action of ADMSC on obesity treatment. The transplantation of ADMSCs reduces adipose tissue inflammation, restores glucose homeostasis by improving insulin sensitivity and promoting insulin production, and reverses liver steatosis.

1.5.2. Genetic modification of ADMSC: CRISPR/Cas9 gene editing

Genetic engineering of ADMSC has been proposed as a strategy to enhance the therapeutic potential of these cells and improve the clinical outcomes after transplantation. Several genetic engineering methods have been described to modify the ADMSC gene expression profile. These techniques can be broadly classified as viral- and non-viral-based transfection as well as Clustered Regularly Interspaced Short Palindromic Repeats (CRISPR)-Cas9 gene editing technology.

Due to its high efficiency, specificity, simple design and cost-effectiveness, CRISPR/Cas is becoming the most widely used genome editing technology^{218,219}. CRISPR/Cas9 system is based on the nucleolytic activity of the endonuclease protein Cas9, which is conducted to a specific site in the genome by a guide RNA (gRNA). The Cas9 protein binds to the target site determined by the gRNA and performs a double-strand break (DSB) followed by the introduction of mutations at the cleavage site by the non-homologous end-joining repair mechanism of the cell. Using a predesigned repair template, this system can not only knock out genes but also knock in (CRISPR/Cas9-SAM-System) or even insert specific mutations^{218,220,221} (Figure 10).

The efficiency of the CRISPR/Cas9 system has already been tested in MSC by targeting critical genes involved in adipocyte differentiation and function as *Pparg2*, *Prdm16*, *Zfp423*, or *Ucp1*²²², demonstrating that this system could efficiently manipulate gene expression in pre- and mature adipocytes *in vitro*. This gene editing technology has also been optimized in ADMSC obtained from human AT. Kamble *et al.* developed a method for gene knock out by introducing CRISPR/Cas9 system by electroporation in ADMSC. They knock out *PPARG* genes with more than 90% efficiency, blocking the differentiation of ADMSC into adipocytes²²³.

Regarding *in vivo* models, CRISPR/Cas9 technology was used to engineer human white adipocytes to display phenotypes similar to brown fat, by targeting endogenous expression of uncoupling protein 1 (UCP1)²²⁴ or nuclear receptor-interacting protein 1 (NRIP1)²²⁵. Both studies showed the benefits of using CRISPR/Cas9 technology to treat metabolic complications and demonstrated that it is a safe alternative, as *ex vivo* delivered Cas9 and sgRNA are entirely degraded by receptor cells after high-efficiency genomic modification without detectable off-target editing.

Hence, CRISPR/Cas9 gene editing in ADMSC seems to be a promising tool for therapeutical applications. However, all these investigations are still at an early stage, and more positive results are needed for their translation into the clinic.

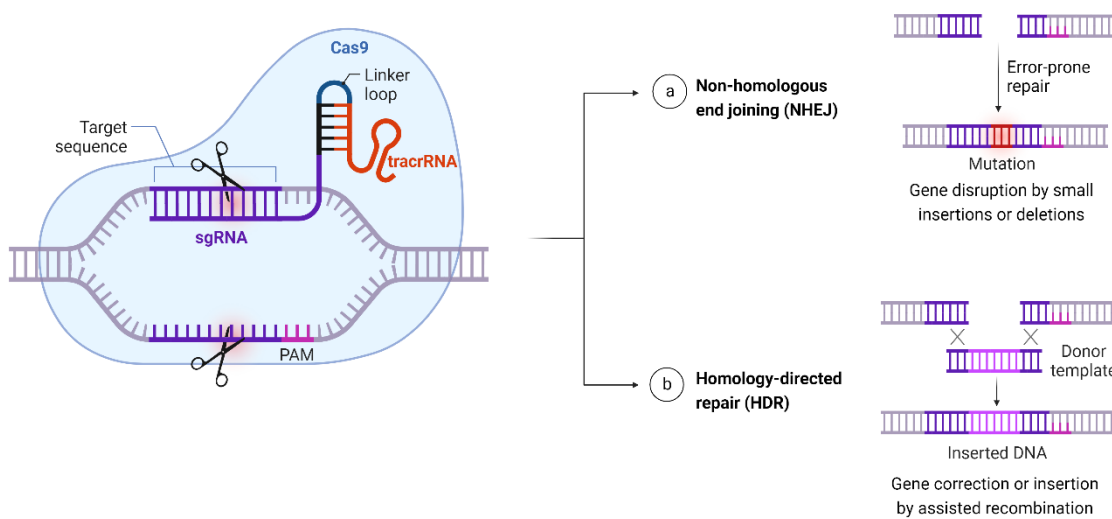


Figure 10. Clustered Regularly Interspaced Short Palindromic Repeats (CRISPR)-Cas9 gene editing technology.

This section is further detailed in the following review: Lopez-Yus M, García-Sobreviela MP, Del Moral-Bergos R, Arbones-Mainar JM. Gene Therapy Based on Mesenchymal Stem Cells Derived from Adipose Tissue for the Treatment of Obesity and Its Metabolic Complications. *Int J Mol Sci.* 2023 Apr 18;24(8):7468. doi: 10.3390/ijms24087468. PMID: 37108631; PMCID: PMC10138576. (Annex I).

2. HYPOTHESIS AND OBJECTIVES

2.1. Hypothesis

Obesity is a major risk factor for the development of metabolic diseases. It is well established that each individual possesses an intrinsic limit on their capacity to store lipids in scWAT. When scWAT reaches its maximal storage capacity, AT fails to store lipids appropriately redirecting this lipid flux to other organs like visWAT and liver, leading to visceral obesity and liver steatosis respectively. Therefore, it is reasonable to think that the understanding of molecular mechanisms leading to the expansion of scWAT may be a key factor for prediction and treatment of metabolic diseases associated to obesity.

Our central hypothesis is that the use of high-throughput technologies will reveal novel mechanisms regulating the expansion of scWAT. This will contribute to identify novel biomarkers or potential new targets for obesity and its metabolic complications.

Moreover, we hypothesize that genomic editing using CRISPR/Cas9 technology of the hADMSC resident in the adipose tissue can modify differentiation and functional capacity of these adipocyte precursors and lead to mature adipocytes with extended expandability potential. Thereby, increased expansive capacity of adipocytes could reduce accumulation of ectopic fat in peripheral organs such as liver and, therefore, have therapeutic activity against obesity related disorders like fatty liver disease.

2.2. Objectives

The general objective of this work is to elucidate the physiological processes involved in the healthy expansion of the scWAT and to detect and treat any altered mechanism in scWAT linked to NAFLD.

This objective was divided in three specific goals:

- 1) To determine if some genes involved in the expansion of the scWAT may have a potential role as non-invasive biomarkers for the diagnosis of metabolically healthy or unhealthy obesity.
- 2) To obtain new insights into the molecular mechanisms underlying the causative role of scWAT in NAFLD, identifying targetable genes in scWAT potentially involved in the development and progression of NAFLD.
- 3) To determine the viability of a cellular-based therapy for obesity related disorders by modulating the expression of specific genes in hADMSC-derived adipocytes.

3. MATERIALS AND METHODS

3.1. Human cohort description

The cohort used for this study was the FATE cohort, a longitudinal cohort of obese patients undergoing bariatric surgery in Miguel Servet University Hospital (HUMS, Zaragoza, Spain), that donated blood samples, subcutaneous and visceral AT biopsies and eventually liver biopsies. The FATE cohort is a live cohort in which patients have been recruited at different time points since 2013 and undergone different procedures and techniques according to the research needs⁶¹.

Patients were screened to exclude alcohol or drugs abuse, autoimmune disease, chronic inflammatory diseases or chronic infectious diseases (HIV, HBV, HCV). All subjects in the cohort provided written consent and the study was approved by the Regional Institutional Review Board of Ethics at Aragón, Spain (CEIC-A). Samples and data from patients included in this study were provided by the Biobank of the Aragon Health System (PT20/00112), integrated in the Spanish National Biobanks Network and they were processed following standard operating procedures with the appropriate approval of the Ethics and Scientific Committees.

3.2. Characterization of human cohort

3.2.1. Tissue samples collection

Biopsies (~3 cm³) of AT from both the subcutaneous and the visceral fat depot were obtained with a bipolar/ultra-sonic device (Thunderbeat. Olympus, Spain) and extracted via a 12 mm trocar (Applied Medical Europe, Spain) inserted in the left hypochondrium during laparoscopic surgery.

Liver biopsies were also obtained during the surgery and were deemed adequate when they were 16 mm in length and included at least 6 portal tracts.

3.2.2. Plasma biochemistry

Plasma biochemistries were performed at the Clinical Biochemistry department at the HUMS using state of the art analyzers. All analyses are in compliance with the requirements for quality and competence (ISO 15189:2012) for medical laboratories.

The following metabolic parameters were analyzed: glucose, HOMA (homeostatic model assessment), glycated hemoglobin (HbA1c), C-Reactive protein (CRP), cross-linked C-terminal telopeptide of type I collagen (CTX), triglyceride (TG), total cholesterol, high density lipoproteins (HDL), gamma glutamyl transferase (GGT), alanine transaminase (ALT), aspartate transaminase (AST) and leptin.

Additionally, adiponectin, adipsin, monocyte chemoattractant protein-1 (MCP-1) and resistin were measured in selected samples. The process was carried out in the Cell Sorting and Cytometry Unit of the Aragonese Institute of Health Sciences (IACS), using the LegendPlex immunoassay (Biolegend) by flow cytometry, following manufacturer's instructions.

3.2.3. Computer tomography analysis

The visceral and subcutaneous fat area was measured by computer tomography (CT) with an 8 mm single slice at the umbilical level. All CT examinations were acquired with the subject positioned supine in a 64 detector CT scanner (Aquilion 64 Toshiba Tokyo, Japan) and tube voltage set to 120 kVp with automatic tube current modulation and rotation time of 0.5 s. Acquired images were then transferred to a workstation and analyzed with the Vitrea CT Fat Measurement software (Vital Imaging Inc. The Netherlands). Selected fat densities were ranged between -150 and -70 Hounsfield Units (HU) and the Total Fat Area (TFA), Subcutaneous Fat Area (SFA) and Visceral Fat Area (VFA) were measured in cm². SFA and VFA were respectively defined as pixels (area) located outside or inside the outer surface of the abdominal muscle wall. Subsequently, the ratio between subcutaneous fat area divided by the area of visceral fat was calculated.

3.2.4. Histological examination

Paraffin sections of livers were stained with hematoxylin-eosin (H&E). Pathological features of steatosis, lobular inflammation, hepatocellular ballooning and fibrosis were scored by an experienced pathologist, according to criteria established by the Nonalcoholic Steatohepatitis Clinical Research Network²²⁶.

Total NAFLD Activity Score (NAS) (ranging from 0-8) was calculated by adding the scores for steatosis, lobular inflammation, and hepatocellular ballooning as described²²⁶.

3.3. Isolation of hADMSC

hADMSC were obtained from scWAT of patients included in the cohort described above (FATE) that donated a sufficient amount of scWAT ($> 5\text{g}$) to allow the isolation and establishment of hADMSC cell lines. The collected fat biopsies were washed in DPBS with antibiotic and mechanically separated from other tissues and minced with a scalpel. The obtained fraction was disaggregated with 5 ml of digestion medium (low glucose DMEM (#BE12-707F, Lonza), 10 mg/ml albumin (#49647, Sigma Aldrich), 1.5 mg/ml collagenase (#C5138, Sigma Aldrich), 0.6% antibiotic (#A5955, Sigma Aldrich)) and samples were incubated for 40-50 minutes at 37°C and agitation.

The digestate was then centrifuged at 1200 rpm for 10 min at room temperature (r. t). After centrifugation, the supernatant was removed and the pellet was resuspended in 5 ml of red cell lysis buffer (150 mM NaH₄Cl, 10 mM NaHCO₃, 1.27 mM EDTA). The supernatant was incubated for 2 min at r. t. with gentle manual agitation and then centrifuged again at 1200 rpm for 10 min. Subsequently, supernatant was removed, pellet was washed with 10 ml of DPBS to eliminate red blood cell debris and another round of centrifugation was performed. Finally, the cell pellet was resuspended in 5 ml of low glucose DMEM supplemented with 10 % fetal bovine serum (FBS) and 1% antibiotic. Cells were plated in a 25 cm^2 cell culture flask.

Cells were cultured under hypoxic conditions (5% O₂, 5% CO₂) and washed with DPBS after 24 h to remove tissue debris. The culture was maintained and expanded to establish the primary culture. Isolated hADMSC were tested by fluorescence-activated cell sorting analysis using specific antibodies to detect mesenchymal markers: CD34 PercpCy5.5 (#347222, BD Biosciences), CD73-phycoerythrin (PE) (#550257, BD Biosciences), CD90-PE (#555596, BD Biosciences), CD105-FITC (#FAB10971F, R&D Systems), and HLA-DR-APC (#HLA-DRA2-100T, Immunostep).

3.4. Cell culture

3.4.1. hADMSC culture and differentiation

hADMSC cultures were maintained in 10% FBS-low-glucose DMEM under hypoxic conditions (5% O₂, 5% CO₂) and 37°C . Two days after confluence, hADMSC were differentiated into adipocytes using an adipogenic cocktail in normoxic conditions (21%

O₂, 5% CO₂) for additional 5 days. The standard adipogenic cocktail consisted of 10% FBS–high-glucose DMEM plus (Gibco), 1.5 μM insulin (Novo Nordisk), 1 μM dexamethasone (Sigma), 500 μM 3-isobutyl-1-methylxanthine (Sigma), and 2 μM rosiglitazone (Sigma). hADMSC-derived adipocytes were maintained in 10% FBS–high-glucose DMEM and were considered to have reached mature phenotype at 8 days post-differentiation²²⁷.

3.4.2. HepG2 culture

Human hepatoma HepG2 cells were grown in high-glucose DMEM supplemented with 10% FBS at 37 °C in normoxic conditions (21% O₂, 5% CO₂). Experiments were performed at 70-80 % confluence.

3.4.3. HepG2-adipocytes co-culture

Co-culture of adipocytes and HepG2 cells was conducted in cell culture inserts (#141078, Thermo Fisher). First, adipocytes were seeded and differentiated in 12-well plates. Two days before cells completely differentiated into adipocytes, HepG2 cells were plated into membrane inserts (4 μm pore size) and were allowed to grow. After these two days, inserts were transferred to plate wells containing differentiated adipocytes. This resulted in an assembly of the two cell types sharing the culture medium but being separated by the membrane of the insert. Distance from the bottom of the culture dish to the membrane was 0.9 mm. Co-cultures were conducted for 48 h. At the end of the co-culture period, characterization experiments were performed.

3.5. CRISPR/Cas9 genomic modification of hADMSC

CRISPR/Cas9 technology was used to knockout the expression of target genes in hADMSC. First, specific single guide RNAs (sgRNAs) were designed for each target gene, and then, hADMSC were transfected with these sgRNAs and Cas9 as follows.

3.5.1. Design and selection of a single guide RNA

sgRNAs were designed using CHOPCHOP guide design web tool (<https://chopchop.cbu.uib.no>)²²⁸. All sgRNA designs were also evaluated by standard guide RNA design considerations before chosen for experiments²²⁹. Two sgRNAs were

selected for each target gene, that are described in Table 2. TrueGuide™ sgRNA Negative Control, non-targeting 1 (#A35526, Thermo Fisher) was included as a negative control.

Table 2. Selected sgRNA sequences.

Gene ID	Sequence (5'→ 3')	
<i>SOCS3</i>	sgRNA 1	AGCCTATTACATCTACTCCGGGG
	sgRNA 2	CGGATCAGAAAGGTGCCGGCGGG
<i>SIK1</i>	sgRNA 1	TGGGTTTTACGACATCGAGCGG
	sgRNA 2	CGCCATGTAAGTGTCCCCGGGGGG
<i>DUSP1</i>	sgRNA 1	TACTAGCGTCCCTGACAGCGCGG
	sgRNA 2	CGTCCAGCAACACCACGGCGTGG

3.5.2. Cells transfection with sgRNAs and Cas9

Once the sgRNA were designed, various methods were tested to introduce the sgRNA and the Cas9 nuclease into hADMSCs (lentiviral infection, plasmid transfection, electroporation with ribonucleoprotein...). The most efficient one was the electroporation, that is detailed below.

hADMSC were electroporated with sgRNA and Cas9 ribonucleoprotein (RNP) using Neon Transfection system (1300 V, 20 ms, two pulses) 10 µL Kit (Invitrogen). Before electroporation, 12 pmol/reaction of TrueCut™ Cas9 protein v2 (Thermo Fisher) and 48 pmol/reaction of sgRNA (ratio 1:2) were mixed in buffer R and incubated for 20 minutes at r. t. to form a RNP complex.

Cells were harvested and dissolved in buffer R and then mixed with the RNP complex. 100.000 cells were transfected in each electroporation reaction. After transfection, cells were plated into a 75 cm² cell culture flask and cultured as previously described.

3.6. Assessment of genomic mutation efficiency

hADMSC genomic DNA (gDNA) was isolated, sequenced and analyzed in order to determine the efficiency of the sgRNAs.

3.6.1. Genomic DNA isolation

gDNA from control and knockout cells was isolated using DNeasy Blood & Tissue Kit (#69504, Qiagen) following manufacturer's protocol. In brief, cells were cultured in 48-well plates and lysed with 200 µl of lysis buffer containing 20 µl proteinase K. Then, samples were transferred to vials and 200 µl of buffer AL were added. After that, 200 µl of 100% ethanol were added and mixed thoroughly by vortexing. Subsequently, the mixture was pipetted into the DNeasy Mini spin column placed in a 2 ml collection tube and centrifuged at ≥ 6000 g for 1 min. The flow-through was discarded and 500 µl of buffer AW1 were added to the column, that was then centrifuged for 1 min at ≥ 6000 g. The flow-through was discarded again and 500 µl of buffer AW2 were added to the column, that was then centrifuged for 3 min at 20000 g to dry completely the DNeasy membrane. Finally, the DNeasy Mini spin column was placed in a clean vial and DNA was eluted with 200 µl of buffer AE.

The concentration and purity of the gDNA were determined by measuring absorbance at 260/280 nm and 260/230 nm using a Nanodrop 2000 (Thermo Fisher).

3.6.2. PCR

PCR amplification of the target sequences was carried out with specific primers designed 200-300 pb upstream and downstream (forward and reverse primers, respectively) of the sgRNA binding site to ensure the amplification of the edited sequence. Primer sequences are described in Table 3. PCR reaction was performed with 10 ng gDNA, 0.005 U Q5 High-Fidelity DNA Polymerase (#M0491, NEB), 5X Q5 Reaction Buffer, 10 mM dNTPs and 10 µM primers. PCR conditions were: 30 s at 98 °C, followed by 25 cycles of 10 s at 98 °C, 30 s at annealing temperature specified in Table 3 for each primer couple (Tm) and 30 s at 72 °C, and 2 min at 72 °C.

3.6.3. Sanger sequencing

PCR products were purified using QIAquick PCR Purification Kit (#28104, Qiagen) and 50 ng of PCR products were Sanger sequenced using the forward amplification primers. Primers were designed 200-300 pb upstream of the edit site, resulting in a read where the first hundred base pairs are of high quality and the following bases are potentially mixed in modified cells (indicating an edited population with heterogeneous outcomes).

Table 3. Sequences of primers used to amplify edited region of genomic DNA.

Gene ID	sgRNA		Sequence (5'→ 3')	Tm
<i>SOCS3</i>	1	Forward Reverse	CGCCACTTCTTCACGCTCAG TCCTGGTTGGCTTCTTGTGC	69
<i>SOCS3</i>	2	Forward Reverse	CCACACTCCTGGAGACCTAAC GAGGAGGGTTCACTAGGTGG	68
<i>SIK1</i>	1	Forward Reverse	TCTATGAGAGCGGGTCCGTG TCTGAGTCCATGAACCACACTGC	68
<i>SIK1</i>	2	Forward Reverse	TTGTGTCTCTCCAACGCAGC AAAGGCAAGCCACCACATCACG	69
<i>DUSP1</i>	1	Forward Reverse	TTGGCTTGTTGGCTCTGG AGCAAGTTCATTCGTAGAGC	66
<i>DUSP1</i>	2	Forward Reverse	CAGACAAAGAGCACCGCAGG ATAAAATGTACTCCAGCGCCCAC	68

3.6.4. ICE analysis

Sanger sequence results were analyzed using the Syntego Inference of CRISPR Edits (ICE) software tool (<https://ice.synthego.com/#/>, last accessed 30 September 2023), that generates different editing proposals using the control sample, and uses regression to compute how much of each editing outcome is observed in the mixed Sanger read²³⁰.

3.7. Gene expression analysis

3.7.1. RNA isolation

Total RNA was isolated from frozen biopsies of scWAT as well as cell cultures using TRIzol (#T9424, Sigma Aldrich) according to the manufacturer's protocol. To lysate AT fractions, 1 ml of TRIzol per sample was added to a homogenizer, while 1 ml of TRIzol per 10 cm³ of plate and a scraper were used for cell cultures.

Cell lysates or tissue disaggregates were transferred to a vial and incubated 5 min at r. t. to dissociate nuclear components. Then, 0.2 ml of 100% chloroform/ml of TRIzol was added. It was vigorously shaken, incubated for 15 min at r. t. and centrifuged for 15 min at 12000 g and 4 °C.

After centrifugation, three phases were generated. The aqueous phase containing the ribonucleic acids was isolated and 0.5 ml of 100 % isopropanol were added to precipitate the RNA. It was mixed, incubated for 10 min on ice and then centrifuged at 12000 g for 15 min at 4 °C. Subsequently, supernatant was removed by decanting and the nucleotide pellet was resuspended in 1 ml of 75% ethanol for washing. The pellet was homogenized and centrifuged at 7500 g for 5 min and 4 °C. The supernatant was then removed and the pellet was dried for 5 minutes at r. t. Finally, the RNA was resuspended in DEPC water. To remove genomic DNA residues, all the RNA samples were treated with RNase-Free DNase (Life Technologies). The concentration and purity of the RNA were determined by measuring absorbance at 260/280 nm and 260/230 nm using a Nanodrop 2000 (Thermo Fisher). The quality of the extracted RNA was visualized in an agarose gel.

3.7.2. RNA retro-transcription

RNA was reverse-transcribed using PrimeScript Reverse Transcriptase (Takara Bio), 500 ng of RNA were used per reaction in a total volume of 10 µl. An Applied Biosystems 2720 Thermal Cycler was used with the following protocol: 25 °C for 10 min, 37 °C for 2 h and 85°C for 5 min.

3.7.3. Real-time PCR

10 ng of the cDNA product was amplified by real-time PCR in a total volume of 15 µl per reaction with SYBR Select Master Mix (Applied Biosystems), adding 0.5 µl of gene-specific primers at 10 µM. Primers used are specified in Table 4. cDNA amplification was conducted in StepOnePlus system (Applied Biosystems), using a protocol as follows: 95°C for 10 min, 40 cycles of 15 sec at 95°C and 1 min at 60°C, 15 sec at 95°C, 1 min at 60°C, and 15 sec at 95°C. Relative gene expression was normalized to β-actin expression using the $2^{-\Delta\Delta CT}$ method.

Table 4. List of primers used for qPCR.

Gene ID	Sequence (5'→ 3')	
<i>ACTIN</i>	Forward	CATGTACGTTGCTATCCAGGC
	Reverse	CTCCTTAATGTCACGCACGAT
<i>CCDC3</i>	Forward	TGACTGGAAATCCAGGAAGA
	Reverse	CGTGGTCCTCCTCAAAC

<i>CDKNIA</i>	Forward	ACATCGCCAAGGAAAAACGC
	Reverse	GTCTGTTCGGTACTGTCATCC
<i>CTGF</i>	Forward	CTTGCAGACTGACCTGGAAG
	Reverse	CCGTCGGTACATACTCCACAGA
<i>DUSP1</i> (first exon)	Forward	TTCTTCCTCAAAGGAGGATACG
	Reverse	GTGGGGTACTGCAGGAACGT
<i>DUSP1</i> (last exon)	Forward	ACCACCACCGTGTCAACTT
	Reverse	AGAGGTCGTAATGGGGCTCT
<i>FABP4</i>	Forward	ACTGGGCCAGGAATTGACG
	Reverse	CTCGTGGAAAGTGACGCCTT
<i>GADD45B</i>	Forward	TGCTGTGACAACGACATCAAC
	Reverse	GTGAGGGTTCGTGACCAGG
<i>ISM1</i>	Forward	CTTCCCCAGACCGCGATT
	Reverse	CGACCACCTCTATGGTGACCT
<i>PPARG</i>	Forward	AGATGACAGCGACTTGGCAAT
	Reverse	ACTCAGGGTGGTCAGCTTC
<i>SIK1</i> (first exon)	Forward	GCTTCTGAACCATCCACACAT
	Reverse	GTGCCCGTTGGAAGTCAAATA
<i>SIK1</i> (last exon)	Forward	GCTCAAGGAGTATCGGAATGC
	Reverse	AGCAAGGCAGGTGGAAAG
<i>SOCS3</i> (first exon)	Forward	GTCCCCCCCAGAACAGAGCCTATT
	Reverse	TTGACGGTCTTCCGACAGAGAT
<i>SOCS3</i> (last exon)	Forward	CCATTGGGAGTTCTGGAC
	Reverse	TTGGCTTCTTGCTTGTGC
<i>S100A9</i>	Forward	TCGGCTTGACAGAGTGCAGA
	Reverse	TGCCAGCTCACAGAGTA
<i>S100A12</i>	Forward	TTCCTGTGCATTGAGGGGTTA
	Reverse	TTAATGCCCTCCGAAC TGAG

3.7.4. AmpliSeq transcriptome analysis

RNA samples were quantitated using the Qubit RNA high-sensitivity (HS) assay kit (#Q32855, ThermoFisher) and the Qubit 3.0 fluorometer (ThermoFisher). RNA integrity was checked by the 2200 TapeStation system (Agilent) with the High Sensitivity RNA ScreenTape (5067–5579, Agilent). All samples had an RNA integrity number (RIN) > 7. RNA (20 ng) was converted to cDNA using the SuperScript IV VILO Master Mix (#11756050, ThermoFisher) and automated library preparation was carried out with the Ion AmpliSeq transcriptome human gene expression panel Chef-ready kit (#A31446,

ThermoFisher) on the Ion Chef Prep station, chef package version IC.5.4.0 (ThermoFisher).

Sequencing was performed *per* the manufacturer's protocols using the Ion 540 Kit-Chef (# A30011, ThermoFisher) on the Ion Torrent S5-XL (ThermoFisher). Eight samples *per* 540 chip were sequenced obtaining 7.5 to 10 million reads/sample.

Next, bam files were further processed using the Ion AmpliSeq RNA plugin v5.4.01 on the Torrent Server (Torrent Suite Software, v5.4, ThermoFisher) to obtain normalized reads *per* kilobase of transcript *per* million reads mapped (RPKM). A principal component analysis (PCA) method was adopted to identify potential outliers among the samples²³¹.

3.8. Protein analysis

3.8.1. Protein isolation

Proteins were isolated from cell culture and human scWAT biopsies using RIPA lysis buffer (50 nm TRIS, 150 mM NaCl, 1 % Igepal (#I8896, Sigma Aldrich), 0.5 % sodium deoxycholate (#49647, Sigma Aldrich), 0.01 % SDS (#BP-166-100, Thermo Fisher), pH 8). For cell culture proteins isolation, cells were grown in 6-well plates. Culture media was removed and cells were washed with DPBS. To lysate the cells, 100 µl of RIPA buffer per well was added and cultures were incubated for 20 min at 4 °C with agitation. Subsequently, a scraper was used to mechanically lysate the cells. To isolate proteins from AT biopsies, a cell homogenizer was used. 500 µl of RIPA buffer were added to the AT fractions and the homogenizer disaggregated the samples until a homogeneous lysate was obtained. The cellular lysates and tissue disaggregates were then transferred to a vial and centrifuged for 5 min at 15000 rpm at 4°C. The supernatant was stored, discarding the biological membranes and other cellular debris contained in the pellet.

3.8.2. Protein quantification

The protein concentration of the samples was measured with the colorimetric Kit Pierce™ BCA Protein Assay (#23225, Thermo Fisher Scientific). Bovine serum albumin (BSA) (#49647, Sigma Aldrich) at different concentrations, ranging from 25 to 2000 µg/ml, was used as standard curve. To perform the assay, 5 µl of each standard or unknown sample

were pipetted in replicate into a 96-well plate. Then, 200 µl of BCA reagent, previously prepared according to the manufacturer's instructions by mixing reagents A and B (50:1), were added to each well. The reaction was incubated for 30 minutes at 37 °C and measured by absorbance at 562 nm in a Synergy HT plate reader. The absorbances were interpolated to the albumin standard curve to determine the concentrations of the unknown samples.

3.8.3. Sodium dodecyl sulfate-polyacrylamide gel electrophoresis

For analysis of proteins expression, aliquots of cellular lysates, tissue disaggregates or human serum were subjected to reducing sodium dodecyl sulfate-polyacrylamide gel electrophoresis (SDS-PAGE). A Mini-PROTEAN® Tetra System was used for the electrophoretic separation of proteins.

To prepare protein samples, 20 to 80 µg of protein were mixed with 4X Laemmli buffer (125 mM Tris-HCl, 40 % Glycerol, 4 % SDS, 0.05 % bromophenol blue (#B/P620/44, Thermo Fisher) 10 % β-Mercaptoethanol (#M-6250, Sigma Aldrich), pH 6,8) in a total volume of 25 µl and were boiled at 95 °C for 5 min.

Subsequently, 12% polyacrylamide gels were placed in the electrophoresis cuvette and electrophoresis buffer (25 mM Tris-HCl, 0.192 M Glycine, 1 % SDS (#BP-166-100, Thermo Fisher), pH 8.3) was added. Then, prepared samples were loaded into the wells.

Electrophoresis was performed by setting the PowerPac™ Basic Power Supply for 10 minutes at 90 volts to concentrate all proteins to the same level. The power was then increased to 120 volts for 1 hour and 30 minutes for electrophoretic separation.

3.8.4. Western blot

After electrophoresis, the proteins in the gel were transferred to a polyvinylidene difluoride membrane (PVDF) for immunodetection. The gel and the PVDF membrane, previously activated with 100 % methanol, were placed in the transfer cassette. Subsequently, the cassette was inserted into the cuvette of the Mini-PROTEAN® Tetra System and filled with transfer buffer (25 mM Tris-HCl, 0.192M de Glycine, 10 % methanol). The power supply was programmed to maintain an amperage of 400 millamps for 2 hours.

After transfer, PVDF membranes were blocked with 5% dry skimmed milk for 2 h under agitation at r. t. The blocking solution was then removed, and membranes were washed with TPBS (0.2 % Tween20 (#P1379, Sigma Aldrich) in PBS 1X) and probed with primary antibody against different proteins overnight at 4 °C with mild shaking. Different concentrations for each antibody were used, depending on the abundance of the protein in the sample and the specificity of the antibody, that are specified in Table 5.

Table 5. List of antibodies used.

Protein	Primary antibody	Dilution	Secondary antibody	Dilution
β-Actin	SC-47778	1:1000	mouse Ab, SC-525409	1:20000
AFABP	SC-271529	1:1000	mouse Ab, SC-525409	1:20000
DUSP1	SC-373841	1:500	mouse Ab, SC-525409	1:20000
GADD45B	ORB-215494	1:500	rabbit Ab, SC-2357	1:5000
ISM1	PA5-24968	1:1000	rabbit Ab, SC-2357	1:5000
SIK1	1045-1-AP	1:500	rabbit Ab, SC-2357	1:5000
SOCS3	SC-51699	1:500	mouse Ab, SC-525409	1:20000

After incubation, primary antibody was removed and membranes were washed three times for 10 min with TPBS. Finally, membranes were incubated with peroxidase-conjugated secondary antibodies for 1 h at r.t. with mild shaking and washed with TPBS. The results were visualized using Novex® ECL Chemiluminescent Substrate Reagent.

3.8.5. ELISA

To determine novel adipokines concentration in human plasma, ELISA kits were used (Table 6). First, selected plasma samples were diluted according to the concentration of target protein in the test sample to be in the optimal detection range of the kit.

Table 6. List of ELISA Kits used. ISM1, Isthmin 1; CCDC3, Coiled-Coil Domain Containing 3.

Protein	Ref.	Plasma dilution
ISM1	#EH4520, Fine Test	1:50
CCDC3	#EH0082, Fine Test	1:2

100 µl of diluted samples as well as standards were pipetted into the ELISA plate and incubated at 37 °C for 90 min. Then, the plate content was discarded and washed two times with wash buffer. Subsequently, 100 µl of biotin-labeled antibody working solution per well were added, plate was incubated at 37 °C for 60 min and then washed three times with wash buffer. After that, 100 µl of HRP-Streptavidin Conjugate (SABC) working solution were added, plate was incubated 37°C for 30 min and washed five times. To visualize the result, 90 µl of 3,3'-5,5'-Tetramethylbenzidine (TMB substrate) were added, incubated at 37°C in dark within 10-20 min and 50 µl of stop solution was added. The color turned yellow immediately and absorbance was measured at 450 nm in a Synergy HT plate reader.

3.9. Cell characterization assays

3.9.1. Cellular staining

3.9.1.1. *Oil Red O staining*

To quantify intracellular lipid in hMSC-derived adipocytes, Oil Red O staining was used. First, culture media was removed and cells were washed with DPBS (#17-512F, Lonza). To fix adipocytes, 10% formalin was added and incubated for 30 min at r. t. Then, cells were gently washed with 60% isopropanol twice and were stained with Oil Red O working solution (2.1 mg/ml Oil Red O in dH₂O). Cells were incubated with staining solution during 30 min at r. t. with mild shaking. After that, Oil Red O solution was removed and cells were washed with dH₂O three times.

To visualize stained lipid droplets, an inverted microscope (AE31, Motic) was used. After visualization, staining was quantified adding 100% isopropanol, incubating for 10 min with gentle shaking and measuring the extracted dye at 510 nm in a plate spectrophotometer (Sinergy HT, Biotek).

3.9.1.2. *Fluorescent staining*

To perform fluorescent staining assays, culture media was removed and cells were fixed with 4% paraformaldehyde (PFA) for 15 min at r. t. Then, PFA was removed and cultured cells were washed twice with DPBS. To stain nuclei and intracellular lipid accumulation, Hoechst 33342 (#H21492, Life Technologies) diluted 1:5000 and 4,4-Difluoro-1,3,5,7,8-

Pentamethyl-4-Bora-3a,4a-Diaza-s-Indacene (BODIPY 493/503) (#D-3922, Life Technologies) diluted 1:1000 were used, respectively. Cells were incubated with the dyes for 15 min and then washed four times with DPBS.

Images were acquired using an Axio Observer.Z1 inverted fluorescence microscope (Zeiss) and the AxioVision software; while quantification was performed using the Cell Insight CX5 High Content Screening (HCS) Platform.

3.9.2. Lipid metabolic assays

Lipid metabolic assays were performed in hMSC-derived adipocytes using radiolabeled isotopes. Lipolysis, *de novo* lipogenesis and FAs uptake were measured in adipocytes as follows.

3.9.2.1. Lipolysis

Cells were cultured and differentiated in 24-well plates to perform lipolysis assay. First, adipocytes were incubated overnight with 1 nCi/ μ l [9,10-³H(N)]-palmitic acid (#NET043005MC, Perkin-Elmer). Then, cells were washed with DPBS (#17-512F, Lonza) to remove the labeled palmitic acid not taken up by the adipocytes. To quantify basal, isoprenaline-stimulated, and insulin-inhibited lipolysis, cells were then incubated with serum-free DMEM containing 2% BSA (Sigma) without or with 10 μ M isoprenaline (Reig Jofre) or 1 μ M insulin (Novo Nordisk), respectively. After four hour of incubation, conditioned media was collected. To measure labeled FA release, 500 μ l of medium was added to 2 ml of scintillation liquid Ultima Gold (#6013326, Perkin-Elmer). It was homogenized and radioactivity was measured using Rackbeta liquid scintillation counter (Tri-Carb 2560 TR/XL, Packard).

3.9.2.2. De novo lipogenesis

Cells were cultured and differentiated in 24-well plates to perform *de novo* lipogenesis assay. Adipocytes were incubated overnight with 1 nCi/ μ l [³H]-acetic acid (#NET003005MC, Perkin-Elmer). After incubation time, cells were washed, lipids were extracted, and cells were lysed. Lipids extraction was performed by incubating cells with isopropanol 100% for 1 h at 4 °C with mild shaking. The supernatant was then collected and centrifuged at 1,000 rpm for 5 min at r. t. The upper organic phase containing the lipid cellular fraction was collected, and radioactivity was measured. Isotopes were

analyzed in a Rackbeta liquid scintillation counter (Tri-Carb 2560 TR/XL, Packard) after adding Ultimate Gold scintillate (Perkin-Elmer). Cells were lysed with a lysis buffer (0.2 N of NaOH, 0.1% SDS), and protein concentration was quantified using a Pierce BCA protein assay kit. Results were normalized to cellular protein.

3.9.2.3. Fatty acids uptake

Cells were cultured and differentiated in 24-well plates to perform FAs uptake assay. First, adipocytes were incubated overnight with 1 nCi/ μ l [9,10-3H(N)]-palmitic acid (#NET043005MC, Perkin-Elmer). Then, media was removed and adipocytes were incubated with proliferation media without or with 1 μ M insulin (Novo Nordisk) for two hours to determined basal and stimulated uptake, respectively. After incubation time, cells were washed, lipids were extracted, and cells were lysed. Lipids extraction was performed by incubating cells with isopropanol 100% for 1 h at 4 °C with mild shaking. The supernatant was then collected and centrifuged at 1,000 rpm for 5 min at r. t. The upper organic phase containing the lipid cellular fraction was collected, and radioactivity was measured. Isotopes were analyzed in a Rackbeta liquid scintillation counter (Tri-Carb 2560 TR/XL, Packard) after adding Ultimate Gold scintillate (Perkin-Elmer). Cells were lysed with a lysis buffer (0.2 N of NaOH, 0.1% SDS), and protein concentration was quantified using a Pierce BCA protein assay kit. Results were normalized to cellular protein.

3.10. Statistical analysis

Results are expressed as means \pm standard error of the mean (SE) or median [interquartile range]. Pairwise group comparisons were calculated using Student's t test for Gaussian-distributed variables and Mann–Whitney U test for non-Gaussian-distributed data. The statistical analysis was performed using R version 4.0.3 (<http://www.r-project.org>), and the significance level was set at 0.05. Every assay was carried out in at least three independent experiments.

3.10.1. Differential gene expression analysis

Differential expression analysis was performed with the edgeR R package (v. 3.40.02)²³². Briefly, samples were normalized using a weighted trimmed mean of M-values (TMM) and fitted to a quasi-likelihood negative binomial generalized log-linear model followed

by empirical Bayes quasi-likelihood F-tests. Genes with log₂ fold changes [$|\log_2(\text{FC})| \geq 1$] and Benjamini and Hochberg false discovery rates (FDR) < 0.001 were classified as differentially expressed genes (DEGs)²³³.

3.10.2. Gene ontology enrichment analysis

DEGs were then tested for enrichment of gene ontology (GO): biological processes (BP) terms using the clusterProfiler R package (v. 4.6.2)²³⁴. A minimum size of three genes was used for the functional enrichment. GO: BP terms with q value < 0.05 were considered enriched.

3.10.3. Construction of weighted gene co-expression networks and identification of modules

Gene co-expression network analysis was performed with the R package WGCNA¹⁶ using RNA-seq and clinical data from the discovery cohort. Genes with low variance (<25%) or low levels of expression (average < 5 RPKM) were excluded from the analysis. Sample clustering was also performed to detect outliers.

Scale independence and mean connectivity analysis of modules with different power values were performed to determine the soft threshold of module analysis. The power value was determined when the scale independence value was >0.9. Then, the adjacency matrix was calculated using the determined power value to ensure an unsigned scale-free network. Minimal module size and merge cut height were set at 30 and 0.25 respectively. A clustering dendrogram of genes, with dissimilarity based on topological overlap, was generated. Next, we identified modules that were significantly associated with the measured clinical trait by correlating eigengenes with the fatty liver index.

4. RESULTS

4.1. Chapter I

Isthmin-1 (ISM1), a novel adipokine that reflects abdominal adipose tissue distribution in individuals with obesity

The contents of this chapter have been adapted from the following published work:

Lopez-Yus, Marta *et al.* “Isthmin-1 (ISM1), a novel adipokine that reflects abdominal adipose tissue distribution in individuals with obesity.” *Cardiovascular diabetology* vol. 22, 1 335. 8 Dec. 2023, doi:10.1186/s12933-023-02075-0

Isthmin-1 (ISM1), a novel adipokine that reflects abdominal adipose tissue distribution in individuals with obesity

Marta Lopez-Yus^{1,2}, Carmen Casamayor^{2,3}, Juan Jose Soriano-Godes⁴, Sofia Borlan^{2,3}, Yolanda Gonzalez-Irazabal^{2,5}, Maria Pilar Garcia-Sobreviela^{1,2}, Beatriz Garcia-Rodriguez^{2,5}, Raquel del Moral-Bergos^{1,2}, Pilar Calmarza^{2,4,6}, Jose Maria Artigas⁷, Silvia Lorente-Cebrian^{1,2,8}, Vanesa Bernal-Monterde^{2,9}, Alejandro Sanz-Paris^{2,10}, Jose M. Arbones-Mainar^{1,2,11}

¹ Adipocyte and Fat Biology Laboratory (AdipoFat), Translational Research Unit, University Hospital Miguel Servet, Instituto Aragonés de Ciencias de la Salud (IACS)

² Instituto de Investigación Sanitaria (IIS) Aragón, 50009 Zaragoza, Spain

³ Endocrine, Bariatric and Breast Surgery Unit, General and Digestive Surgery Department, Miguel Servet University Hospital, Zaragoza, Spain

⁴ Department of Radiology, Royo-Villanova Hospital, Zaragoza, Spain

⁵ Clinical Biochemistry Department, Miguel Servet University Hospital, Zaragoza, Spain

⁶ CIBER Enfermedad Cardiovascular (CIBERCV), Instituto Salud Carlos III

⁷ Department of Radiology, Miguel Servet University Hospital, Zaragoza, Spain

⁸ Departamento de Farmacología, Fisiología y Medicina Legal y Forense, Universidad de Zaragoza, Zaragoza, Spain. Instituto Agroalimentario de Aragón (IA2) (Universidad de Zaragoza-CITA), Zaragoza

⁹ Gastroenterology Department, Miguel Servet University Hospital, Zaragoza, Spain

¹⁰ Endocrinology and Nutrition Department, Miguel Servet University Hospital, Zaragoza, Spain

¹¹ CIBER Fisiopatología Obesidad y Nutrición (CIBERObn), Instituto Salud Carlos III, Madrid, Spain

ABSTRACT

Background: The assessment of obesity-related health risks has traditionally relied on the Body Mass Index and waist circumference, but their limitations have propelled the need for a more comprehensive approach. The differentiation between visceral (VIS) and subcutaneous (SC) fat provides a finer-grained understanding of these risks, yet practical assessment methods are lacking. We hypothesized that combining the SC-VIS fat ratio with non-invasive biomarkers could create a valuable tool for obesity-related risk assessment.

Methods and results: A clinical study of 125 individuals with obesity revealed significant differences in abdominal fat distribution measured by CT-scan among genders and distinct models of obesity, including visceral, subcutaneous, and the SC/VIS ratio. Stratification based on these models highlighted various metabolic changes. The SC/VIS ratio emerged as an excellent metric to differentiate metabolic status. Gene expression analysis identified candidate biomarkers, with ISM1 showing promise. Subsequent

validation demonstrated a correlation between ISM1 levels in SC and plasma, reinforcing its potential as a non-invasive biomarker for fat distribution. Serum adipokine levels also correlated with the SC/VIS ratio. The Receiver Operating Characteristic analysis revealed ISM1's efficacy in discriminating individuals with favorable metabolic profiles based on adipose tissue distribution. Correlation analysis also suggested that ISM1 was involved in glucose regulation pathways.

Conclusion: The study's results support the hypothesis that the SC-VIS fat ratio and its derived non-invasive biomarkers can comprehensively assess obesity-related health risks. ISM1 could predict abdominal fat partitioning and be a potential biomarker for evaluating obesity-related health risks.

Keywords: CT-Scan, biomarker, subcutaneous fat, expandability

1. INTRODUCTION

The Body Mass Index (BMI) and waist circumference have been widely used to assess obesity, but their limitations have prompted calls for a more comprehensive approach. BMI's sole reliance on weight and height overlooks variations in body composition, potentially misclassifying muscular individuals as obese. Similarly, while considering fat distribution, waist circumference, and waist/hip ratio can be limited as they cannot adequately differentiate between subcutaneous and visceral fat, which is crucial for assessing obesity-related health risks.

White visceral adipose tissue (visWAT), located within the abdominal cavity and intertwined with vital organs, is associated with cardiovascular disease, type 2 diabetes (T2DM), hypertension, and fatty liver (1–3). It can release pro-inflammatory mediators, contributing to these health risks (4). In contrast, subcutaneous fat (scWAT), found just beneath the skin's surface, while still contributing to overall body fat, is less metabolically active and does not pose a metabolic threat (5–7). This differentiation between visceral and subcutaneous fat provides a finer-grained understanding of an individual's obesity-related health risks. It is hence of paramount importance the evaluation of the quantity and distribution of fat in the body. Consequently, focusing on this ratio would be valuable in identifying individuals at higher risk and tailoring interventions to lower morbidity and mortality rates.

However, the challenge lies in implementing this assessment. Imaging techniques, such as magnetic resonance imaging (MRI), computed tomography (CT), and dual-energy x-ray absorptiometry (DXA), provide accurate results but are often complex and impractical in many clinical settings. In this context, non-invasive biomarkers come into play. These indicators, like specific adipokines or hormonal markers, can be measured in blood or urine samples. By measuring these biomarkers, clinicians could estimate the subcutaneous-visceral fat ratio without the need for sophisticated analysis.

Adipokines such as adiponectin and leptin have been associated with fat distribution patterns and metabolic health (8, 9). However, the current knowledge of these adipokine concentration variations is still unable to explain the heterogeneity of metabolic risk. Therefore, there is still a need to identify a promising biomarker that appropriately reflects the adipose tissue distribution and, consequently, the metabolic status of an individual.

We hypothesize that by combining the concept of the subcutaneous-visceral fat ratio with non-invasive biomarkers, we can create a powerful tool to assess obesity-related health risks comprehensively and practically. This approach would enable healthcare professionals to identify at-risk individuals more effectively, allowing for timely interventions and enabling personalized medicine in obesity. Accordingly, the objectives of this study are twofold: We aim to 1) investigate the relationship between abdominal adipose components (scWAT and visWAT) and metabolic dysfunction associated with obesity and 2) identify non-invasive biomarkers associated with abdominal adipose distribution that do not require the use of advanced imaging techniques.

2. MATERIALS AND METHODS

2.1. Human samples and cohort description

Individuals with obesity were recruited at either the Miguel Servet University Hospital (HUMS, Zaragoza, Spain) or the Royo-Villanova Hospital (HRV, Zaragoza, Spain) as described previously (10). Briefly, all patients scheduled for elective bariatric surgery were offered the opportunity to participate in the study by donating blood, biopsies of subcutaneous and visceral adipose tissue, and undergoing a computerized tomography (CT) scan for the quantitative determination of subcutaneous and visceral abdominal fat depots. All patients provided written consent and the study was approved by the Regional Institutional Review Board of Ethics at Aragón, Spain (CEIC-A). Samples and data from patients included in this study were provided following standard operating procedures by the Biobank of the Aragon Health System (PT20/00112), integrated into the Spanish National Biobanks Network.

2.2. Determination of abdominal fat distribution

The visceral and subcutaneous fat areas were measured by CT with an 8 mm single slice at the umbilical level. All CT examinations were acquired with the subject positioned supine in a 64 detector CT scanner (Aquilion 64 Toshiba, Japan) and tube voltage set to 120 kVp with automatic tube current modulation and rotation time of 0.5 s. Acquired images were then transferred to a workstation and analyzed with the Vitrea CT Fat Measurement software (Vital Imaging Inc. The Netherlands). Selected fat densities ranged between -150 and -70 Hounsfield Units (HU) and the areas of the total

subcutaneous (SFA) and visceral fat (VFA) were measured in cm². SFA and VFA were respectively defined as pixels (area) located outside or inside the outer surface of the abdominal muscle wall. Subsequently, we calculated the ratio between subcutaneous fat area divided by the area of visceral fat area (SFA/VFA ratio).

2.3. Biochemical assays

C-reactive protein (CRP), glycated hemoglobin (Hb1Ac), cross-linked C-terminal telopeptide of type I collagen (CTX), triglyceride (TG), cholesterol associated with high-density lipoproteins (HDLc), non-esterified fatty acids (NEFA), gamma glutamyl transferase (GGT), alanine transaminase (ALT), and leptin were determined at the Clinical Biochemistry department at the HUMS using state of the art analyzers. All analyses were in compliance with the requirements for quality and competence (ISO 15189:2012) for medical laboratories. Homeostatic Model Assessment for Insulin Resistance (HOMA) was calculated as previously described (11).

Adiponectin, adiponisin, MCP-1 and resistin were measured using the LegendPlex immunoassay (Biolegend) by flow cytometry, following manufacturer's instructions. The process was carried out in the Cell Sorting and Cytometry Unit of the Aragonese Institute of Health Sciences (IACS). ISM1 and CCDC3 were determined by FineTest ELISA kits (refs. EH4520 and EH0082, respectively) according to the manufacturer's instructions (Fine Biotech Co.).

2.4. RNA isolation

Total RNA was isolated from frozen biopsies of scWAT and visWAT using TRIzol (Sigma) according to the manufacturer's protocol. All the RNA samples were treated with RNase-Free DNase (Life Technologies) to remove genomic DNA.

2.5. AmpliSeq human transcriptome analysis

RNA content was measured using the Qubit RNA high-sensitivity (HS) assay kit (#Q32855, ThermoFisher) with the Qubit 3.0 fluorometer (ThermoFisher). RNA integrity was checked by the 2200 TapeStation system (Agilent) with the High Sensitivity RNA ScreenTape (5067–5579, Agilent). All samples had an RNA integrity number (RIN) > 7. RNA (20 ng) was converted to cDNA using the SuperScript IV VILO Master Mix (#11756050, ThermoFisher) and libraries were made with the Ion AmpliSeq

transcriptome human gene expression panel (#A31446, ThermoFisher) on the Ion Chef Prep station (ThermoFisher).

Sequencing was performed using the Ion 540 Kit-Chef (# A30011, ThermoFisher) on the Ion Torrent S5-XL (ThermoFisher). Eight samples *per* 540 chip were sequenced, obtaining 7.5 to 10 million reads/sample. The entire sequencing process was carried out in the Genomics Unit of the Aragonese Institute of Health Sciences (IACS).

Next, bam files were processed using the Ion AmpliSeq RNA plugin v5.4.01 on the Torrent Server (Torrent Suite Software, v5.4, ThermoFisher) to obtain to obtain the count matrices. Differential expression analysis was performed with the edgeR R package (v. 3.40.02) (12). The gene expressions of the scWAT samples included in the first tertile were compared to the scWAT samples included in the third tertile. Briefly, samples were normalized using a weighted trimmed mean of M-values (TMM) and fitted to a quasi-likelihood negative binomial generalized log-linear model followed by empirical Bayes quasi-likelihood F-tests. Genes with \log_2 fold changes $|\log_2(\text{FC})| \geq 1$ and Benjamini and Hochberg false discovery rates (FDR, (13)) < 0.1 were classified as differentially expressed genes (DEGs).

2.6. RT-qPCR

RNA was reverse-transcribed using PrimeScript Reverse Transcriptase (Takara Bio). Real-time PCR was performed using the StepOnePlus system (Applied Biosystems). 2 μl of the cDNA product was amplified using gene-specific primers in a total volume of 15 μl *per* reaction with SYBR Select Master Mix (Applied Biosystems). Relative gene expression was normalized to $\beta\text{-ACTIN}$ expression using the $2^{-\Delta\Delta\text{Ct}}$ method. The following primers were used: *ISMI*-F, 5'-CTTCCCCAGACCGCGATT-3'; *ISMI*-R, 5'-CGACCACCTCTATGGTGACCT-3'; *CCDC3*-F, 5'-TGACTGGAAATCCAGGAAGA-3'; *CCDC3*-R, 5'-CGTGGTCCTCCTCAAAC-3'; *ACTIN*-F, 5'-CATGTACGTTGCTATCCAGGC-3'; *ACTIN*-R, 5'-CTCCTTAATGTCACGCACGAT-3'.

2.7. Western blot analysis

For analysis of protein expression, aliquots of serum or adipose tissue biopsies lysates were subjected to reducing sodium dodecyl sulfate-polyacrylamide gel electrophoresis (SDS-PAGE), using 12% polyacrylamide gels. Electrophoresis was carried out at 100

volts for 2 hours. Proteins were then transferred to polyvinylidene difluoride membranes (PVDF), which were blocked with 5% dry skimmed milk for 2 hours and probed with primary antibody against ISM1 or β -ACTIN overnight at 4 °C with mild shaking. The results were visualized using fluorophore-conjugated secondary antibodies that were incubated 1 hour at room temperature with mild shaking. Antibody used were: β -Actin (Santa Cruz #SC-47778) diluted 1:1000, ISM1 (Thermo Fisher #PA5-24968) diluted 1:1000, mouse secondary antibody (Thermo Fisher # A-11001) diluted 1:30000, rabbit secondary antibody (Thermo Fisher # A-) diluted 1:30000.

2.8. Statistical analysis

Boxplots were used to display the distribution and summary statistics. The line within the box indicates the median value, the box represents the interquartile range (IQR), and the whiskers extend from the edges of the box to the minimum and maximum values within 1.5 times the IQR. Data points beyond this range are plotted individually as points. Spearman correlation analysis was used to investigate the association between continuous variables. We calculated p-values for trends in ordered categories (tertiles) using the Pearson or the Spearman tests for normal- or non normal-distributed variables, respectively. We utilized Receiver Operating Characteristic (ROC) curves to assess the predictive power and discriminative ability of our classification model. We quantified the overall performance of our model by calculating the area under the ROC curve (AUC). The statistical analysis was performed using R version 4.0.3 (<http://www.r-project.org>) and the appropriate packages, p-values < 0.05 were considered significant.

3. RESULTS

3.1. Metabolic characterization of the different subtypes of obesity

This clinical study included 125 individuals with obesity. The median age was 49 yrs (range 20-66) and 57% were women. The median BMI and waist circumference were 42 kg/m² and 120 cm, respectively, with no observed sex-based differences in these parameters (as shown in Table 1). All participants underwent a CT-scan imaging test to determine abdominal fat distribution, measuring Subcutaneous Fat Area (SFA) and Visceral Fat Area (VFA). Significant disparities emerged in adipose partition, with women having higher subcutaneous fat and lower visceral adipose tissue than men.

Table 1. Clinical and biochemical characteristics of the subjects in the cohort. Data are median [interquartile range]. p: p-value for the sex differences (Mann-Whitney).

	[ALL] N=125	Men N=54	Women N=71	p
Age (years)	49.0 [41.0;56.0]	48.5 [45.0;58.0]	49.0 [40.0;54.0]	0.308
Body mass index (BMI, kg/m ²)	41.0 [35.9;44.6]	40.4 [35.9;44.5]	41.0 [36.3;44.5]	0.884
Waist circumference (cm)	120 [112;126]	122 [114;130]	120 [112;125]	0.335
Subcutaneous Fat Area (cm ²)	355 [248;478]	270 [205;375]	403 [310;494]	<0.001
Visceral Fat Area (cm ²)	239 [154;335]	332 [268;418]	190 [121;250]	<0.001

We categorized obesity into three distinct models based on the enlargement of adipose deposits: 1) Visceral obesity (classical android obesity) characterized by increased VFA and constant SFA, 2) Subcutaneous obesity (classical gynoid pattern) characterized by enlarged SFA and constant VFA, and 3) the SFA/VFA ratios, utilized to assess the propensity for visceral versus subcutaneous fat storage. We further divided these models into tertiles to facilitate comparisons among them. Notably, the first two types of obesity exhibited an increase in waist circumference across obesity tertiles, whereas the third type maintained a consistent waist circumference across tertiles (Fig. 1).

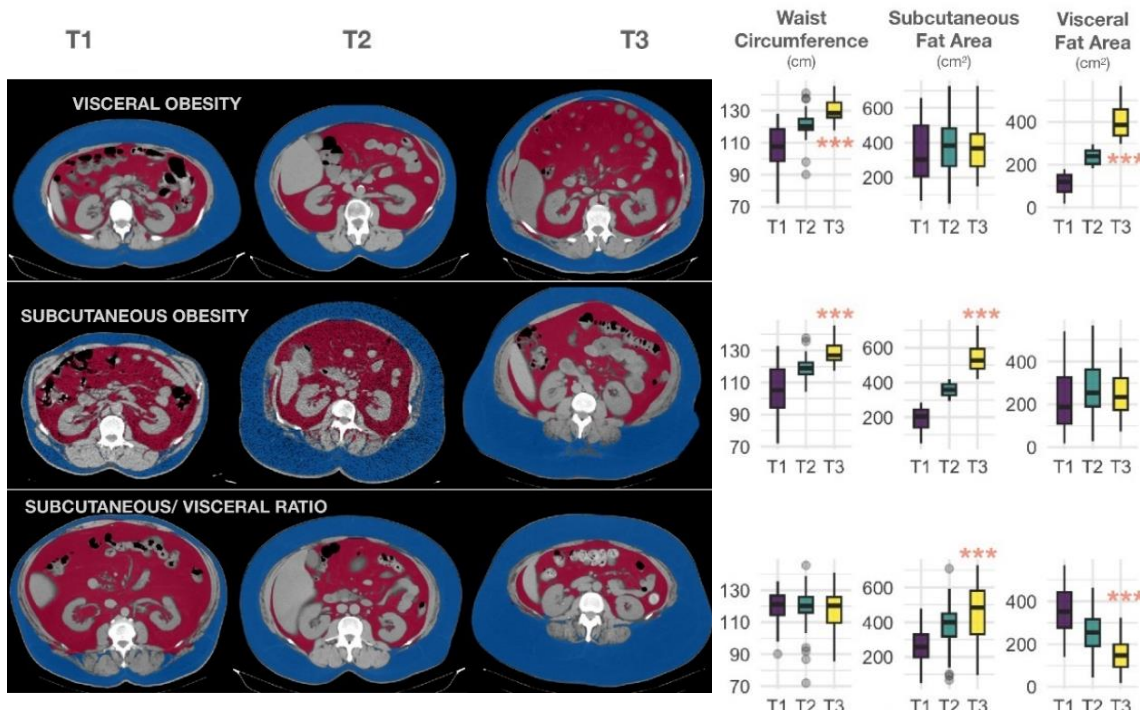


Figure 1. Representative CT scan of abdominal adipose tissue segmentation for each group of people with obesity, according to visceral, subcutaneous adipose tissue accumulation or subcutaneous/visceral ratio. Subcutaneous and visceral fat are colored in blue and red.

Clinical and biochemical parameters were measured and analyzed according to the different classifications of obesity (Fig. 2). Upon stratification based on visceral obesity, we noted a compromised metabolic profile characterized by markedly elevated HOMA index, Hb1Ac levels, and hepatic enzymes GGT and ALT across the tertiles. Conversely, there was a significant reduction in HDL cholesterol levels within these tertiles. When patients were stratified according to their subcutaneous fat content, we found increased CRP levels and lower CTx serum concentration across the SFA tertiles. Lastly, patient stratification according to the SFA/VFA ratio showed the most significant changes among tertiles. Subjects in the upper tertile presented significantly higher levels of CRP and HDL, while HOMA index, hemoglobin, CTx, triglycerides, and GGT were reduced (Figure 2). We also explored the association of SFA/VFA ratio with cardiometabolic traits in sex-adjusted logistic models. The ratio was associated with reduced odds ratios (ORs) for dyslipidemia (OR:0.370, CI95%: 0.125-0.816, p= 0.038), high blood pressure (OR: 0.321, CI95%: 0.126-0.652, p= 0.007), and type 2 diabetes (OR: 0.286, CI95%: 0.084-0.710, p=0.022). These results prove that the SFA/VFA ratio is an excellent metric to differentiate the metabolic status of individuals with similar perceived obesity (same BMI and same waist circumference in the three tertiles).

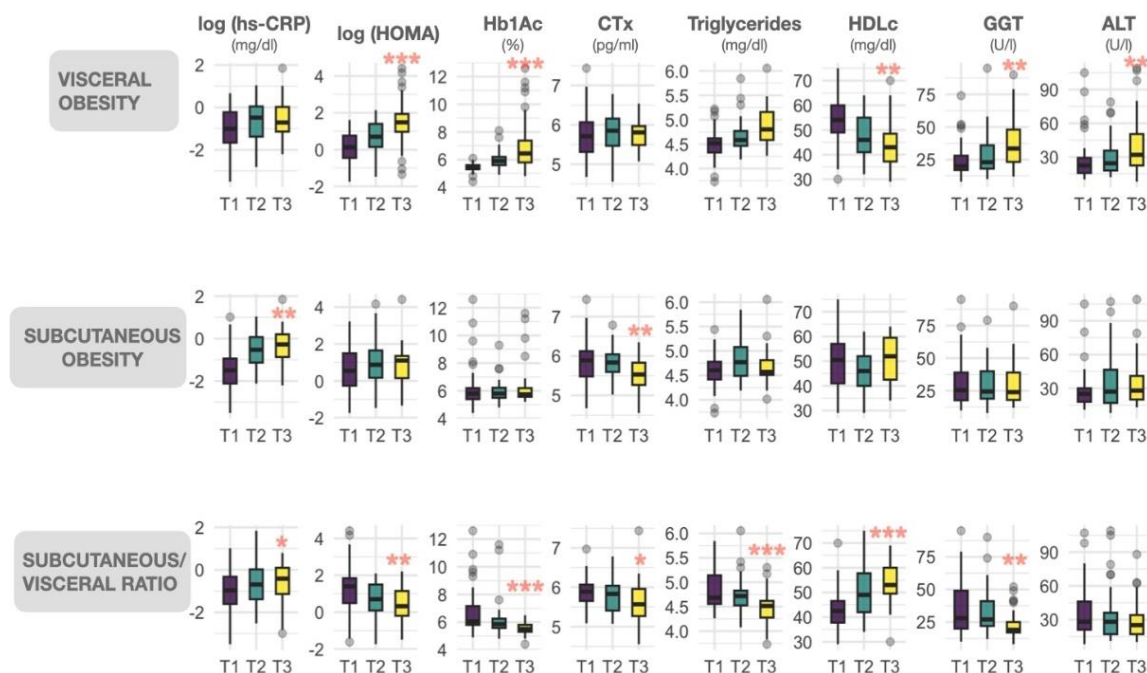


Figure 2. Morphometric and metabolic parameters in the lower, middle and upper tertiles of visceral and subcutaneous adipose tissue accumulation and subcutaneous/visceral ratio in people with obesity. Hs-CRP: high-sensitivity C-reactive protein, HOMA: homeostasis model assessment of insulin resistance, Hb1Ac: glycated hemoglobin, Ctx: cross-linked C-terminal telopeptide of type I collagen, TG: triglycerides, HDLc: high density lipoproteins, GGT: gamma glutamyl transferase, ALT: alanine transaminase. p for trend across tertiles: * <0.05 , ** <0.01 , *** <0.001

3.2. Identification of genes differentially expressed in subcutaneous adipose tissue according to the SFA/VFA ratio

To identify potential biomarkers that reflect the abdominal fat partitioning, we carried out a global gene expression analysis in scWAT biopsies from 45 donors using edgeR (12) and contrasting the lower tertile (T1) vs. the upper tertile (T3) of de SFA/SVA ratio. Ten differential expressed genes (DEGs) with false discovery rate (FDR) <0.1 were identified (Figure 3A). Four of them (*CCDC3*, *GRIP1*, *ISM1*, and *TRDN*) showed a positive association, increasing their expression as SFA/VFA ratio increased, while six of them (*CD9*, *FJX1*, *GATA6*, *IARS*, *MPZL2*, and *ZFY*) showed a negative association (Fig. 3B).

Among those DEGs, *CCDC3* and *ISM1* were genes encoding proteins previously reported to be secreted by adipose tissue. As our final goal was to find a non-invasive biomarker, these candidate genes were selected for subsequent analysis.

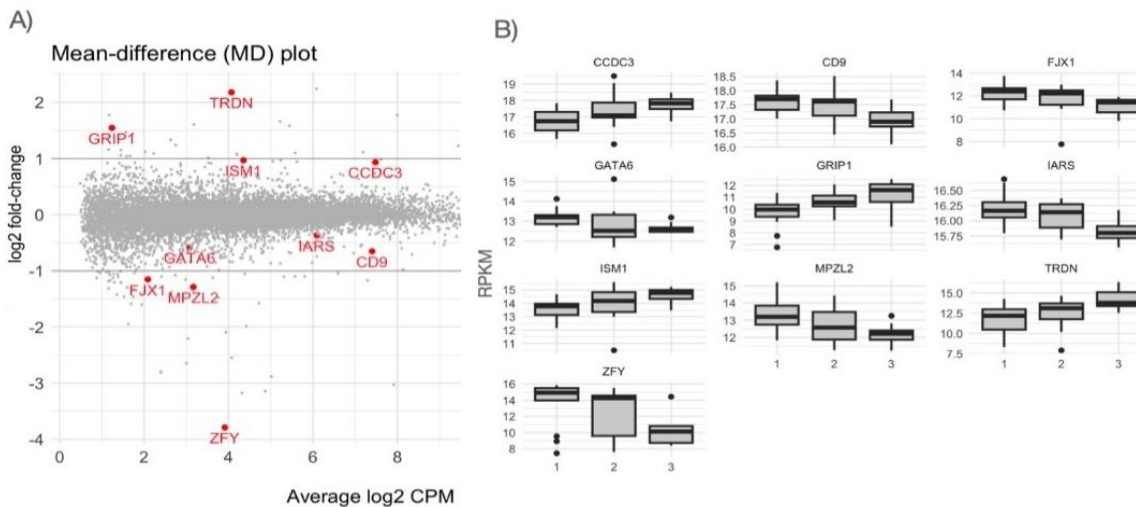


Figure 3. Genes differentially expressed in scWAT according to the SFA/VFA ratio. A) MD plot showing the log-fold change and average abundance of each gene. Significantly (FDR ≤ 0.1) up and down DE genes are highlighted in red. B) Variation of differentially expressed genes across tertiles of the SFA/VFA ratio. RPKM: Reads Per Kilobase per Million mapped reads.

3.3. Validation of adipose tissue expression and serum levels of *CCDC3* and *ISM1*

mRNA levels of *CCDC3* and *ISM1* were measured by qPCR in scWAT and visWAT. We found a high correlation between qPCR- and amplicon-sequencing-measured expression levels ($\rho=0.83$ and $\rho=0.75$ for *CCDC3* and *ISM1*, respectively, both $p<0.001$). We also found a depot-specific expression in which *ISM1* mRNA levels were significantly higher in scWAT ($p=0.015$), while *CCDC3* was more expressed in visWAT ($p<0.001$) (Fig 4A).

Next, we investigated the correlation of plasma values of ISM1 and CCDC3 measured by ELISA and their expression values in scWAT and visWAT. Interestingly, this correlation was observed only for ISM1 in scWAT ($r=0.46$, $p=0.007$) but not in visWAT (Fig 4B). Conversely, CCDC3 plasma levels did not correlate with the expression levels in either scWAT or visWAT.

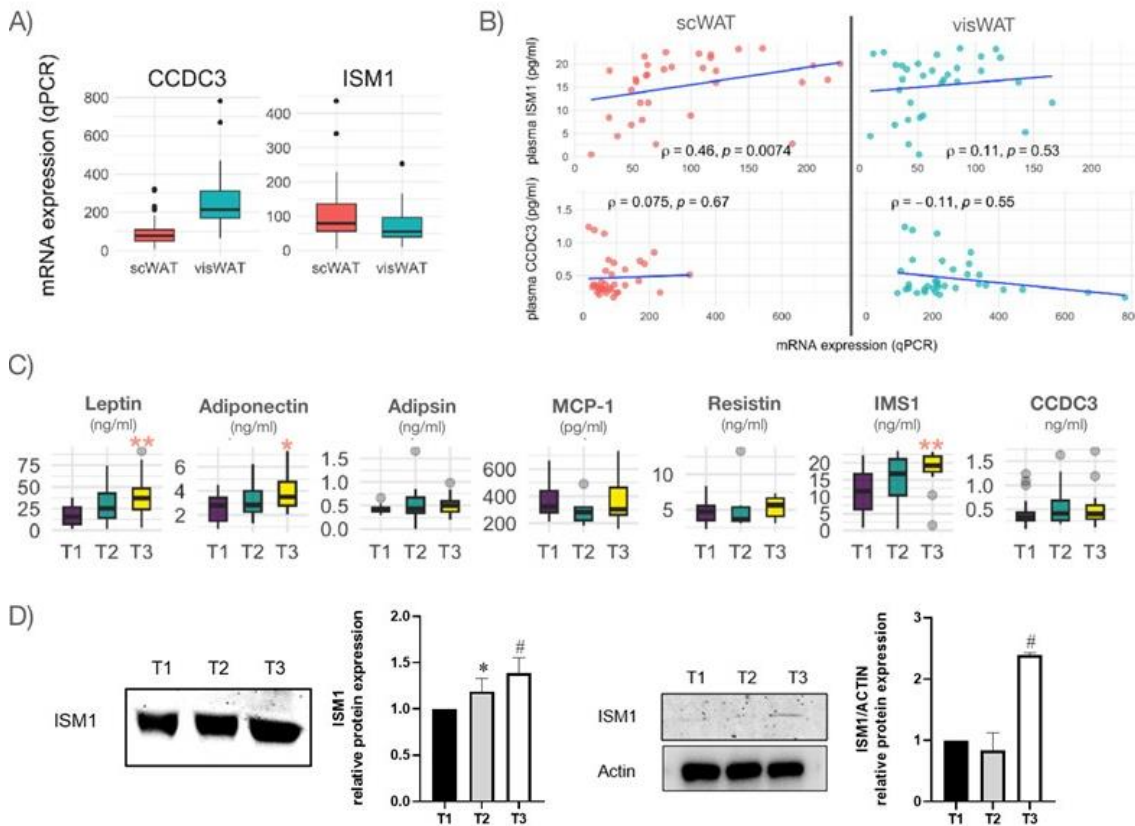


Figure 4. Expression of CCDC3 and ISM1 by qPCR in the subcutaneous and visceral adipose depots and association of the SFA/VFA ratio with serum adipokines. A) mRNA expression of CCDC3 and ISM1 in subcutaneous (scWAT) and visceral (visWAT) adipose tissues. B) Depot specific correlation of serum CCDC3 and ISM1 with mRNA expression levels. C) Serum levels of different adipokines in individual with obesity, stratified by the SFA/VFA ratio. p for trend across tertiles: * <0.05 , ** <0.01

3.4. Association of the SFA/VFA ratio with serum adipokines

Finally, we measured the serum levels of well-characterized adipokines and correlated these values with the SFA/VFA ratio. We did not observe an association of adipsin, MCP-1, or resistin, but a significant increase across SFA/VFA ratio tertiles was observed for leptin and adiponectin (Fig. 4C).

Regarding the newly identified adipokines, we did not observe an association of CCDC3 with the SFA/VFA, which aligns with the lack of association between scWAT expression and serum levels. However, a significant increase across SFA/VFA ratio tertiles was observed for ISM1. This upward trend in ISM1 was further validated through Western blot analysis in both plasma and scWAT (Fig. 4D), confirming the potential of this adipokine as a biomarker of adipose tissue distribution.

3.5. Biomarker Evaluation and Insights into ISM1's Metabolic Role

We conducted a Receiver Operating Characteristic (ROC) analysis to assess the efficacy of ISM1 and CCDC3 as biomarkers in distinguishing subjects within the upper tertile of the SFA/VFA ratio, representing individuals with the most favorable metabolic profile. Our analysis found that CCDC3 had an Area Under the ROC Curve (AUC) value of 0.57, indicating that it performed relatively poorly as a predictor (Fig 5).

However, ISM1 exhibited a significantly higher AUC of 0.75, demonstrating a fair ability to discriminate between individuals in the upper tertile of the SFA/VFA ratio and those outside this category, underscoring its potential clinical relevance and utility in the stratification of obese subjects with superior metabolic profiles based on adipose tissue distribution.

Lastly, we performed a correlation analysis among plasma ISM1 and other metabolic parameters to obtain some clues about the potential role of ISM1 in metabolic regulation in obesity. We found significant correlations with several metabolic markers. Notably, it displayed strong associations with leptin and PCR. Additionally, ISM1 showed correlations with adiponectin and CTx, both linked to glucose metabolism, indicating possible involvement in glucose regulation pathways. In contrast, no significant correlations were observed between ISM1 and adiponectin, NEFA, resistin, or plasma triglycerides. These findings imply that ISM1 may play multifaceted roles in metabolic regulation, warranting further investigation into its specific mechanisms and functions within these metabolic pathways.

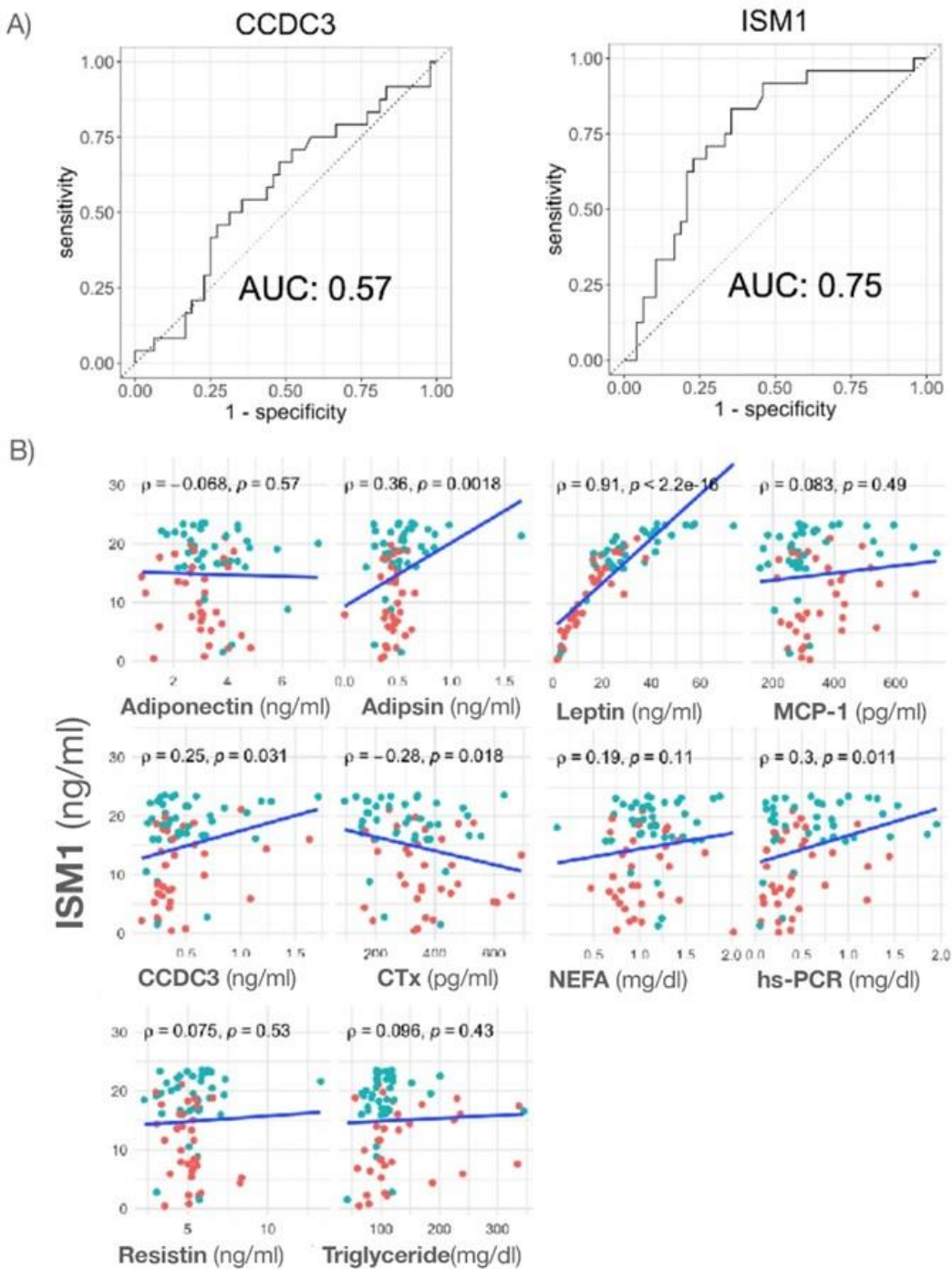


Figure 5. Sensitivity and specificity of CCDC3 and ISM1 as biomarkers of elevated SFA/VFA ratio and correlation analysis of ISM1 and other metabolic parameters. A) Receiver operator curves (ROC) for prediction of being in the first tertile (T_1) of the SFA/VFA ratio. B) Correlations between serum ISM1 and other metabolic parameters. AUC: Area under the ROC curve.

4. DISCUSSION

The primary aim of this study was to discover a non-invasive biomarker to predict the distribution of abdominal adipose tissue in individuals with obesity, and consequently, to assess the metabolic risks linked to fat mass accumulation. To achieve this goal, we conducted a transcriptomic analysis on scWAT biopsies to identify candidate genes associated with the SFA/VFA ratio. Subsequently, we assessed their levels in serum. We unveiled a novel adipokine, ISM1, whose serum levels correlated with the SFA/VFA ratio. These findings suggest that ISM1 could predict abdominal fat partitioning and be a potential biomarker for evaluating obesity-related health risks.

Obesity increases the risk of developing metabolic disorders, such as cardiovascular disease, type 2 diabetes, hypertension, or fatty liver (14, 15). However, not all forms of obesity are equally dangerous: despite higher percentages of body fat, some individuals are at less risk for certain chronic obesity-related complications (4, 6). Data suggest that fat's physical location dramatically influences disease risk (5, 7). Accumulation of adipose tissue in the upper body, in the abdominal region (android obesity), is associated with the development of obesity-related comorbidities and even all-cause mortality (16). In contrast, population studies have shown that fat accumulation in the lower body, in the gluteal-femoral region (gynoid obesity), is associated with protective lipid and glucose profiles and decreased cardiovascular and metabolic disease prevalence (5–7).

However, the situation becomes more intricate when considering that the association of abdominal obesity with metabolic risk is primarily observed when subcutaneous white adipose tissue (scWAT) reaches its maximum storage capacity and fails to handle lipid storage adequately. This results in the redirection of lipid flux to visceral white adipose tissue (visWAT), leading to the accumulation of ectopic fat. Such a process triggers insulin resistance through mechanisms involving lipotoxicity and inflammations (17), as outlined in the adipose tissue expandability hypothesis (18). Therefore, it is critical to evaluate not only the quantity and the location of fat in the body but also to distinguish between visceral and subcutaneous abdominal depots. Considering that, the first objective of our work was to verify whether the scWAT/visWAT ratio was suitable to stratify patients with obesity according to their metabolic risk (19, 20).

Several studies have lent some support to this theory, demonstrating that in obesity, the regional distribution of adipose tissue strongly correlates with several important

metabolic variables (3). It has been broadly reported that VFA, but not total adiposity or SFA, is associated with glucose intolerance, suggesting an insulin-resistant state (21, 22). In addition to being associated with disturbances in insulin-glucose homeostasis, visceral obesity has been related to alterations in plasma lipoprotein-lipid levels, particularly increased plasma triglyceride and low HDL concentrations (23, 24), as well as with liver disease (25).

Our results align with these previous data, being the stratification according to the SFA/VFA ratio the one that showed the major metabolic differences between tertiles. Patients in the upper tertile of SFA/VFA ratio (more subcutaneous and less visceral fat) had similar BMI and waist circumference than those in the lower tertile. However, they presented lower levels of indicators of metabolic risk, with better carbohydrate metabolism (reduced HOMA as well as Hb1Ac and CTx levels), better lipid profile (lower triglycerides and higher HDL serum concentration), and decreased levels of liver damage markers (GGT and ALT). This suggests that despite similar antropometric measurements (BMI, waist circumference), body fat distribution was linked metabolic disease severity markers, as expected.

Paradoxically, we found that hs-CRP levels increased with subcutaneous expansion (subcutaneous obesity model or upper SFA/VFA ratio). CRP is the most frequently employed marker for acute-phase reactants associated with inflammation (26). Previous studies had reported a positive association between CRP and visceral fat (27, 4). The association observed with scWAT in our cohort could be attributed to the augmented size (hypertrophy) of adipocytes in the subcutaneous depot (28, 29), leading us to hypothesize that heightened hs-CRP levels may potentially indicate the threshold of adipose expansion in our patients with morbid obesity.

Considering previous data and our results, the SFA/VFA ratio is a good indicator of metabolic risk. Nevertheless, the challenge lies in implementing this assessment, as advanced techniques like body composition analysis and imaging are often complex and impractical in many clinical settings. Therefore, our second aim was to identify a non-invasive biomarker that accurately reflects adipose tissue distribution.

Adipokines have been broadly proposed as non-invasive biomarkers of obesity, as their production is often dysregulated in obese individuals and contributes to the pathogenesis of obesity-associated metabolic complications (30, 31). For instance, circulating

adiponectin levels have been inversely correlated with body weight, visceral fat accumulation, and metabolic disease risk (32, 33). At the same time, a positive association has been reported between leptin levels and the percentage of fat mass (34). This evidence is also observed in our cohort, where adiponectin levels decreased as visceral fat decreased and leptin levels increased as total subcutaneous fat mass increased. Since the synthesis of adipokines reflects adipose tissue function in overall metabolic homeostasis, we assumed that perhaps differences in the expression of not-yet known adipokines produced by the scWAT could reveal divergence in the metabolic phenotype. Therefore, we performed an RNAseq analysis in scWAT, and we identified two genes whose expression increased as the SFA/VFA ratio increased and which were predicted to encode adipose tissue-secreted proteins; CCDC3 and ISM1.

CCDC3 is a secretory protein reported to be highly expressed in adipose tissue, regulated by insulin and pioglitazone, and suppressed by TNF-alpha, isoproterenol, and norepinephrine (35). Its hormone-like role in regulating lipid metabolism has been described in an autocrine manner, regulating adipocyte lipogenesis (36), and in a paracrine manner, regulating liver lipid metabolism (37). Moreover, it has been linked to obesity, especially visceral fat accumulation (38). Our results showed a positive association between CCDC3 expression in scWT and the SFA/VFA ratio. However, this correlation was not replicated in serum CCDC3 levels, which excludes this adipokine as a valid biomarker of scWAT functionality. CCDC3 expression levels were higher in visceral instead of subcutaneous fat, and there could be different mechanisms regulating its expression and secretion in both fat depots.

The second potential biomarker was ISM1, a secreted protein initially discovered in fetal brain development and expressed in the vasculature, skin, immune cells, and lungs [reviewed in (39)]. ISM1 has been recently identified in mouse and human adipocytes as an adipokine that has essential metabolic roles in multiple tissues, promoting glucose uptake, inhibiting hepatic lipogenesis (40, 41), and stimulating protein synthesis (42), thus improving hyperglycemia and reducing lipid accumulation in mouse models. Moreover, ISM1 expression in adipocytes and circulating ISM1 levels have been associated with obesity and reduced risk of type 2 diabetes mellitus (T2DM) (43, 44). However, nothing is known about its association with adipose tissue distribution.

Our data showed that ISM1 mRNA expression levels scWAT were strongly associated with the SFA/VFA ratio. However, no such association was observed in visWAT. In the same vein, circulating ISM1 levels were positively associated with SFA and the SFA/VFA ratio but not with VFA. This suggests that the elevated ISM1 levels observed could potentially originate from subcutaneous adipose cells and exert endocrine influences on other tissues. We posit that that ISM1 secreted by scWAT has a beneficial role in whole-body energy homeostasis, which aligns with the protective function previously reported for this adipokine (41).

In our study, we conducted a comprehensive correlation analysis to shed light on the metabolic regulation of ISM1. We found significant correlations between ISM1 and CCDC3 and hs-PCR, the later could be indicative of the presence of an exhausted scWAT adipocytes reaching their limit of expansion. Notably, ISM1 was also associated with adipsin and CTx, both linked to glucose metabolism (45, 46), hinting at a role of this new adipokine in glucose regulation. Interestingly, we found ISM1 plasma levels highly correlated with leptin levels. Leptin is a well-known adipokine mainly produced by scWAT in proportion to the amount of fat mass and is involved in regulating food intake and glucose and lipid metabolism, among others (30). Although leptin is a well-characterized adipokine, studies associating this hormone with ISM1 are scarce. Recent evidence revealed a simultaneous increase in the expression of ISM1 and leptin in the adipose tissue of mice fed high fat diet (41). At the same time, no significant associations were identified between serum levels of these two adipokines in pre-puberal boys (44). This association warrants further investigation as a common regulatory mechanism for both adipokines could exist. Both ISM1 and leptin seem to be expressed mainly by scWAT, increasing their levels in obesity. In addition, both seem to have a role in regulating glucose metabolism, so that future research could clarify the role of the combined function of these adipokines in the maintenance of energy homeostasis.

These findings collectively underscore ISM1's potential involvement in various metabolic processes, laying the foundation for future research into its precise metabolic functions. However, important questions also arise from our current findings: the molecular mechanism regulating ISM1 expression in scWAT and its association with leptin, or the target tissues and function of this adipokine. Besides, our results mainly concern individuals with obesity, and how this protein is expressed and secreted in non-obese also warrants further investigations. Moreover, further validation in an independent cohort

must be performed before proving its potential as a biomarker of adipose tissue distribution.

In conclusion, our research proves the importance of distinguishing adipose tissue location to classify obesity phenotypes. It proposes ISM1 as a novel non-invasive biomarker to predict abdominal fat partitioning and, consequently, to evaluate obesity-related health risks.

Acknowledgments

We want to particularly acknowledge all the patients included in the study, as well as the IACS Functional Genomics and Sequencing Core and the Biobank of the Aragon Health System (PT20/00112) integrated in the Spanish National Biobanks Network.

Conflict of Interest

The authors declare that they have no conflicts of interest.

Author Contributions

M.L.-Y., and J.M.A.-M. were involved in the conception, design, and conduct of the study and the analysis and interpretation of the results. C.C, J.J.S.-G., S.B., Y.G.-I., M.P.G.-S., B.G.-R., R.delM.-B., P.C., and J.M.A. made substantial contributions to the acquisition of data. V.B.-M and A.S.-P. contributed to the clinical interpretation of the data. M.L.-Y. and S.L.-C. wrote the first draft of the manuscript, and all authors edited, reviewed, and approved the final version of the manuscript.

Funding

This study was partially supported by a grant (PI22/01366) from the Instituto de Salud Carlos III and by FEDER funds: “Una manera de hacer Europa” and by the regional government of Aragón (B03_23R), co-financed with the FEDER Aragón 2014–2020: “Construyendo Europa desde Aragón”.

Data Availability Statement

Gene expression and patient data is held by the Aragón Institute of Health Sciences (IACS). Access may be granted to those who meet pre-specified criteria for confidential access, available at <https://www.iacs.es/instituto-aragones-ciencias-la-salud/oficina-virtual/solicitud-de-acceso-a-datos-para-realizacion-de-un-proyecto-de-investigacion-rpi01-3a> and with prior authorization by the Ethics Committee of Aragon (CEIC-A) which can be obtained at <https://www.iacs.es/investigacion/comite-de-etica-de-la-investigacion-de-aragon-ceica/ceica-evaluaciones-y-otras-presentaciones/>.

5. REFERENCES

1. Sparrow D, Borkan GA, Gerzof SG, Wisniewski C, Silbert CK. Relationship of fat distribution to glucose tolerance. Results of computed tomography in male participants of the Normative Aging Study. *Diabetes* 35: 411–415, 1986. doi: 10.2337/diab.35.4.411.
2. Després J-P, Nadeau A, Tremblay A, Ferland M, Moorjani S, Lupien PJ, Thériault G, Pinault S, Bouchard C. Role of Deep Abdominal Fat in the Association Between Regional Adipose Tissue Distribution and Glucose Tolerance in Obese Women. *Diabetes* 38: 304–309, 1989. doi: 10.2337/diab.38.3.304.
3. Neeland IJ, Ross R, Després J-P, Matsuzawa Y, Yamashita S, Shai I, Seidell J, Magni P, Santos RD, Arsenault B, Cuevas A, Hu FB, Griffin B, Zambon A, Barter P, Fruchart J-C, Eckel RH, International Atherosclerosis Society, International Chair on Cardiometabolic Risk Working Group on Visceral Obesity. Visceral and ectopic fat, atherosclerosis, and cardiometabolic disease: a position statement. *Lancet Diabetes Endocrinol* 7: 715–725, 2019. doi: 10.1016/S2213-8587(19)30084-1.
4. Pou KM, Massaro JM, Hoffmann U, Vasan RS, Maurovich-Horvat P, Larson MG, Keaney JF Jr, Meigs JB, Lipinska I, Kathiresan S, Murabito JM, O'Donnell CJ, Benjamin EJ, Fox CS. Visceral and Subcutaneous Adipose Tissue Volumes Are Cross-Sectionally Related to Markers of Inflammation and Oxidative Stress. *Circulation* 116: 1234–1241, 2007. doi: 10.1161/circulationaha.107.710509.
5. Klein S, Fontana L, Young VL, Coggan AR, Kilo C, Patterson BW, Mohammed BS. Absence of an Effect of Liposuction on Insulin Action and Risk Factors for Coronary Heart Disease. *New England Journal of Medicine* 350: 2549–2557, 2004. doi: 10.1056/NEJMoa033179.
6. McLaughlin T, Lamendola C, Liu A, Abbasi F. Preferential Fat Deposition in Subcutaneous Versus Visceral Depots Is Associated with Insulin Sensitivity. *The Journal of Clinical Endocrinology & Metabolism* 96: E1756–E1760, 2011. doi: 10.1210/jc.2011-0615.
7. Porter SA, Massaro JM, Hoffmann U, Vasan RS, O'Donnell CJ, Fox CS. Abdominal Subcutaneous Adipose Tissue: A Protective Fat Depot? *Diabetes Care* 32: 1068–1075, 2009. doi: 10.2337/dc08-2280.
8. Park K-G, Park KS, Kim M-J, Kim H-S, Suh Y-S, Ahn JD, Park K-K, Chang Y-C, Lee I-K. Relationship between serum adiponectin and leptin concentrations and body fat distribution. *Diabetes Research and Clinical Practice* 63: 135–142, 2004. doi: 10.1016/j.diabres.2003.09.010.
9. Staiger H, Tschritter O, Machann J, Thamer C, Fritsche A, Maerker E, Schick F, Häring H-U, Stumvoll M. Relationship of Serum Adiponectin and Leptin Concentrations with Body Fat Distribution in Humans. *Obesity Research* 11: 368–376, 2003. doi: 10.1038/oby.2003.48.
10. Torres-Perez E, Valero M, Garcia-Rodriguez B, Gonzalez-Irazabal Y, Calmarza P, Calvo-Ruata L, Ortega C, Garcia-Sobreviela M, Sanz-Paris A, Artigas J, Lagos J, Arbones-Mainar J. The FAT expandability (FATE) Project: Biomarkers to determine the limit of expansion and the complications of obesity. *Cardiovascular Diabetology* 14: 40, 2015. doi: 10.1186/s12933-015-0203-6.
11. Matthews DR, Hosker JP, Rudenski AS, Naylor BA, Treacher DF, Turner RC. Homeostasis model assessment: insulin resistance and β -cell function from fasting plasma glucose and insulin concentrations in man. *Diabetologia* 28: 412–419, 1985.

12. Robinson MD, McCarthy DJ, Smyth GK. edgeR: a Bioconductor package for differential expression analysis of digital gene expression data. *bioinformatics* 26: 139–140, 2010.
13. Benjamini Y, Hochberg Y. Controlling the false discovery rate: a practical and powerful approach to multiple testing. *Journal of the Royal statistical society: series B (Methodological)* 57: 289–300, 1995.
14. Article O. Health Effects of Overweight and Obesity in 195 Countries over 25 Years. .
15. Estes C, Razavi H, Loomba R, Younossi Z, Sanyal AJ. Modeling the epidemic of nonalcoholic fatty liver disease demonstrates an exponential increase in burden of disease. *Hepatology* 67: 123–133, 2018. doi: 10.1002/hep.29466.
16. Després J-P, Lemieux I, Bergeron J, Pibarot P, Mathieu P, Larose E, Rod' es-Cabau J, Bertrand OF, Poirier P. Abdominal Obesity and the Metabolic Syndrome: Contribution to Global Cardiometabolic Risk. *Arteriosclerosis, Thrombosis, and Vascular Biology* 28: 1039–1049, 2008. doi: 10.1161/atvaha.107.159228.
17. Kang YM, Jung CH, Cho YK, Jang JE, Hwang JY, Kim EH, Lee WJ, Park JY, Kim HK. Visceral adiposity index predicts the conversion of metabolically healthy obesity to an unhealthy phenotype. *PLoS ONE* 12, 2017. doi: 10.1371/journal.pone.0179635.
18. Virtue S, Vidal-Puig A. Adipose tissue expandability, lipotoxicity and the Metabolic Syndrome - An allostatic perspective. *Biochimica et Biophysica Acta - Molecular and Cell Biology of Lipids* 1801: 338–349, 2010. doi: 10.1016/j.bbalip.2009.12.006.
19. Ladeiras-lopes R, Sampaio F, Bettencourt N, Fontes-carvalho R, Ferreira N, Leite-moreira A, Gama V. The Ratio Between Visceral and Subcutaneous Abdominal Fat Assessed by Computed Tomography Is an Independent Predictor of Mortality and Cardiac Events. *Revista Española de Cardiología* , 2016.
20. Kwon S, Han AL. The Correlation between the Ratio of Visceral Fat Area to Subcutaneous Fat Area on Computed Tomography and Lipid Accumulation Product as Indexes of Cardiovascular Risk. *Journal of Obesity & Metabolic Syndrome* 28: 186–193, 2019. doi: 10.7570/jomes.2019.28.3.186.
21. Després J-P. Body Fat Distribution and Risk of Cardiovascular Disease. *Circulation* 126: 1301–1313, 2012. doi: 10.1161/circulationaha.111.067264.
22. De Larocheillière E, Côté J, Gilbert G, Bibeau K, Ross M-K, Dion-Roy V, Pibarot P, Després J-P, Larose É. Visceral/epicardial adiposity in nonobese and apparently healthy young adults: association with the cardiometabolic profile. .
23. Walton C, Lees B, Crook D, Worthington M, Godsland IF, Stevenson JC. Body fat distribution, rather than overall adiposity, influences serum lipids and lipoproteins in healthy men independently of age. *American Journal of Medicine* 99: 459–464, 1995.
24. Spalding KL, Bernard S, Näslund E, Salehpour M, Possnert G, Appelsved L, Fu KY, Alkass K, Druid H, Thorell A, Rydén M, Arner P. Impact of fat mass and distribution on lipid turnover in human adipose tissue. *Nature Communications* 8, 2017. doi: 10.1038/ncomms15253.
25. Thamer C, Machann J, Haap M, Stefan N, Heller E, Schnödt B, Stumvoll M, Claussen C, Fritzsche A, Schick F, Häring H. Intrahepatic Lipids Are Predicted by Visceral Adipose Tissue Mass in Healthy Subjects. *Diabetes Care* 27: 2726–2729, 2004. doi: 10.2337/diacare.27.11.2726.

26. Ridker PM, Hennekens CH, Buring JE, Rifai N. C-Reactive Protein and Other Markers of Inflammation in the Prediction of Cardiovascular Disease in Women. *New England Journal of Medicine* 342: 836–843, 2000. doi: 10.1056/NEJM200003233421202.
27. Forouhi NG, Sattar N, McKeigue PM. Relation of C-reactive protein to body fat distribution and features of the metabolic syndrome in Europeans and South Asians. *Int J Obes* 25: 1327–1331, 2001. doi: 10.1038/sj.ijo.0801723.
28. Bahceci M, Gokalp D, Bahceci S, Tuzcu A, Atmaca S, Arikan S. The correlation between adiposity and adiponectin, tumor necrosis factor α , interleukin-6 and high sensitivity C-reactive protein levels. Is adipocyte size associated with inflammation in adults? *J Endocrinol Invest* 30: 210–214, 2007. doi: 10.1007/BF03347427.
29. Stenkula KG, Erlanson-Albertsson C. Adipose cell size: importance in health and disease. *Am J Physiol Regul Integr Comp Physiol* 315: 284–295, 2018. doi: 10.1152/ajpregu.00257.2017.-Adipose.
30. Saito T, Murata M, Otani T, Tamemoto H, Kawakami M, Ishikawa S. Association of subcutaneous and visceral fat mass with serum concentrations of adipokines in subjects with type 2 diabetes mellitus. *Endocrine journal* 59: 39–45, 2012.
31. Korac A, Srdic-Galic B, Kalezic A, Stancic A, Otasevic V, Korac B, Jankovic A. Adipokine signatures of subcutaneous and visceral abdominal fat in normal-weight and obese women with different metabolic profiles. *Archives of Medical Science* 17: 323–336, 2021. doi: 10.5114/aoms/92118.
32. Cnop M, Havel PJ, Utzschneider KM, Carr DB, Sinha MK, Boyko EJ, Retzlaff BM, Knopp RH, Brunzell JD, Kahn SE. Relationship of adiponectin to body fat distribution, insulin sensitivity and plasma lipoproteins: Evidence for independent roles of age and sex. *Diabetologia* 46: 459–469, 2003. doi: 10.1007/s00125-003-1074-z.
33. Kim C, Park J, Park J, Kang E, Ahn C, Cha B, Lim S, Kim K, Lee H. Comparison of body fat composition and serum adiponectin levels in diabetic obesity and non-diabetic obesity. *Obesity* 14: 1164–1171, 2006. doi: 10.1038/oby.2006.133.
34. Ostlund Jr R, Yang JW, Klein S, Gingerich R. Relation between plasma leptin concentration and body fat, gender, diet, age, and metabolic covariates. *The journal of clinical endocrinology & metabolism* 81: 3909–3913, 1996.
35. Kobayashi S, Fukuhara A, Taguchi T, Matsuda M, Tochino Y, Otsuki M, Shimomura I. Identification of a new secretory factor, CCDC3/Favine, in adipocytes and endothelial cells. *Biochemical and Biophysical Research Communications* 392: 29–35, 2010. doi: 10.1016/j.bbrc.2009.12.142.
36. Kobayashi S, Fukuhara A, Otsuki M, Suganami T, Ogawa Y, Morii E, Shimomura I. Fat/vessel-derived secretory protein (Favine)/CCDC3 is involved in lipid accumulation. *Journal of Biological Chemistry* 290: 7443–7451, 2015. doi: 10.1074/jbc.M114.592493.
37. Liao W, Liu H, Zhang Y, Jung JH, Chen J, Su X, Kim YC, Flores ER, Wang SM, Czarny-Ratajczak M, Li W, Zeng SX, Lu H. Ccdc3: A New P63 Target Involved in Regulation Of Liver Lipid Metabolism. *Sci Rep* 7: 9020, 2017. doi: 10.1038/s41598-017-09228-8.
38. Ugi S, Maeda S, Kawamura Y, Kobayashi MA, Imamura M, Yoshizaki T, Morino K, Sekine O, Yamamoto H, Tani T, Rokushima M, Kashiwagi A, Maegawa H. CCDC3 is specifically upregulated

- in omental adipose tissue in subjects with abdominal obesity. *Obesity* 22: 1070–1077, 2014. doi: 10.1002/oby.20645.
- 39. Stanford K, Burlacu A, Akhmedov A. *A brief overview about the adipokine: Isthmin-1*. 2021.
 - 40. Menghuan L, Yang Y, Qianhe M, Na Z, Shicheng C, Bo C, XueJie YI. Advances in research of biological functions of Isthmin-1. .
 - 41. Jiang Z, Zhao M, Voilquin L, Jung Y, Aikio MA, Sahai T, Dou FY, Roche AM, Carcamo-Orive I, Knowles JW, Wabitsch M, Appel EA, Maikawa CL, Camporez JP, Shulman GI, Tsai L, Rosen ED, Gardner CD, Spiegelman BM, Svensson KJ. Isthmin-1 is an adipokine that promotes glucose uptake and improves glucose tolerance and hepatic steatosis. *Cell Metabolism* 33: 1836-1852.e11, 2021. doi: 10.1016/j.cmet.2021.07.010.
 - 42. Zhao M, Danneskiold-Samsøe NB, Ulicna L, Nguyen Q, Voilquin L, Lee DE, White JP, Jiang Z, Cuthbert N, Paramasivam S, Bielczyk-Maczynska E, Van Rechem C, Svensson KJ. Phosphoproteomic mapping reveals distinct signaling actions and activation of muscle protein synthesis by Isthmin-1. *eLife* 11, 2022. doi: 10.7554/eLife.80014.
 - 43. Wang J, Du J, Ge X, Peng W, Guo X, Li W, Huang S. Circulating Ism1 Reduces the Risk of Type 2 Diabetes but not Diabetes-Associated NAFLD. *Frontiers in Endocrinology* 13, 2022. doi: 10.3389/fendo.2022.890332.
 - 44. Ruiz-Ojeda FJ, Anguita-Ruiz A, Rico MC, Leis R, Bueno G, Moreno LA, Gil-Campos M, Gil Á, Aguilera CM. Serum levels of the novel adipokine isthmin-1 are associated with obesity in pubertal boys. .
 - 45. Lo JC, Ljubicic S, Leibiger B, Kern M, Leibiger IB, Moede T, Kelly ME, Chatterjee Bhowmick D, Murano I, Cohen P, Banks AS, Khandekar MJ, Dietrich A, Flier JS, Cinti S, Blüher M, Danial NN, Berggren P-O, Spiegelman BM. Adipsin Is an Adipokine that Improves β Cell Function in Diabetes. *Cell* 158: 41–53, 2014. doi: 10.1016/j.cell.2014.06.005.
 - 46. Xuan Y, Sun L-H, Liu D-M, Zhao L, Tao B, Wang W-Q, Zhao H-Y, Liu J-M, Ning G. Positive Association Between Serum Levels of Bone Resorption Marker CTX and HbA1c in Women With Normal Glucose Tolerance. *The Journal of Clinical Endocrinology & Metabolism* 100: 274–281, 2015. doi: 10.1210/jc.2014-2583.

4.2. Chapter II

Identification of novel targets in adipose tissue involved in non-alcoholic fatty liver disease progression

The contents of this chapter have been adapted from the following published work:

Lopez-Yus, Marta *et al.* “Identification of novel targets in adipose tissue involved in non-alcoholic fatty liver disease progression.” *FASEB journal: official publication of the Federation of American Societies for Experimental Biology* vol. 36,8 (2022): e22429.
doi:10.1096/fj.202200118RR

Identification of novel targets in adipose tissue involved in non-alcoholic fatty liver disease progression

Marta Lopez-Yus^{1,2}, Silvia Lorente-Cebrian^{1,2,3}, Raquel del Moral-Bergos^{1,2}, Carlos Hörndler^{2,4},
Maria Pilar Garcia-Sobreviela^{1,2}, Carmen Casamayor^{2,5}, Alejandro Sanz-Paris^{2,6}, Vanesa Bernal-
Monterde^{2,7}, Jose M. Arbones-Mainar^{1,2,8}

¹ Adipocyte and Fat Biology Laboratory (AdipoFat), Translational Research Unit, University Hospital Miguel Servet, Instituto Aragonés de Ciencias de la Salud (IACS),

² Instituto de Investigación Sanitaria (IIS) Aragón, 50009 Zaragoza, Spain

³ Departamento de Farmacología, Fisiología y Medicina Legal y Forense, Universidad de Zaragoza.
Instituto Agroalimentario de Aragón (IA2) (Universidad de Zaragoza-CITA), Zaragoza, Spain.

⁴ Pathology Department, Miguel Servet University Hospital, 50009 Zaragoza, Spain

⁵ Endocrine, Bariatric and Breast Surgery Unit, General and Digestive Surgery Department, Miguel
Servet University Hospital, 50009 Zaragoza, Spain

⁶ Nutrition Department, Miguel Servet University Hospital, 50009 Zaragoza, Spain

⁷ Gastroenterology Department, Miguel Servet University Hospital, 50009 Zaragoza, Spain

⁸ CIBER Fisiopatología Obesidad y Nutrición (CIBERObn), Instituto Salud Carlos III, Madrid, Spain

ABSTRACT

Obesity is a major risk factor for the development of Nonalcoholic fatty liver disease (NAFLD). We hypothesize that a dysfunctional subcutaneous white adipose tissue (scWAT) may lead to an accumulation of ectopic fat in liver. Our aim was to investigate the molecular mechanisms involved in the causative role of scWAT in NALFD progression. We performed a RNA-sequencing analysis in a discovery cohort (n=45) to identify genes in scWAT correlated with fatty liver index, a qualitative marker of liver steatosis. We then validated those targets in a second cohort (n=47) of obese patients who had liver biopsies available. Finally, we obtained scWAT mesenchymal stem cells (MSCs) from 13 obese patients at different stages of NAFLD and established *in vitro* models of human MSC (hMSC)-derived adipocytes. We observed impaired adipogenesis in hMSC-derived adipocytes as liver steatosis increased, suggesting that an impaired adipogenic capacity is a critical event in the development of NAFLD. Four genes showed a differential expression pattern in both scWAT and hMSC-derived adipocytes, where their expression paralleled steatosis degree: *SOCS3*, *DUSP1*, *SIK1* and *GADD45B*. We propose these genes as key players in NAFLD progression. They could eventually constitute potential new targets for future therapies against liver steatosis.

Key words: adipose tissue, fatty liver, obesity, mesenchymal stem cell

1. INTRODUCTION

White adipose tissue (WAT) is a metabolic organ of paramount importance in the regulation of whole-body energy homeostasis. WAT functions as a key energy reservoir and secretes various cytokines (adipokines) and other metabolites to control systemic energy expenditure¹. Subcutaneous white adipose tissue (scWAT) is located under the skin and is the largest storage site for excess lipids. It is endowed with a high plasticity, being able to contract and expand in response to changes in energy balance. The expansion of scWAT is determined by two main processes which include the differentiation of new mature adipocytes from their precursors, known as mesenchymal stem cells (MSC), and the ability to enlarge from those already formed adipocytes².

It is well established that each individual possesses an intrinsic limit on their capacity to store lipids in scWAT (i.e. the adipose tissue expandability hypothesis³). Subcutaneous adipocytes are the preferable storage fat depot, they can enlarge as result of a prolonged positive energy balance. When scWAT reaches its maximal storage capacity, adipose tissue fails to store lipids appropriately redirecting this lipid flux to other organs where it is accumulated as ectopic fat causing insulin resistance through lipotoxic- and inflammation-related mechanisms⁴. This ectopic accumulation occurs primarily in the visceral adipose tissue (visWAT) and liver, leading to visceral obesity and liver steatosis respectively⁵.

Nonalcoholic fatty liver disease (NAFLD) is a general term for a variety of liver conditions caused by hepatic fat accumulation in people who drink little or no alcohol⁶. It is rapidly becoming one of the most common liver diseases worldwide⁷. Steatosis represents the first step of the NAFLD progression and is mostly benign and remains clinically silent. However, in several cases ($\approx 30\%$) these complications ultimately lead to steatohepatitis (NASH), fibrosis, cirrhosis or even hepatocarcinoma, where liver functions are severely altered⁸.

Current evidence undoubtedly demonstrates a complex and dynamic interrelationship between adipose tissue and liver, where adipose tissue seems to play a major causative role governing hepatosteatosis⁹. However, the key factors determining ectopic liver fat accumulation are not fully understood. We hypothesize that gene modifications at scWAT level may represent a rational approach to specifically reduce ectopic liver fat accumulation.

Considering that, the main objective of this study was to obtain new insights into the molecular mechanisms underlying the causative role of scWAT in NAFLD. This aim was addressed by: 1) identifying targetable upregulated genes in scWAT potentially involved in the development and progression of NAFLD and, 2) establishing a functionally relevant *in vitro* model of human MSC (hMSC)-derived adipocytes throughout the progression of NAFLD. To this end, we sequentially combined a global RNA-sequencing analysis from scWAT from a discovery cohort with specific qPCR validation in a second independent cohort where paired adipose/liver biopsies and hMSC-derived adipocytes were available.

The scientific impact of our findings relies on the fact that subsequent modifications (e.g., gene edition) of these newly identified genes could represent a promising strategy to prevent or correct the development of NAFLD.

2. MATERIALS AND METHODS

2.1. Human samples and cohort description

Human abdominal scWAT and liver biopsies were obtained from well-characterized patients who underwent elective surgical procedures at the Miguel Servet University Hospital (HUMS, Zaragoza, Spain) as described previously¹⁰. Importantly, patients were screened to exclude chronic viral hepatitis or autoimmune hepatitis, and drug- or alcohol-related hepatotoxicity.

For this study, three different cohorts were recruited: 1) The discovery cohort included 45 patients with different adiposity levels with or without other metabolic conditions such as dyslipidemia, diabetes or hypertension. 2) The validation cohort encompassed 47 patients from whom scWAT and laparoscopic liver biopsies had been obtained in the same surgical procedure. 3) The hMSC cohort included 13 participants who donated a sufficient amount of scWAT (>5g) to allow the isolation and establishment of hMSC cell lines. Study design and workflow are depicted in Figure 1.

All subjects were categorized as dyslipidemic, diabetic or hypertensive following National Cholesterol Education Program-Adult Treatment Panel III (NCEP–ATPIII) criteria¹¹. All patients provided written consent and the study was approved by the Regional Institutional Review Board of Ethics at Aragón, Spain (CEIC-A). Samples and

data from patients included in this study were provided by the Biobank of the Aragon Health System (PT20/00112), integrated in the Spanish National Biobanks Network and they were processed following standard operating procedures with the appropriate approval of the Ethics and Scientific Committees.

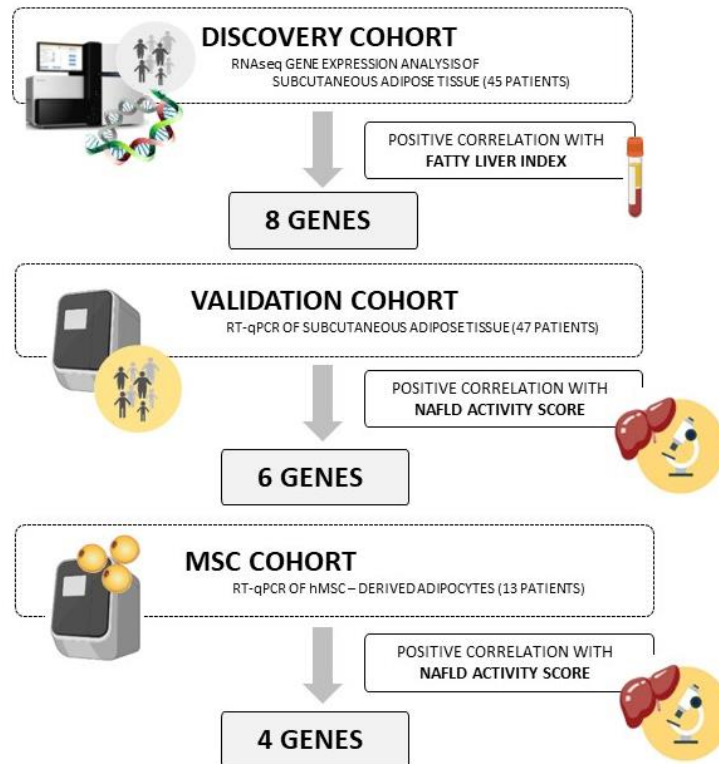


Figure 1. Study design and workflow.

2.2. Biochemical assays

Plasma biochemistries were performed at the Clinical Biochemistry department at the HUMS using state of the art analyzers. All analyses are in compliance with the requirements for quality and competence (ISO 15189:2012) for medical laboratories. The fatty liver index (FLI) is a formula that includes waist circumference, body mass index (BMI), triglycerides, and gamma-glutamyl-transferase (GGT) for prediction of fatty liver¹².

2.3. Histological examination

Liver biopsies were deemed adequate when they were 16 mm in length and included at least 6 portal tracts. Paraffin sections of livers were stained with hematoxylin-eosin (H&E). Pathological features of steatosis (0–3), lobular inflammation (0–3), hepatocellular ballooning (0–2), and fibrosis (0–4) were scored by an experienced

pathologist, according to criteria established by the Nonalcoholic Steatohepatitis Clinical Research Network¹³. Total NAFLD Activity Score (NAS) (ranging from 0-8) was calculated by adding the scores for steatosis, lobular inflammation, and hepatocellular ballooning as described¹³.

2.4. Isolation of hMSC from human adipose tissue

hMSC were isolated from scWAT obtained from 13 subjects as previously described¹⁴. In brief, minced adipose tissue was digested with collagenase (Sigma-Aldrich). The digestate was then spun and the cell pellet was resuspended in 10% fetal bovine serum (FBS)-low-glucose DMEM (Gibco) and seeded in six-well plates.

2.5. hMSC culture and differentiation

hMSC cultures were maintained in 10% FBS-low-glucose DMEM under hypoxic conditions (5% O₂, 5% CO₂) and 37°C. Two days after confluence, hMSC were differentiated into adipocytes using an adipogenic cocktail in normoxic conditions for additional 5 days. The standard adipogenic cocktail consisted of 10% FBS–high-glucose DMEM plus (Gibco), 1.5 µM insulin (Novo Nordisk), 1 µM dexamethasone (Sigma), 500 µM 3-isobutyl-1-methylxanthine (Sigma), and 2 µM rosiglitazone (Sigma). hMSC-derived adipocytes were maintained in 10% FBS–high-glucose DMEM and were considered to have reached mature phenotype at 8 days post-differentiation. Intracellular lipids were stained with Oil Red O and then the dye was extracted with isopropanol and quantified at 500 nm absorbance as previously described¹⁵.

2.6. RNA isolation

Total RNA was isolated from frozen biopsies of scWAT using TRIzol (Sigma) according to the manufacturer's protocol. All the RNA samples were treated with RNase-Free DNase (Life Technologies) to remove genomic DNA.

2.7. AmpliSeq human transcriptome analysis

RNA samples were quantitated using the Qubit RNA high-sensitivity (HS) assay kit (#Q32855, ThermoFisher) and the Qubit 3.0 fluorometer (ThermoFisher). RNA integrity was checked by the 2200 TapeStation system (Agilent) with the High Sensitivity RNA ScreenTape (5067–5579, Agilent). All samples had an RNA integrity number (RIN) > 7. RNA (20 ng) was converted to cDNA using the SuperScript IV VILO Master Mix (#11756050, ThermoFisher) and automated library preparation was carried out with the

Ion AmpliSeq transcriptome human gene expression panel Chef-ready kit (#A31446, ThermoFisher) on the Ion Chef Prep station, chef package version IC.5.4.0 (ThermoFisher). Sequencing was performed *per* the manufacturer's protocols using the Ion 540 Kit-Chef (# A30011, ThermoFisher) on the Ion Torrent S5-XL (ThermoFisher). Eight samples *per* 540 chip were sequenced obtaining 7.5 to 10 million reads/sample. Next, bam files were further processed using the Ion AmpliSeq RNA plugin v5.4.01 on the Torrent Server (Torrent Suite Software, v5.4, ThermoFisher) to obtain normalized reads *per* kilobase of transcript *per* million reads mapped (RPKM). A principal component analysis (PCA) method was adopted to identify potential outliers among the samples.

Differentially expressed genes (DEGs) were subsequently determined by correlation analysis (Spearman) between the normalized RPKMs for each single gene and the fatty liver index. The false discovery rate (FDR) adjustment for multiple testing was accounted for using q-values.

2.8. Construction of weighted gene co-expression networks and identification of modules associated with the fatty liver index

Gene co-expression network analysis was performed with the R package WGCNA¹⁶ using RNA-seq and clinical data from the discovery cohort. Genes with low variance (<25%) or low levels of expression (average < 5 RPKM) were excluded from the analysis. Sample clustering was also performed to detect outliers.

Scale independence and mean connectivity analysis of modules with different power values were performed to determine the soft threshold of module analysis. The power value was determined when the scale independence value was >0.9. Then, the adjacency matrix was calculated using the determined power value to ensure an unsigned scale-free network. Minimal module size and merge cut height were set at 30 and 0.25 respectively. A clustering dendrogram of genes, with dissimilarity based on topological overlap, was generated. Next, we identified modules that were significantly associated with the measured clinical trait by correlating eigengenes with the fatty liver index.

To understand the functional significance of genes from modules of interest, the gene ontology (GO) enrichment analysis-biological processes (BP) was used. We determined the over-representative GO categories in a module, based on the Fisher's exact test with a Bonferroni correction for multiple testing.

2.9. RT-qPCR

RNA was reverse-transcribed using PrimeScript Reverse Transcriptase (Takara Bio). Real-time PCR was performed using the StepOnePlus system (Applied Biosystems). 2 µl of the cDNA product was amplified using gene-specific primers (Table 1) in a total volume of 15 µl per reaction with SYBR Select Master Mix (Applied Biosystems). Relative gene expression was normalized to β -ACTIN or FABP4 expression using the $2^{-\Delta\Delta Ct}$ method.

Table 1. Sequences of primers used in the study.

Gene ID		Sequence (5'→3')
<i>ACTIN</i>	Forward	CATGTACGTTGCTATCCAGGC
	Reverse	CTCCTTAATGTCACGCACGAT
<i>FABP4</i>	Forward	ACTGGGCCAGGAATTGACG
	Reverse	CTCGTGGAAAGTGACGCCTT
<i>SOCS3</i>	Forward	GTCCCCCCCAGAACAGAGCTATT
	Reverse	TTGACGGTCTTCCGACAGAGAT
<i>DUSP1</i>	Forward	TTCTTCCTCAAAGGAGGATACG
	Reverse	GTGGGGTACTGCAGGAAC
<i>SIK1</i>	Forward	GCTTCTGAACCATCCACACAT
	Reverse	GTGCCCGTTGGAAGTCAAATA
<i>GADD45B</i>	Forward	TGCTGTGACAACGACATCAAC
	Reverse	GTGAGGGTTCGTGACCAGG
<i>S100A9</i>	Forward	TCGGCTTGACAGAGT GCAAGA
	Reverse	TGCCCCAGCTTCACAGAGTA
<i>S100A12</i>	Forward	TTCCTGTGCATTGAGGGTTA
	Reverse	TTAATGCCCTTCCGAACTGAG
<i>CTGF</i>	Forward	CTTGCAGCTGACCTGGAAG
	Reverse	CCGTCGGTACATACTCCACAGA
<i>CDKN1A</i>	Forward	ACATGCCAAGGAAAAACGC
	Reverse	GTCTGTTCGGTACTGTCATCC

2.10. Western blot analysis

For analysis of proteins expression, aliquots of cellular lysates were subjected to reducing sodium dodecyl sulfate-polyacrylamide gel electrophoresis (SDS-PAGE), using 12% polyacrylamide gels. Electrophoresis was carried out at 100 volts for 2 hours. Proteins were then transferred to polyvinylidene difluoride membranes (PVDF), that were blocked with 5% dry skimmed milk for 2 hours and probed with primary antibody against different proteins overnight at 4 °C with mild shaking. The results were visualized using peroxidase-conjugated secondary antibodies, that were incubated 1 hour at r.t. with mild

shaking. Antibody used were: β -Actin (Santa Cruz #SC-47778) diluted 1:1000, AFABP (Santa Cruz #SC-271529) diluted 1:1000, SOCS3 (Santa Cruz #SC-51699) diluted 1:500, GADD45B (Biorbyt #ORB215494) diluted 1:500, SIK1 (Proteintec #51045-1-AP) diluted 1:500, mouse secondary antibody (Santa Cruz #sc-525409) diluted 1:20000, rabbit secondary antibody (Santa Cruz #sc-2357) diluted 1:5000.

2.11. Statistical analysis

Results are expressed as either mean \pm standard error of the mean (SEM) or median [interquartile range]. Pairwise group comparisons were calculated using Student's t test for Gaussian-distributed variables and Mann–Whitney U test for non-Gaussian-distributed data. The p value for trend was computed from the Pearson test to investigate whether or not the NAS systematically increases or decreases over the levels of the variables of interest. The statistical analysis was performed using R 4.0.3 (<http://www.r-project.org>) and the appropriate packages, and the level of significance was set at 0.05.

3. RESULTS

3.1. Identification of candidate genes potentially involved in adipose tissue – liver crosstalk

To obtain new insight into the molecular mechanisms underlying NAFLD progression, a global gene expression analysis from scWAT biopsies was carried out in 45 individuals. Table 2 describes phenotypical characteristics (clinical and biochemical) of selected patients (discovery cohort). This cohort encompasses both female (60%) and male patients (40%) with different BMI levels (7% normoweight, 7% overweight and 86% obese) and considerable presence of general descriptors of metabolic syndrome features.

In the discovery phase of this study, we used the Fatty Liver Index (FLI) as a proxy for the severity of liver steatosis¹². To explore the broad molecular mechanisms behind the liver fat accumulation, we performed a weighted correlation network analysis (WGCNA). This systems biology method is useful for finding and summarizing clusters of highly correlated genes (modules)¹⁶. The mRNA levels of 11651 genes expressed in scWAT biopsies with clinical information were included in the analysis and a power of $\beta = 5$ was selected to ensure a scale-free network (Figure 2A). We detected 9 gene modules (8 co-expression modules and 1 module with the remaining uncorrelated genes), among which

the number of genes ranged from 89 to 3501 (Figure 2B). We then calculated associations of each module with the FLI. Two modules (Pink and Red) were positively associated with FLI while 3 modules (Brown, Yellow, and Grey) showed a negative correlation with FLI (Figure 2C). Gene Ontology enrichment analysis showed that the Pink module consisted of genes involved in white blood cell migration and chemotaxis processes, while most of the genes in the Red modules engaged in immune responses (Figure 2D). On the other hand, the biological processes-enrichment analysis also showed that the Brown module was significantly enriched for genes involved in the regulation of transcription, while genes in the Yellow module were associated with sensory perception, which might reflect the cross-talk between the nervous system and the adipose tissue. Lastly, the genes included in the Grey module were connected with regulation of molecular functions.

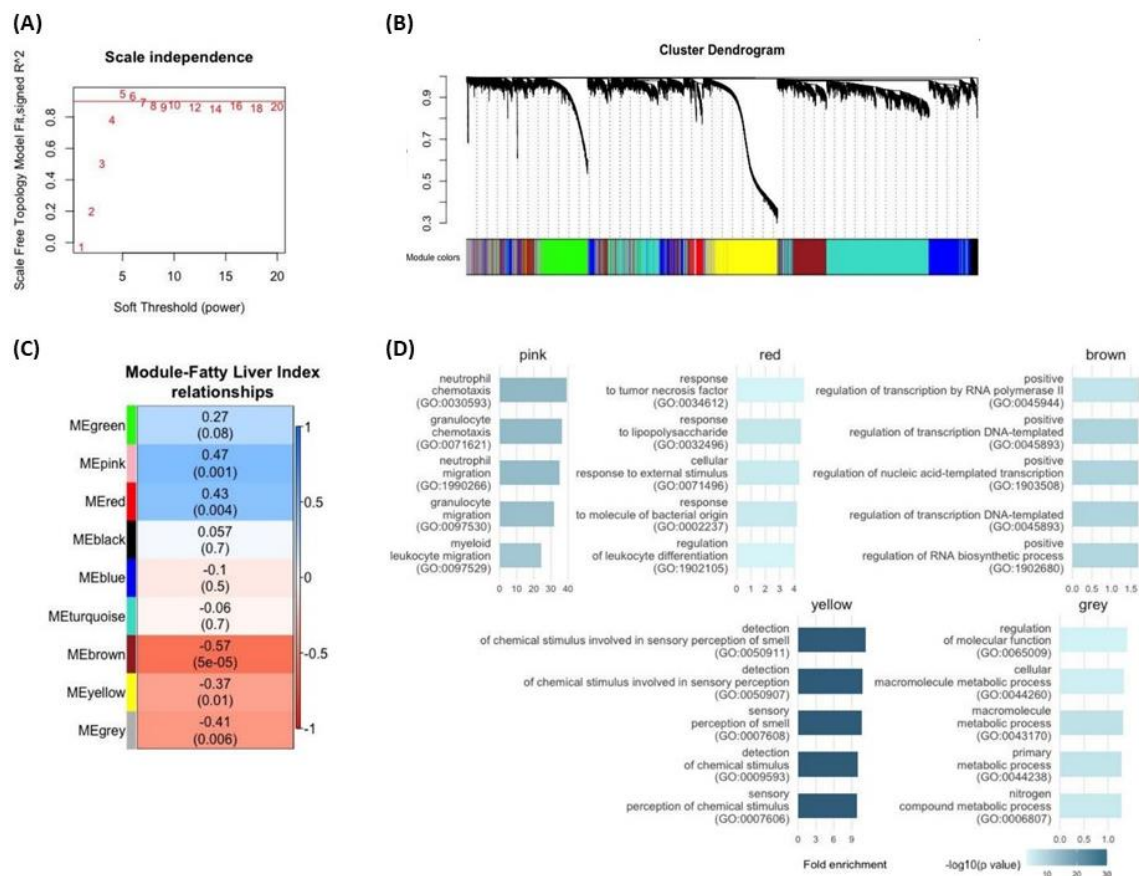


Figure 2. Weighted gene co-expression network analysis (WGCNA). (A) Determination of soft-thresholding power. (B) Hierarchical clustering of identified co-expressed genes in modules. Colored rows represent a color-coded module which contains a group of highly connected genes. (C) Heatmap of the correlation between module eigengenes (ME) and the fatty liver index. Each cell contains the correlation coefficient and the associated p-value. (D) Top five enrichment results of GO-Biological process for significant modules. The number of genes in the selected co-expression modules were 79 (Pink), 397 (Red), 1632 (Brown), 1610 (Yellow), and 1270 (Grey).

Table 2. Clinical and biochemical characteristics of the three cohorts and their statistical differences. Data are presented as number (%) or median [interquartile range]. Subjects were categorized as hypertensive, dyslipemic or diabetic following ATPIII criteria ¹¹. Differences between groups were tested with the Student's t-test; BMI, body mass index (kg/m²); GGT, gamma-glutamyl transpeptidase; AST, aspartate transaminase; ALT, alanine transaminase.

Cohort			Comparison		
Discovery	Validation	hMSC	p.Discovery vs Validation	p.Discovery vs hMSC	p.Validation vs hMSC
N = 45 N = 47 N = 13					
Sex:			0.870	0.853	0.853
Male	18 (40.0%)	17 (36.2%)	7 (53.8%)		
Female	27 (60.0%)	30 (63.8%)	6 (46.2%)		
Age (years)	48 [41.0; 54.0]	45 [40.5; 50.0]	47 [42.0; 51.0]	0.716	0.716
BMI	39.9 [35.9;44.6]	47.3 [42.8;50.7]	44.1 [41.7;50.3]	<0.001	0.003
BMI Category			0.023	1.000	1.000
Normoweight	3 (6.67%)	0 (0.00%)	0 (0.00%)		
Overweight	3 (6.67%)	0 (0.00%)	0 (0.00%)		
Obesity	39 (86.7%)	47 (100%)	13 (100%)		
Hypertension	19 (42.2%)	25 (53.2%)	6 (46.2%)	1.000	1.000
Dyslipidemia	13 (28.9%)	17 (36.2%)	7 (53.8%)	0.601	0.334
Diabetes	10 (22.2%)	17 (36.2%)	5 (38.5%)	0.432	0.432
Glucose (mg/dl)	96.5 [85.5;108]	103 [89.5;117]	117 [102;134]	0.119	0.040
Triglycerides (mg/dl)	98.0 [88.0;124]	127 [95.0;180]	144 [110;165]	0.049	0.049
Cholesterol (mg/dl)	191 [175;226]	188 [165;214]	188 [145;206]	0.596	0.596
GGT (U/l)	24.0 [18.0;40.0]	35.0 [23.5;44.0]	37.5 [25.0;48.5]	0.042	0.061
AST (U/l)	28.5 [22.0;35.2]	22.0 [18.5;31.0]	25.0 [22.8;28.8]	0.053	0.555
ALT (U/l)	28.0 [18.0;36.5]	25.0 [20.0;41.0]	40.0 [24.2;43.2]	0.699	0.268
Leptin (ng/mL)	22.1 [8.95;36.5]	51.3 [33.9;80.6]	50.5 [27.2;72.9]	<0.001	0.003
Glycated hemoglobin (mmol/mol)	5.70 [5.40;6.00]	5.80 [5.60;6.70]	5.60 [5.45;6.70]	0.211	0.690
					0.669

For a more focused candidate-gene approach, we applied Spearman correlation to identify a set of genes whose expression profiles varied with the severity of the fatty liver. Out of 17747 genes, we found 475 genes strongly correlated with the FLI score ($\rho > 0.5$ or $\rho < -0.5$, $p < 0.0001$) (Figure 3A). Those candidate genes were distributed over all 22 autosomes and the X chromosome. None were found on the Y chromosome (Figure 3B). Using a false discovery rate (FDR) threshold of $q < 0.003$, we observed 81 differentially expressed genes (DEG) associated with FLI (Supplementary Figure 1). In the next step, we selected only positively correlated genes ($n = 30$), since our main objective was to find targets susceptible of being knocked-down.

Among those transcripts which displayed this positive association, a thorough bibliographic analysis was carried out to rank these genes according to their potential relevance and whose function had been previously linked to fatty acid metabolism and/or liver function. We finally selected 8 genes: *SOCS3*, *DUSP1*, *SIK1*, *GADD45B*, *S100A9*, *S100A12*, *CTGF* and *CDKN1A* (Figure 3C). It should be noted that all these genes were included in the Red module delimited by the WCNA, except for *S100A9* and *S100A12* which appeared in the Pink module. These candidate genes were further considered for subsequent analysis.

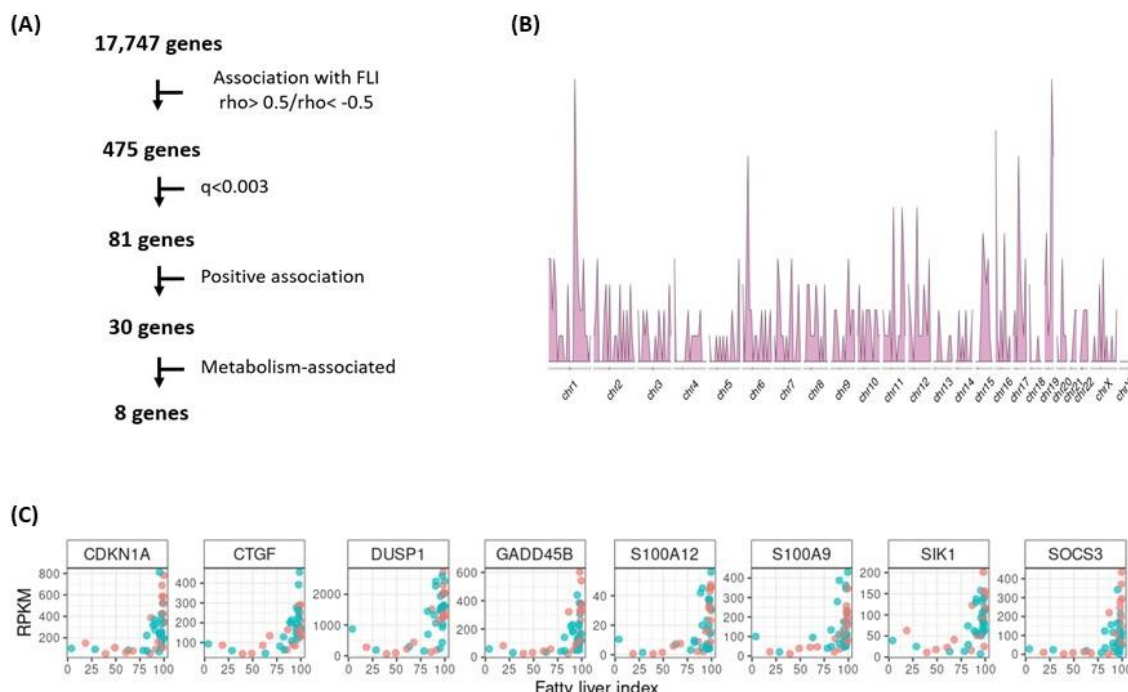


Figure 3. Identification of candidate genes potentially involved in adipose tissue – liver crosstalk. (A) Workflow of RNA-Seq analysis. (B) Chromosomal distribution of genes whose expression profiles varied with the severity of the NAFLD. (C) Expression of selected genes according to fatty liver index (FLI); male in red and female in blue; RPKM (Reads per kilo base per million mapped reads).

3.2. Validation of candidate genes in scWAT biopsies from a second (validation) cohort

To validate those candidate genes obtained from previous RNA sequencing analysis, their mRNA expression was determined in scWAT from a second validation cohort. This validation cohort included 47 subjects with a similar age and sex distribution to the discovery cohort. This validation cohort encompassed only obese patients ($BMI > 30 \text{ kg/m}^2$) who presented increased values of triglycerides, GGT, and leptin compared to their discovery cohort counterparts (Table 2).

Subsequently, mRNA levels of selected genes were quantified in scWAT by real-time qRT-PCR. All candidates showed mRNA levels within widely accepted range of Ct values indicative of a constitutive adipose tissue expression ($Ct \approx 16-25$). Proving that the strength of this validation cohort is that it encompasses both scWAT and liver biopsies from the same patient, subjects were categorized according to their liver biopsies NAFLD activity score (NAS) into 3 groups: NAS = 0 - 1 ($n = 26$), NAS = 2 - 3 ($n = 14$), NAS 4 - 5 ($n = 7$). Consistent with the previous RNA-seq data in scWAT, mRNA levels of *SOCS3*, *DUSP1*, *SIK1*, *GADD45B*, *S100A9* and *S100A12* were also positively associated ($p < 0.05$) with hepatic steatosis (NAS) in this second validation cohort (Figure 4A-F, Supplementary Table 1). *CDKN1A* and *CTGF* did not replicate that association and were excluded from subsequent analyses (Figure 4G-H, Supplementary Table 1).

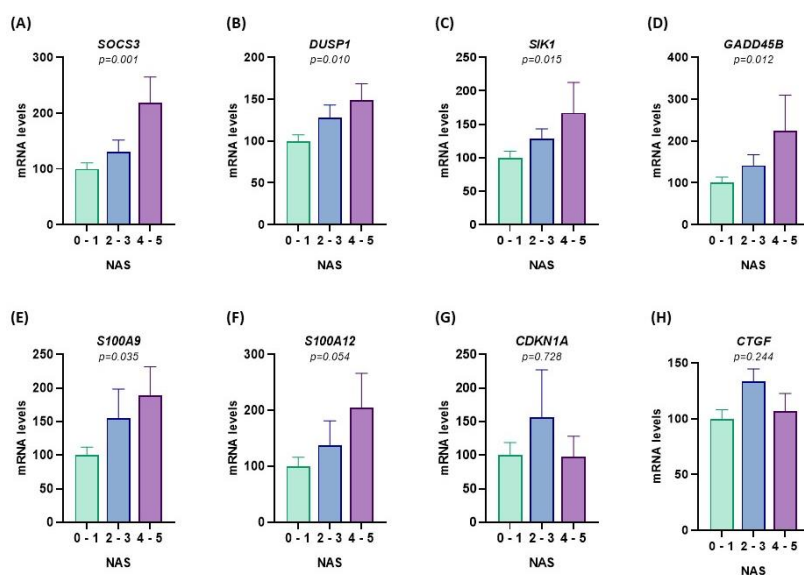


Figure 4. mRNA expression of *SOCS3* (A), *DUSP1* (B), *SIK1* (C), *GADD45B* (D), *S100A9* (E), *S100A12* (F), *CDKN1A* (G) and *CTGF* (H) in scWAT of patients from the validation cohort grouped according to their Nonalcoholic fatty liver disease Activity Score (NAS) (NAS = 0 - 1, $n = 26$; NAS = 2 - 3, $n = 14$; NAS 4 - 5, $n = 7$). Relative gene expression was normalized to β -ACTIN and values are expressed as mean \pm SEM. P: p-value for the trend.

Furthermore, expression of selected genes was also analyzed in paired visWAT biopsies ($n = 47$) from this second validation cohort. The association observed in scWAT was replicated in visWAT for *S100A9* and *S100A12*, but not for *SOCS3*, *DUSP1*, *SIK1*, *GADD45B*, *CDKN1A* and *CTGF*, suggesting a specific gene regulation of these candidates in scWAT fat depot (Supplementary Table 1).

3.3. Lipid content of adipocyte differentiated hMSC and their corresponding liver biopsies

Next, we sought to further characterize the specific role of adipocytes in fatty liver progression. To this end, hMSCs were isolated from scWAT biopsies and differentiated into adipocytes¹⁴. Thirteen different donors were included in this new *in vitro* hMSC cohort. Importantly, we observed no significant differences in any relevant clinical or biochemical parameter when comparing the hMSC donors and the discovery cohort (Table 2).

In order to test the functional feasibility of our hMSC cohort, adipogenic differentiation capacity of the selected 13 hMSC cell lines was compared by 1) quantifying oil red O (ORO) staining of lipid droplets in adipocytes and 2) by analyzing mRNA expression of a well-established adipocyte-related transcript, fatty acid binding protein 4 (*FABP4*)¹⁷. At day 8 post-differentiation, we observed a strong correlation between these two differentiation markers ($r = 0.45$, $p = 0.012$) which demonstrated that both are reliable indicators of the degree of adipocyte differentiation (Supplementary Figure 2).

To elucidate whether hMSC-derived adipocyte differentiation potential was associated with the liver phenotype of the donor, those 13 cell lines were grouped according to the NAS of the patient (NAS 0 – 1, $n = 4$; NAS 2 – 3, $n = 5$; NAS 4 – 5, $n = 4$). We observed an increased differentiation capacity, measured by both ORO and *FABP4* mRNA expression, from first group (NAS 0 - 1) compared to the third group (NAS 4 - 5) which had the lowest differentiation potential (Figure 5).

These results suggest that a lower lipid storage capacity of differentiated subcutaneous adipocytes *in vitro* could be related to an increased fat accumulation in liver. Therefore, these data validate our model and cohort of hMSC derived-adipocyte as a reliable tool to further characterize fatty liver disease progression.

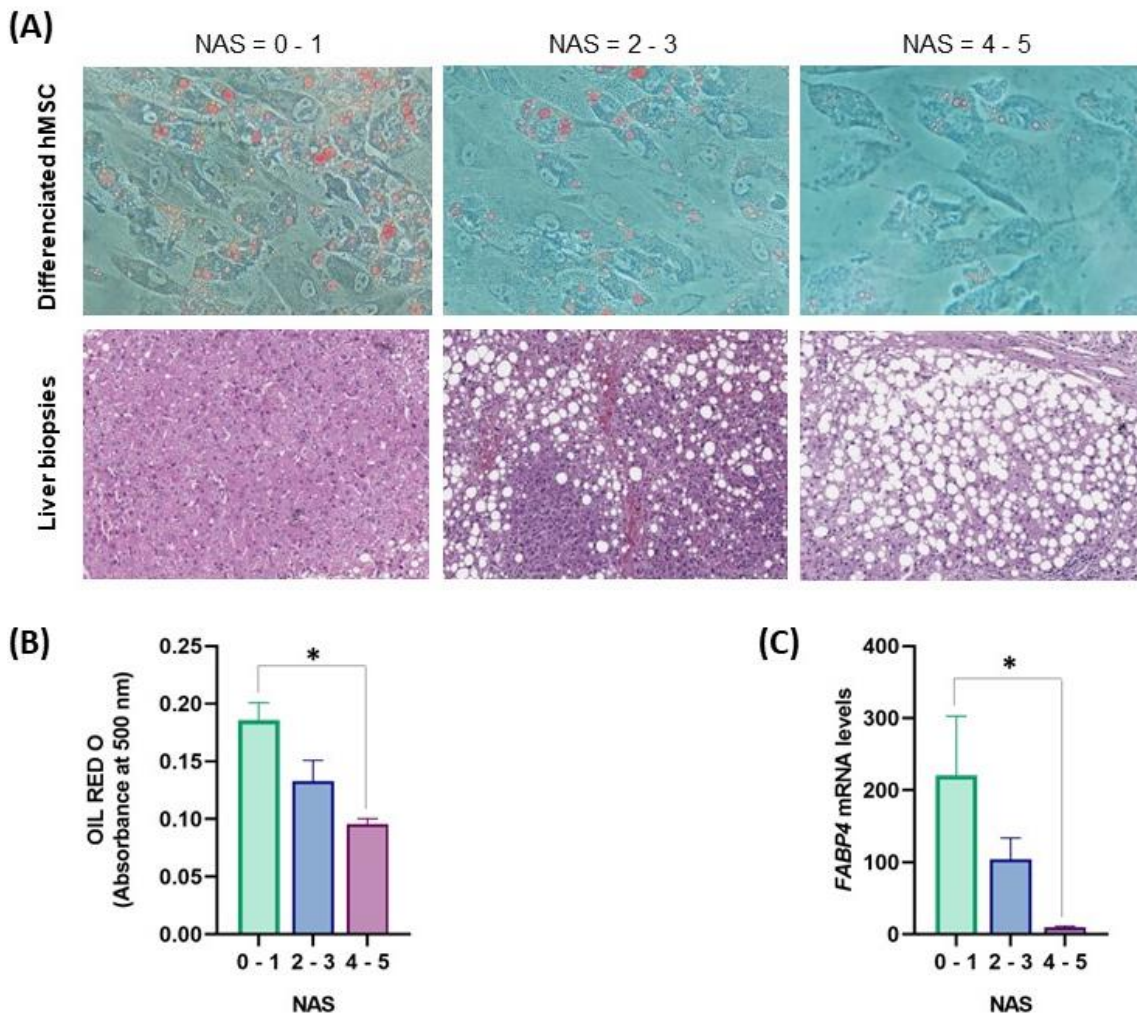


Figure 5. Fat content of adipocyte differentiated hMSC and their corresponding liver biopsies.
(A). Oil Red O staining of hMSC-derived adipocyte (top panel) and liver histological examination stained with H&E (lower panel) from the same patient, each one representative of the overall subgroup. Quantification (absorbance at 500 nm) of Oil Red O staining (B) and FABP4 mRNA expression (C) in 13 lines of hMSC-derived adipocytes grouped according to the Nonalcoholic fatty liver disease Activity Score (NAS) of the donor. Relative mRNA expression was normalized to β -ACTIN and values are expressed as mean \pm SEM. *, P < 0.05.

3.4. Expression of selected genes in differentiated hMSC of patients with different degrees of liver steatosis

To verify whether the previously observed differences in gene expression at scWAT level were adipocyte-specific or occurred in other cell types within the scWAT, we next investigated the expression levels of our candidate genes in previously characterized hMSC-derived adipocytes.

We observed a wide variation in the degree of differentiation of hMSC into adipocytes depending of the cell line (Figure 5). As mRNA levels refer to gene expression in the whole culture (including differentiated and undifferentiated cells), *FABP4* was used to normalize differences in adipocyte differentiation across the cell lines. We found high levels of mRNA expression of *SOCS3*, *DUSP1*, *SIK1* and *GADD45B*, but no expression of *S100A9* or *S100A12* was observed in any of the cell lines (data not shown). Moreover, a statistical significant increase was observed in mRNA levels of *SOCS3* ($p=0.015$), *DUSP1* ($p=0.05$), *SIK1* ($p=0.009$) and *GADD45B* ($p=0.016$) as donor's NAS increased (Figure 6A-D, Supplementary Table 2). These results confirm that these genes have a differential regulation pattern in adipocytes, that correlates with the degree of steatosis.

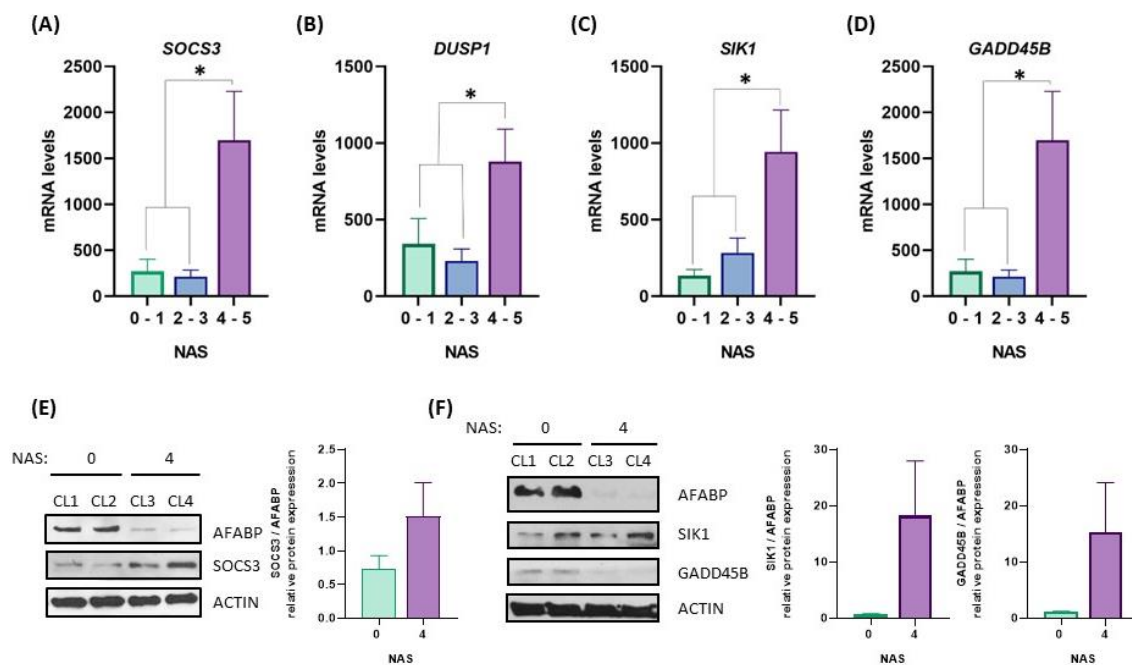


Figure 6. Expression of selected genes in hMSC-derived adipocytes of patients with different degrees of liver steatosis. (A-D) mRNA expression of *SOCS3* (A), *DUSP1* (B), *SIK1* (C) and *GADD45B* (D) in 13 cell lines of hMSC-derived adipocytes of patients grouped according to their Nonalcoholic fatty liver disease Activity Score (NAS) (NAS = 0-1, n=4; NAS = 2-3, n=5; NAS = 4-5, n=4). Relative gene expression was normalized to *FABP4* mRNA levels. (E-F) Western blot protein expression analysis of AFABP, *SOCS3*, *SIK1* and *GADD45B* in four different hMSC-derived adipocytes cell lines, two of them (CL1, CL2) obtained from scWAT of patients without liver steatosis (NAS = 0) and the other two (CL3, CL4) from patients with hepatosteatosis (NAS = 4). 20 μ g of cellular lysate were loaded for *SOCS3* detection (E) and 80 μ g for *SIK1* and *GADD45B* (F). Both Actin and AFABP were used as internal controls. Densitometry quantification was performed normalizing levels of protein expression to AFABP. Results show mean values of 3 independent experiments. Values are expressed as mean \pm SEM. *, $P < 0.05$. CL, cell line.

To further characterize the role of these genes, we performed a protein expression analysis in four different cell lines, two of them obtained from scWAT of patients without liver steatosis (NAS = 0) and the other two from patients with high degree of hepatosteatosis (NAS = 4). Consistent with mRNA data, AFABP protein expression was significantly upregulated in cell lines of patients with lower steatosis, showing the higher adipogenic capacity of these lines. To reduce differences in adipocyte differentiation across the cell lines, candidates' protein expression was normalized to AFABP. We observed a significant increase of SOCS3, SIK1 and GADD45B protein expression as steatosis increases (Figure 6E, F), following a concordant regulatory pattern between gene and protein expression. However, we could not replicate *DUSP1* mRNA expression outcomes at the protein level.

4. DISCUSSION

The main objective of this study was to clarify the physiological role that impaired scWAT expansion plays in the development and progression of NAFLD. To this end, we have analyzed scWAT biopsies to reveal genes associated with NAFLD progression and we have also established and validated an *in vitro* model to study adipose tissue in NAFLD based on hMSC-derived adipocytes isolated from patients with this condition. Our main outcome is that we identify four genes whose expression increases accordingly to the degree of hepatic steatosis both in scWAT and hMSC-derived adipocytes: *SOCS3*, *DUSP1*, *SIK1* and *GADD45B*.

The first objective of our study was to uncover novel genes whose regulation in scWAT could be essential in the progression of NAFLD. We initially performed a high throughput gene expression analysis from scWAT of patients with different degrees of liver steatosis and correlated these results with FLI. Although previous studies have proposed this biochemical parameter as a strong surrogate biomarker of liver steatosis¹⁸, FLI calculation is built upon anthropometric and biological variables that are altered in other metabolic disturbances, therefore these associations might be due to other non-liver-related diseases^{19–21}. However, we excluded this possibility by testing our candidate genes in a second cohort with similar prevalence of obesity-associated conditions (i.e. hypertension, dyslipidemia, and diabetes) and more importantly, where subjects were categorized according to their NAS. This histological score obtained from liver biopsies

is, to this date, the most accurate method to diagnose liver steatosis¹³. This two-step validation of our findings in two independent cohorts of patients highlights the relevance of our experimental design as a cornerstone in addressing our research purpose.

The second objective of this study was to establish an *in vitro* model of hMSC-derived adipocytes that could reflect the different stages of NAFLD. Several studies have shown that hMSC isolated from scWAT of patients with metabolic disorders like obesity and diabetes are defective in various functionalities and properties²² including differentiation²³, multipotent state^{24,25}, metabolism^{26,27} and immunomodulation²⁸. Considering that, we tried to address if there were also a correlation between the physiological status of hMSC and the degree of liver steatosis in order to directly link adipose tissue expandability capacity to dysfunctional liver crosstalk.

As observed in hMSC from morbid obese patients²⁹, lipid accumulation in hMSC-derived adipocytes from NAFLD patients was decreased, indicating impaired adipogenesis of these pre-adipocytes along with NAFLD severity. This negative association between the adipogenic potential of hMSC and the degree of liver steatosis suggests that impaired hMSC differentiation relates to altered WAT expandability and thus, could be a crucial step in development and progression of NAFLD. Indeed, a lower lipid storage capacity in adipocytes may eventually promote fat accumulation in the liver, which is in agreement with previous reports³⁰ and consistent with our WAT expandability hypothesis. It can be argued that 5 out of 13 patients are diabetic in our hMSC cohort and impaired adipogenesis is also associated with diabetes²³. However, we observed the same inverse association between markers of adipogenic differentiation (Oil Red O and FABP4) and NAFLD severity in both diabetic and non-diabetic patients (Supplementary Figure 3). This lends more plausibility to the relationship between adipogenesis and NAFLD progression.

These data validate our *in vitro* model and cohort of hMSC-derived adipocytes as a reliable and robust tool to further characterize the implication of scWAT in fatty liver disease progression. This model could overcome the possible limitations found in other *in vitro* approaches³¹, providing that our model not only discriminates between healthy and unhealthy patients but also distinguishes between different stages of the disease. Eventually, this “proposed” model (clinical data and associated hMSC-derived

adipocytes) could be also of interest to address other research questions related to obesity-associated disorders such as diabetes, insulin resistance or cardiovascular diseases.

Taking advantage of the two main points underlined in this study, we further corroborated that the differential regulation of these four genes observed at scWAT level actually come from single adipocytes and not from other non-adipose cell types within this tissue. *SOCS3*, *DUSP1*, *SIK1* and *GADD45B* showed the same regulatory pattern in hMSC-derived adipocytes as observed in scWAT, reinforcing the idea that these genes are directly involved in NAFLD progression by exerting regulatory actions specifically in adipocytes (f. i., re-directing lipid flux from adipose tissue to the liver) thus, limiting scWAT fat accumulation capacity and lipid metabolism.

Interestingly, the regulatory pattern observed at mRNA level was translated to protein level for *SOCS3*, *SIK1* and *GADD45B*, but we did not observe the presence of *DUSP1* at the protein level in fully differentiated hMSC-derived adipocytes. Ferguson et al. have shown that this protein is only produced by 3T3L1 cells in the early phase of adipocyte differentiation³². Therefore, we hypothesize that *DUSP1* may be playing an important role in scWAT *in vivo*, where there are hMSC at different stages of differentiation. Alternatively, *DUSP1* mRNA could have regulatory effects in the early phase of adipocyte differentiation without being translated into protein.

On the other hand, the expression of these genes in visWAT do not correlate with liver steatosis, suggesting a specific regulation of *SOCS3*, *DUSP1*, *SIK1* and *GADD45B* in scWAT, that differs from visWAT. However, genes which are not expressed in adipocytes, *S100A9* and *S100A12*, showed the same regulatory pattern in both fat depots. These results suggest that the expression of *S100A9* and *S100A12* in WAT is also related with NAFLD but it comes from other cellular type(s) within the WAT, probably immune system cells³³. This hypothesis is supported by our bioinformatic analysis which found that the *S100A9* and *S100A12* genes included in the cluster enriched for genes related to white blood cell metabolism.

Previous studies support our findings, reporting a critical role of these newly identified genes in lipid metabolism (including lipid synthesis, breakdown and oxidation) in several models. For instance, liver-specific *SOCS3* deletion in mice enhances hepatic insulin sensitivity and lipogenesis resulting in fatty liver and obesity^{34,35}, while its overexpression in scWAT causes local insulin resistance^{36,37}. However, whether these

results are translated to humans remains still elusive. Other studies have also reported *DUSP1* overexpression in scWAT and peripheral blood mononuclear cells of obese humans³⁸, while its liver-specific overexpression in mice is linked to the promotion of hepatosteatosis³⁹. Moreover, *DUSP1* regulates signaling during early 3T3-L1 adipocytes differentiation³². On the other hand, *SIK1* is involved in regulation of hepatic lipogenesis by controlling SREBP-1c phosphorylation⁴⁰ and promotes insulin resistance in obesity in mouse models⁴¹, whereas *GADD45B* has been shown to play a role in coordination of liver fatty acid uptake and metabolic health⁴² and regulates hepatic gluconeogenesis in mice⁴³.

This evidence points out the relevance of these genes in NAFLD progression and future functional studies will contribute to decipher their actions in humans and within metabolic disease context. However, important questions also arise from our current findings: for instance, how the temporal expression dynamics and the potential interaction of these candidates affect the clinical phenotype (NAFLD development and its severity). Indeed, these newly identified genes could be also considered as potential biomarkers of disease progression (alone or combined with other parameters) although some limitations exist and should be also considered with caution (scWAT biopsies availability). Besides, our results concern mainly to individuals with obesity and whether these changes fully translate to non-obese also warrants further investigations.

In conclusion, our results constitute a proof-of-evidence of the paramount importance of adipose-liver crosstalk and suggest that impaired adipogenic capacity of hMSC is a critical event in promoting the development of NAFLD. Restoration of fully functional hMSC phenotype (such as through specific gene(s) modulation) might be an additional strategy to address NAFLD and its associated complications. We propose four genes from scWAT: *SOCS3*, *DUSP1*, *SIK1*, and *GADD45B* as key players in NAFLD progression. Although more functional interventions are warranted to test the cause and effect relationship, these genes could constitute potential new targets for future therapies.

Acknowledgments

We thank Prof. Emilio Sancho, Arturo Perez, and J. Rodriguez for their guidance in our studies on liver toxicity.

We want to particularly acknowledge all the patients included in the study, as well as the IACS Functional Genomics and Sequencing Core and the Biobank of the Aragon Health System (PT20/00112) integrated in the Spanish National Biobanks Network.

Conflict of Interest

The authors declare that they have no conflicts of interest.

Author Contributions

M.L.-Y., S.L.-C., and J.M.A.-M. designed the study. M.L.-Y., R.d.M.-B. and M.P.G.-S. performed research, V. B.-M., C.H., C.C. and A. S.-P. provided and analyzed samples, M.L.-Y., S.L.-C. and J.M.A.-M. analyzed data and wrote the manuscript; R.d.M.-B., M.P.G.-S., V. B.-M., C.H., C.C. and A. S.-P. reviewed the manuscript. All authors have read and agreed to the published version of the manuscript.

Funding

This study was sponsored by a grant (PI17/02268) from the Instituto de Salud Carlos III and by FEDER funds: “Una manera de hacer Europa” and by the regional government of Aragón (B03_20R), co-financed with the FEDER Aragón 2014–2020: “Construyendo Europa desde Aragón”.

Data Availability Statement

Gene expression and patient data is held by the Aragón Institute of Health Sciences (IACS). Access may be granted to those who meet pre-specified criteria for confidential access, available at <https://www.iacs.es/instituto-aragones-ciencias-la-salud/oficina-virtual/solicitud-de-acceso-a-datos-para-realizacion-de-un-proyecto-de-investigacion-rpi01-3a> and with prior authorization by the Ethics Committee of Aragon (CEIC-A) which can be obtained at <https://www.iacs.es/investigacion/comite-de-etica-de-la-investigacion-de-aragon-ceica/ceica-evaluaciones-y-otras-presentaciones/>.

5. REFERENCES

- 1 Large V, Peroni O, Letexier D, Ray H, Beylot M. Metabolism of lipids in human white adipocyte. *Diabetes Metab.* 2004;30(4):294–309.
- 2 Choe SS, Huh JY, Hwang IJ, Kim JI, Kim JB. Adipose tissue remodeling: Its role in energy metabolism and metabolic disorders. *Front Endocrinol (Lausanne)*. 2016;7(APR):1–16.
- 3 Virtue S, Vidal-Puig A. Adipose tissue expandability, lipotoxicity and the Metabolic Syndrome - An allostatic perspective. *Biochim Biophys Acta - Mol Cell Biol Lipids*. 2010;1801(3):338–349.
- 4 Hammarstedt A, Gogg S, Hedjazifar S, Nerstedt A, Smith U. Impaired adipogenesis and dysfunctional adipose tissue in human hypertrophic obesity. *Physiol Rev*. 2018;98(4):1911–1941.
- 5 McQuaid SE, Hodson L, Neville MJ et al. Downregulation of adipose tissue fatty acid trafficking in obesity: A driver for ectopic fat deposition? *Diabetes*. 2011;60(1):47–55.
- 6 Ipsen DH, Lykkesfeldt J, Tveden-Nyborg P. Molecular mechanisms of hepatic lipid accumulation in non-alcoholic fatty liver disease. *Cell Mol Life Sci*. 2018;75(18):3313–3327.
- 7 Younossi Z, Anstee QM, Marietti M et al. Global burden of NAFLD and NASH: trends, predictions, risk factors and prevention. *Nat Rev Gastroenterol Hepatol*. 2018;15(1):11–20.
- 8 Stefan N, Kantartzis K, Häring H-U. Causes and metabolic consequences of Fatty liver. *Endocr Rev*. 2008;29(7):939–960.
- 9 Azzu V, Vacca M, Virtue S, Allison M, Vidal-Puig A. Adipose Tissue-Liver Cross Talk in the Control of Whole-Body Metabolism: Implications in Nonalcoholic Fatty Liver Disease. *Gastroenterology*. 2020;158(7):1899–1912.
- 10 Torres-Perez E, Valero M, Garcia-Rodriguez B et al. The FAT expandability (FATe) Project: Biomarkers to determine the limit of expansion and the complications of obesity. *Cardiovasc Diabetol*. 2015;14(1):1–8.
- 11 Piepoli MF, Hoes AW, Agewall S et al. 2016 European Guidelines on cardiovascular disease prevention in clinical practice: The Sixth Joint Task Force of the European Society of Cardiology and Other Societies on Cardiovascular Disease Prevention in Clinical Practice (constituted by representati. *Eur Heart J*. 2016;37(29):2315–2381.
- 12 Bedogni G, Bellentani S, Miglioli L et al. The fatty liver index: A simple and accurate predictor of hepatic steatosis in the general population. *BMC Gastroenterol*. 2006;6:1–7.
- 13 Kleiner DE, Brunt EM, Van Natta M et al. Design and validation of a histological scoring system for nonalcoholic fatty liver disease. *Hepatology*. 2005;41(6):1313–1321.
- 14 Perez-Diaz S, Garcia-Rodriguez B, Gonzalez-Irazaba Y, Valero M, Lagos-Lizan J, Arbones-Mainar JM. Knockdown of PTRF ameliorates adipocyte differentiation and functionality of human mesenchymal stem cells. *Am J Physiol - Cell Physiol*. 2017;312(1):C83–C91.
- 15 Ramírez-Zacarías JL, Castro-Muñozledo F, Kuri-Harcuch W. Quantitation of adipose conversion and triglycerides by staining intracytoplasmic lipids with oil red O. *Histochemistry*. 1992;97(6):493–497.
- 16 P. Langfelder and S. Horvath. WGCNA: an R package for weighted correlation network analysis. *BMC Bioinformatics*, Dec 29;9:559.
- 17 Garin-Shkolnik T, Rudich A, Hotamisligil GS, Rubinstein M. FABP4 attenuates PPAR γ and

- adipogenesis and is inversely correlated with PPAR γ in adipose tissues. *Diabetes*. 2014;63(3):900–911.
- 18 Kitazawa A, Maeda S, Fukuda Y. Fatty liver index as a predictive marker for the development of diabetes: A retrospective cohort study using Japanese health check-up data. *PLoS One*. 2021;16(9 September):1–15.
- 19 Guiu B, Crevisy-Girod E, Binquet C et al. Prediction for steatosis in type-2 diabetes: Clinico-biological markers versus 1H-MR spectroscopy. *Eur Radiol*. 2012;22(4):855–863.
- 20 Kahl S, Straßburger K, Nowotny B et al. Comparison of liver fat indices for the diagnosis of hepatic steatosis and insulin resistance. *PLoS One*. 2014;9(4).0094059.
- 21 Fedchuk L, Nascimbeni F, Pais R, Charlotte F, Housset C, Ratziu V. Performance and limitations of steatosis biomarkers in patients with nonalcoholic fatty liver disease. *Aliment Pharmacol Ther*. 2014;40(10):1209–1222.
- 22 Louwen F, Ritter A, Kreis NN, Yuan J. Insight into the development of obesity: functional alterations of adipose-derived mesenchymal stem cells. *Obes Rev*. 2018;19(7):888–904.
- 23 Oliva-Olivera W, Coin-Aragüez L, Lhamyani S et al. Adipogenic impairment of adipose tissue-derived mesenchymal stem cells in subjects with metabolic syndrome: Possible protective role of FGF2. *J Clin Endocrinol Metab*. 2017;102(2):478–487.
- 24 Oñate B, Vilahur G, Camino-López S et al. Stem cells isolated from adipose tissue of obese patients show changes in their transcriptomic profile that indicate loss in stemcellness and increased commitment to an adipocyte-like phenotype. *BMC Genomics*. 2013;14(1):1–12.
- 25 Pérez LM, Bernal A, De Lucas B et al. Altered metabolic and stemness capacity of adipose tissue-derived stem cells from obese mouse and human. *PLoS One*. 2015;10(4):1–22.
- 26 Pérez LM, Suárez J, Bernal A, De Lucas B, San Martin N, Gálvez BG. Obesity-driven alterations in adipose-derived stem cells are partially restored by weight loss. *Obesity*. 2016;24(3):661–669.
- 27 Mastrangelo A, Panadero MI, Perez LM et al. New insight on obesity and adipose-derived stem cells using comprehensive metabolomics. *Biochem J*. 2016;473(14):2187–2203.
- 28 Serena C, Keiran N, Ceperuelo-Mallafre V, Ejarque M, Fradera R, Roche K, Nuñez-Roa C VJ. Obesity and Type 2 Diabetes Alters the Immune Properties of Human Adipose Derived Stem Cells. *Stem Cells Express*. 2016;:2078–2084.
- 29 Silva KR, Liechocki S, Carneiro JR et al. Stromal-vascular fraction content and adipose stem cell behavior are altered in morbid obese and post bariatric surgery ex-obese women. *Stem Cell Res Ther*. 2015;6(1):1–13.
- 30 Qureshi K, Abrams GA. Metabolic liver disease of obesity and role of adipose tissue in the pathogenesis of nonalcoholic fatty liver disease. *World J Gastroenterol*. 2007;13(26):3540–3553.
- 31 Kanuri G, Bergheim I. In vitro and in vivo models of non-alcoholic fatty liver disease (NAFLD). *Int J Mol Sci*. 2013;14(6):11963–11980.
- 32 Ferguson BS, Nam H, Stephens JM, Morrison RONF. Mitogen-Dependent Regulation of DUSP1 Governs ERK and p38 Signaling During Early 3T3-L1 Adipocyte Differentiation. *J Cell Physiol*. 2016;231(7):1562–1574.
- 33 Mossel DM, Moganti K, Riabov V et al. Epigenetic Regulation of S100A9 and S100A12

- Expression in Monocyte-Macrophage System in Hyperglycemic Conditions. *Front Immunol.* 2020;11(June):1–19.
- 34 Ogata H, Chinen T, Yoshida T et al. Loss of SOCS3 in the liver promotes fibrosis by enhancing STAT3-mediated TGF- β 1 production. 2006;(February):2520–2530.
- 35 Sachithanandan N, Fam BC, Fynch S et al. Liver-Specific Suppressor of Cytokine Signaling-3 Deletion in Mice Enhances Hepatic Insulin Sensitivity and Lipogenesis Resulting in Fatty Liver and Obesity. *Hepatology*. 2010:1632–1642.
- 36 Shi H, Cave B, Inouye K, Bjørbaek C, Flier JS. Overexpression of Suppressor of Cytokine Signaling 3 in Adipose Tissue Causes Local but Not Systemic Insulin Resistance. *Diabetes*. 2006;(April). doi:10.2337/diabetes.55.03.06.db05-0841.
- 37 Papers JBC, Doi M, Shi H, Tzameli I, Bjørbaek C, Flier JS. Suppressor of Cytokine Signaling 3 Is a Physiological Regulator of Adipocyte Insulin Signaling. *J Biol Chem*. 2004;279(33):34733–34740.
- 38 Khadir A, Tiss A, Abubaker J et al. Map kinase phosphatase dusp1 is overexpressed in obese humans and modulated by physical exercise. *Am J Physiol - Endocrinol Metab*. 2015;308(1):E71–E83.
- 39 Lawan A, Zhang L, Gatzke F et al. Hepatic mitogen-activated protein kinase phosphatase 1 selectively regulates glucose metabolism and energy homeostasis. *Mol Cell Biol*. 2015;35(1):26–40.
- 40 Yoon YS, Seo WY, Lee MW, Kim ST, Koo SH. Salt-inducible kinase regulates hepatic lipogenesis by controlling SREBP-1c phosphorylation. *J Biol Chem*. 2009;284(16):10446–10452.
- 41 Nixon M, Stewart-fitzygibbon R, Fu J et al. Skeletal muscle salt inducible kinase 1 promotes insulin resistance in obesity. *Mol Metab*. 2016;5(1):34–46.
- 42 Fuhrmeister J, Zota A, Sijmonsma TP et al. Fasting-induced liver GADD 45 b restrains hepatic fatty acid uptake and improves metabolic health. *EMBO Mol Med*. 2016;8(6):654–669.
- 43 Kim H, Lee DS, An TH et al. GADD45 β Regulates Hepatic Gluconeogenesis via Modulating the Protein Stability of FoxO1. 2021;:1–13.

Supplementary material

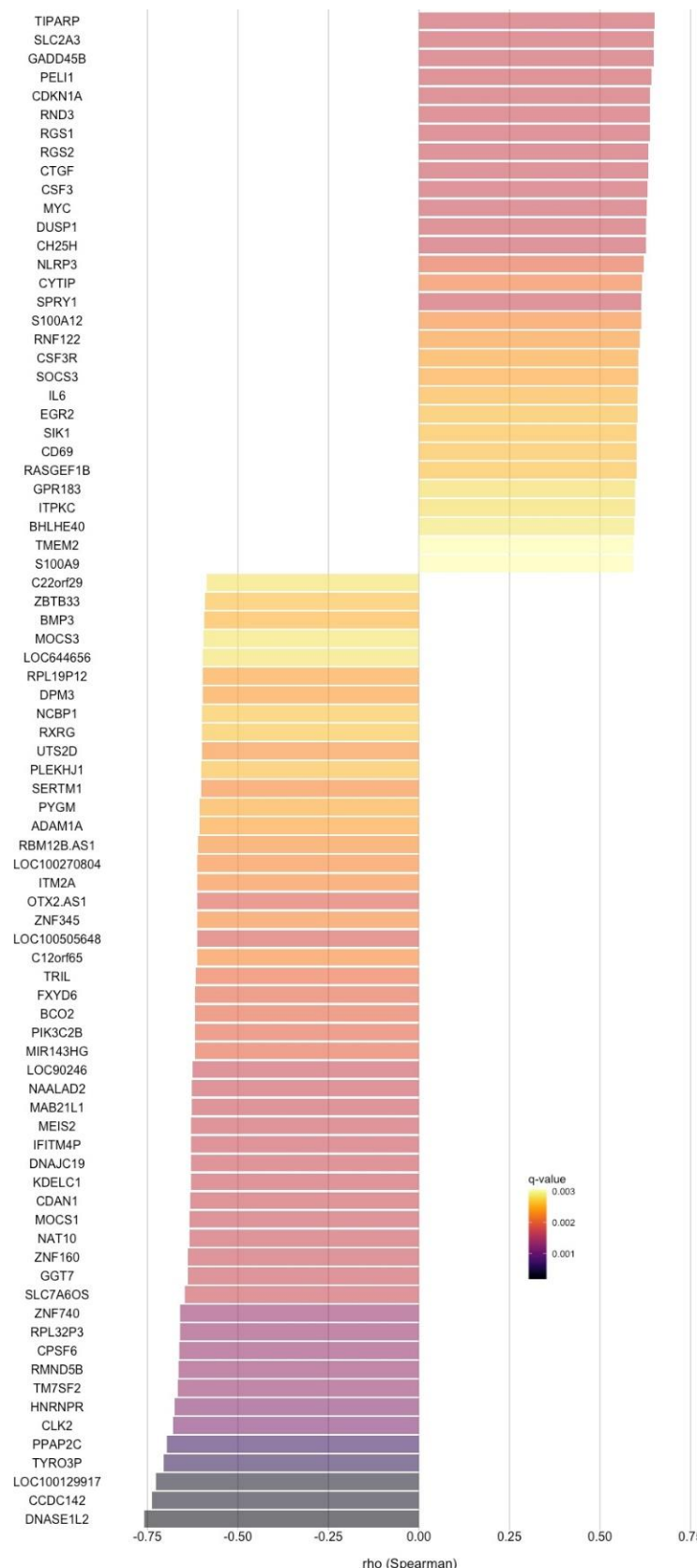
Supplementary Table 1. Correlations of mRNA expression levels of selected genes with Nonalcoholic fatty liver disease Activity Score (NAS) in scWAT and visWAT of patients of second cohort ($n = 47$). The table shows Pearson's correlation coefficient (r) and p-value for each gene in both fat depots.

		<i>SOCS3</i>	<i>DUSP1</i>	<i>SIK1</i>	<i>GADD45B</i>	<i>S100A9</i>	<i>S100A12</i>	<i>CDKN1A</i>	<i>CTGF</i>
<i>scWAT</i>	r	0.531	0.415	0.491	0.460	0.316	0.303	0.012	0.118
	p-value	< .001	0.005	< .001	0.001	0.032	0.040	0.939	0.428
<i>visWAT</i>	r	0.173	0.138	0.245	0.073	0.513	0.539	0.014	-0.158
	p-value	0.244	0.354	0.096	0.627	< .001	< .001	0.923	0.290

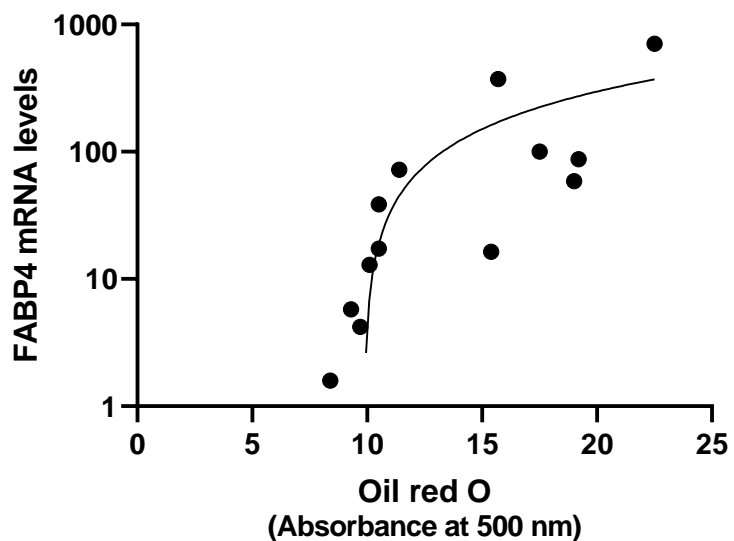
Supplementary Table 2. Correlations (Pearson's correlation coefficient, r and p-value) of mRNA expression levels of selected genes with Nonalcoholic fatty liver disease Activity Score (NAS) in 13 hMSC-derived adipocytes.

	<i>SOCS3</i>	<i>DUSP1</i>	<i>SIK1</i>	<i>GADD45B</i>
<i>r</i>	0.359	0.271	0.353	0.321
<i>p-value</i>	0.005	0.033	0.006	0.011

Supplemental Figure 1. Selected genes and correlation coefficients with the fatty liver index in the discovery cohort. Bar color indicates rho-associated q-value (all p-values<0.001).



Supplementary Figure 5. Correlation between Oil Red O staining and FABP4 mRNA expression (\log_{10}) in 13 cell lines of hMSC-derived adipocytes from different donors.



4.3. Chapter III

CRISPR/Cas9-mediated deletion of adipocyte genes associated with NAFLD alters adipocyte lipid handling and reduces steatosis in hepatocytes *in vitro*

The contents of this chapter have been adapted from the following published work:

Lopez-Yus, Marta *et al.* “CRISPR/Cas9-mediated deletion of adipocyte genes associated with NAFLD alters adipocyte lipid handling and reduces steatosis in hepatocytes *in vitro*.” *American journal of physiology. Cell physiology*, 10.1152/ajpcell.00291.2023. 18 Sep. 2023, doi:10.1152/ajpcell.00291.2023

CRISPR/Cas9-mediated deletion of adipocyte genes associated with NAFLD alters adipocyte lipid handling and reduces steatosis in hepatocytes *in vitro*

Marta Lopez-Yus^{1,2,3}, Scott Frendo-Cumbo⁴, Raquel del Moral Bergos^{1,2,3}, Maria Pilar Garcia-Sobreviela^{1,3}, Vanesa Bernal-Monterde^{1,3,5}, Mikael Rydén⁴, Silvia Lorente-Cebrian^{1,6}, Jose M. Arbones-Mainar^{1,2,3,7}

¹ Adipocyte and Fat Biology Laboratory (AdipoFat), Translational Research Unit, University Hospital Miguel Servet, Instituto Aragonés de Ciencias de la Salud (IACS), Zaragoza, Spain

² Instituto Aragonés de Ciencias de la Salud (IACS), Zaragoza, Spain

³ Instituto de Investigación Sanitaria (IIS) Aragón, 50009, Zaragoza, Spain

⁴ Department of Medicine (H7), Karolinska Institutet, Karolinska University Hospital Huddinge, SE-141 83, Huddinge, Sweden.

⁵ Gastroenterology Department, Miguel Servet University Hospital, 50009, Zaragoza, Spain

⁶ Departamento de Farmacología, Fisiología y Medicina Legal y Forense, Universidad de Zaragoza.

Instituto Agroalimentario de Aragón (IA2) (Universidad de Zaragoza-CITA), Zaragoza, Spain.

⁷ CIBER Fisiopatología Obesidad y Nutrición (CIBERObn), Instituto Salud Carlos III, Madrid, Spain

ABSTRACT

Obesity is a major risk factor for the development of non-alcoholic fatty liver disease (NAFLD) and the subcutaneous white adipose tissue (scWAT) is the primary lipid storage depot and regulates lipid fluxes to other organs. Our previous work identified genes up-regulated in scWAT of patients with NAFLD: *SOCS3*, *DUSP1*, and *SIK1*. Herein, we knocked down (KD) their expression in human adipose-derived mesenchymal stem cells (hADMSCs) using CRISPR/Cas9 technology and characterized their phenotype.

We found that *SOCS3*, *DUSP1*, and *SIK1* expression in hADMSC-derived adipocytes was not critical for adipogenesis. However, the metabolic characterization of the cells suggested that the genes played important roles in lipid metabolism. Reduction of *SIK1* expression significantly increased both *de novo* lipogenesis (DNL) and palmitate-induced lipogenesis (PIL). Editing out *SOCS3* reduced DNL while increasing isoproterenol-induced lipolysis and insulin-induced palmitate accumulation. Conversely, *DUSP1* reduced PIL and DNL. Moreover, RNA-sequencing analysis of edited cells showed that these genes not only altered lipid metabolism but also other biological pathways related to inflammatory processes, in the case of *DUSP1*, extracellular matrix remodeling for *SOCS3*, or cellular transport for *SIK1*. Finally, to evaluate a possible adipocyte-

hepatocyte axis, human hepatoma HepG2 cells were co-cultured with edited hADMSCs-derived adipocytes in the presence of [³H]-palmitate. All HepG2 cells cultured with DUSP1-, SIK1-, or SOCS3-KD adipocytes decreased [³H]-palmitate accumulation compared with control adipocytes.

These results support our hypotheses that *SOCS3*, *DUSP1*, and *SIK1* regulate multiple aspects of adipocyte function which may play a role in the progression of obesity-associated comorbidities, such as NAFLD.

Keywords: fatty liver, adipose tissue, hADMSC, SOCS3, SIK1, DUSP1

1. INTRODUCTION

Accumulating evidence indicates that obesity is closely associated with an increased risk of metabolic diseases, such as insulin resistance, type 2 diabetes (T2DM), or non-alcoholic fatty liver disease (NAFLD) (1). The development of these obesity-associated comorbidities depends largely on how functionally resilient the adipose tissue (AT) is in response to excessive nutrient supply. The subcutaneous white adipose tissue (scWAT) is the primary lipid storage organ and regulates systemic energy homeostasis by controlling metabolic flexibility and lipid fluxes to other organs (2, 3). As an individual gains weight, scWAT expands to store the excess calories from the diet. Once the storage capacity is exceeded, the scWAT fails to accumulate lipids appropriately, redirecting the lipid flux to other organs (4). This ectopic fat accumulation occurs primarily in the visceral adipose tissue (visWAT) and liver, leading to visceral obesity and liver steatosis, respectively (3), and promotes comorbidities associated with obesity as T2DM or NAFLD (5).

The lipid accumulation capacity of scWAT is determined by the differential expression of genes, proteins, microRNAs, and metabolites from different cell types. Although many genes are well known to be involved in regulating this process, the complete molecular mechanism that determines this expansibility limit still needs to be fully understood (6).

Therefore, it is critical to identify novel target genes in adipocytes whose differential expression determines the lipid accumulation capacity of scWAT. Moreover, it is rational to hypothesize that modifying the expression of these critical genes could be a promising strategy to increase the expansibility capacity of scWAT and, consequently, reduce the ectopic fat accumulation that promotes comorbidities associated with obesity.

In this context, CRISPR/Cas9 gene editing technology has emerged as a promising tool to modify AT function (7). The efficiency of CRISPR/Cas9 to edit AT has already been tested in adipose tissue-derived mesenchymal stem cells (ADMSC) to knockout the expression of crucial genes such as *PPARG* (8), *UCP1* (9) or *NRIP1* (10), proving the potential of this gene editing tool to treat metabolic complications associated to obesity. However, all these investigations are still in an early stage, and more positive results are needed for their translation into clinical practice.

Our previous work identified four genes up-regulated in scWAT of patients with NAFLD: *SOCS3*, *DUSP1*, *SIK1*, and *GADD45B*, that may be involved in regulating adipocyte

function (11). To further investigate the role of these genes in adipocytes, we specifically knocked down their expression in human ADMSC (hADMSC) using CRISPR/Cas9 technology and characterized the phenotype of the differentiated adipocytes. With our work, we aimed to: 1) develop CRISPR/Cas9 technology in our model of hADMSC, 2) address the relevance of specific gene knockdown of previously identified target genes in adipocyte function, and 3) determine if modification at cellular/adipocyte level could be potentially translated into alterations of fat accumulation capacity of hepatocytes in a human co-culture model of hepato-adipocytes.

2. MATERIAL AND METHODS

2.1. Cell culture and differentiation

The proliferation and differentiation of human adipocytes were performed as previously described (12). Cells were isolated from the abdominal scWAT of one healthy male donor undergoing elective surgery. Informed written consent was given and tissue collection was approved by Regionala Etikprövningsnämnden in Stockholm, Sweden, on the 16th of December 2009 (permit number 2009/1881-31/1).

In brief, scWAT was digested with type II collagenase (Sigma-Aldrich) and the stroma vascular fraction (SVF), which includes the adipocyte progenitors (hADMSC), was isolated. The cells were washed and subsequently expanded for 6-8 passages in proliferation medium (DMEM, 10 mmol/l HEPES, 10% FBS, 50 µg/mL Penicillin-Streptomycin) supplemented with 2.5 ng/mL fibroblast growth factor-2 (FGF2) (Sigma-Aldrich). hADMSC were plated at a cell density of 20 000 cells/cm² and maintained at 37°C with 5% CO₂. Two days post-confluence, in vitro differentiation was induced using DMEM/F12 without glucose supplemented with an adipogenic cocktail (1 µM dexamethasone, 100 µM 3-isobutyl-1-methylxanthine (IBMX), 10 µM rosiglitazone, 0.2 nM triiodothyronine (T3), 10 µg/mL transferrin, 5 µg/mL insulin). On day three of differentiation, dexamethasone and IBMX were removed. At day ten, rosiglitazone was removed, and the cells were allowed to undergo complete adipogenic differentiation up to day thirteen.

HepG2 were grown in DMEM supplemented with 10% fetal bovine serum at 37 °C with 5% CO₂.

2.2. Design and selection of a single guide RNA

To knock out the expression of target genes, single guide RNAs (sgRNAs) were designed using the CHOPCHOP guide design web tool (<https://chopchop.cbu.uib.no>, last accessed 31 May 2023) (13). All sgRNA designs were evaluated by standard guide RNA design considerations before being chosen for experiments (14). Two sgRNAs were selected for each target gene (described in Table 1). A non-targeting TrueGuideTM sgRNA (Thermo Fisher) was included as a negative control.

Table 1. Selected sgRNA sequences.

Gene ID		Sequence (5'→ 3')
<i>SOCS3</i>	sgRNA 1	AGCCTATTACATCTACTCCGGGG
	sgRNA 2	CGGATCAGAAAGGTGCCGGCGGG
<i>SIK1</i>	sgRNA 1	TGGGTTTTACGACATCGAGCGG
	sgRNA 2	CGCCATGTAAGTGTCCCCGGGGG
<i>DUSP1</i>	sgRNA 1	TACTAGCGTCCTGACAGCGCGG
	sgRNA 2	CGTCCAGCAACACCACGGCGTGG

2.3. Cells transfection with sgRNAs and Cas9

hADMSC were electroporated with sgRNA and Cas9 ribonucleoprotein (RNP) using a Neon Transfection system (1300 V, 20 ms, two pulses) 10 µL Kit (Invitrogen). Before electroporation, 12 pmol/reaction of TrueCutTM Cas9 protein v2 (Thermo Fisher) and 48 pmol/reaction of sgRNA (ratio 1:2) were mixed in buffer R and incubated for 20 minutes at room temperature to form an RNP complex. hADMSC were harvested, dissolved in buffer R, and mixed with the RNP complex. 100 000 cells were transfected in each electroporation reaction. After transfection, cells were plated into a 75 cm² cell culture flask and culture as previously described.

2.4. Assessment of genomic mutation efficiency using Sanger sequencing

Genomic DNA from control and knockdown cells were isolated using DNeasy Blood & Tissue Kit (Qiagen). PCR amplification of the target sequence was carried out with 10 ng gDNA, 0.005 U Q5 High-Fidelity DNA Polymerase (NEB), 5X Q5 Reaction Buffer, 10 mM dNTPs, and 10 µM primers described in Table 2. PCR conditions were: 30 s at 98 °C, followed by 25 cycles of 10 s at 98 °C, 30 s at the annealing temperature specified in

Table 1 for each primer couple (Tm), and 30 s at 72 °C, and 2 min at 72 °C. PCR products were purified using QIAquick PCR Purification Kit (Qiagen) and 50 ng of PCR products were Sanger-sequenced using the forward amplification primers. Primers were designed 200-300 bp upstream of the edit site. This resulted in a read where the first hundred base pairs are of high quality and the following bases are potentially mixed (indicating an edited population with heterogeneous outcomes). Sanger sequence results were analyzed using the Syntego Inference of CRISPR Edits (ICE) software tool (<https://ice.synthego.com/#/>, last accessed 28 Jun 2023) (15), that generates different editing proposals using the control sample, and uses regression to compute how much of each editing outcome is observed in the mixed Sanger read.

Table 2. Sequences of primers used to amplify edited region of genomic DNA.

Gene ID	sgRNA		Sequence (5'→3')	Tm
<i>SOCS3</i>	1	Forward	CGCCACTTCTTCACGCTCAG	69
		Reverse	TCCTGGTTGGCTTCTTGTC	
<i>SOCS3</i>	2	Forward	CCACACTCCTGGAGACCTAAC	68
		Reverse	GAGGAGGGTTCAGTAGGTGG	
<i>SIK1</i>	1	Forward	TCTATGAGAGCGGGTCCGTG	68
		Reverse	TCTGAGTCCATGAACCACTGC	
<i>SIK1</i>	2	Forward	TTGTGTCTCTCCAACGCAGC	69
		Reverse	AAAGGCAAGCCACCATCACG	
<i>DUSP1</i>	1	Forward	TTGGCTTGTTGGCTCTGG	66
		Reverse	AGCAAGTTCATTCGTAGAGC	
<i>DUSP1</i>	2	Forward	CAGACAAAGAGCACCGCAGG	68
		Reverse	ATAAATGTACTCCAGCGCCCAC	

2.5. Cellular Staining

Cells were fixed in 4% PFA for 15 min at room temperature and washed twice with PBS. Cells were incubated with BODIPY (diluted 1:1000) and Hoechst (diluted 1:5000) for 15 min to stain accumulated lipids and nuclei, respectively, and cells were then washed four times with PBS. Images were acquired using an Axio Observer Z1 inverted fluorescence microscope (Zeiss) and the AxioVision software, while quantification was performed

using the Cell Insight CX5 High Content Screening (HCS) Platform. The quantification was performed in 2 independent experiments, with 4 biological replicates for experiment.

2.6. Lipid metabolic assays

Lipolysis, fatty acids uptake, and *de novo* lipogenesis were assayed as previously described (16, 17). Briefly, for lipolysis and fatty acids uptake assays, adipocytes were incubated overnight with 1 nCi/ μ l [9,10-³H(N)]-palmitic acid (Perkin-Elmer). To quantify basal, isoprenaline-stimulated and insulin-inhibited lipolysis, cells were then incubated with serum-free DMEM containing 2 % BSA (Sigma) without or with 10 μ M isoprenaline (Reig Jofre) or 1 μ M insulin (Novo Nordisk), respectively. After four hours of incubation, conditioned media was collected and labeled fatty acid release was quantified. To determine fatty acid accumulation, adipocytes were incubated with proliferation media with or without 1 μ M insulin (Novo Nordisk) for two hours. Cells were then washed, lipids were extracted and cells were lysed. For the *de novo* lipogenesis assay, adipocytes were incubated overnight with 1 nCi/ μ l [³H]-acetic acid (Perkin-Elmer). After incubation time, cells were washed, lipids were extracted, and cells were lysed. Lipids extraction was performed incubating cells with isopropanol 100% for 1 h at 4°C with mild shaking. The supernatant was then collected and centrifuged at 1000 r.p.m. for 5 min at r. t. The upper organic phase containing the lipidic cellular fraction was collected and radioactivity was measured. Isotopes were analyzed in a Rackbeta liquid scintillation counter (Tri-Carb 2560 TR/XL, Packard) after adding Ultimate Gold scintillate (Perkin-Elmer). Cells were lysed with a lysis buffer (0.2 N NaOH, 0.1 % SDS) and protein concentration was quantify using a Pierce™ BCA Protein Assay Kit. Results were normalized to cellular protein.

2.7. Co-culture with HepG2

Co-culture of adipocytes and HepG2 cells was conducted in cell culture inserts (Thermo Fisher). Briefly, adipocytes were seeded and differentiated in 12-well plates. HepG2 were plated into membrane inserts (4 μ m pore size) and transferred to plate wells incubating differentiated adipocytes. This resulted in an assembly of the two cell types sharing the culture medium but separated by the insert's membrane. The distance from the bottom of the culture dish to the membrane was 0.9 mm. Co-cultures were conducted for 48 h. At the end of the co-culture period, a palmitate uptake assay was performed in both cell lines, as previously described.

2.8. RNA isolation, cDNA synthesis, and qPCR analysis

Total RNA was extracted from hADMSC and differentiated adipocytes using column-based commercial kits (RNeasy Lipid Tissue Mini Kit, Qiagen) according to the provided instructions. The concentration and purity of the RNA were measured using Nanodrop 2000 (Thermo Fisher) and samples were reverse transcribed using PrimeScript Reverse Transcriptase (Takara Bio). 10 ng of the cDNA product was amplified by qPCR in a total volume of 15 µl per reaction with SYBR Select Master Mix (Applied Biosystems), adding 0.5 µl of gene-specific primers at 10 µM (specified in Table 3). cDNA amplification was conducted in StepOnePlus system (Applied Biosystems), using a protocol as follows: 95°C for 10 min, 40 cycles of 15 sec at 95°C and 1 min at 60°C, 15 sec at 95°C, 1 min at 60°C, and 15 sec at 95°C. Relative gene expression was normalized to β-actin expression using the $2^{-\Delta\Delta CT}$ method.

Table 3. Primers used for qPCR.

Gene ID		Sequence (5'→ 3')
<i>Actin</i>	Forward	CATGTACGTTGCTATCCAGGC
	Reverse	CTCCTTAATGTCACGCACGAT
<i>PPARG</i>	Forward	AGATGACAGCGACTTGGCAAT
	Reverse	ACTCAGGGTGTTTCAGCTTC
<i>SOCS3</i>	Forward	CCATTGGGAGTTCCCTGGAC
	Reverse	TTGGCTTCTTGTGCTTGTGC
<i>SIK1</i>	Forward	CCTTCTCTGCGAGCAAAAGC
	Reverse	TGAGTCAGTGAGGTGTCCGA
<i>DUSP1</i>	Forward	ACCACCACCGTGTCAACTT
	Reverse	AGAGGTCGTAATGGGGCTCT

2.9. AmpliSeq transcriptome analysis

RNA samples were quantitated using the Qubit RNA high-sensitivity (HS) assay kit (#Q32855, ThermoFisher) and the Qubit 3.0 fluorometer (ThermoFisher). RNA integrity was checked by the 2200 TapeStation system (Agilent) with the High Sensitivity RNA ScreenTape (5067–5579, Agilent). All samples had an RNA integrity number (RIN) > 7. RNA (20 ng) was converted to cDNA using the SuperScript IV VILO Master Mix (#11756050, ThermoFisher) and automated library preparation was carried out with the

Ion AmpliSeq transcriptome human gene expression panel Chef-ready kit (#A31446, ThermoFisher) on the Ion Chef Prep station, chef package version IC.5.4.0 (ThermoFisher). Sequencing was performed per the manufacturer's protocols using the Ion 540 Kit-Chef (# A30011, ThermoFisher) on the Ion Torrent S5-XL (ThermoFisher). Eight samples per 540 chip were sequenced, obtaining 7.5 to 10 million reads/sample. Next, bam files were further processed using the Ion AmpliSeq RNA plugin v5.4.01 on the Torrent Server (Torrent Suite Software, v5.4, ThermoFisher) to obtain the count matrices.

2.10. Statistical and differential gene expression analyses

Results are expressed as means \pm standard error of the mean (SEM). Every assay was carried out in at least two independent experiments. Differences between groups were tested with the Student's t-test. The statistical analysis was performed using R version 4.0.3 (<http://www.r-project.org>), and the significance level was set at 0.05.

Differential expression analysis was performed with the edgeR R package (v. 3.40.02) (18) in which the gene expressions of the control hADMSC-derived adipocytes were compared to knocked out hADMSC-derived adipocytes (i.e., control vs. DUSP1-KD, control vs. SIK1-KD, and control vs. SOCS3-KD). Briefly, samples were normalized using a weighted trimmed mean of M-values (TMM) and fitted to a quasi-likelihood negative binomial generalized log-linear model followed by empirical Bayes quasi-likelihood F-tests. Genes with \log_2 fold changes $[|\log_2(\text{FC})| \geq 1]$ and Benjamini and Hochberg false discovery rates (FDR, (19)) < 0.001 were classified as differentially expressed genes (DEGs). DEGs were then tested for enrichment of Gene Ontology (GO): Biological processes (BP) terms using the clusterProfiler R package (v. 4.6.2) (20). A minimum size of three genes was used for the functional enrichment. GO: BP terms with q-value < 0.05 were considered enriched.

3. RESULTS

3.1. Ribonucleoprotein (RNP) complex effectively edited genomic DNA

Our previous work identified four genes up-regulated in scWAT of patients with NAFLD: *SOCS3*, *DUSP1*, *SIK1*, and *GADD45B* (11). To investigate if these genes played a causal role in the accumulation of liver fat beyond the mere statistical association, we tried to

knockdown their expression in hADMSC. As *GADD45B* was previously described as a critical regulator of cell viability and its suppression caused cell death (21), we decided to exclude this gene from subsequent analyses. To knockdown the expression of target genes in hADMSC, sgRNAs against *SOCS3*, *SIK1*, and *DUSP1* were designed and RNP complexes were delivered by electroporation as described in Materials and Methods. Two different sgRNA targeting each gene were used, resulting in two knockdown cell lines for each gene, henceforth referred to as KD1 and KD2 (Fig 1A), while a non-targeting sgRNA was used to generate the control cell line.

The efficiency of the sgRNAs was first evaluated at the DNA level in hADMSC 48 h post-transfection. We compared the control and the edited sequences using the Inference of CRISPR Edits (ICE) algorithm to quantify the identity and prevalence of edits resulting from non-homologous end joining (NHEJ) after RNP's cut. Results showed that all six sgRNAs efficiently cut the gDNA, with more than 87% of edited sequences in all the cases (Fig 1B, Supplementary Figure 1). Regarding *SOCS3*, sgRNA 1 worked slightly better than sgRNA 2: 92 vs. 87%, respectively. The highest mutation efficiency was achieved by *SIK1* for both guides, with 96%. Moreover, both *DUSP1* sgRNAs achieved similar knockout efficiency, 92 and 91%, respectively. The predominant modification was one base pair (bp) insertion in the case of *DUSP1* (both guides) and *SOCS3* sgRNA 2, and one bp deletion for *SIK1* (both guides) and *SOCS3* sgRNA 1 (Fig 1B, Supplementary Figure 1). We also analyzed the gDNA of modified hADMSC after 4 cell passages and full differentiation to adipocytes. Interestingly, the percentage of inferred sequences was similar before and after differentiation in all the KD-cell lines, keeping the same relative proportion of edition (not shown). That may indicate that none of the editions modify the viability of the cells.

Next, we measured the mRNA levels of target genes in control and modified hADMSC before differentiation into adipocytes (day 0) and 13 days after initiating the differentiation process. Compared to control cultures, the mRNA levels of *DUSP1* in DUSP1-KD1 and DUSP1-KD2 cell lines were significantly decreased at both time points ($p < 0.05$) (Fig 1C). A similar reduction was observed for *SIK1* expression levels in SIK1-KD1 and SIK1-KD2 differentiated cells ($p < 0.05$) (Fig 1D). However, none of the SOCS3-KD cells showed a significant reduction in *SOCS3* gene expression, although a decreasing trend in expression can be observed in day 13 adipocytes ($p=0.07$ for SOCS3-KD1 and $p=0.12$ for SOCS3-KD2) (Fig 1E).

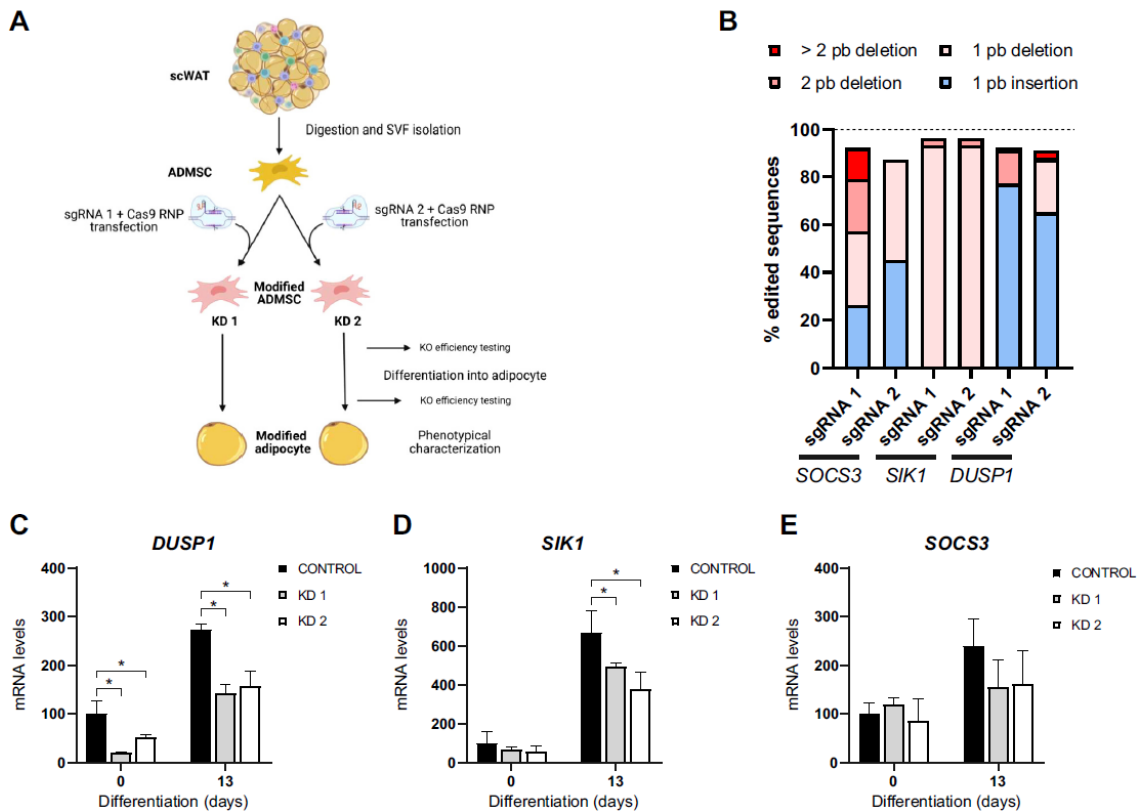


Figure 1. Evaluation of efficiency of sgRNA-Cas9 RNP complex. **A.** Schematic representation of the experimental setup of the entire process, from obtaining a biopsy of human adipose tissue, isolation of the stromal vascular fraction (SVF) to characterization of modified adipocytes from adipose-derived mesenchymal stem cells (ADMSC). **B.** Gene editing profiles generated by the Inference of CRISPR Edits (ICE) software tool showing the percentage of edited sequences as well as the type of edition for each sgRNA used. **C-E.** mRNA expression levels of target genes in control and edited cells (KD1 and KD2) before and after differentiation. Relative gene expression was normalized to β -ACTIN and values are expressed as mean \pm SEM. *p < 0.05.

3.2. Loss-of-function of targeted genes did not affect adipocyte differentiation

Next, we evaluated whether the specific gene editing performed in human hADMSC-derived adipocytes could alter the adipogenic process. The expression of *PPARG* remained similar between all KD-cell lines throughout the differentiation process (Fig 2A), suggesting that *SOCS3*, *SIK1*, and *DUSP4* expression did not affect this well-characterized adipogenic marker.

To confirm this observation, the degree of differentiation was also measured by lipid accumulation on fully differentiated knockdown hADMSC-derived adipocytes. Likewise, no significant change was observed on intracellular lipid staining in all KD-adipocyte cell lines as compared to control (Fig 2B, C). Of note, cells from control and knockdown cultures reached confluence on the same day, and the number of cells

determined by nuclei count at day 13 of differentiation was similar (not showed), ruling out off-target effects on proliferation and viability of modified cells.

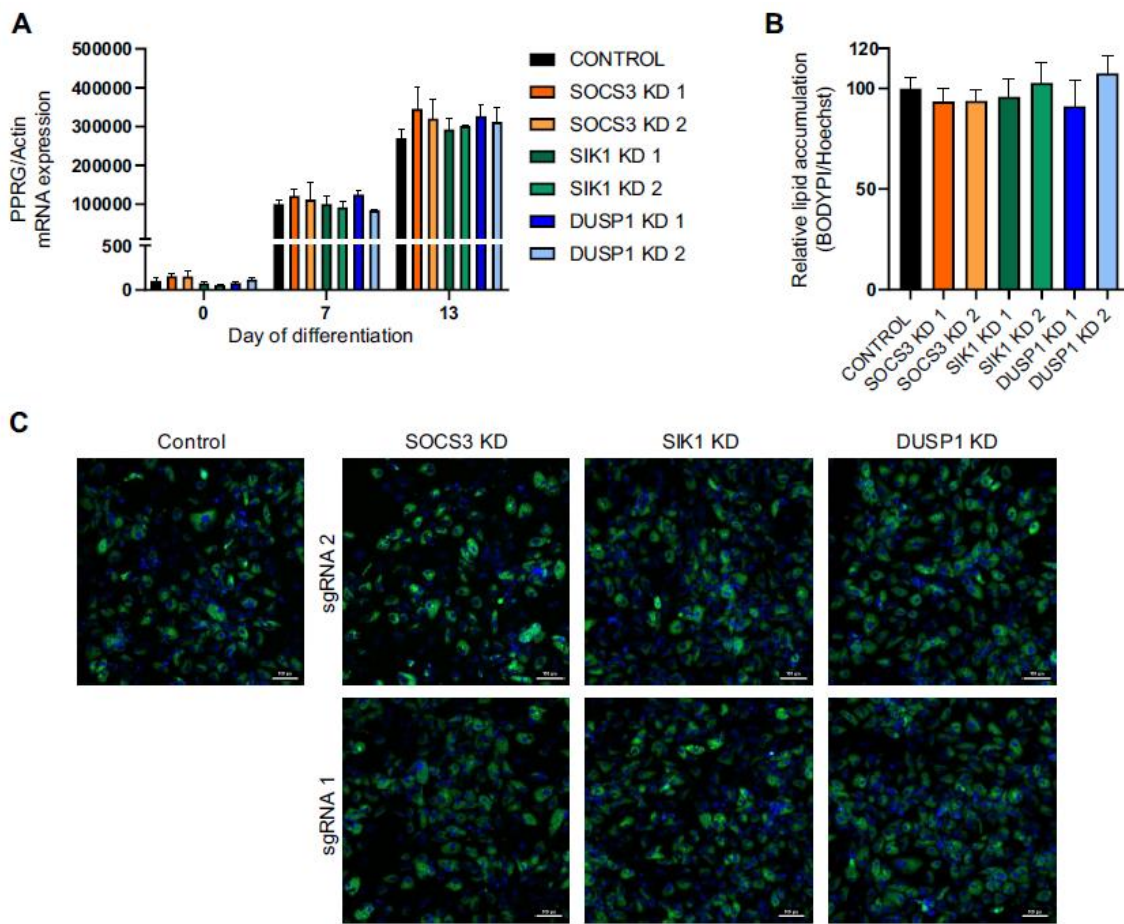


Figure 2. Assessment of hADMSC differentiation into adipocytes after knocking out target genes. **A.** PPARG mRNA expression levels in edited cells compared to control during the differentiation process. **B.** Lipid accumulation in control and edited mature adipocytes quantified by Bodipy staining, normalized by nuclei count. Bars represent the mean \pm SEM of 2 independent experiments, with 4 biological replicates for experiment. **C.** Representative images of control and edited adipocytes; lipid droplets stain with Bodipy (green) and nuclei with Hoechst (blue).

3.3. Loss-of-function of targeted genes altered lipid metabolism in hADMSCs-derived adipocytes

We then investigated the effect of the edited genes on adipocyte lipid handling, characterizing lipolysis, *de novo* lipogenesis, and palmitate-induced lipogenesis in control and modified hADMSCs-derived adipocytes. As we did not observe a significant difference in the effect of alternative sgRNAs (KD1 & KD2) for either gene, averaged results from both cell lines were analyzed together (Fig 3).

To test the functional lipolytic capacity of hADMSC-derived adipocytes, they were loaded with [³H]-palmitate overnight, which was incorporated into triglycerides. Subsequently, the release of radiolabeled palmitate was determined in basal condition and after stimulation with insulin or isoprenaline. SOCS3, DUSP1, SIK1 KD-cell lines showed a significant increase of palmitate released into the culture medium after isoprenaline incubation, whereas insulin exerted anti-lipolytic effects significantly reducing palmitate release (Fig 3A). The results showed that editing out the *DUSP1* gene did not change palmitate release compared with the control cell line at any tested condition. However, SOCS3-KD significantly increased isoprenaline-induced lipolysis ($p=0.021$), while a significant reduction was observed for SIK1-KD in basal and insulin-inhibited lipolysis ($p=0.049$, $p=0.046$, respectively) (Fig 3A).

We also evaluated *de novo* lipogenesis using [³H]-acetate as a precursor. Compared with the control adipocytes, this radio-assay increased ³H accumulation in the lipid fraction of SIK1-KD cells ($p=0.039$), while it was significantly decreased in DUSP1-KD ($p=0.026$) and SOCS3-KD ($p=0.008$) cells (Fig 3B).

Finally, [³H]-palmitate-induced lipogenesis was measured in basal and insulin-stimulated conditions. Compared with control cells, *DUSP1* loss-of-function significantly reduced ($p=0.005$, $p=0.014$), while SIK1 increased ($p=0.005$, $p<0.001$), palmitate uptake both in basal and stimulated conditions. On the other hand, *SOCS3* significantly took in more labeled palmitate only in response to insulin ($p=0.007$) (Fig 3C). Together, these studies support that DUSP1, SIK1 and SOCS3 are important regulators of adipocyte lipid handling, which may contribute to scWAT dysfunction in obesity.

3.4. Gene editing in adipocytes affected lipid deposition in hepatocytes

As these candidate genes were reported to be up-regulated in adipocytes of patients with NAFLD (11), we next investigated if the metabolic changes observed in modified adipocytes could be translated into variations of fat deposition in the hepatocytes. To address this question, we co-cultured control and edited adipocytes with HepG2 hepatocytes and analyzed palmitate uptake in both cell types.

Human hepatoma HepG2 cells were co-cultured with edited hADMSCs-derived adipocytes in the presence of [³H]-palmitate. All HepG2 cells cultured with either DUSP1-KD, SIK1-KD, or SOCS3-KD adipocytes decreased [³H]-palmitate accumulation compared to control adipocytes. A 12% reduction in palmitate-induced

lipogenesis was observed in HepG2 co-cultured with DUSP1-KD, although it did not reach statistical signification ($p=0.12$). Greater reductions in lipogenesis were obtained in HepG2 co-cultured with either SIK1-KD (-22%, $p=0.001$) or SOCS3-KD adipocytes (-33%, $p<0.001$) (Fig 3D).

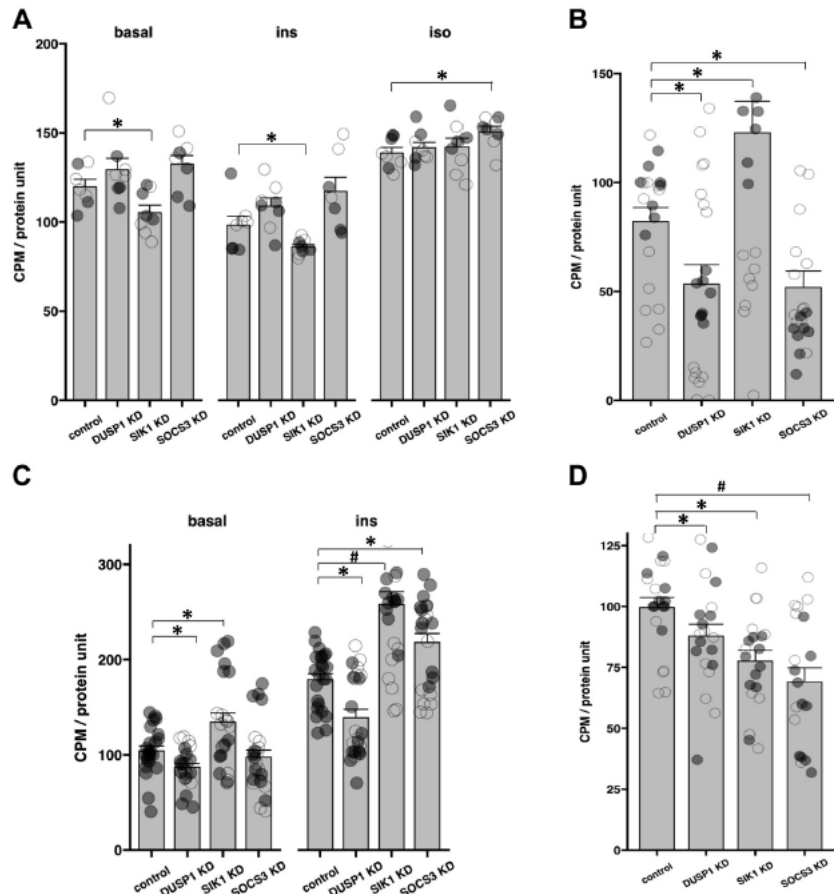


Figure 3. Metabolic characterization of edited hADMSC-derived adipocytes. **A.** The lipolysis assay was performed by measuring the release of 9,10-[³H] palmitate into the cell supernatant without (basal) or with insulin (ins) or isoproterenol (iso). **B.** The de novo lipogenesis assay was carried out by measuring the incorporation of [³H]-acetate into the lipid fraction of the cells. Palmitate-induced lipogenesis was quantified by measuring the incorporation of 9,10-[³H]-palmitate into the cellular lipid fraction of adipocytes without (basal) or insulin-stimulated (ins) (**C**), and HEPG2 in coculture (**D**), as described in M&M. Bars represent the mean \pm SEM of counts per minute (CPM) per protein unit for the pooled individual replicates of the two KDs for each edited and control gene. (KD1: grey circles, KD2: white circles). *, $p < 0.05$; #, $p < 0.001$.

3.5. Identification of other altered pathways in knockdown hADMSCs-derived adipocytes

A global gene expression analysis was conducted in all KD-adipocytes derived from the edited hADMSCs to identify altered processes or molecular pathways. Differential gene expression analysis was performed using edgeR (18) with the following contrast designs; control vs. DUSP1-KD, control vs. SIK1-KD, and control vs. SOCS3-KD. The principal

component analysis (PCA) shows clusters of each condition's replicates (KD1 and KD2 and 2 technical replicates) (Fig 4A). All replicates for each condition, except SIK1-KD1 replicate 2, clustered together. Accordingly, results were further analyzed jointly and data from the SIK-KD1.2 sample were removed from the analysis.

Next, statistically significant differentially expressed genes (DEGs) between the control and each knockdown group were identified based on their calculated log₂ fold changes [$|\log_2(\text{FC})| \geq 1$] and false discovery rates (FDR < 0.001). A mean-difference (MD) plot depicts the log-fold change and average abundance of each gene. A total of 22 DEGs (13 up-regulated and 9 down-regulated) were found after editing out *DUSP1* (Fig 4B, Supplementary Table 1) and *SIK1* (2 up-regulated and 20 down-regulated) (Fig 4C, Supplementary Table 1) compared with control adipocytes, while 340 DEGs (110 up-regulated and 230 down-regulated) were identified in SOCS3-KD cells (Fig 4D, Supplementary Table 1).

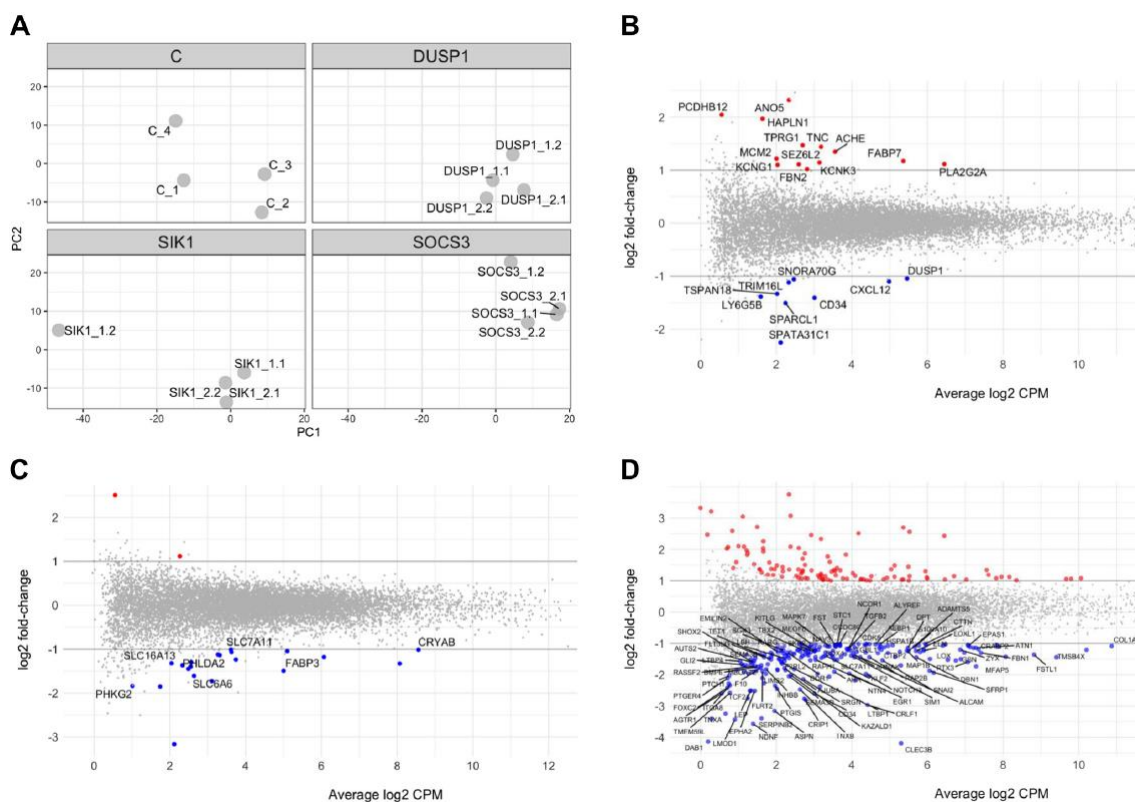


Figure 4. Gene expression profile of modified cells. **A.** Principal component analysis (PCA) of the AmpliSeq-resulting count matrices for outlier sample detection. **B, C and D.** M-A plot displaying the \log_2 fold-change compared with \log_2 average expression of differentially expressed genes (DEGs) resulting from the comparison of control vs. *DUSP1-KD* (**B**), *SIK1-KD* (**C**), and *SOCS3-KD* (**D**) adipocytes with default \log_2 fold-change thresholds of -1 and 1 . Down-regulated and up-regulated DEGs are plotted in blue and red, respectively. Labels correspond to DEGs that appeared enriched in a biological process according to the Gene Ontology analyses.

A Gene Ontology (GO) and the Kyoto Encyclopedia of Genes and Genomes (KEGG) enrichment analyses were performed to further identify and characterize the molecular basis of DEGs in each KD cell line. Figure 5 and Supplementary Table 2 depict those biological processes (BP) enriched with at least 3 DEGs and $q\text{-value} < 0.05$.

For DUSP1-KD cells, the up-regulated *TNC*, *ACHE*, and *FBN2* DEGs clustered together in BPs related to osteoblast differentiation (GO:0001649 and GO:0001503), while *TNC*, *SEZ6L2*, and *ACHE* enriched the GO term "synapse organization" (GO:0050808). Down-regulated genes, including *CD34*, *DUSP1*, and *CXCL12*, enriched the term "leukocyte migration" (GO:0050900), and their diminished expression could help prevent a chronic inflammatory state. No significant BPs were up-regulated when silencing *SIK1* in hADMSCs-derived adipocytes. However, GO analysis identified 5 significant down-regulated BPs associated with transporters across the plasma membrane in *SIK1*-KD cells, including *SLC16A13*, *SLC7A11*, *SLC6A6*, and *FABP3*. Notably, these candidates were involved in the transport of different nutrients, such as carboxylic and organic acids as well as organic anions (GO:0098657, GO:0046942, GO:0015849, and GO:0015711). Finally, *SOCS3* silencing yielded the highest number of down-regulated genes as compared to control adipocytes. GO analysis showed 33 down-regulated BPs mostly related to collagen and cellular matrix formation, as well as regulation of transmembrane receptor protein serine/threonine kinase signaling pathways (Fig 5). Interestingly, genes already known to interact with *SOCS3* are significantly down-regulated in this cell line as *LEP* (22) or *TGF- β 2* (23).

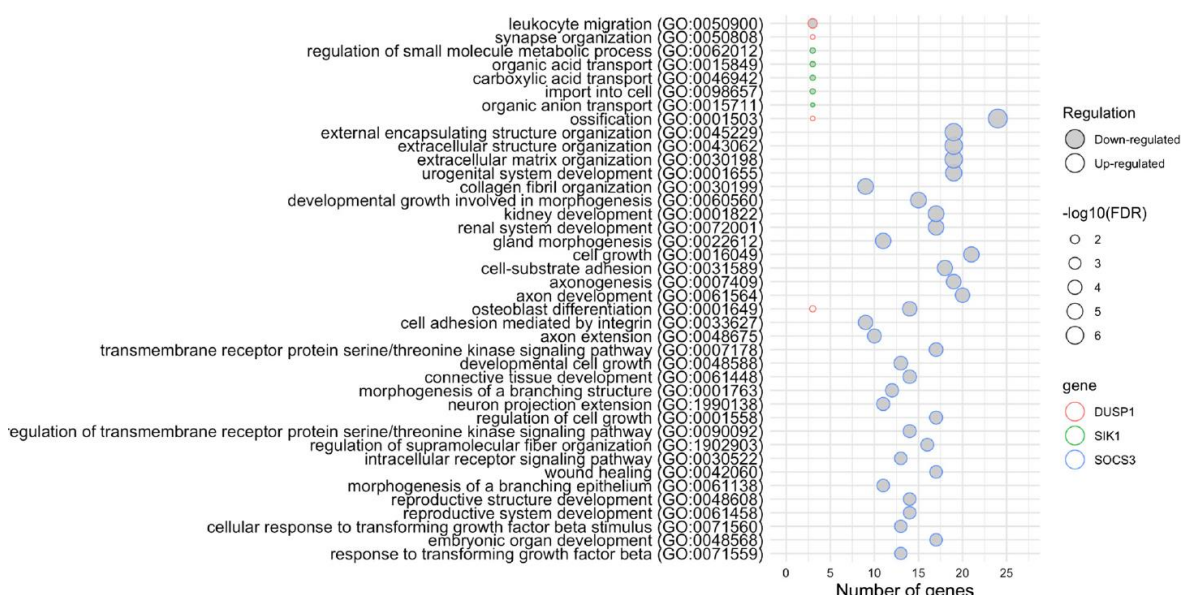


Figure 5. Gene Ontology (GO) pathway enrichment analysis of up- and down-regulated DEGs.

4. DISCUSSION

The main objectives of this study were 1) to clarify the physiological role of three genes previously reported to be up-regulated in scWAT of patients with NAFLD and 2) to hypothesize whether their genetic modification could be a therapeutic approach for this condition. To this end, we optimized a CRISPR/Cas9 protocol that successfully edited the gDNA of hADMSC. We then differentiated these modified cells into adipocytes and evaluated their adipogenic capacity and phenotypical changes at the transcriptomic and metabolic levels. Our results suggest the potential of CRISPR/Cas9 technology to treat metabolic complications and provide new insight into the role of *SOCS3*, *SIK1*, and *DUSP1* in human adipocytes.

Our first aim was to optimize a CRISPR/Cas9 protocol to edit hADMSC without affecting their adipogenic potential. Transfecting the RNP-sgRNA complex by electroporation achieved a very high percentage of edited cells, thus avoiding the subsequent selection of modified cells that involves multiple passages that may impair hAMSC differentiation capacity (8). Moreover, our experimental setup using two different sgRNA for each target gene reduced the odds of observing possible off-target effects of this method, as similar phenotypical changes were observed independently of the sgRNA used. Importantly, specific gene knockdown of our targets did not compromise adipocyte differentiation potential/capacity. Of note, the genomic edition translated into a significant reduction of target gene mRNA levels in the *DUSP1*- and *SIK1*-KD cells. The fact that this did not occur in the *SOCS3*-KD cells could be explained by the transcription of CRISPR/Cas9 edited DNA into modified mRNA and its detection by the PCR primers used.

Our second goal was to study some candidate genes previously described to increase their expression both in scWAT and mature adipocytes of human patients according to the degree of hepatic steatosis (11). *SOCS3*, *SIK1*, and *DUSP1* were found to be regulating scWAT dysfunction, which is critical for NAFLD development and progression (5). Therefore, a deeper understanding of its role in the regulation of adipocyte function could be beneficial for future NAFLD therapies.

Multiple studies have shown that *SOCS3* expression is elevated in obesity and associated with several metabolic disorders, including reduced energy expenditure, increased food intake and adiposity, and insulin and leptin resistance (reviewed in (24)). Interestingly, liver-specific *SOCS3* deletion in mice enhances hepatic insulin sensitivity and lipogenesis

but provokes fatty liver and obesity (25, 26). On the other hand, *SOCS3* over-expression in scWAT causes local insulin resistance (27), suggesting that attenuation of *SOCS3* locally could lead to beneficial metabolic effects and, therefore, be a promising target for treating metabolic complications associated with obesity (28). However, whether these results are translated to human adipocytes remains still elusive. To address this question, we generated human *SOCS3*-KD adipocytes. Our *in vitro* results aligned in part with previously described *in vivo* results and clinical data. *SOCS3* knockdown significantly reduced de novo lipogenesis while improving insulin response in adipocytes by increasing notably fatty acids accumulation after incubation with this hormone. Moreover, when co-cultured with hepatocytes, this increase was translated into a reduction of fatty acids in hepatocytes, suggesting a potentially anti-steatotic effect in hepatocytes.

We also reported that *SOCS3* suppression significantly altered the adipocytes' transcriptome. In line with phenotypical changes observed, fatty acid transport pathways were altered in *SOCS3*-KD cells. Other interesting transcriptomic alteration observed in *SOCS3*-KD cells was related to extracellular matrix (ECM) remodeling. Two regulators of *SOCS3*, leptin and tumor growth factor $\beta 2$ (*TGF- $\beta 2$*), both known to be involved in ECM remodeling and promotion of fibrosis (23, 29), were altered in *SOCS3*-KD adipocytes. Moreover, multiple genes involved in this process were down-regulated: Secreted frizzled-related protein 1 (*SFRP1*), known to be down-regulated in obesity and to control AT expansion (30); lysyl oxidase (*LOX*), also up-regulated in AT of human and rats under pro-inflammatory conditions (31, 32); snail Family Transcriptional Repressor 2 (*SNAI2*) and asposin (*ASPN*), both modulators of AT mass (33, 34); serglycin (*SRGN*), involved in AT inflammation in obesity (35); among others. Moreover, Insulin Like Growth Factor Binding Protein 2 (*IGFBP2*) is one of the most upregulated genes. This factor is known to regulate the phosphatidylinositol 3-kinase (PI3K)/ alpha serine/threonine-protein kinase (Akt) signaling pathway and known to be dysregulated in obesity (reviewed in (36)). Its overexpression in the absence of *SOCS3* might suggest a compensatory mechanism for the control of this key pathway. Altogether, our results suggest that *SOCS3* is not just critical for AT maintenance because of its well-known function as insulin signaling regulator but also because its implication in AT remodeling.

Our *SIK1*-KD adipocytes showed an increased capacity for fatty acid uptake in both basal and insulin-stimulated response, as well as in de novo lipogenesis and reduced basal

lipolysis. The fact that reduced *SIK1* expression stimulates lipid anabolic pathways (while inhibits lipid catabolism) is concordant with our initial hypothesis: reduced *SIK1* expression in adipocytes might increase adipocyte capacity to store lipids and thus, could prevent ectopic lipid flux to other non-adipose cells such as hepatocytes. Importantly, our co-culture results also support this since *SIK1*-KD adipose cells seem to partially prevent hepatocyte lipid accumulation due to a decrease in fatty acid uptake. Other previous studies in mouse and human models are in agreement to our findings showing a protective role of reduced *SIK1* in regulating lipid flux and metabolism (reviewed in (37)) Although substantial improvement at the metabolic level was observed in *SIK1*-KD cells, scarce differences were found at the transcriptomic level. It could be explained by the fact that *SIK1* is a kinase, so its metabolic regulatory activity is mainly post-transcriptional. Further phosphoproteomic analysis of KD-adipocytes could clarify the metabolic role of this protein. Nevertheless, pathways related to the energy reserve metabolic process and cellular transport of different nutrients such as amino acids, carboxic acids, or organic acids appeared altered in *SIK1*-KD adipocytes. Among the dysregulated genes outlined, *SLC16A13* and *FABP3*, both transporters previously described to be involved in ectopic lipid accumulation and insulin resistance in mice (38) and humans, respectively (39, 40).

Regarding *DUSP1*, little is known about its role in lipid metabolism regulation. Just one study reported *DUSP1* overexpression in scWAT and peripheral blood mononuclear cells of individuals with obesity (41), while its liver-specific overexpression in mice is linked to the promotion of hepatosteatosis (42). Our outcomes in *DUSP1*-KD adipocytes might suggest only a modest relevance of *DUSP1* as regulator of lipid metabolism since lipogenic capacity of *DUSP1*-KD adipocytes seems to be partially blunted. This may be explained by the fact that the MAPK-specific dual-specificity phosphatases (DUSPs) are a large family of phosphatases that act coordinately to regulate MAPK signaling. Therefore, there may be a compensation of function by other phosphatases in the family (43). Indeed, several of these DUSPs have also been reported to be up-regulated in obese animals, suggesting a cooperative and compensatory role of these phosphatases in the maintenance of adipocyte function (44). Interesting transcriptional alterations were observed in *DUSP1*-KD adipocytes regarding immune system cell migration-related genes. For instance, *CXCL12*, a chemokine reported to be secreted by AT to induce insulin resistance (45) and to interact with *DUSP1* in other cellular types (46), is one of the most down-regulated genes in *DUSP1*-KD adipocytes. Similarly, *SPARCL1*, an AT-

secreted glycoprotein known to regulate inflammatory response through C-C motif chemokine ligand 2 (*CCL2*) (47), followed the same expression pattern. These observations were in line with previous data showing that *DUSP1* expression in AT was divergently regulated at the gene expression level based on the inflammatory environment resulting from obesity (44). Indeed, the protective role of *DUSP1*-KD adipocytes might be linked to secondary improvements of adipocyte-inflammatory status rather than direct alterations in adipocyte lipid metabolism. Taken together, data suggest that NAFLD-associated inflammation and not obesity per se appears responsible for elevated *DUSP1* gene expression in AT.

These pieces of evidence point out the relevance of our candidate genes in adipocytes and, consequently, in NAFLD progression. However, the study has some limitations, so future functional studies are needed to fully decipher their actions in humans and within the metabolic disease context. For instance, our cellular characterization concern mainly mRNA expression and phenotypical changes and whether these changes fully translate to functional protein levels also warrants further investigations. Indeed, all these proteins have a post-transcriptional regulatory function. Therefore, protein studies could help elucidate the molecular pathways regulated by these proteins. Moreover, the RNA-seq analysis was performed under basal conditions, and more relevant alterations could be observed in modified adipocytes following insulin stimulation.

In conclusion, our results constitute a proof-of-concept of the potential of CRISPR/Cas9 technology to treat metabolic complications and provide new insight into the role of *SOCS3*, *SIK1*, and *DUSP1* in human adipocytes.

Acknowledgements: We acknowledge the scientific inputs and advice from Prof. A. Álvarez-Alfaro.

Disclosure of conflict of interest: The authors declare that they have no conflicts of interest.

Authors Contributions: M.L.-Y. and J.M.A.-M. designed the study. M.L.-Y, S.F.-C., R.M.-B., and M.P.G.-S performed experiments. M.L.-Y., S.L-C., V.B.-M., and J.M.A.-M interpreted the results of the experiments. M.L.-Y., S.L-C., M.R., and J.M.A.-M drafted and edited the manuscript. All authors approved the final version of the manuscript.

Funding: JMA-M is partially supported by the project PI22/01366 (Instituto de Salud Carlos III and co-financed by Fondo Europeo de Desarrollo Regional (FEDER): “Una manera de hacer Europa”) and also has support from the regional government of Aragón (B03_23R, co-financed with the FEDER Aragón: “Construyendo Europa desde Aragón”). ML-Y is the recipient of a fellowship from the Gobierno de Aragón and a EMBO Scientific Exchange Grant (#9603). MR is supported by grants from the Swedish Research Council, ERC-SyG SPHERES (856404), the NovoNordisk Foundation (the MeRIAD consortium Grant number 0064142), Knut and Alice Wallenbergs, the Center for Innovative Medicine, the Swedish Diabetes Foundation, the Stockholm County Council and the Strategic Research Program in Diabetes at Karolinska Institutet. SL-C is supported by Spanish Ministry of Science (BFU2015-65937-R) and University of Zaragoza (JIUZ-2021-BIO-03). SF-C is supported by a Novo Nordisk postdoctoral fellowship run in partnership with Karolinska Institutet.

5. REFERENCES

1. Blüher M. Obesity: global epidemiology and pathogenesis. *Nature Reviews Endocrinology*. 2019;15(5):288–98.
2. Louwen F, Ritter A, Kreis NN, Yuan J. Insight into the development of obesity: Functional alterations of adipose-derived mesenchymal stem cells. *Obesity Reviews*. 2018;
3. McQuaid SE, Hodson L, Neville MJ, Dennis AL, Cheeseman J, Humphreys SM, et al. Downregulation of adipose tissue fatty acid trafficking in obesity: A driver for ectopic fat deposition? *Diabetes*. 2011;60(1):47–55.
4. Virtue S, Vidal-Puig A. Adipose tissue expandability, lipotoxicity and the Metabolic Syndrome--an allostatic perspective. *Biochimica et biophysica acta*. 2010 Mar;1801(3):338–49.
5. Azzu V, Vacca M, Virtue S, Allison M, Vidal-Puig A. Adipose tissue-liver cross talk in the control of whole-body metabolism: implications in nonalcoholic fatty liver disease. *Gastroenterology*. 2020;158(7):1899–912.
6. Torres-Perez E, Valero M, Garcia-Rodriguez B, Gonzalez-Irazabal Y, Calmarza P, Calvo-Ruata L, et al. The FAT expandability (FATe) Project: Biomarkers to determine the limit of expansion and the complications of obesity. *Cardiovascular Diabetology*. 2015;14(1):40.
7. Doudna JA, Charpentier E. The new frontier of genome engineering with CRISPR-Cas9. *Science*. 2014;346(6213):1258096.
8. Kamble PG, Hetty S, Vranic M, Almby K, Castillejo-López C, Abalo XM, et al. Proof-of-concept for CRISPR/Cas9 gene editing in human preadipocytes: Deletion of FKBP5 and PPARG and effects on adipocyte differentiation and metabolism. *Scientific Reports*. 2020 Dec;10(1).
9. Wang CH, Lundh M, Fu A, Kriszt R, Huang TL, Lynes MD, et al. CRISPR-engineered human brown-like adipocytes prevent diet-induced obesity and ameliorate metabolic syndrome in mice. *Science Translational Medicine*. 2020 Aug;12(558).
10. Tsagkaraki E, Nicoloro SM, DeSouza T, Solivan-Rivera J, Desai A, Lifshitz LM, et al. CRISPR-enhanced human adipocyte browning as cell therapy for metabolic disease. *Nature Communications*. 2021 Dec;12(1).
11. Lopez-Yus M, Lorente-Cebrian S, del Moral-Bergos R, Hörndlér C, García-Sobreviela MP, Casamayor C, et al. Identification of novel targets in adipose tissue involved in non-alcoholic fatty liver disease progression. *The FASEB Journal*. 2022 Aug 1;36(8):e22429.
12. Ehrlund A, Mejhert N, Lorente-Cebrián S, Åström G, Dahlman I, Laurencikiene J, et al. Characterization of the Wnt Inhibitors Secreted Frizzled-Related Proteins (SFRPs) in Human Adipose Tissue. *The Journal of Clinical Endocrinology & Metabolism*. 2013 Mar 1;98(3):E503–8.
13. Labun K, Montague TG, Krause M, Torres Cleuren YN, Tjeldnes H, Valen E. CHOPCHOP v3: Expanding the CRISPR web toolbox beyond genome editing. *Nucleic Acids Research*. 2019 Jul;47(W1):W171–4.
14. Van Campenhout C, Cabochette P, Veillard AC, Laczik M, ZelisKD-Schmidt A, Sabaté C, et al. Guidelines for optimized gene knockdown using CRISPR/Cas9. *BioTechniques*. 2019;66(6):295–302.
15. Conant D, Hsiau T, Rossi N, Maures T, Waite K, Yang J, et al. Inference of CRISPR Edits from Sanger Trace Data. *CRISPR Journal*. 2022;123–30.

16. Gamundi-Segura S, Serna J, Oehninger S, Horcajadas JA, Arbones-Mainar JM. Effects of adipocyte-secreted factors on decidualized endometrial cells: modulation of endometrial receptivity in vitro. *Journal of Physiology and Biochemistry [Internet]*. 2015 Feb 17 [cited 2015 Feb 18]; Available from: <http://www.ncbi.nlm.nih.gov/pubmed/25686566>
17. Perez-Diaz S, Garcia-Sobreviela MP, Gonzalez-Irazabal Y, Garcia-Rodriguez B, Espina S, Arenaz I, et al. PTRF acts as an adipokine contributing to adipocyte dysfunctionality and ectopic lipid deposition. *Journal of Physiology and Biochemistry [Internet]*. 2018; Available from: <http://link.springer.com/10.1007/s13105-018-0638-9>
18. Robinson MD, McCarthy DJ, Smyth GK. edgeR: a Bioconductor package for differential expression analysis of digital gene expression data. *bioinformatics*. 2010;26(1):139–40.
19. Benjamini Y, Hochberg Y. Controlling the false discovery rate: a practical and powerful approach to multiple testing. *Journal of the Royal statistical society: series B (Methodological)*. 1995;57(1):289–300.
20. Yu G, Wang LG, Han Y, He QY. clusterProfiler: an R package for comparing biological themes among gene clusters. *Omics: a journal of integrative biology*. 2012;16(5):284–7.
21. Nasri M, Mir P, Dannenmann B, Amend D, Skroblyn T, Xu Y, Schulze-Osthoff K, Klimiankou M, Welte K, Skokowa J. Fluorescent labeling of CRISPR/Cas9 RNP for gene knockout in HSPCs and iPSCs reveals an essential role for GADD45b in stress response. *Blood Adv*. 2019 Jan 8;3(1):63-71.
22. Yang Z, Hulver M, Mcmillan RP, Cai L, Kershaw EE, Yu L, et al. Regulation of Insulin and Leptin Signaling by Muscle Suppressor of Cytokine Signaling 3 (SOCS3). *Journal of Clinical Investigation*. 2012;7(10):2–11.
23. Dees C, Pötter S, Zhang Y, Bergmann C, Zhou X, Luber M, et al. TGF- β -induced epigenetic deregulation of SOCS3 facilitates STAT3 signaling to promote fibrosis. *Journal of Clinical Investigation*. 2020 May;130(5):2347–63.
24. Wunderlich CM, Hövelmeyer N, Wunderlich FT. Mechanisms of chronic JAK-STAT3-SOCS3 signaling in obesity. *Journal of Clinical Investigation*. 2013;June:1–7.
25. Ogata H, Chinen T, Yoshida T, Kinjyo I, Takaesu G, Shiraishi H, et al. Loss of SOCS3 in the liver promotes fibrosis by enhancing STAT3-mediated TGF- β 1 production. *Journal of Clinical Investigation*. 2006;(February):2520–30.
26. Sachithanandan N, Fam BC, Fynch S, DzamKD N, Watt MJ, Wormald S, et al. Liver-Specific Suppressor of Cytokine Signaling-3 Deletion in Mice Enhances Hepatic Insulin Sensitivity and Lipogenesis Resulting in Fatty Liver and Obesity. *Journal of Clinical Investigation*. 2010;1632–42.
27. Shi H, Cave B, Inouye K, Bjørbæk C, Flier JS. Overexpression of Suppressor of Cytokine Signaling 3 in Adipose Tissue Causes Local but Not Systemic Insulin Resistance. *Journal of Clinical Investigation*. 2006;(April).
28. Pedroso JAB, Ramos-Lobo AM, Donato J. SOCS3 as a future target to treat metabolic disorders. *Hormones*. 2019 Jun;18(2):127–36.
29. Zhang Z, Wang F, Wang BJ, Chu G, Cao Q, Sun BG, et al. Inhibition of leptin-induced vascular extracellular matrix remodelling by adiponectin. *Journal of Molecular Endocrinology*. 2014 Jun;53(2):145–54.
30. Lagathu C, Christodoulides C, Tan CY, Virtue S, Laudes M, Campbell M, et al. Secreted frizzled-related protein 1 regulates adipose tissue expansion and is dysregulated in severe obesity. *International Journal of Obesity*. 2010 Dec;34(12):1695–705.

31. Huang A, Lin Y, Kao L, Chiou Y, Lee G, Lin H, et al. Inflammation-induced macrophage lysyl oxidase in adipose stiffening and dysfunction in obesity. *Clinical and Translational Medicine*. 2021 Sep;11(9).
32. Miana M, Galán M, Martínez-Martínez E, Varona S, Jurado-López R, Bausa-Miranda B, et al. The lysyl oxidase inhibitor β -aminopropionitrile reduces body weight gain and improves the metabolic profile in diet-induced obesity in rats. *DMM Disease Models and Mechanisms*. 2015 Jun;8(6):543–51.
33. Pérez-Mancera PA, Bermejo-Rodríguez C, González-Herrero I, Herranz M, Flores T, Jiménez R, et al. Adipose tissue mass is modulated by SLUG (SNAI2). *Human Molecular Genetics*. 2007 Dec;16(23):2972–86.
34. Sakashita H, Yamada S, Kinoshita M, Kajikawa T, Iwayama T, Murakami S. Mice lacking PLAP-1/asporin counteracts high fat diet-induced metabolic disorder and alveolar bone loss by controlling adipose tissue expansion. *Scientific Reports*. 2021 Dec;11(1).
35. Doncheva AI, Norheim FA, Hjorth M, Grujic M, Paivandy A, Dankel SN, et al. Serglycin Is Involved in Adipose Tissue Inflammation in Obesity. *The Journal of Immunology*. 2022 Jan;208(1):121–32.
36. Boughanem H, Yubero-Serrano EM, López-Miranda J, Tinahones FJ, Macias-Gonzalez M, Sala LL. Molecular Sciences Potential Role of Insulin Growth-Factor-Binding Protein 2 as Therapeutic Target for Obesity-Related Insulin Resistance. *Int J Mol Sci*. 2021;22:1133–1133.
37. Yoon YS, Seo WY, Lee MW, Kim ST, KDo SH. Salt-inducible kinase regulates hepatic lipogenesis by controlling SREBP-1c phosphorylation. *Journal of Biological Chemistry*. 2009;284(16):10446–52.
38. Schumann T, König J, von Loeffelholz C, Vatner DF, Zhang D, Perry RJ, et al. Deletion of the diabetes candidate gene Slc16a13 in mice attenuates diet-induced ectopic lipid accumulation and insulin resistance. *Communications Biology*. 2021 Dec;4(1).
39. Vergnes L, Chin R, Young SG, Reue K. Heart-type fatty acid-binding protein is essential for efficient brown adipose tissue fatty acid oxidation and cold tolerance. *Journal of Biological Chemistry*. 2011 Jan;286(1):380–90.
40. Zhang Y, Kent JW, Lee A, Cerjak D, Ali O, Diasio R, et al. Fatty acid binding protein 3 (fabp3) is associated with insulin, lipids and cardiovascular phenotypes of the metabolic syndrome through epigenetic modifications in a northern european family population. *BMC Medical Genomics*. 2013;6(1).
41. Khadir A, Tiss A, Abubaker J, Abu-Farha M, Al-Khairi I, Cherian P, et al. Map kinase phosphatase dusp1 is overexpressed in obese humans and modulated by physical exercise. *American Journal of Physiology - Endocrinology and Metabolism*. 2015;308(1):E71–83.
42. Lawan A, Zhang L, Gatzke F, Min K, Jurczak MJ, Al-mutairi M, et al. Regulates Glucose Metabolism and Energy Homeostasis. 2015;35(1):26–40.
43. Dickinson RJ, Keyse SM. Diverse physiological functions for dual-specificity MAP kinase phosphatases. *Journal of Cell Science*. 2006 Nov;119(22):4607–15.
44. Ferguson BS, Nam H, Stephens JM, Morrison RONF. Mitogen-Dependent Regulation of DUSP1 Governs ERK and p38 Signaling During Early 3T3-L1 Adipocyte Differentiation. 2015;(April):1562–74.

45. Kim D, Kim J, Yoon JH, Ghim J, Yea K, Song P, et al. CXCL12 secreted from adipose tissue recruits macrophages and induces insulin resistance in mice. *Diabetologia*. 2014;57(7):1456–65.
46. Dedobbeleer M, Willems E, Lambert J, Lombard A, Digregorio M, Lumapati PN, et al. MKP1 phosphatase is recruited by CXCL12 in glioblastoma cells and plays a role in DNA strand breaks repair. *Carcinogenesis*. 2020 Jun;41(4):417–29.
47. Rodrigues RM, Guan Y, Gao B. Targeting adipose tissue to tackle NASH: SPARCL1 as an emerging player. *Journal of Clinical Investigation*. 2021;131(20).

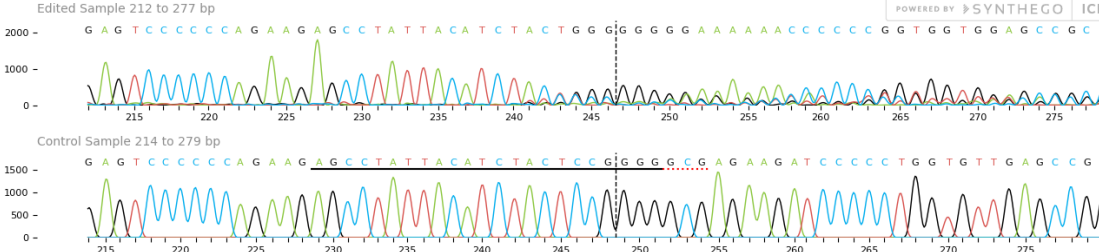
Supplementary material

Supplemental Tables S1 and S2: <https://doi.org/10.5281/zenodo.8302260>.

Supplemental Table 1. Analysis of genome-editing event using Sanger sequencing data with Synthego ICE tool (<https://ice.synthego.com/>). “Traces” tab (A) and “contribution” tab (B) are showed for each edited cell line. **A.** “Trace” tab shows edited and wild-type (control) sequences in the region around the guide sgRNA cut. The horizontal black underlined region represents the guide sequence. The horizontal red underline is the PAM site. The vertical black dotted line represents the actual cut site. Cutting and error-prone repair usually results in mixed sequencing bases after the cut, which are represented as a mix chromatogram pick. **B.** “Contribution” tab shows the inferred sequences present in the edited population, explaining the type of edit (indel) and its relative proportion (contribution). Cut sites are represented by black vertical dotted lines, nucleotides that have been deleted are indicated by a dash, and letter 'N' indicates a mix chromatogram pick.

Gene	sgRNA	PAM sequence	% efficiency
<i>SOCS3</i>	AGCCTATTACATCTACTCCGGGG	GCG	92

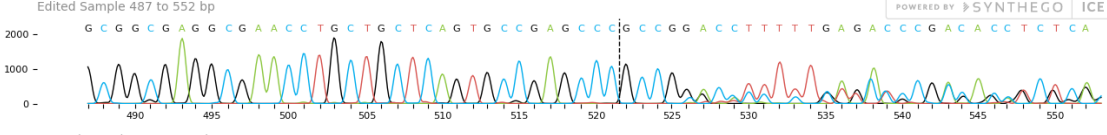
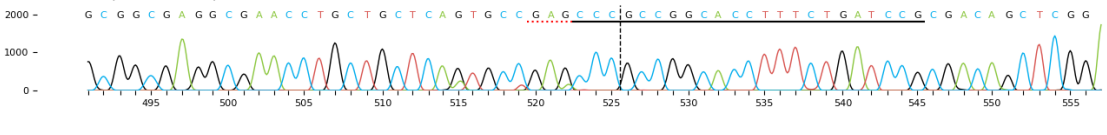
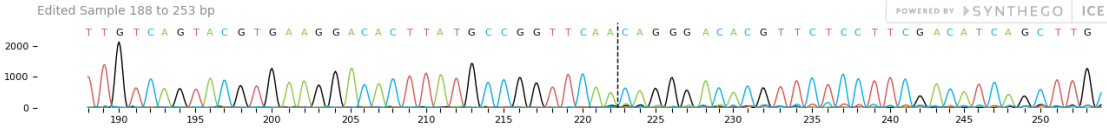
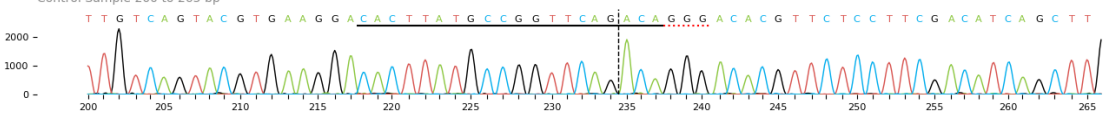
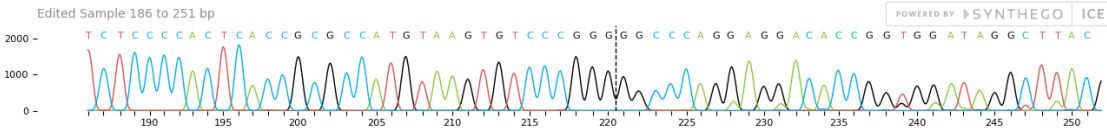
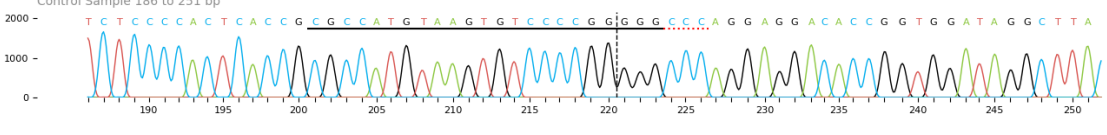
A.



POWERED BY SYNTHEGO ICE

B.

INDEL	CONTRIBUTION	SEQUENCE
+1	26%	AGAAAGAGCCTATTACATCTACTCCG N G G G G C G A G A A G A T C C C C T G G T G T T G A G C C G G C C C C T C T C C T C C A A C G T
-1	23%	AGAAAGAGCCTATTACATCTACTCCG - G G G G C G A G A A G A T C C C C T G G T G T T G A G C C G G C C C C T C T C C T C C A A C G T G
-2	22%	AGAAAGAGCCTATTACATCTACTCC G G G G G C G A G A A G A T C C C C T G G T G T T G A G C C G G C C C C T C T C C T C C A A C G T G
-1	8%	AGAAAGAGCCTATTACATCTACTCC G G G G G C G A G A A G A T C C C C T G G T G T T G A G C C G G C C C C T C T C C T C C A A C G T G
-3	7%	AGAAAGAGCCTATTACATCTACT G G G G G C G A G A A G A T C C C C T G G T G T T G A G C C G G C C C C T C T C C T C C A A C G T G
-5	6%	AGAAAGAGCCTATTACATCTA G G G G G C G A G A A G A T C C C C T G G T G T T G A G C C G G C C C C T C T C C T C C A A C G T G

<i>SOCS3</i>	CGGATCAGAAAGGTGCCGGCGGG	CTC	87
A.			
	Edited Sample 487 to 552 bp  Control Sample 491 to 556 bp 		
B.			
	INDEL CONTRIBUTION ▾ SEQUENCE +1 45% G A A C C T G C T G C T C A G T G C C G A G C C C N G C C G G C A C C T T T C T G A T C C G C G A C A G C T C G G A C C A G C G C C A C T T C T C A -1 42% G A A C C T G C T G C T C A G T G C C G A G C C C - C C G G C A C C T T T C T G A T C C G C G A C A G C T C G G A C C A G C G C C A C T T C T C A C		
Gene	sgRNA	PAM sequence	% efficiency
<i>SIKI</i>	CACTTATGCCGGTTCAGACA	GGG	96
A.			
	Edited Sample 188 to 253 bp  Control Sample 200 to 265 bp 		
B.			
	INDEL CONTRIBUTION ▾ SEQUENCE -1 89% G T G A A G G A C A C T T A T G C C G G T T C A - A C A G G G A C A C G T T C T C C T C T G A C A T C A G C T T G C C C G A G A A G A T T C A G T C T -1 * 4% G T G A A G G A C A C T T A T G C C G G T T C A G - C A G G G A C A C G T T C T C C T C T G A C A T C A G C T T G C C C G A G A A G A T T C A G T C T -2 * 3% G T G A A G G A C A C T T A T G C C G G T T C - A C A G G G A C A C G T T C T C C T C T G A C A T C A G C T T G C C C G A G A A G A T T C A G T C T		
<i>SIKI</i>	CGCCATGTAAGTGTCCCCGGGGG	CCC	96
A.			
	Edited Sample 186 to 251 bp  Control Sample 186 to 251 bp 		
B.			
	INDEL CONTRIBUTION ▾ SEQUENCE -1 93% C A C C G C G C C A T G T A A G T G T C C C G G - G G C C C A G G A G G A C A C C G G T G G A T A G G C T T A C G G T C A C G T G A G G G T G G G -2 * 3% C A C C G C G C C A T G T A A G T G T C C C G G - G G C C C A G G A G G A C A C C G G T G G A T A G G C T T A C G G T C A C G T G A G G G T G G G		

Gene	sgRNA	PAM sequence	% efficiency																									
<i>DUSPI</i>	TACTAGCGTCCCTGACAGCG	AAT	91																									
A.																												
<p>Edited Sample 178 to 243 bp</p> <p>Control Sample 183 to 248 bp</p>																												
B.																												
<p>INDEL CONTRIBUTION ▾ SEQUENCE</p> <table border="1"> <tr> <td>+1</td> <td>77%</td> <td>CTGAGTACTAGCGTCCCCCTGACAGCG</td> <td> NCGGAATCTGGGTGCAGTCCCTGCAGTACCCCAC</td> <td>TCTACGATCAGGTTAG</td> </tr> <tr> <td>-2</td> <td>7%</td> <td>CTGAGTACTAGCGTCCCCCTGACAGCG-</td> <td>-GGAATCTGGGTGCAGTCCCTGCAGTACCCCAC</td> <td>TCTACGATCAGGTTAGT</td> </tr> <tr> <td>-2</td> <td>6%</td> <td>CTGAGTACTAGCGTCCCCCTGACAGCG</td> <td>--GAATCTGGGTGCAGTCCCTGCAGTACCCCAC</td> <td>TCTACGATCAGGTTAGT</td> </tr> <tr> <td>-6</td> <td>1%</td> <td>CTGAGTACTAGCGTCCCCCTGAC-----</td> <td>--GAATCTGGGTGCAGTCCCTGCAGTACCCCAC</td> <td>TCTACGATCAGGTTAGT</td> </tr> <tr> <td>-2</td> <td>1%</td> <td>CTGAGTACTAGCGTCCCCCTGACAG--</td> <td>CGGAAATCTGGGTGCAGTCCCTGCAGTACCCCAC</td> <td>TCTACGATCAGGTTAGT</td> </tr> </table>				+1	77%	CTGAGTACTAGCGTCCCCCTGACAGCG	NCGGAATCTGGGTGCAGTCCCTGCAGTACCCCAC	TCTACGATCAGGTTAG	-2	7%	CTGAGTACTAGCGTCCCCCTGACAGCG-	-GGAATCTGGGTGCAGTCCCTGCAGTACCCCAC	TCTACGATCAGGTTAGT	-2	6%	CTGAGTACTAGCGTCCCCCTGACAGCG	--GAATCTGGGTGCAGTCCCTGCAGTACCCCAC	TCTACGATCAGGTTAGT	-6	1%	CTGAGTACTAGCGTCCCCCTGAC-----	--GAATCTGGGTGCAGTCCCTGCAGTACCCCAC	TCTACGATCAGGTTAGT	-2	1%	CTGAGTACTAGCGTCCCCCTGACAG--	CGGAAATCTGGGTGCAGTCCCTGCAGTACCCCAC	TCTACGATCAGGTTAGT
+1	77%	CTGAGTACTAGCGTCCCCCTGACAGCG	NCGGAATCTGGGTGCAGTCCCTGCAGTACCCCAC	TCTACGATCAGGTTAG																								
-2	7%	CTGAGTACTAGCGTCCCCCTGACAGCG-	-GGAATCTGGGTGCAGTCCCTGCAGTACCCCAC	TCTACGATCAGGTTAGT																								
-2	6%	CTGAGTACTAGCGTCCCCCTGACAGCG	--GAATCTGGGTGCAGTCCCTGCAGTACCCCAC	TCTACGATCAGGTTAGT																								
-6	1%	CTGAGTACTAGCGTCCCCCTGAC-----	--GAATCTGGGTGCAGTCCCTGCAGTACCCCAC	TCTACGATCAGGTTAGT																								
-2	1%	CTGAGTACTAGCGTCCCCCTGACAG--	CGGAAATCTGGGTGCAGTCCCTGCAGTACCCCAC	TCTACGATCAGGTTAGT																								
<i>DUSPI</i>	CGTCCAGAACACCACGGCG	TAG	91																									
A.																												
<p>Edited Sample 231 to 296 bp</p> <p>Control Sample 234 to 299 bp</p>																												
B.																												
<p>INDEL CONTRIBUTION ▾ SEQUENCE</p> <table border="1"> <tr> <td>+1</td> <td>65%</td> <td>GCGGCCCTGCTGGCGGCCCTACCA</td> <td> NCGCCGTGGTGCTGGACGAGCGCAGCGCCGCCCTGGACGGCGCCAAG</td> <td></td> </tr> <tr> <td>-1</td> <td>22%</td> <td>GCGGCCCTGCTGGCGGCCCTACCA</td> <td>-GCGCTGGTGCTGGACGAGCGCAGCGCCGCCCTGGACGGCGCCAAGC</td> <td></td> </tr> <tr> <td>-30</td> <td>2%</td> <td>GCGGCCCTGCTGGCGGCCCTACCA</td> <td>-----AGCGCAGCGCCGCCCTGGACGGCGCCAAGC</td> <td></td> </tr> <tr> <td>-6</td> <td>1%</td> <td>GCGGCCCTGCTGGCGGCCCTACCA</td> <td>-----GGTTGCTGGACGAGCGCAGCGCCGCCCTGGACGGCGCCAAGC</td> <td></td> </tr> <tr> <td>-2</td> <td>1%</td> <td>GCGGCCCTGCTGGCGGCCCTACCA</td> <td>--CCGTGGTGCTGGACGAGCGCAGCGCCGCCCTGGACGGCGCCAAGC</td> <td></td> </tr> </table>				+1	65%	GCGGCCCTGCTGGCGGCCCTACCA	NCGCCGTGGTGCTGGACGAGCGCAGCGCCGCCCTGGACGGCGCCAAG		-1	22%	GCGGCCCTGCTGGCGGCCCTACCA	-GCGCTGGTGCTGGACGAGCGCAGCGCCGCCCTGGACGGCGCCAAGC		-30	2%	GCGGCCCTGCTGGCGGCCCTACCA	-----AGCGCAGCGCCGCCCTGGACGGCGCCAAGC		-6	1%	GCGGCCCTGCTGGCGGCCCTACCA	-----GGTTGCTGGACGAGCGCAGCGCCGCCCTGGACGGCGCCAAGC		-2	1%	GCGGCCCTGCTGGCGGCCCTACCA	--CCGTGGTGCTGGACGAGCGCAGCGCCGCCCTGGACGGCGCCAAGC	
+1	65%	GCGGCCCTGCTGGCGGCCCTACCA	NCGCCGTGGTGCTGGACGAGCGCAGCGCCGCCCTGGACGGCGCCAAG																									
-1	22%	GCGGCCCTGCTGGCGGCCCTACCA	-GCGCTGGTGCTGGACGAGCGCAGCGCCGCCCTGGACGGCGCCAAGC																									
-30	2%	GCGGCCCTGCTGGCGGCCCTACCA	-----AGCGCAGCGCCGCCCTGGACGGCGCCAAGC																									
-6	1%	GCGGCCCTGCTGGCGGCCCTACCA	-----GGTTGCTGGACGAGCGCAGCGCCGCCCTGGACGGCGCCAAGC																									
-2	1%	GCGGCCCTGCTGGCGGCCCTACCA	--CCGTGGTGCTGGACGAGCGCAGCGCCGCCCTGGACGGCGCCAAGC																									

5. DISCUSSION

The main objective of this work was to identify dysregulated genes in scWAT involved in the correct expansion of AT, that could have a potential role as: 1) biomarkers for prediction of metabolic diseases progression or 2) novel targets for future therapies against ectopic fat accumulation. To this end, we analyzed the transcriptome of scWAT of patients with varying degrees of adiposity and associated the results with different indicators of the metabolic status of an individual.

The cohort used for this study was the FATE cohort, a longitudinal cohort of obese patients undergoing bariatric surgery that donated biological samples. This cohort is divided in two sub-cohorts. The first one is composed by patients that underwent a CT imaging test for the quantitative determination of subcutaneous and visceral abdominal fat; while the second is characterized by the availability of liver biopsies to determine the degree of hepatosteatosis.

Considering that, we set two independent but related lines of research, each of them taking advantage of the information provided by each of the sub-cohorts. In fact, both clinical data, the abdominal fat distribution and the degree of liver steatosis, give us valuable information about the expandability capacity of scWAT, as visceral fat and liver are the main organs that accumulate ectopic fat when scWAT accumulation capacity is exceeded. Therefore, both lines of research were aligned with our final goal of understanding the molecular mechanisms leading to the correct expansion of scWAT in obese patients.

Our first line of research was focused on how physical location of fat in the abdominal region determines the different obesity phenotypes, highlighting the importance of identifying a non-invasive biomarker that reflects AT distribution and, consequently, that could predict complications of obesity.

It has been broadly studied that the physical location of fat dramatically influences obesity-related disease risk²³⁵⁻²³⁷. Accumulation of AT in the upper body, in the abdominal region, is associated with the development of metabolic comorbidities; while deposition of fat in the lower body, in the gluteofemoral region, is associated with a protective lipid and glucose profile as well as a decrease in cardiovascular and metabolic disease prevalence^{63,64}. This association of abdominal obesity with metabolic risk is primarily attributed to visWAT expansion⁶⁰. visWAT expansion occurs when scWAT reaches its maximal storage capacity and fails to store lipids appropriately, redirecting the

lipid flux to visWAT and other peripheral organs, where it is accumulated as ectopic fat. This excessive fat causes insulin resistance through lipotoxic and inflammation-related mechanisms⁶⁹, increasing health risk.

Considering that, the differentiation between visceral and subcutaneous abdominal fat seems to be critical to assess the metabolic status of an individual^{238,239}. Therefore, we decided to focus on a parameter that consider the area of both fat depots, the sc/vis ratio. We stratified the patients in our cohort according to this sc/vis ratio, thanks to the data obtained from the CT imaging test, and confirmed that this value was a good indicator of metabolic risk. Patients with more subcutaneous and less abdominal fat (higher sc/vis ratio) presented lower levels of indicators of metabolic risk, having less insulin resistance (lower HOMA), less lipids alteration (lower triglycerides and higher HDL serum concentration) and lower levels of liver damage markers (GGT and ALT). All in agreement with previous data that associated visceral obesity with disturbances in insulin-glucose homeostasis^{240–242}, alterations in plasma lipoprotein-lipid levels^{243,244} and liver dysfunction^{245,246}.

However, this indicator has important limitations as predictor of metabolic risk, as imaging techniques are required to determine its value, what is often complex and impractical in many clinical settings. Therefore, our next step was to identify a cost-efficient and clinically applicable biomarker that accurately reflect sc/vis AT distribution.

Secreted factors, like adipokines, are biomarkers of preferable choice for metabolic diseases since their production is often dysregulated in obese individuals and contribute to the pathogenesis of obesity-associated metabolic complications^{247,248}. Considering that the synthesis of adipokines reflects AT function in overall metabolic homeostasis, we assumed that differences in the expression of specific adipokines in scWAT could reveal divergence in the metabolic phenotype.

We identified two genes, *CCDC3* and *ISM1*, previously reported to encode adipokines and whose expression in scWAT correlated with the sc/vis ratio. However, we could not reproduce *CCDC3* AT expression to serum concentration levels, excluding this adipokine as a valid biomarker for AT distribution. It could be explained by the fact that *CCDC3* expression levels were higher in visceral rather in subcutaneous fat and could be different mechanisms regulating its expression and secretion in both fat depots. These results are in line with previous data that linked *CCDC3* expression with visceral obesity²⁴⁹.

By contrary, we observed a strong positive correlation between circulating ISM1 levels and the sc/vis ratio. Moreover, visWAT *ISM1* expression was much lower and did not show any correlation with serum levels. It could indicate that the higher ISM1 serum levels observed in individuals with the most favorable metabolic profile (higher sc/vis ratio) might be secreted by subcutaneous adipose cells and might exert endocrine protective effects in other tissues.

This potential function of ISM1 in regulating whole body metabolism is in line with previous published data. ISM1 has been recently identified in mouse and human adipocytes as an adipokine that has important metabolic roles in multiple tissues, promoting glucose uptake, inhibiting hepatic lipogenesis^{250,251}, and stimulating protein synthesis²⁵², thus improving hyperglycemia and reducing lipid accumulation in mouse models. Moreover, ISM1 expression in adipocytes, as well as circulating ISM1 levels, have been associated with obesity and type 2 diabetes mellitus (T2DM)^{253,254}.

Considering that and to further understand the metabolic regulation of ISM1, we conducted a comprehensive correlation analysis. We found significant correlations between ISM1 and several key factors, highlighting a strong association with leptin. Both ISM1 and leptin seem to be expressed mainly by scWAT, increasing their levels in obesity. In addition, both seem to have a role in the regulation of glucose metabolism, so future research is needed to elucidate a common regulatory mechanism or a combined function of these adipokines in the maintenance of energy homeostasis.

In conclusion, the first part of our research proves the importance of distinguishing AT location to classify obesity phenotypes and proposes ISM1 as novel non-invasive biomarker to predict abdominal fat partitioning and, consequently, to evaluate obesity-related health risks.

Once we studied the general classification of obesity phenotypes, we decided to focus on one of the main comorbidities associated to obesity, NAFLD. As discussed above, AT dysfunction is one of the main causes of fat deposition in the liver and it usually occurs when AT exceeded its fat storage capacity^{95,113}.

Therefore, and aligned with our final goal of understanding the molecular mechanism leading to the correct expansion of scWAT in obese patients, we tried to uncover novel

genes whose regulation in scWAT could be essential in liver fat deposition and, consequently, in the development and progression of NAFLD.

For that purpose, we initially performed a high throughput gene expression analysis from scWAT of patients with different degrees of liver steatosis and correlated these results with FLI, a surrogate biomarker of liver steatosis^{255,256}. We then validated the results in a second independent cohort, where pair scWAT-liver biopsies were available and patients were classified according to their NAS, a histological score that accurately reflect liver steatosis²⁵⁷. This two-step validation of our findings in two independent cohorts allowed us to identify six genes whose expression in scWAT increases accordingly to the degree of hepatic steatosis: *DUSP1*, *GADD45B*, *SIK1*, *SOCS3*, *S100A9* and *S100A12*.

To verify whether the previously observed differences in gene expression at scWAT level were adipocyte-specific or occurred in other cell types within the scWAT, we established an *in vitro* model based on hADMSC-derived adipocytes isolated from patients with different degrees of liver steatosis. Several studies have shown that hADMSC isolated from patients with metabolic disorders like obesity and diabetes are defective in various functionalities and properties²⁵⁸ including differentiation²⁵⁹, multipotent state^{260,261}, metabolism^{262,263} and immunomodulation²⁶⁴. Considering that, we tried to address if there were also a correlation between the physiological status of hADMSC and the degree of liver steatosis in order to directly link AT expandability capacity to dysfunctional liver crosstalk.

Interestingly, we observed a decrease in lipid accumulation in hADMSC-derived adipocytes from NAFLD patients indicating impaired adipogenesis of these pre-adipocytes along with NAFLD severity. This negative association between the adipogenic potential of hMSC and the degree of liver steatosis suggests that impaired hMSC differentiation relates to altered WAT expandability and thus, could be a crucial step in development and progression of NAFLD. Indeed, a lower lipid storage capacity in adipocytes may eventually promote fat accumulation in the liver, which is in agreement with previous reports⁹⁶ and consistent with our WAT expandability hypothesis.

Once our *in vitro* model was characterized, expression levels of our target genes were measured in hADMSC-derived adipocytes. Surprisingly, *S100A9* and *S100A12* did not show expression in adipocytes, suggesting that the differential expression observed at scWAT level comes from other cellular type(s) within the WAT, probably immune

system cells²⁶⁵. However, *SOCS3*, *DUSP1*, *SIK1* and *GADD45B* showed the same regulatory pattern in hADMSC-derived adipocytes as observed in scWAT, reinforcing the idea that these genes are directly involved in NAFLD progression by exerting regulatory actions specifically in adipocytes.

Therefore, we decided to focus on these adipocyte-expressed genes and go further in clarifying its physiological role in scWAT and in NAFLD progression. To this end, we optimized a CRISPR/Cas9 protocol to reduce the expression of our target genes (*SOCS3*, *DUSP1* and *SIK1*) in hADMSC without affecting their adipogenic potential. We then differentiated these modified cells into adipocytes and evaluated their adipogenic capacity and phenotypical changes at the transcriptomic and metabolic levels.

The efficiency of CRISPR/Cas9 to edit AT has already been tested in hADMSC to knockout the expression of crucial adipocyte genes such as *PPARG*²²³, *UCPI*²²⁴ or *NRIP1*²⁶⁶, proving the potential of this gene editing tool to treat metabolic complications associated to obesity. We were able to optimize a CRISPR/Cas9 protocol for our *in vitro* model of hADMSC obtained from obese patients. We transfected the RNP-sgRNA complex by electroporation and achieved a very high percentage of edited cells, thus avoiding the subsequent selection of modified cells that involves multiple passages that may impair hAMSC differentiation capacity²²³. Moreover, the genomic edition translated into a significant reduction of *SOCS3*, *DUSP1* and *SIK1* mRNA levels, allowing us to characterize these cell lines and to determine the physiological role of the target genes.

As discussed in detail in the discussion section of the third manuscript, the reduction of the expression of these genes had important consequences in the adipocyte's lipid metabolic function, altering processes as lipolysis (basal and isoprenaline-stimulated) *de novo* lipogenesis or palmitate uptake. Moreover, RNA-sequencing analysis of edited cells showed that these genes not only altered lipid metabolism but also other biological pathways related to inflammatory processes, in the case of *DUSP1*, extracellular matrix remodeling for *SOCS3*, or cellular transport for *SIK1*. These results support our hypotheses that *SOCS3*, *DUSP1*, and *SIK1* regulate multiple aspects of adipocyte function which may play a role in the progression of obesity-associated comorbidities.

Finally, we evaluate a possible adipocyte-hepatocyte axis to determine if the metabolic changes observed in modified adipocytes could be translated into variations of fat deposition in the hepatocytes. Our HepG2-adipocyte co-culture model showed a

significant reduction in palmitate accumulation in hepatocytes co-culture with modified adipocytes, suggesting a communication between both cellular types.

Therefore, the results of our second line of research constitute a proof-of-evidence of the paramount importance of adipose-liver crosstalk and suggest that impaired adipogenic capacity of hADMSC is a critical event in promoting the development of NAFLD. Moreover, we identified three genes, *SOCS3*, *DUSP1*, and *SIK1*, dysregulated in patients with liver steatosis and key regulators of AT functionality. We demonstrated that restoration of fully functional hADMSC phenotype (such as through specific gene(s) modulation using CRISPR/Cas9 technology) might be an additional strategy to address NAFLD and its associated complications.

These findings collectively underscore the importance of AT fat accumulation capacity in maintenance of whole body homeostasis. We demonstrated that dysregulation of key genes in scWAT alters AT functionality, what determines ectopic fat deposition mainly in the visWAT, leading to visceral obesity, and in the liver, leading to NAFLD.

However, the study has some limitations that need to be discussed. The main limitation is the cohort in which the study has been conducted. The cohort is composed mainly by individuals with obesity, and how these results translate to non-obese also warrants further investigations. For instance, it would be necessary to evaluate *ISM1* expression and secretion levels in non-obese patient before confirming its potential as biomarker. Similarly, *SOCS3*, *SIK1*, and *DUSP1* expression in adipocytes obtained from healthy donors should be checked to confirm that their dysregulation is associated specifically to NAFLD and not to other comorbidities associated to obesity.

Our current findings lay the foundation for future research, as they raise important questions. For instance, the molecular mechanism regulating *ISM1* expression in scWAT and its association with leptin; or the target tissues and function of this adipokine. Similarly, functional studies are needed to fully decipher the metabolic actions of *SOCS3*, *SIK1* and *DUSP1* in humans and within the metabolic disease context.

In conclusion, our results highlight the importance of scWAT fat storage capacity. We propose some genes as key regulators of AT functionality, which is critical for visceral obesity and NAFLD development and progression. Moreover, our results constitute a proof-of-concept of the potential of CRISPR/Cas9 technology to treat metabolic complications.

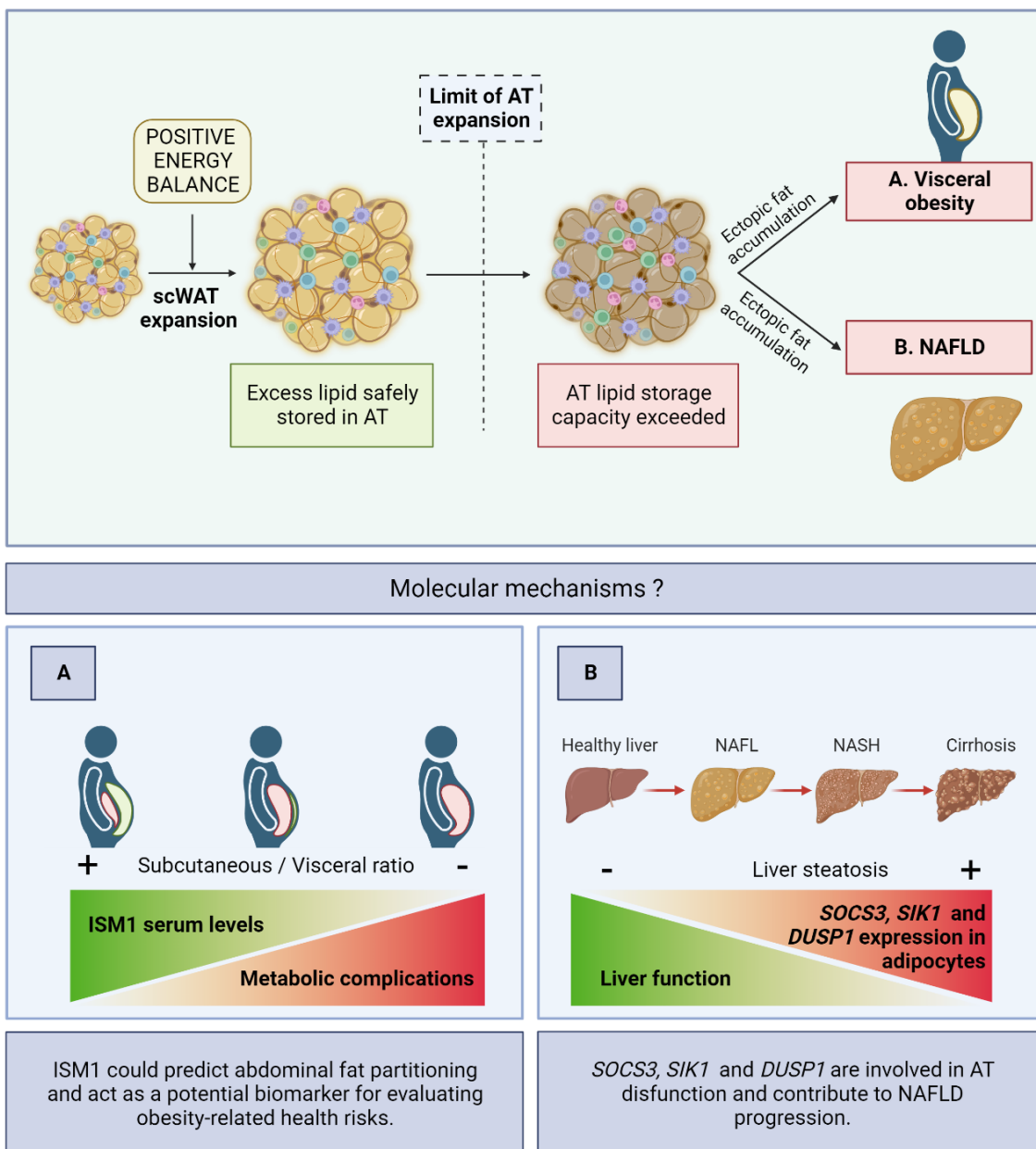


Figure 11. Graphical abstract of the thesis.

6. CONCLUSIONS

The following conclusions can be drawn from the results presented above:

- 1- It is critical to distinguish adipose tissue location to classify obesity phenotypes. The SFA/VFA ratio is an accurate metric to classify the metabolic status of individuals with similar perceived obesity (same BMI and same waist circumference).
- 2- ISM1 expression levels in scWAT and its serum levels exhibited a correlation with the SFA/VFA ratio. These findings suggest that ISM1 could predict abdominal fat partitioning and act as a potential biomarker for evaluating obesity-related health risks.
- 3- Adipogenic capacity of ADMSC decreased as liver steatosis increased, proposing that an impaired adipogenic capacity is a critical event in the development of NAFLD.
- 4- *SOCS3*, *DUSP1*, *SIK1* and *GADD45B* showed a differential expression pattern in both scWAT and hADMSC-derived adipocytes of patients with NAFLD. Their expression paralleled steatosis degree.
- 5- Editing out *SOCS3*, *DUSP1*, and *SIK1* using CRISP/Cas9 technology reduced their expression in hADMSC without conditioning its adipogenic capacity, highlighting the potential of this gene editing tool to treat metabolic complications.
- 6- *SOCS3*, *DUSP1*, and *SIK1* downregulation in adipocytes altered lipid metabolism, suggesting that these genes regulate multiple aspects of adipocyte function and may play a role in the progression of obesity-associated comorbidities, such as NAFLD.

De los resultados presentados pueden extraerse las siguientes conclusiones:

- 1- Es fundamental distinguir la localización del tejido adiposo para clasificar los distintos fenotipos de la obesidad. La relación entre el área de grasa subcutánea y visceral (ratio sub/vis) es una métrica precisa para clasificar el estado metabólico de individuos con obesidad aparentemente similar (mismo IMC y mismo perímetro de cintura).
- 2- Los niveles de expresión de *ISM1* en tejido adiposo subcutáneo y sus niveles séricos mantienen una correlación directa con el ratio sub/vis. Esto sugiere que *ISM1* podría predecir la distribución de la grasa abdominal y actuar como biomarcador para evaluar los riesgos de desarrollar comorbilidades relacionados con la obesidad.
- 3- La capacidad adipogénica de las hADMSC disminuye a medida que aumenta la esteatosis hepática, proponiendo que una capacidad adipogénica alterada es un evento crítico en el desarrollo de la enfermedad de hígado graso no alcohólico.
- 4- *SOCS3*, *DUSP1*, *SIK1* y *GADD45B* muestran un patrón de expresión diferencial en tejido adiposo subcutáneo y en adipocitos derivados de pacientes con hígado graso. Su expresión mantiene una correlación directa con el grado de esteatosis.
- 5- La edición genética de *SOCS3*, *DUSP1* y *SIK1* mediante la tecnología CRISP/Cas9 reduce su expresión en adipocitos sin condicionar su capacidad adipogénica, destacando el potencial de esta herramienta de edición genética para tratar complicaciones metabólicas.
- 6- La supresión de la expresión de *SOCS3*, *DUSP1* y *SIK1* en adipocitos altera el metabolismo lipídico, lo que sugiere que estos genes regulan múltiples aspectos de la función de los adipocitos y pueden desempeñar un papel en la progresión de comorbilidades asociadas a la obesidad, como la enfermedad de hígado graso no alcohólico.

7. REFERENCES

1. Kwok KHM, Lam KSL, Xu A. Heterogeneity of white adipose tissue: Molecular basis and clinical implications. *Exp Mol Med.* 2016;48(3). doi:10.1038/emm.2016.5
2. Sakers A, De Siqueira MK, Seale P, Villanueva CJ. Adipose-tissue plasticity in health and disease. *Cell.* 2022;185(3):419-446. doi:10.1016/j.cell.2021.12.016
3. Luo L, Liu M. Adipose tissue in control of metabolism. *Journal of Endocrinology.* 2016;231(3):R77-R99. doi:10.1530/JOE-16-0211
4. Zwick RK, Guerrero-Juarez CF, Horsley V, Plikus M V. Anatomical, Physiological, and Functional Diversity of Adipose Tissue. *Cell Metab.* 2018;27(1):68-83. doi:10.1016/j.cmet.2017.12.002
5. Arner P, Rydén M. Human white adipose tissue: A highly dynamic metabolic organ. *J Intern Med.* 2022;291(5):611-621. doi:10.1111/joim.13435
6. Carpentier AC, Blondin DP, Haman F, Richard D. Brown Adipose Tissue-A Translational Perspective. *Endocr Rev.* 2023;44(2):143-192. doi:10.1210/endrev/bnac015
7. Pilkington AC, Paz HA, Wankhade UD. Beige Adipose Tissue Identification and Marker Specificity—Overview. *Front Endocrinol (Lausanne).* 2021;12. doi:10.3389/fendo.2021.599134
8. Frank AP, De Souza Santos R, Palmer BF, Clegg DJ. Determinants of body fat distribution in humans may provide insight about obesity-related health risks. *J Lipid Res.* 2019;60(10):1710-1719. doi:10.1194/jlr.R086975
9. Zwick RK, Guerrero-Juarez CF, Horsley V, Plikus M V. Anatomical, Physiological, and Functional Diversity of Adipose Tissue. *Cell Metab.* 2018;27(1):68-83. doi:10.1016/j.cmet.2017.12.002
10. Ibrahim MM. Subcutaneous and visceral adipose tissue: Structural and functional differences. *Obesity Reviews.* 2010;11(1):11-18. doi:10.1111/j.1467-789X.2009.00623.x
11. Pittenger MF, Discher DE, Péault BM, Phinney DG, Hare JM, Caplan AI. Mesenchymal stem cell perspective: cell biology to clinical progress. *NPJ Regen Med.* 2019;4(1). doi:10.1038/s41536-019-0083-6
12. Roobrouck VD, Ulloa-Montoya F, Verfaillie CM. Self-renewal and differentiation capacity of young and aged stem cells. *Exp Cell Res.* 2008;314(9):1937-1944. doi:10.1016/j.yexcr.2008.03.006

13. Spalding KL, Arner E, Westermark PO, et al. Dynamics of fat cell turnover in humans. *Nature*. 2008;453(7196):783-787. doi:10.1038/nature06902
14. Ghaben AL, Scherer PE. Adipogenesis and metabolic health. *Nat Rev Mol Cell Biol*. 2019;20(4):242-258. doi:10.1038/s41580-018-0093-z
15. Cristancho AG, Lazar MA. Forming functional fat: A growing understanding of adipocyte differentiation. *Nat Rev Mol Cell Biol*. 2011;12(11):722-734. doi:10.1038/nrm3198
16. Farmer SR. *Transcriptional Control of Adipocyte Formation*.
17. Blázquez-Medela AM, Jumabay M, Boström KI. Beyond the bone: Bone morphogenetic protein signaling in adipose tissue. *Obesity Reviews*. 2019;20(5):648-658. doi:10.1111/obr.12822
18. Chang E, Kim CY. Natural products and obesity: A focus on the regulation of mitotic clonal expansion during adipogenesis. *Molecules*. 2019;24(6). doi:10.3390/molecules24061157
19. Madsen MS, Siersbæk R, Boergesen M, Nielsen R, Mandrup S. Peroxisome Proliferator-Activated Receptor γ and C/EBP α Synergistically Activate Key Metabolic Adipocyte Genes by Assisted Loading. *Mol Cell Biol*. 2014;34(6):939-954. doi:10.1128/mcb.01344-13
20. *Cross-Regulation of C/EBP and PPAR Controls the Transcriptional Pathway of Adipogenesis and Insulin Sensitivity*.
21. Gregoire FM, Smas CM, Sul S. *Understanding Adipocyte Differentiation*. Vol 78.; 1998.
22. Ambele MA, Dhanraj P, Giles R, Pepper MS. Adipogenesis: A complex interplay of multiple molecular determinants and pathways. *Int J Mol Sci*. 2020;21(12):1-27. doi:10.3390/ijms21124283
23. Massier L, Jalkanen J, Elmastas M, et al. An integrated single cell and spatial transcriptomic map of human white adipose tissue. *Nat Commun*. 2023;14(1):1438. doi:10.1038/s41467-023-36983-2
24. Scherer PE. Adipose tissue: From lipid storage compartment to endocrine organ. In: *Diabetes*. Vol 55. ; 2006:1537-1545. doi:10.2337/db06-0263
25. Luo L, Liu M. Adipose tissue in control of metabolism. *Journal of Endocrinology*. 2016;231(3):R77-R99. doi:10.1530/JOE-16-0211
26. Song Z, Xiaoli AM, Yang F. Regulation and metabolic significance of De Novo lipogenesis in adipose tissues. *Nutrients*. 2018;10(10). doi:10.3390/nu10101383

27. Luo L, Liu M. Adipose tissue in control of metabolism. *Journal of Endocrinology*. 2016;231(3):R77-R99. doi:10.1530/JOE-16-0211
28. Carpentier AC. 100th anniversary of the discovery of insulin perspective: Insulin and adipose tissue fatty acid metabolism. *Am J Physiol Endocrinol Metab*. 2021;320(4):E653-E670. doi:10.1152/AJPENDO.00620.2020
29. Batchuluun B, Pinkosky SL, Steinberg GR. Lipogenesis inhibitors: therapeutic opportunities and challenges. *Nat Rev Drug Discov*. 2022;21(4):283-305. doi:10.1038/s41573-021-00367-2
30. Grabner GF, Xie H, Schweiger M, Zechner R. Lipolysis: cellular mechanisms for lipid mobilization from fat stores. *Nat Metab*. 2021;3(11):1445-1465. doi:10.1038/s42255-021-00493-6
31. Duncan RE, Ahmadian M, Jaworski K, Sarkadi-Nagy E, Sul HS. Regulation of lipolysis in adipocytes. *Annu Rev Nutr*. 2007;27:79-101. doi:10.1146/annurev.nutr.27.061406.093734
32. Lass A, Zimmermann R, Oberer M, Zechner R. Lipolysis - A highly regulated multi-enzyme complex mediates the catabolism of cellular fat stores. *Prog Lipid Res*. 2011;50(1):14-27. doi:10.1016/j.plipres.2010.10.004
33. Saponaro C, Gaggini M, Carli F, Gastaldelli A. The subtle balance between lipolysis and lipogenesis: A critical point in metabolic homeostasis. *Nutrients*. 2015;7(11):9453-9474. doi:10.3390/nu7115475
34. Scheja L, Heeren J. The endocrine function of adipose tissues in health and cardiometabolic disease. *Nat Rev Endocrinol*. 2019;15(9):507-524. doi:10.1038/s41574-019-0230-6
35. Trayhurn P. Endocrine and signalling role of adipose tissue: New perspectives on fat. In: *Acta Physiologica Scandinavica*. Vol 184. ; 2005:285-293. doi:10.1111/j.1365-201X.2005.01468.x
36. Friedman JM. Leptin and the endocrine control of energy balance. *Nat Metab*. 2019;1(8):754-764. doi:10.1038/s42255-019-0095-y
37. Karbowska J, Kochan Z. *Role of Adiponectin in the Regulation of Carbohydrate and Lipid Metabolism*; 2006. <https://www.researchgate.net/publication/6574741>
38. Al-Mansoori L, Al-Jaber H, Prince MS, Elrayess MA. Role of Inflammatory Cytokines, Growth Factors and Adipokines in Adipogenesis and Insulin Resistance. *Inflammation*. 2022;45(1):31-44. doi:10.1007/s10753-021-01559-z

39. Bond ST, Calkin AC, Drew BG. Adipose-Derived Extracellular Vesicles: Systemic Messengers and Metabolic Regulators in Health and Disease. *Front Physiol.* 2022;13. doi:10.3389/fphys.2022.837001
40. Kulaj K, Harger A, Bauer M, et al. Adipocyte-derived extracellular vesicles increase insulin secretion through transport of insulinotropic protein cargo. *Nat Commun.* 2023;14(1). doi:10.1038/s41467-023-36148-1
41. Jung UJ, Choi MS. Obesity and its metabolic complications: The role of adipokines and the relationship between obesity, inflammation, insulin resistance, dyslipidemia and nonalcoholic fatty liver disease. *Int J Mol Sci.* 2014;15(4):6184-6223. doi:10.3390/ijms15046184
42. Zorena K, Jachimowicz-Duda O, Ślęzak D, Robakowska M, Mrugacz M. Adipokines and obesity. Potential link to metabolic disorders and chronic complications. *Int J Mol Sci.* 2020;21(10). doi:10.3390/ijms21103570
43. Fitch AK, Bays HE. Obesity definition, diagnosis, bias, standard operating procedures (SOPs), and telehealth: An Obesity Medicine Association (OMA) Clinical Practice Statement (CPS) 2022. *Obesity Pillars.* 2022;1:100004. doi:10.1016/j.obpill.2021.100004
44. Heymsfield SB, Wadden TA. Mechanisms, Pathophysiology, and Management of Obesity. *New England Journal of Medicine.* 2017;376(3):254-266. doi:10.1056/nejmra1514009
45. Health Effects of Overweight and Obesity in 195 Countries over 25 Years. *New England Journal of Medicine.* 2017;377(1):13-27. doi:10.1056/NEJMoa1614362
46. Pi-Sunyer X. The medical risks of obesity. *Postgrad Med.* 2009;121(6):21-33. doi:10.3810/pgm.2009.11.2074
47. Kahn SE, Hull RL, Utzschneider KM. Mechanisms linking obesity to insulin resistance and type 2 diabetes. *Nature.* 2006;444(7121):840-846. doi:10.1038/nature05482
48. Sarwar R, Pierce N, Koppe S. Obesity and nonalcoholic fatty liver disease: Current perspectives. *Diabetes Metab Syndr Obes.* 2018;11:533-542. doi:10.2147/DMSO.S146339
49. Loomba R, Friedman SL, Shulman GI. Mechanisms and disease consequences of nonalcoholic fatty liver disease. *Cell.* 2021;184(10):2537-2564. doi:10.1016/j.cell.2021.04.015

50. Lopez-Jimenez F, Almahmeed W, Bays H, et al. Obesity and cardiovascular disease: mechanistic insights and management strategies. A joint position paper by the World Heart Federation and World Obesity Federation. *Eur J Prev Cardiol.* 2022;29(17):2218-2237. doi:10.1093/eurjpc/zwac187
51. Henning RJ. *Obesity and Obesity-Induced Inflammatory Disease Contribute to Atherosclerosis: A Review of the Pathophysiology and Treatment of Obesity.* Vol 11.; 2021. www.AJCD.us/ISSN:2160-200X/AJCD0135880
52. Shariq OA, Mckenzie TJ. Obesity-related hypertension: A review of pathophysiology, management, and the role of metabolic surgery. *Gland Surg.* 2020;9(1):80-93. doi:10.21037/gs.2019.12.03
53. Avgerinos KI, Spyrou N, Mantzoros CS, Dalamaga M. Obesity and cancer risk: Emerging biological mechanisms and perspectives. *Metabolism.* 2019;92:121-135. doi:10.1016/j.metabol.2018.11.001
54. Lin X, Li H. Obesity: Epidemiology, Pathophysiology, and Therapeutics. *Front Endocrinol (Lausanne).* 2021;12. doi:10.3389/fendo.2021.706978
55. Blüher M. Obesity: global epidemiology and pathogenesis. *Nat Rev Endocrinol.* 2019;15(5):288-298. doi:10.1038/s41574-019-0176-8
56. Nuttall FQ. Body mass index: Obesity, BMI, and health: A critical review. *Nutr Today.* 2015;50(3):117-128. doi:10.1097/NT.0000000000000092
57. Frankenfield DC, Rowe WA, Cooney RN, Smith JS, Becker D. *Limits of Body Mass Index to Detect Obesity and Predict Body Composition.* Vol 17.; 2001.
58. Hammarstedt A, Gogg S, Hedjazifar S, Nerstedt A, Smith U. Impaired Adipogenesis and Dysfunctional Adipose Tissue in Human Hypertrophic Obesity. *Physiol Rev.* 1911;98. doi:10.1152/physrev
59. Goossens GH. The Metabolic Phenotype in Obesity: Fat Mass, Body Fat Distribution, and Adipose Tissue Function. *Obes Facts.* 2017;10(3):207-215. doi:10.1159/000471488
60. Kang YM, Jung CH, Cho YK, et al. Visceral adiposity index predicts the conversion of metabolically healthy obesity to an unhealthy phenotype. *PLoS One.* 2017;12(6). doi:10.1371/journal.pone.0179635
61. Torres-Perez E, Valero M, Garcia-Rodriguez B, et al. The FAT expandability (FATE) Project: Biomarkers to determine the limit of expansion and the complications of obesity. *Cardiovasc Diabetol.* 2015;14(1):1-8. doi:10.1186/s12933-015-0203-6

62. Pinnick KE, Nicholson G, Manolopoulos KN, et al. Distinct developmental profile of lower-body adipose tissue defines resistance against obesity-associated metabolic complications. *Diabetes*. 2014;63(11):3785-3797. doi:10.2337/db14-0385
63. Spalding KL, Bernard S, Näslund E, et al. Impact of fat mass and distribution on lipid turnover in human adipose tissue. *Nat Commun.* 2017;8. doi:10.1038/ncomms15253
64. Frank AP, De Souza Santos R, Palmer BF, Clegg DJ. Determinants of body fat distribution in humans may provide insight about obesity-related health risks. *J Lipid Res.* 2019;60(10):1710-1719. doi:10.1194/jlr.R086975
65. Jo J, Gavrilova O, Pack S, et al. Hypertrophy and/or hyperplasia: Dynamics of adipose tissue growth. *PLoS Comput Biol.* 2009;5(3). doi:10.1371/journal.pcbi.1000324
66. Stenkula KG, Erlanson-Albertsson C. Adipose cell size: importance in health and disease. *Am J Physiol Regul Integr Comp Physiol.* 2018;315:284-295. doi:10.1152/ajpregu.00257.2017.-Adipose
67. Muir LA, Neeley CK, Meyer KA, et al. Adipose tissue fibrosis, hypertrophy, and hyperplasia: Correlations with diabetes in human obesity. *Obesity*. 2016;24(3):597-605. doi:10.1002/oby.21377
68. Trayhurn P. Hypoxia and Adipose Tissue Function and Dysfunction in Obesity. *Physiol Rev.* 2013;93:1-21. doi:10.1152/physrev.00017.2012.-The
69. Kawai T, Autieri M V., Scalia R. Adipose tissue inflammation and metabolic dysfunction in obesity. *Am J Physiol Cell Physiol.* 2021;320(3):C375-C391. doi:10.1152/ajpcell.00379.2020
70. Wondmkun YT. Obesity, insulin resistance, and type 2 diabetes: Associations and therapeutic implications. *Diabetes, Metabolic Syndrome and Obesity*. 2020;13:3611-3616. doi:10.2147/DMSO.S275898
71. Virtue S, Vidal-Puig A. Adipose tissue expandability, lipotoxicity and the Metabolic Syndrome - An allostatic perspective. *Biochim Biophys Acta Mol Cell Biol Lipids*. 2010;1801(3):338-349. doi:10.1016/j.bbalip.2009.12.006
72. McQuaid SE, Hodson L, Neville MJ, et al. Downregulation of adipose tissue fatty acid trafficking in obesity: A driver for ectopic fat deposition? *Diabetes*. 2011;60(1):47-55. doi:10.2337/db10-0867

73. Ipsen DH, Lykkesfeldt J, Tveden-Nyborg P. Molecular mechanisms of hepatic lipid accumulation in non-alcoholic fatty liver disease. *Cellular and Molecular Life Sciences*. 2018;75(18):3313-3327. doi:10.1007/s00018-018-2860-6
74. Moreno-Indias I, Tinahones FJ. Impaired adipose tissue expandability and lipogenic capacities as ones of the main causes of metabolic disorders. *J Diabetes Res*. 2015;2015. doi:10.1155/2015/970375
75. Gray SL, Vidal-Puig AJ. Adipose Tissue Expandability in the Maintenance of Metabolic Homeostasis. *Nutr Rev*. 2007;65(6):7-12. doi:10.1301/nr.2007.jun.s7-s12
76. Lé B, Wajchenberg O. *Subcutaneous and Visceral Adipose Tissue: Their Relation to the Metabolic Syndrome*; 2000. <https://academic.oup.com/edrv/article/21/6/697/2424212>
77. Quek J, Chan KE, Wong ZY, et al. Global prevalence of non-alcoholic fatty liver disease and non-alcoholic steatohepatitis in the overweight and obese population: a systematic review and meta-analysis. *Lancet Gastroenterol Hepatol*. 2023;8(1):20-30. doi:10.1016/S2468-1253(22)00317-X
78. Younossi ZM, Golabi P, Paik JM, Henry A, Van Dongen C, Henry L. The global epidemiology of nonalcoholic fatty liver disease (NAFLD) and nonalcoholic steatohepatitis (NASH): a systematic review. *Hepatology*. 2023;77(4):1335-1347. doi:10.1097/hep.0000000000000004
79. Paik JM, Golabi P, Younossi Y, Mishra A, Younossi ZM. Changes in the Global Burden of Chronic Liver Diseases From 2012 to 2017: The Growing Impact of NAFLD. *Hepatology*. 2020;72(5):1605-1616. doi:10.1002/hep.31173
80. El-Zayadi AR. Hepatic steatosis: A benign disease or a silent killer. *World J Gastroenterol*. 2008;14(26):4120-4126. doi:10.3748/wjg.14.4120
81. Loomba R, Adams LA. The 20% Rule of NASH Progression: The Natural History of Advanced Fibrosis and Cirrhosis Caused by NASH. *Hepatology*. 2019;70(6):1885-1888. doi:10.1002/hep.30946
82. Younossi Z, Anstee QM, Marietti M, et al. Global burden of NAFLD and NASH: Trends, predictions, risk factors and prevention. *Nat Rev Gastroenterol Hepatol*. 2018;15(1):11-20. doi:10.1038/nrgastro.2017.109
83. Caturano A, Acierno C, Nevola R, et al. Non-alcoholic fatty liver disease: From pathogenesis to clinical impact. *Processes*. 2021;9(1):1-18. doi:10.3390/pr9010135

84. Schreuder TCHA, Verwer BJ, van Nieuwkerk CMJ, Mulder CJJ. Nonalcoholic fatty liver disease: An overview of current insights in pathogenesis, diagnosis and treatment. *World J Gastroenterol.* 2008;14(16):2474-2486. doi:10.3748/wjg.14.2474
85. Buzzetti E, Pinzani M, Tsochatzis EA. The multiple-hit pathogenesis of non-alcoholic fatty liver disease (NAFLD). *Metabolism.* 2016;65(8):1038-1048. doi:10.1016/j.metabol.2015.12.012
86. Kim DY, Park JY. Genetic risk factors associated with NAFLD. *Hepatoma Res.* 2020;2020. doi:10.20517/2394-5079.2020.96
87. Anstee QM, Day CP. The Genetics of Nonalcoholic Fatty Liver Disease: Spotlight on PNPLA3 and TM6SF2. *Semin Liver Dis.* 2015;35(3):270-290. doi:10.1055/s-0035-1562947
88. Kabbani M, Michailidis E, Steensels S, et al. Human hepatocyte PNPLA3-148M exacerbates rapid non-alcoholic fatty liver disease development in chimeric mice. *Cell Rep.* 2022;40(11). doi:10.1016/j.celrep.2022.111321
89. Luukkonen PK, Nick A, Hölttä-Vuori M, et al. Human PNPLA3-I148M variant increases hepatic retention of polyunsaturated fatty acids. *JCI Insight.* 2019;4(16). doi:10.1172/jci.insight.127902
90. Mahdessian H, Taxiarchis A, Popov S, et al. TM6SF2 is a regulator of liver fat metabolism influencing triglyceride secretion and hepatic lipid droplet content. *Proc Natl Acad Sci U S A.* 2014;111(24):8913-8918. doi:10.1073/pnas.1323785111
91. Li XY, Liu Z, Li L, Wang HJ, Wang H. TM6SF2 rs58542926 is related to hepatic steatosis, fibrosis and serum lipids both in adults and children: A meta-analysis. *Front Endocrinol (Lausanne).* 2022;13. doi:10.3389/fendo.2022.1026901
92. Zeybel M, Mann DA, Mann J. Epigenetic modifications as new targets for liver disease therapies. *J Hepatol.* 2013;59(6):1349-1353. doi:10.1016/j.jhep.2013.05.039
93. Hyun J, Jung Y. Dna methylation in nonalcoholic fatty liver disease. *Int J Mol Sci.* 2020;21(21):1-26. doi:10.3390/ijms21218138
94. Pooya S, Blaise S, Moreno Garcia M, et al. Methyl donor deficiency impairs fatty acid oxidation through PGC-1 α hypomethylation and decreased ER- α , ERR- α , and HNF-4 α in the rat liver. *J Hepatol.* 2012;57(2):344-351. doi:10.1016/j.jhep.2012.03.028

95. Azzu V, Vacca M, Virtue S, Allison M, Vidal-Puig A. Adipose Tissue-Liver Cross Talk in the Control of Whole-Body Metabolism: Implications in Nonalcoholic Fatty Liver Disease. *Gastroenterology*. 2020;158(7):1899-1912. doi:10.1053/j.gastro.2019.12.054
96. Qureshi K, Abrams GA. Metabolic liver disease of obesity and role of adipose tissue in the pathogenesis of nonalcoholic fatty liver disease. *World J Gastroenterol*. 2007;13(26):3540-3553. doi:10.3748/wjg.v13.i26.3540
97. Polyzos SA, Kountouras J, Zavos C, Tsiaousi E. The role of adiponectin in the pathogenesis and treatment of non-alcoholic fatty liver disease. *Diabetes Obes Metab*. 2010;12(5):365-383. doi:10.1111/j.1463-1326.2009.01176.x
98. Mohamed MS, Youssef TM, Abdullah EE, Ahmed AE. Correlation between adiponectin level and the degree of fibrosis in patients with non-alcoholic fatty liver disease. *Egyptian Liver Journal*. 2021;11(1). doi:10.1186/s43066-021-00134-3
99. Mavilia MG, Wu GY. Liver and serum adiponectin levels in non-alcoholic fatty liver disease. *J Dig Dis*. 2021;22(4):214-221. doi:10.1111/1751-2980.12980
100. Jiménez-Cortegana C, García-Galey A, Tami M, et al. Role of leptin in non-alcoholic fatty liver disease. *Biomedicines*. 2021;9(7). doi:10.3390/biomedicines9070762
101. Rotundo L, Persaud A, Feurdean M, Ahlawat S, Kim HS. The Association of leptin with severity of non-alcoholic fatty liver disease: A population-based study. *Clin Mol Hepatol*. 2018;24(4):392-401. doi:10.3350/cmh.2018.0011
102. Martínez-Uña M, López-Mancheño Y, Diéguez C, Fernández-Rojo MA, Novelle MG. Unraveling the role of leptin in liver function and its relationship with liver diseases. *Int J Mol Sci*. 2020;21(24):1-33. doi:10.3390/ijms21249368
103. Jacome-Sosa MM, Parks EJ. Fatty acid sources and their fluxes as they contribute to plasma triglyceride concentrations and fatty liver in humans. *Curr Opin Lipidol*. 2014;25(3):213-220. doi:10.1097/MOL.0000000000000080
104. Postic C, Girard J. Contribution of de novo fatty acid synthesis to hepatic steatosis and insulin resistance: Lessons from genetically engineered mice. *Journal of Clinical Investigation*. 2008;118(3):829-838. doi:10.1172/JCI34275
105. Geng Y, Faber KN, de Meijer VE, Blokzijl H, Moshage H. How does hepatic lipid accumulation lead to lipotoxicity in non-alcoholic fatty liver disease? *Hepatol Int*. 2021;15(1):21-35. doi:10.1007/s12072-020-10121-2

106. Alkhouri N, Dixon LJ, Feldstein AE. Lipotoxicity in nonalcoholic fatty liver disease: Not all lipids are created equal. *Expert Rev Gastroenterol Hepatol.* 2009;3(4):445-451. doi:10.1586/egh.09.32
107. Win S, Than TA, Zhang J, Oo C, Min RWM, Kaplowitz N. New insights into the role and mechanism of c-Jun-N-terminal kinase signaling in the pathobiology of liver diseases. *Hepatology.* 2018;67(5):2013-2024. doi:10.1002/hep.29689
108. Chen Q, Lu X, Zhang X. Noncanonical nf-κb signaling pathway in liver diseases. *J Clin Transl Hepatol.* 2021;9(1):81-89. doi:10.14218/JCTH.2020.00063
109. Du Plessis J, Van Pelt J, Korf H, et al. Association of Adipose Tissue Inflammation with Histologic Severity of Nonalcoholic Fatty Liver Disease. *Gastroenterology.* 2015;149(3):635e14-648.e14. doi:10.1053/j.gastro.2015.05.044
110. Wang J, Wang J, He W, et al. Mutual interaction between endoplasmic reticulum and mitochondria in nonalcoholic fatty liver disease. *Lipids Health Dis.* 2020;19(1). doi:10.1186/s12944-020-01210-0
111. Delli Bovi AP, Marciano F, Mandato C, Siano MA, Savoia M, Vajro P. Oxidative Stress in Non-alcoholic Fatty Liver Disease. An Updated Mini Review. *Front Med (Lausanne).* 2021;8. doi:10.3389/fmed.2021.595371
112. Paradies G, Paradies V, Ruggiero FM, Petrosillo G. Oxidative stress, cardiolipin and mitochondrial dysfunction in nonalcoholic fatty liver disease. *World J Gastroenterol.* 2014;20(39):14205-14218. doi:10.3748/wjg.v20.i39.14205
113. Lee E, Korf H, Vidal-Puig A. An adipocentric perspective on the development and progression of non-alcoholic fatty liver disease. *J Hepatol.* Published online May 2023. doi:10.1016/j.jhep.2023.01.024
114. Pujia R, Tarsitano MG, Arturi F, et al. Advances in Phenotyping Obesity and in Its Dietary and Pharmacological Treatment: A Narrative Review. *Front Nutr.* 2022;9. doi:10.3389/fnut.2022.804719
115. Górnicka M, Szewczyk K, Białkowska A, et al. Anthropometric Indices as Predictive Screening Tools for Obesity in Adults; The Need to Define Sex-Specific Cut-Off Points for Anthropometric Indices. *Applied Sciences (Switzerland).* 2022;12(12). doi:10.3390/app12126165
116. Khanna D, Peltzer C, Kahar P, Parmar MS. Body Mass Index (BMI): A Screening Tool Analysis. *Cureus.* Published online February 11, 2022. doi:10.7759/cureus.22119

117. Ross R, Neeland IJ, Yamashita S, et al. Waist circumference as a vital sign in clinical practice: a Consensus Statement from the IAS and ICCR Working Group on Visceral Obesity. *Nat Rev Endocrinol.* 2020;16(3):177-189. doi:10.1038/s41574-019-0310-7
118. Wall-Medrano A, Faramarzi E, Romero-Saldaña M, Es Z. *Diagnostic Accuracy of the Waist-to-Height Ratio and Other Anthropometric Indices for Metabolically Healthy Obesity in the Working Population.*
119. Sommer I, Teufer B, Szelag M, et al. The performance of anthropometric tools to determine obesity: a systematic review and meta-analysis. *Sci Rep.* 2020;10(1). doi:10.1038/s41598-020-69498-7
120. Piqueras P, Ballester A, Durá-Gil J V., Martinez-Hervas S, Redón J, Real JT. Anthropometric Indicators as a Tool for Diagnosis of Obesity and Other Health Risk Factors: A Literature Review. *Front Psychol.* 2021;12. doi:10.3389/fpsyg.2021.631179
121. Kim SR, Lerman LO. Diagnostic imaging in the management of patients with metabolic syndrome. *Translational Research.* 2018;194:1-18. doi:10.1016/j.trsl.2017.10.009
122. Shuster A, Patlas M, Pinthus JH, Mourtzakis M. The clinical importance of visceral adiposity: A critical review of methods for visceral adipose tissue analysis. *British Journal of Radiology.* 2012;85(1009):1-10. doi:10.1259/bjr/38447238
123. Onuma T, Kamishima T, Sasaki T, Sakata M. Absolute reliability of adipose tissue volume measurement by computed tomography: application of low-dose scan and minimal detectable change—a phantom study. *Radiol Phys Technol.* 2015;8(2):312-319. doi:10.1007/s12194-015-0322-5
124. Kjønigsen LJ, Harneshaug M, Fløtten AM, et al. Reproducibility of semiautomated body composition segmentation of abdominal computed tomography: a multiobserver study. *Eur Radiol Exp.* 2019;3(1). doi:10.1186/s41747-019-0122-5
125. Fukuda T, Bouchi R, Takeuchi T, et al. Ratio of visceral-to-subcutaneous fat area predicts cardiovascular events in patients with type 2 diabetes. *J Diabetes Investig.* 2018;9(2):396-402. doi:10.1111/jdi.12713
126. Kwon SH, Han AL. The correlation between the ratio of visceral fat area to subcutaneous fat area on computed tomography and lipid accumulation product as indexes of cardiovascular risk. *J Obes Metab Syndr.* 2019;28(3):186-193. doi:10.7570/JOMES.2019.28.3.186

127. Ladeiras-Lopes R, Sampaio F, Bettencourt N, et al. The Ratio Between Visceral and Subcutaneous Abdominal Fat Assessed by Computed Tomography Is an Independent Predictor of Mortality and Cardiac Events. *Revista Española de Cardiología (English Edition)*. 2017;70(5):331-337. doi:10.1016/j.rec.2016.09.010
128. Ladeiras-Lopes R, Sampaio F, Bettencourt N, et al. The Ratio Between Visceral and Subcutaneous Abdominal Fat Assessed by Computed Tomography Is an Independent Predictor of Mortality and Cardiac Events. *Revista Española de Cardiología (English Edition)*. 2017;70(5):331-337. doi:10.1016/j.rec.2016.09.010
129. Cintenza EE, Cintenza M. Biomarkers in obesity. *Rev Rom Med Lab*. 2018;26(3):353-358. doi:10.2478/rrlm-2018-0027
130. Nimptsch K, Konigorski S, Pischon T. Diagnosis of obesity and use of obesity biomarkers in science and clinical medicine. *Metabolism*. 2019;92:61-70. doi:10.1016/j.metabol.2018.12.006
131. Aleksandrova K, Mozaffarian D, Pischon T. Addressing the perfect storm: Biomarkers in obesity and pathophysiology of cardiometabolic risk. *Clin Chem*. 2018;64(1):142-153. doi:10.1373/clinchem.2017.275172
132. Unamuno X, Gómez-Ambrosi J, Rodríguez A, Becerril S, Frühbeck G, Catalán V. Adipokine dysregulation and adipose tissue inflammation in human obesity. *Eur J Clin Invest*. 2018;48(9). doi:10.1111/eci.12997
133. Article 540_Are Adipokines Functional Biomarkers of Obesity.
134. Liuzzi A, Savia G, Tagliaferri M, et al. *Serum Leptin Concentration in Moderate and Severe Obesity: Relationship with Clinical, Anthropometric and Metabolic Factors*. <http://www.stockton-press.co.uk/ijo>
135. Shimizu H, Shimomura Y, Hayashi R, et al. *Serum Leptin Concentration Is Associated with Total Body Fat Mass, but Not Abdominal Fat Distribution*.
136. Perakakis N, Farr OM, Mantzoros CS. Leptin in Leanness and Obesity: JACC State-of-the-Art Review. *J Am Coll Cardiol*. 2021;77(6):745-760. doi:10.1016/j.jacc.2020.11.069
137. Gruber T, Pan C, Contreras RE, et al. Obesity-associated hyperleptinemia alters the gliovascular interface of the hypothalamus to promote hypertension. *Cell Metab*. 2021;33(6):1155-1170.e10. doi:10.1016/j.cmet.2021.04.007

138. Poetsch MS, Strano A, Guan K. Role of Leptin in Cardiovascular Diseases. *Front Endocrinol (Lausanne)*. 2020;11. doi:10.3389/fendo.2020.00354
139. Chai SB, Sun F, Nie XL, Wang J. Leptin and coronary heart disease: A systematic review and meta-analysis. *Atherosclerosis*. 2014;233(1):3-10. doi:10.1016/j.atherosclerosis.2013.11.069
140. Kishida K, Funahashi T, Shimomura I. Adiponectin as a routine clinical biomarker. In: *Best Practice and Research: Clinical Endocrinology and Metabolism*. Vol 28. Bailliere Tindall Ltd; 2014:119-130. doi:10.1016/j.beem.2013.08.006
141. Lu JY, Huang KC, Chang LC, et al. Adiponectin: A biomarker of obesity-induced insulin resistance in adipose tissue and beyond. *J Biomed Sci*. 2008;15(5):565-576. doi:10.1007/s11373-008-9261-z
142. Hong X, Zhang X, You L, et al. Association between adiponectin and newly diagnosed type 2 diabetes in population with the clustering of obesity, dyslipidaemia and hypertension: a cross-sectional study. *BMJ Open*. 2023;13(2). doi:10.1136/bmjopen-2021-060377
143. Srikanthan K, Feyh A, Visweshwar H, Shapiro JI, Sodhi K. Systematic review of metabolic syndrome biomarkers: A panel for early detection, management, and risk stratification in the West Virginian population. *Int J Med Sci*. 2016;13(1):25-38. doi:10.7150/ijms.13800
144. Liu Z, Liang S, Que S, Zhou L, Zheng S, Mardinoglu A. Meta-analysis of adiponectin as a biomarker for the detection of metabolic syndrome. *Front Physiol*. 2018;9(SEP). doi:10.3389/fphys.2018.01238
145. Marques V, Afonso MB, Bierig N, et al. Adiponectin, Leptin, and IGF-1 Are Useful Diagnostic and Stratification Biomarkers of NAFLD. *Front Med (Lausanne)*. 2021;8. doi:10.3389/fmed.2021.683250
146. Barrios V, Gómez-Huelgas R, Rodríguez R, de Pablos-Velasco P, Barrios Alonso V. *Adiponectin: An Emerging Cardiovascular Risk Factor. The REFERENCE Study ORIGINAL ARTICLES*. <https://www.revespcardiol.org/?ref=421468218>,
147. Kishida K, Funahashi T, Shimomura I. Adiponectin as a routine clinical biomarker. In: *Best Practice and Research: Clinical Endocrinology and Metabolism*. Vol 28. Bailliere Tindall Ltd; 2014:119-130. doi:10.1016/j.beem.2013.08.006
148. Djoussé L, Bartz TM, Ix JH, et al. Fatty acid-binding protein 4 and incident heart failure: the Cardiovascular Health Study. *Eur J Heart Fail*. 2013;15(4):394-399. doi:10.1093/eurjhf/hfs196

149. Romacho T, Sánchez-Ferrer CF, Peiró C. Visfatin/Nampt: An adipokine with cardiovascular impact. *Mediators Inflamm.* 2013;2013. doi:10.1155/2013/946427
150. Kahn SE, Hull RL, Utzschneider KM. Mechanisms linking obesity to insulin resistance and type 2 diabetes. *Nature.* 2006;444(7121):840-846. doi:10.1038/nature05482
151. Wiebe N, Muntner P, Tonelli M. Associations of body mass index, fasting insulin, and inflammation with mortality: a prospective cohort study. *Int J Obes.* 2022;46(12):2107-2113. doi:10.1038/s41366-022-01211-2
152. Xun P, Wu Y, He Q, He K. Fasting insulin concentrations and incidence of hypertension, stroke, and coronary heart disease: As meta-analysis of prospective cohort studies 1-3. *American Journal of Clinical Nutrition.* 2013;98(6):1543-1554. doi:10.3945/ajcn.113.065565
153. Patel N, Taveira TH, Choudhary G, Whitlatch H, Wu WC. Fasting serum C-peptide levels predict cardiovascular and overall death in nondiabetic adults. *J Am Heart Assoc.* 2012;1(6). doi:10.1161/JAHA.112.003152
154. Pikkemaat M, Melander O, Mölstad S, Garberg G, Boström KB. C-peptide concentration, mortality and vascular complications in people with Type 2 diabetes. The Skaraborg Diabetes Register. *Diabetic Medicine.* 2015;32(1):85-89. doi:10.1111/dme.12608
155. Talia C, Connolly L, Fowler PA. The insulin-like growth factor system: A target for endocrine disruptors? *Environ Int.* 2021;147. doi:10.1016/j.envint.2020.106311
156. Sandhu MS, Heald AH, Gibson JM, Cruickshank JK, Dunger DB, Wareham NJ. Circulating concentrations of insulin-like growth factor-I and development of glucose intolerance: a prospective observational study. *The Lancet.* 2002;359(9319):1740-1745. doi:10.1016/S0140-6736(02)08655-5
157. Drogan D, Schulze MB, Boeing H, Pischon T. Insulin-Like Growth Factor 1 and Insulin-Like Growth Factor-Binding Protein 3 in Relation to the Risk of Type 2 Diabetes Mellitus: Results from the EPIC-Potsdam Study. *Am J Epidemiol.* 2016;183(6):553-560. doi:10.1093/aje/kwv188
158. Khanna D, Khanna S, Khanna P, Kahar P, Patel BM. Obesity: A Chronic Low-Grade Inflammation and Its Markers. *Cureus.* Published online February 28, 2022. doi:10.7759/cureus.22711

159. Graßmann S, Wirsching J, Eichelmann F, Aleksandrova K. Association Between Peripheral Adipokines and Inflammation Markers: A Systematic Review and Meta-Analysis. *Obesity*. 2017;25(10):1776-1785. doi:10.1002/oby.21945
160. Articles C-reactive protein concentration and risk of coronary heart disease, stroke, and mortality: an individual participant meta-analysis. *The Lancet*. 375:132-140. doi:10.1016/S0140
161. Zhang Q, Meng XH, Qiu C, et al. Integrative analysis of multi-omics data to detect the underlying molecular mechanisms for obesity in vivo in humans. *Hum Genomics*. 2022;16(1). doi:10.1186/s40246-022-00388-x
162. Aleksandrova K, Egea Rodrigues C, Floegel A, Ahrens W. Omics Biomarkers in Obesity: Novel Etiological Insights and Targets for Precision Prevention. *Curr Obes Rep*. 2020;9(3):219-230. doi:10.1007/s13679-020-00393-y
163. Loos RJF, Yeo GSH. The genetics of obesity: from discovery to biology. *Nat Rev Genet*. 2022;23(2):120-133. doi:10.1038/s41576-021-00414-z
164. Loos RJF, Janssens ACJW. Predicting Polygenic Obesity Using Genetic Information. *Cell Metab*. 2017;25(3):535-543. doi:10.1016/j.cmet.2017.02.013
165. Müller MJ, Geisler C, Blundell J, et al. The case of GWAS of obesity: does body weight control play by the rules? *Int J Obes*. 2018;42(8):1395-1405. doi:10.1038/s41366-018-0081-6
166. Yengo L, Sidorenko J, Kemper KE, et al. Meta-analysis of genome-wide association studies for height and body mass index in ~700 000 individuals of European ancestry. *Hum Mol Genet*. 2018;27(20):3641-3649. doi:10.1093/hmg/ddy271
167. Locke AE, Kahali B, Berndt SI, et al. Genetic studies of body mass index yield new insights for obesity biology. *Nature*. 2015;518(7538):197-206. doi:10.1038/nature14177
168. Fawcett KA, Barroso I. The genetics of obesity: FTO leads the way. *Trends in Genetics*. 2010;26(6):266-274. doi:10.1016/j.tig.2010.02.006
169. Ehrlich AC, Friedenberg FK. Genetic Associations of Obesity: The Fat-Mass and Obesity-Associated (FTO) Gene. *Clin Transl Gastroenterol*. 2016;7(1):e140. doi:10.1038/ctg.2016.1
170. Melhorn SJ, Askren MK, Chung WK, et al. FTO genotype impacts food intake and corticolimbic activation. *American Journal of Clinical Nutrition*. 2018;107(2):145-154. doi:10.1093/ajcn/nqx029

171. Magno FCCM, Guaraná HC, Fonseca ACP, et al. Influence of FTO rs9939609 polymorphism on appetite, ghrelin, leptin, IL6, TNF α levels, and food intake of women with morbid obesity. *Diabetes, Metabolic Syndrome and Obesity*. 2018;11:199-207. doi:10.2147/DMSO.S154978
172. Cecil JE, Tavendale R, Watt P, Hetherington MM, Palmer CNA. *An Obesity-Associated FTO Gene Variant and Increased Energy Intake in Children A Bs Tr Ac t.*; 2008. www.nejm.org
173. Speakman JR. FTO effect on energy demand versus food intake. *Nature*. 2010;464(7289). doi:10.1038/nature08807
174. Wang CY, Shie S Sen, Hsieh IC, Tsai ML, Wen MS. FTO modulates circadian rhythms and inhibits the CLOCK-BMAL1-induced transcription. *Biochem Biophys Res Commun*. 2015;464(3):826-832. doi:10.1016/j.bbrc.2015.07.046
175. Lan N, Lu Y, Zhang Y, et al. FTO – A Common Genetic Basis for Obesity and Cancer. *Front Genet*. 2020;11. doi:10.3389/fgene.2020.559138
176. Smemo S, Tena JJ, Kim KH, et al. Obesity-associated variants within FTO form long-range functional connections with IRX3. *Nature*. 2014;507(7492):371-375. doi:10.1038/nature13138
177. Sobreira DR, Joslin AC, Zhang Q, et al. Extensive pleiotropism and allelic heterogeneity mediate metabolic effects of IRX3 and IRX5. *Science (1979)*. 2021;372(6546):1085-1091. doi:10.1126/science.abf1008
178. Fan SH, Say YH. Leptin and leptin receptor gene polymorphisms and their association with plasma leptin levels and obesity in a multi-ethnic Malaysian suburban population. *J Physiol Anthropol*. 2014;33(1). doi:10.1186/1880-6805-33-15
179. Howlader M, Sultana MI, Akter F, Hossain MM. Adiponectin gene polymorphisms associated with diabetes mellitus: A descriptive review. *Heliyon*. 2021;7(8). doi:10.1016/j.heliyon.2021.e07851
180. Armenise C, Lefebvre G, Ero`me Carayol J', et al. Transcriptome profiling from adipose tissue during a low-calorie diet reveals predictors of weight and glycemic outcomes in obese, nondiabetic subjects. doi:10.3945/ajcn
181. Nasias D, Dalakoura-Karagkouni K, Vassou D, Papagiannakis G, Papadaki A, Kardassis D. Transcriptome analysis of the adipose tissue in a mouse model of metabolic syndrome identifies gene signatures related to disease pathogenesis. *Genomics*. 2020;112(6):4053-4062. doi:10.1016/j.ygeno.2020.06.053

182. Homuth G, Wahl S, Müller C, et al. Extensive alterations of the whole-blood transcriptome are associated with body mass index: Results of an mRNA profiling study involving two large population-based cohorts. *BMC Med Genomics*. 2015;8(1). doi:10.1186/s12920-015-0141-x
183. Ghosh S, Dent R, Harper ME, Gorman SA, Stuart JS, McPherson R. Gene expression profiling in whole blood identifies distinct biological pathways associated with obesity. *BMC Med Genomics*. 2010;3. doi:10.1186/1755-8794-3-56
184. Mattick JS. *Non-Coding RNAs: The Architects of Eukaryotic Complexity*. Vol 2.; 2001.
185. Iacomino G, Siani A. Role of microRNAs in obesity and obesity-related diseases. *Genes Nutr*. 2017;12(1). doi:10.1186/s12263-017-0577-z
186. Jean-François L, Derghal A, Mounien L. Micrornas in obesity and related metabolic disorders. *Cells*. 2019;8(8). doi:10.3390/cells8080859
187. Ortiz-Dosal A, Rodil-García P, Salazar-Olivo LA. Circulating microRNAs in human obesity: a systematic review. *Biomarkers*. 2019;24(6):499-509. doi:10.1080/1354750X.2019.1606279
188. Ji C, Guo X. The clinical potential of circulating microRNAs in obesity. *Nat Rev Endocrinol*. 2019;15(12):731-743. doi:10.1038/s41574-019-0260-0
189. Rangel-Huerta OD, Pastor-Villaescusa B, Gil A. Are we close to defining a metabolomic signature of human obesity? A systematic review of metabolomics studies. *Metabolomics*. 2019;15(6). doi:10.1007/s11306-019-1553-y
190. Floegel A, Wientzek A, Bachlechner U, et al. Linking diet, physical activity, cardiorespiratory fitness and obesity to serum metabolite networks: Findings from a population-based study. *Int J Obes*. 2014;38(11):1388-1396. doi:10.1038/ijo.2014.39
191. Alves A, Bassot A, Bulteau AL, Pirola L, Morio B. Glycine metabolism and its alterations in obesity and metabolic diseases. *Nutrients*. 2019;11(6). doi:10.3390/nu11061356
192. Tulipani S, Palau-Rodriguez M, Miñarro Alonso A, et al. Biomarkers of Morbid Obesity and Prediabetes by Metabolomic Profiling of Human Discordant Phenotypes. *Clinica Chimica Acta*. 2016;463:53-61. doi:10.1016/j.cca.2016.10.005

193. Siddik MAB, Shin AC. Recent progress on branched-chain amino acids in obesity, diabetes, and beyond. *Endocrinology and Metabolism*. 2019;34(3):234-246. doi:10.3803/EnM.2019.34.3.234
194. Wenk MR. Lipidomics: New tools and applications. *Cell*. 2010;143(6):888-895. doi:10.1016/j.cell.2010.11.033
195. Mousa A, Naderpoor N, Mellett N, et al. Lipidomic profiling reveals early-stage metabolic dysfunction in overweight or obese humans. *Biochim Biophys Acta Mol Cell Biol Lipids*. 2019;1864(3):335-343. doi:10.1016/j.bbalip.2018.12.014
196. Klop B, Elte JWF, Cabezas MC. Dyslipidemia in Obesity: Mechanisms and Potential Targets. *Nutrients*. 2013;5(4):1218-1240. doi:10.3390/nu5041218
197. Sánchez-Vinces S, Garcia PHD, Silva AAR, et al. Mass-Spectrometry-Based Lipidomics Discriminates Specific Changes in Lipid Classes in Healthy and Dyslipidemic Adults. *Metabolites*. 2023;13(2). doi:10.3390/metabo13020222
198. Davies A, Li X, Obeid S, et al. *Short and Medium Chain Acylcarnitines as Markers of Outcome in Diabetic and Non-Diabetic Subjects with Acute Coronary Syndromes*.
https://academic.oup.com/eurheartj/article/41/Supplement_2/ehaa946.1561/6002428
199. Guasch-Ferré M, Ruiz-Canela M, Li J, et al. Plasma acylcarnitines and risk of type 2 diabetes in a mediterranean population at high cardiovascular risk. *Journal of Clinical Endocrinology and Metabolism*. 2019;104(5):1508-1519. doi:10.1210/jc.2018-01000
200. Spiller S, Blüher M, Hoffmann R. Plasma levels of free fatty acids correlate with type 2 diabetes mellitus. *Diabetes Obes Metab*. 2018;20(11):2661-2669. doi:10.1111/dom.13449
201. Xia Q, Campbell JA, Ahmad H, Si L, de Graaff B, Palmer AJ. Bariatric surgery is a cost-saving treatment for obesity—A comprehensive meta-analysis and updated systematic review of health economic evaluations of bariatric surgery. *Obesity Reviews*. 2020;21(1). doi:10.1111/obr.12932
202. Wilding JPH, Batterham RL, Calanna S, et al. Once-Weekly Semaglutide in Adults with Overweight or Obesity. *New England Journal of Medicine*. 2021;384(11):989-1002. doi:10.1056/nejmoa2032183

203. Jastreboff AM, Aronne LJ, Ahmad NN, et al. Tirzepatide Once Weekly for the Treatment of Obesity. *New England Journal of Medicine*. 2022;387(3):205-216. doi:10.1056/nejmoa2206038
204. Lin X, Li H. Obesity: Epidemiology, Pathophysiology, and Therapeutics. *Front Endocrinol (Lausanne)*. 2021;12. doi:10.3389/fendo.2021.706978
205. Lopez-Yus M, García-Sobreviela MP, del Moral-Bergos R, Arbones-Mainar JM. Gene Therapy Based on Mesenchymal Stem Cells Derived from Adipose Tissue for the Treatment of Obesity and Its Metabolic Complications. *Int J Mol Sci*. 2023;24(8). doi:10.3390/ijms24087468
206. Andrzejewska A, Lukomska B, Janowski M. Concise Review: Mesenchymal Stem Cells: From Roots to Boost. *Stem Cells*. 2019;37(7):855-864. doi:10.1002/stem.3016
207. Jovic D, Yu Y, Wang D, et al. A Brief Overview of Global Trends in MSC-Based Cell Therapy. *Stem Cell Rev Rep*. 2022;18(5):1525-1545. doi:10.1007/s12015-022-10369-1
208. Munir H, Ward LSC, Sheriff L, et al. Adipogenic Differentiation of Mesenchymal Stem Cells Alters Their Immunomodulatory Properties in a Tissue-Specific Manner. *Stem Cells*. 2017;35(6):1636-1646. doi:10.1002/stem.2622
209. Wang Y, Chen X, Cao W, Shi Y. Plasticity of mesenchymal stem cells in immunomodulation: Pathological and therapeutic implications. *Nat Immunol*. 2014;15(11):1009-1016. doi:10.1038/ni.3002
210. Yang X, Meng Y, Han Z, Ye F, Wei L, Zong C. Mesenchymal stem cell therapy for liver disease: full of chances and challenges. *Cell Biosci*. 2020;10(1). doi:10.1186/s13578-020-00480-6
211. Melief SM, Zwaginga JJ, Fibbe WE, Roelofs H. Adipose Tissue-Derived Multipotent Stromal Cells Have a Higher Immunomodulatory Capacity Than Their Bone Marrow-Derived Counterparts. *Stem Cells Transl Med*. 2013;2(6):455-463. doi:10.5966/sctm.2012-0184
212. Cao M, Pan Q, Dong H, et al. Adipose-derived mesenchymal stem cells improve glucose homeostasis in high-fat diet-induced obese mice. *Stem Cell Res Ther*. 2015;6(1). doi:10.1186/s13287-015-0201-3
213. Lee CW, Hsiao WT, Lee OKS. Mesenchymal stromal cell-based therapies reduce obesity and metabolic syndromes induced by a high-fat diet. *Translational Research*. Published online 2017:61-74. doi:doi:10.1016/j.trsl.2016.11.003

214. Karaoz E, Okcu A, Ünal ZS, Subasi C, Saglam O, Duruksu G. Adipose tissue-derived mesenchymal stromal cells efficiently differentiate into insulin-producing cells in pancreatic islet microenvironment both in vitro and in vivo. *Cyotherapy*. 2013;15(5):557-570. doi:10.1016/j.jcyt.2013.01.005
215. Nam JS, Kang HM, Kim J, et al. Transplantation of insulin-secreting cells differentiated from human adipose tissue-derived stem cells into type 2 diabetes mice. *Biochem Biophys Res Commun*. 2014;443(2):775-781. doi:10.1016/j.bbrc.2013.10.059
216. Pan F, Liao N, Zheng Y, et al. Intrahepatic transplantation of adipose-derived stem cells attenuates the progression of non-alcoholic fatty liver disease in rats. *Mol Med Rep*. 2015;12(3):3725-3733. doi:10.3892/mmr.2015.3847
217. Shree N, Venkategowda S, Venkatranganna M V., Datta I, Bhonde RR. Human adipose tissue mesenchymal stem cells as a novel treatment modality for correcting obesity induced metabolic dysregulation. *Int J Obes*. 2019;43(10):2107-2118. doi:10.1038/s41366-019-0438-5
218. Shin J, Oh JW. Development of CRISPR/Cas9 system for targeted DNA modifications and recent improvements in modification efficiency and specificity. *BMB Rep*. 2020;53(7):341-348. doi:10.5483/BMBRep.2020.53.7.070
219. Kantor A, McClements ME, Maclaren RE. Crispr-cas9 dna base-editing and prime-editing. *Int J Mol Sci*. 2020;21(17):1-22. doi:10.3390/ijms21176240
220. Nidhi S, Anand U, Oleksak P, et al. Novel crispr-cas systems: An updated review of the current achievements, applications, and future research perspectives. *Int J Mol Sci*. 2021;22(7). doi:10.3390/ijms22073327
221. Doudna JA. The promise and challenge of therapeutic genome editing. *Nature*. 2020;578(7794):229-236. doi:10.1038/s41586-020-1978-5
222. Lundh M, Plucińska K, Isidor MS, Petersen PSS, Emanuelli B. Bidirectional manipulation of gene expression in adipocytes using CRISPRa and siRNA. *Mol Metab*. 2017;6(10):1313-1320. doi:10.1016/j.molmet.2017.07.001
223. Kamble PG, Hetty S, Vranić M, et al. Proof-of-concept for CRISPR/Cas9 gene editing in human preadipocytes: Deletion of FKBP5 and PPARG and effects on adipocyte differentiation and metabolism. *Sci Rep*. 2020;10(1). doi:10.1038/s41598-020-67293-y

224. Wang CH, Lundh M, Fu A, et al. CRISPR-engineered human brown-like adipocytes prevent diet-induced obesity and ameliorate metabolic syndrome in mice. *Sci Transl Med.* 2020;12(558). doi:10.1126/SCITRANSLMED.AAZ8664
225. Shen Y, Cohen JL, Nicoloro SM, et al. CRISPR-delivery particles targeting nuclear receptor–interacting protein 1 (Nrip1) in adipose cells to enhance energy expenditure. *Journal of Biological Chemistry.* 2018;293(44):17291-17305. doi:10.1074/jbc.RA118.004554
226. Kleiner DE, Brunt EM, Van Natta M, et al. Design and validation of a histological scoring system for nonalcoholic fatty liver disease. *Hepatology.* 2005;41(6):1313-1321. doi:10.1002/hep.20701
227. Lopez-Yus M, Lorente-Cebrian S, del Moral-Bergos R, et al. Identification of novel targets in adipose tissue involved in non-alcoholic fatty liver disease progression. *FASEB Journal.* 2022;36(8). doi:10.1096/fj.202200118RR
228. Labun K, Montague TG, Krause M, Torres Cleuren YN, Tjeldnes H, Valen E. CHOPCHOP v3: Expanding the CRISPR web toolbox beyond genome editing. *Nucleic Acids Res.* 2019;47(W1):W171-W174. doi:10.1093/nar/gkz365
229. Van Campenhout C, Cabochette P, Veillard AC, et al. Guidelines for optimized gene knockout using CRISPR/Cas9. *Biotechniques.* 2019;66(6):295-302. doi:10.2144/btn-2018-0187
230. Conant D, Hsiau T, Rossi N, et al. Inference of CRISPR Edits from Sanger Trace Data. *CRISPR Journal.* Published online 2022:123-130. doi:10.1101/251082
231. Chen X, Zhang B, Wang T, Wang T, Bonni A, Zhao G. Robust principal component analysis for accurate outlier sample detection in RNA-Seq data. *BMC Bioinformatics.* 2020;21(1). doi:10.1186/s12859-020-03608-0
232. Robinson MD, McCarthy DJ, Smyth GK. edgeR: A Bioconductor package for differential expression analysis of digital gene expression data. *Bioinformatics.* 2009;26(1):139-140. doi:10.1093/bioinformatics/btp616
233. Benjamini Y, Hochberg Y. *Controlling the False Discovery Rate: A Practical and Powerful Approach to Multiple Testing.* Vol 57.; 1995.
234. Yu G, Wang LG, Han Y, He QY. ClusterProfiler: An R package for comparing biological themes among gene clusters. *OMICS.* 2012;16(5):284-287. doi:10.1089/omi.2011.0118
235. Pereira-Manfro WF, de Lima GR, Nogueira Neto JF, et al. Association between visceral/subcutaneous adipose tissue ratio and plasma inflammatory markers and

- score for cardiovascular risk prediction in a Brazilian cohort: Pró-saúde study. *Brazilian Journal of Medical and Biological Research.* 2021;54(12). doi:10.1590/1414-431X2021e11521
236. Abraham TM, Pedley A, Massaro JM, Hoffmann U, Fox CS. Association between visceral and subcutaneous adipose depots and incident cardiovascular disease risk factors. *Circulation.* 2015;132(17):1639-1647. doi:10.1161/CIRCULATIONAHA.114.015000
237. Lee MJ, Wu Y, Fried SK. Adipose tissue heterogeneity: Implication of depot differences in adipose tissue for obesity complications. *Mol Aspects Med.* 2013;34(1):1-11. doi:10.1016/j.mam.2012.10.001
238. Ladeiras-Lopes R, Sampaio F, Bettencourt N, et al. The Ratio Between Visceral and Subcutaneous Abdominal Fat Assessed by Computed Tomography Is an Independent Predictor of Mortality and Cardiac Events. *Revista Española de Cardiología (English Edition).* 2017;70(5):331-337. doi:10.1016/j.rec.2016.09.010
239. Kwon SH, Han AL. The correlation between the ratio of visceral fat area to subcutaneous fat area on computed tomography and lipid accumulation product as indexes of cardiovascular risk. *J Obes Metab Syndr.* 2019;28(3):186-193. doi:10.7570/JOMES.2019.28.3.186
240. Ahmed B, Sultana R, Greene MW. Adipose tissue and insulin resistance in obese. *Biomedicine and Pharmacotherapy.* 2021;137. doi:10.1016/j.biopha.2021.111315
241. Zhang M, Hu T, Zhang S, Zhou L. Associations of Different Adipose Tissue Depots with Insulin Resistance: A Systematic Review and Meta-analysis of Observational Studies. *Sci Rep.* 2015;5. doi:10.1038/srep18495
242. Patel P, Abate N. Body fat distribution and insulin resistance. *Nutrients.* 2013;5(6):2019-2027. doi:10.3390/nu5062019
243. Spalding KL, Bernard S, Näslund E, et al. Impact of fat mass and distribution on lipid turnover in human adipose tissue. *Nat Commun.* 2017;8. doi:10.1038/ncomms15253
244. Walton C, Lees B, Crook D, Worthington M, Godsland IF, Stevenson JC. *Body Fat Distribution, Rather than Overall Adiposity, Influences Serum Lipids and Lipoproteins in Healthy Men Independently of Age.*

245. Wijarnpreecha K, Ahmed A, Kim D. Body fat distribution: a crucial target for intervention in nonalcoholic fatty liver disease and fibrosis. *Hepatobiliary Surg Nutr.* 2022;11(5):738-742. doi:10.21037/hbsn-22-366
246. Chiyanika C, Wong VWS, Wong GLH, et al. Implications of Abdominal Adipose Tissue Distribution on Nonalcoholic Fatty Liver Disease and Metabolic Syndrome: A Chinese General Population Study. *Clin Transl Gastroenterol.* 2021;12(2):E00300. doi:10.14309/ctg.0000000000000300
247. Saito T, Murata M, Otani T, Tamemoto H, Kawakami M, -E Ishikawa S. *Association of Subcutaneous and Visceral Fat Mass with Serum Concentrations of Adipokines in Subjects with Type 2 Diabetes Mellitus.* Vol 2012.
248. Korac A, Srdic-Galic B, Kalezic A, et al. Adipokine signatures of subcutaneous and visceral abdominal fat in normal-weight and obese women with different metabolic profiles. *Archives of Medical Science.* 2021;17(2):323-336. doi:10.5114/aoms/92118
249. Ugi S, Maeda S, Kawamura Y, et al. CCDC3 is specifically upregulated in omental adipose tissue in subjects with abdominal obesity. *Obesity.* 2014;22(4):1070-1077. doi:10.1002/oby.20645
250. Menghuan L, Yang Y, Qianhe M, et al. Advances in research of biological functions of Isthmin-1. *J Cell Commun Signal.* Published online September 1, 2023. doi:10.1007/s12079-023-00732-3
251. Jiang Z, Zhao M, Voilquin L, et al. Isthmin-1 is an adipokine that promotes glucose uptake and improves glucose tolerance and hepatic steatosis. *Cell Metab.* 2021;33(9):1836-1852.e11. doi:10.1016/j.cmet.2021.07.010
252. Zhao M, Danneskiold-Samsøe NB, Ulicna L, et al. Phosphoproteomic mapping reveals distinct signaling actions and activation of muscle protein synthesis by Isthmin-1. *eLife.* 2022;11. doi:10.7554/eLife.80014
253. Wang J, Du J, Ge X, et al. Circulating Ism1 Reduces the Risk of Type 2 Diabetes but not Diabetes-Associated NAFLD. *Front Endocrinol (Lausanne).* 2022;13. doi:10.3389/fendo.2022.890332
254. Ruiz-Ojeda FJ, Anguita-Ruiz A, Rico MC, et al. Serum levels of the novel adipokine isthmin-1 are associated with obesity in pubertal boys. *World Journal of Pediatrics.* Published online 2023. doi:10.1007/s12519-022-00665-8

255. Bedogni G, Bellentani S, Miglioli L, et al. The fatty liver index: A simple and accurate predictor of hepatic steatosis in the general population. *BMC Gastroenterol.* 2006;6:1-7. doi:10.1186/1471-230X-6-33
256. Kitazawa A, Maeda S, Fukuda Y. Fatty liver index as a predictive marker for the development of diabetes: A retrospective cohort study using Japanese health check-up data. *PLoS One.* 2021;16(9 September):1-15. doi:10.1371/journal.pone.0257352
257. Fedchuk L, Nascimbeni F, Pais R, Charlotte F, Housset C, Ratziu V. Performance and limitations of steatosis biomarkers in patients with nonalcoholic fatty liver disease. *Aliment Pharmacol Ther.* 2014;40(10):1209-1222. doi:10.1111/apt.12963
258. Louwen F, Ritter A, Kreis NN, Yuan J. Insight into the development of obesity: functional alterations of adipose-derived mesenchymal stem cells. *Obesity Reviews.* 2018;19(7):888-904. doi:10.1111/obr.12679
259. Oliva-Olivera W, Coin-Aragüez L, Lhamyani S, et al. Adipogenic impairment of adipose tissue-derived mesenchymal stem cells in subjects with metabolic syndrome: Possible protective role of FGF2. *Journal of Clinical Endocrinology and Metabolism.* 2017;102(2):478-487. doi:10.1210/jc.2016-2256
260. Oñate B, Vilahur G, Camino-López S, et al. Stem cells isolated from adipose tissue of obese patients show changes in their transcriptomic profile that indicate loss in stemcellness and increased commitment to an adipocyte-like phenotype. *BMC Genomics.* 2013;14(1):1-12. doi:10.1186/1471-2164-14-625
261. Pérez LM, Bernal A, De Lucas B, et al. Altered metabolic and stemness capacity of adipose tissue-derived stem cells from obese mouse and human. *PLoS One.* 2015;10(4):1-22. doi:10.1371/journal.pone.0123397
262. Pérez LM, Suárez J, Bernal A, De Lucas B, San Martin N, Gálvez BG. Obesity-driven alterations in adipose-derived stem cells are partially restored by weight loss. *Obesity.* 2016;24(3):661-669. doi:10.1002/oby.21405
263. Mastrangelo A, Panadero MI, Perez LM, et al. New insight on obesity and adipose-derived stem cells using comprehensive metabolomics. *Biochemical Journal.* 2016;473(14):2187-2203. doi:10.1042/BCJ20160241
264. Serena C, Ceperuelo-Mallafre V, Ejarque M, Fradera R, Roche K, Nuñez-Roa C, Vendrell J KN. Obesity and Type 2 Diabetes Alters the Immune Properties of Human Adipose Derived Stem Cells. *Stem Cells Express.* Published online 2016:2078-2084.

265. Mossel DM, Moganti K, Riabov V, et al. Epigenetic Regulation of S100A9 and S100A12 Expression in Monocyte-Macrophage System in Hyperglycemic Conditions. *Front Immunol.* 2020;11(June):1-19. doi:10.3389/fimmu.2020.01071
266. Tsagkaraki E, Nicoloro SM, DeSouza T, et al. CRISPR-enhanced human adipocyte browning as cell therapy for metabolic disease. *Nat Commun.* 2021;12(1). doi:10.1038/s41467-021-27190-y

8. ANNEXES

8.1. Annex I. *Review*

**Gene Therapy Based on Mesenchymal Stem Cells
Derived from Adipose Tissue for the Treatment
of Obesity and Its Metabolic Complications**



Review

Gene Therapy Based on Mesenchymal Stem Cells Derived from Adipose Tissue for the Treatment of Obesity and Its Metabolic Complications

Marta Lopez-Yus ^{1,2,3}, Maria Pilar García-Sobreviela ^{1,3}, Raquel del Moral-Bergos ^{1,2,3}
and Jose M. Arbones-Mainar ^{1,2,3,4,*}

- ¹ Adipocyte and Fat Biology Laboratory (AdipoFat), Translational Research Unit, University Hospital Miguel Servet, 50009 Zaragoza, Spain
² Instituto Aragonés de Ciencias de la Salud (IACS), 50009 Zaragoza, Spain
³ Instituto de Investigación Sanitaria (IIS) Aragón, 50009 Zaragoza, Spain
⁴ CIBER Fisiopatología Obesidad y Nutrición (CIBEROBN), Instituto Salud Carlos III, 28029 Madrid, Spain
* Correspondence: jmarbones.iacs@aragon.es; Tel.: +34-976-769-565

Abstract: Obesity is a highly prevalent condition often associated with dysfunctional adipose tissue. Stem cell-based therapies have become a promising tool for therapeutic intervention in the context of regenerative medicine. Among all stem cells, adipose-derived mesenchymal stem cells (ADMSCs) are the most easily obtained, have immunomodulatory properties, show great ex vivo expansion capacity and differentiation to other cell types, and release a wide variety of angiogenic factors and bioactive molecules, such as growth factors and adipokines. However, despite the positive results obtained in some pre-clinical studies, the actual clinical efficacy of ADMSCs still remains controversial. Transplanted ADMSCs present a meager rate of survival and proliferation, possibly because of the damaged microenvironment of the affected tissues. Therefore, there is a need for novel approaches to generate more functional ADMSCs with enhanced therapeutic potential. In this context, genetic manipulation has emerged as a promising strategy. In the current review, we aim to summarize several adipose-focused treatments of obesity, including cell therapy and gene therapy. Particular emphasis will be given to the continuum from obesity to metabolic syndrome, diabetes, and underlying non-alcoholic fatty liver disease (NAFLD). Furthermore, we will provide insights into the potential shared adipocentric mechanisms involved in these pathophysiological processes and their remediation using ADMSCs.

Keywords: adipose tissue-derived mesenchymal stem cell; ADMSC; cell therapy; gene editing; obesity



Citation: Lopez-Yus, M.; García-Sobreviela, M.P.; del Moral-Bergos, R.; Arbones-Mainar, J.M. Gene Therapy Based on Mesenchymal Stem Cells Derived from Adipose Tissue for the Treatment of Obesity and Its Metabolic Complications. *Int. J. Mol. Sci.* **2023**, *24*, 7468. <https://doi.org/10.3390/ijms24087468>

Academic Editors: Giovanni Pallio and Federica Mannino

Received: 8 March 2023

Revised: 12 April 2023

Accepted: 16 April 2023

Published: 18 April 2023



Copyright: © 2023 by the authors. Licensee MDPI, Basel, Switzerland. This article is an open access article distributed under the terms and conditions of the Creative Commons Attribution (CC BY) license (<https://creativecommons.org/licenses/by/4.0/>).

1. Introduction

According to the definition by the Obesity Medicine Association, “Obesity is a chronic, relapsing, multifactorial, neurobehavioral disease, wherein an increase in body fat promotes adipose tissue (AT) dysfunction and abnormal fat mass physical forces, resulting in adverse metabolic, biomechanical, and psychosocial health consequences” [1]. This definition encompasses three main consequences of obesity, including metabolic disturbances typically associated with high blood sugar levels and altered blood lipids. These alterations lead to an increased risk of cardiovascular disease, cancer, and dysfunction of multiple organs, such as the pancreas and liver [2].

In the last 40 years, the prevalence of obesity has skyrocketed globally. In 2015, more than 600 million adults were obese; a high body mass index (BMI) accounted for 4.0 million deaths worldwide [3]. However, the public health war against obesity has failed to reduce the prevalence of obesity, often producing unintended consequences, such as an excessive weight concern among the population, which can lead to a negative body image and eating

disorders [4]. Consequently, various alternative strategies have emerged to minimize the health-related consequences of obesity.

Currently, bariatric surgery remains the most effective and cost-saving treatment for obesity and its complications [5]; although, because of its complexity, it seems unable to reduce the obesity pandemic expansion. On the other hand, some pharmacological strategies targeting the energy balance regulatory system are now reaching clinically relevant reductions in body weight [6,7]. The appearance of new tools and techniques of genetic engineering as well as advances in understanding the molecular basis of obesity and its metabolic complications have given rise to new precision medicine approaches targeting adipose tissue as an anti-obesity therapy. These innovative approaches include cell-based therapy and gene therapy for obesity.

This narrative review will focus on noninvasive approaches for the adipose-focused treatment of obesity, including cell therapy and gene therapy. Particular emphasis will be given to the continuum from obesity to metabolic syndrome, diabetes, and underlying non-alcoholic fatty liver disease (NAFLD). We aim to provide insight into the potential shared adipocentric mechanisms implied in these pathophysiological processes and their remediation using adipose-derived mesenchymal stem cells (ADMSCs).

2. Adipose Tissue-Derived Mesenchymal Stem Cells

2.1. Adipose Tissue and the Expandability Hypothesis

It is currently accepted that white adipose tissue (WAT) is not a mere energy reservoir and is considered an endocrine organ producing various cytokines (adipokines) and other metabolites to control systemic energy expenditure [8]. Adipose tissue is extraordinarily heterogeneous in terms of its composition and body distribution. Subcutaneous white adipose tissue (scWAT) is located under the skin and is the largest storage site for excess lipids. We know there is an individual limit on the capacity to store lipids in scWAT (i.e., the adipose tissue expandability hypothesis [9]). The expansion of scWAT is determined by two main processes: the differentiation of new mature adipocytes from their precursors, known as mesenchymal stem cells (MSCs), and the ability to enlarge from those already formed adipocytes [10]. This adipogenic process is coordinated by the differential expression of genes, proteins, microRNAs, and metabolites from different cell types.

When scWAT reaches its maximal storage capacity, adipose tissue fails to store lipids appropriately, redirecting this lipid flux to other organs where it is accumulated as ectopic fat and causes lipotoxicity and inflammation [11]. This ectopic accumulation occurs primarily in the visceral adipose tissue (vWAT) and liver, leading to visceral obesity and liver steatosis [12].

2.2. Mesenchymal Stem Cells

MSCs are multipotent stroma cells characterized by the capacity of self-renewal and the ability to differentiate into cell types of mesodermal origin, including adipocytes, osteoblast, and chondrocytes. These cells can be obtained from multiple sources, including adult bone marrow, adipose tissue, peripheral blood, and various neonatal birth-associated tissues [13,14].

MSCs have emerged as a promising therapeutic strategy for various diseases in recent years. Their clinical relevance was initially based on their tissue regeneration capacity, but discovering their paracrine properties has largely extended the range of therapeutic applications [15]. Several characteristics favor their use in treating a wide range of conditions [16]. For instance, MSCs can migrate to a wide range of tissues, specialty inflammatory and pathological sites, because injured tissues secrete chemokines that attract MSCs [17]. Additionally, MSCs possess immunomodulatory properties which are mediated by cell-cell interactions and the secretion of soluble paracrine factors [18]. MSCs can modulate immune system cells' proliferation and activation, inhibiting CD4+ and CD8+ T cells' proliferation, regulatory T (Treg) cells' activation, inducing M2 macrophage polarization, suppressing the

function of dendritic cells (DCs), ameliorating B-cells and natural killers' (NK) proliferation, and decreasing macrophages' and neutrophils' infiltration into inflammation sites [19,20].

Other characteristics that make MSCs good candidates for cell therapy are their potential to differentiate into multiple lineages and their ability to be easily expanded ex vivo while retaining their original lineage differentiation commitment [16]. After transplantation, MSCs can differentiate into chondrocytes and undergo chondrogenesis [21]; cardiomyocyte-like cells that integrate into host tissue [22]; hepatocyte-like cells (HLCs) that contribute to liver regeneration [23]; or into insulin-producing cells (IPCs) that secrete insulin [24].

Therefore, these cells are interesting therapeutic tools to target damaged tissues and act as a reservoir of growth factors and immuno-modulatory molecules.

2.3. Adipose Tissue as Source of MSCs for Cell Therapy

MSCs obtained from adipose tissue have been proposed as an exciting tool for cell therapy due to their easy isolation and abundance. The characteristics of ADMSCs greatly vary depending on the type and anatomical region of AT. Thus, scWAT is the primary source of ADMSCs, mainly because more than 2% of this tissue is constituted by the stroma vascular fraction (SVF) [25]. Compared with bone marrow (BM), where the MSCs fraction only constitutes 0.001% to 0.1%, AT can provide up to 500-fold more MSCs than an equivalent quantity of BM aspirate, reinforcing that AT is the most abundant and efficient source of MSCs [26].

Although most of the characteristics of ADMSCs are similar to MSCs obtained from other sources, some differences also exist. For instance, several investigations have shown that ADMSCs are stronger immunomodulators that can adapt better to oxidative stress or hypoxia-induced apoptosis and have a greater angiogenetic capacity when exposed to unfavorable conditions [27]. These advantages, compared with other MSCs, are mainly explained by the release of higher levels of pro-inflammatory and anti-inflammatory cytokines, including interferon γ (IFN- γ), interleukins (IL-6, IL-8), and transforming growth factor (TGF- β). Moreover, ADMSCs secrete a higher quantity of growth factors such as granulocyte macrophage colony-stimulating factor (GM-CSF), granulocyte colony-stimulating factor (G-CSF), nerve growth factor (NGF), or insulin-like growth factor 1 (IGF-1) that makes them proliferate better than other MSCs [24,28,29]. Additionally, ADMSCs are more suitable for regenerative medicine, as they differentiate better into β -cells, muscle cells, or cardiomyocytes [30–32].

Overall, their abundance, easy isolation, and superior characteristics have boosted interest in using ADMSCs for clinical applications.

3. ADMSCs in the Treatment of Obesity and Its Metabolic Complications

Various interventions have been proposed for obesity and its related disorders in clinical settings. However, effective therapies to prevent and remedy obesity and its comorbidities are still lacking [33]. In this context, ADMSC therapy has emerged as a promising strategy. The results obtained in animal models have confirmed their effects on weight loss, changes in adipose tissue composition, and improvement of related comorbidities such as diabetes or NAFLD. The most promising in vivo results are reviewed below and summarized in Table 1 and Figure 1.

3.1. Body Composition and Weight Loss

Weight loss is a critical step in treating obesity and its related complications. Numerous in vivo experiments have shown the efficiency of ADMSCs in weight loss and the reduction in body fat mass. Cao et al. investigated the effects of ADMSCs on body weight and composition in a mouse model of high-fat diet (HFD)-induced obesity [34]. A single intravenous infusion of ex vivo expanded syngeneic ADMSC significantly reduced body weight and triglyceride levels. In line with these findings, Tung-Qian Ji et al. demonstrated that two episodes of systemic human ADMSC transplantations effectively decrease body

weight in mice [35]. Likewise, Lee et al. showed that the transplantation of human ADMSC, MSC-derived brown adipocytes (M-BA), and MSC lysate into obese mice reduced body weight and hyperlipidemia [36]. In a similar fashion, Liu et al. used leptin receptor-deficient (*db/db*) mice and diet-induced obesity (DIO) mice to compare the effects of the administration of MSCs obtained from different sources: AT and an umbilical cord (UC) [37]. Their results showed that three weeks of ADMSC administration blocked body weight gain and AT weight was decreased in both obesity models. In contrast, UC-MSC administration had little or no effect on the animals' body weight and AT weight, suggesting that MSCs isolated from different sources may differ in their physiological functions.

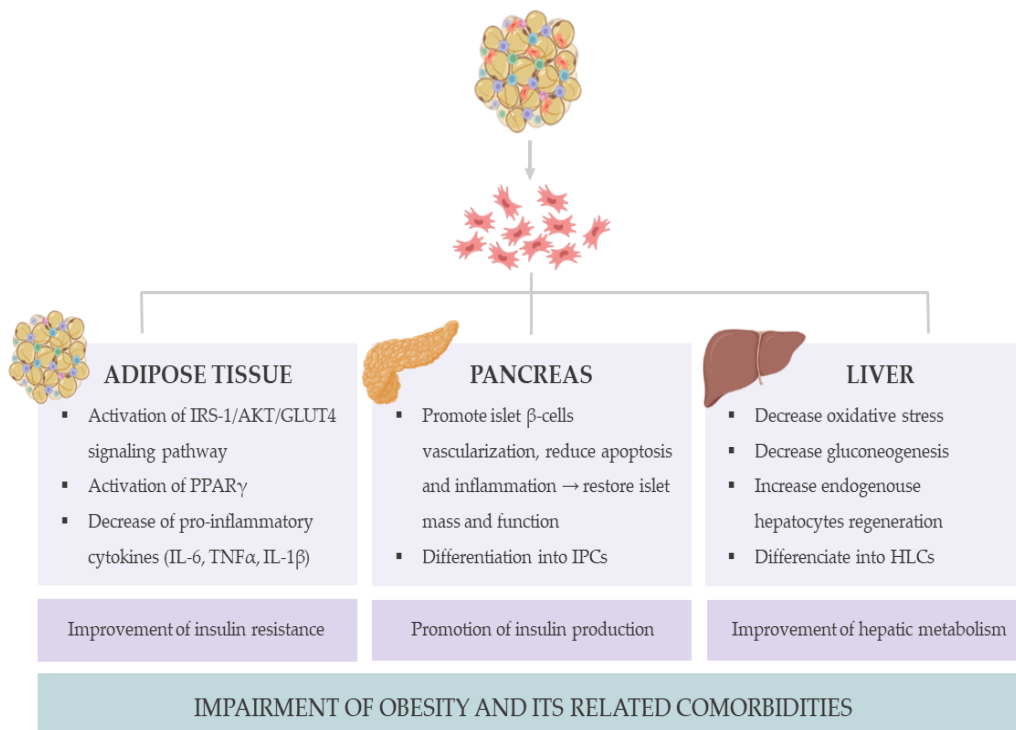


Figure 1. The mechanisms of action of ADMSC on obesity treatment. The transplantation of ADMSC reduces adipose tissue inflammation, restores glucose homeostasis by improving insulin sensitivity and promoting insulin production, and reverses liver steatosis. Abbreviation: ADMSCs, adipose-derived mesenchymal stem cells; AKT, serine/threonine kinase 1; GLUT4, glucose transporter 4; HLCs, hepatocyte-like cells; IL-1 β , interleukin 1 β ; IL-6, interleukin 6; IPCs, insulin-producing cells; IRS-1, insulin receptor substrate 1; PPAR- γ , peroxisome proliferator-activated receptor gamma; and TNF- α , tumor necrosis factor α .

However, another study by Shang et al. showed that treating obese mice with ADMSC did not change body weight, although it reduced adipocyte hypertrophy [38]. Similarly, Jaber et al. showed a significant reduction in body fat mass, despite no change in body weight [39]. Interesting results were also obtained by Shree et al. [40]: HFD-fed mice were treated with human ADMSCs or ADMSCs preconditioned with metformin. It turned out that animals administrated with ADMSCs alone did not change body weight, but significant weight loss was reported in the metformin-preconditioned ADMSC mice.

Distinct animal models, different adipose tissue depots selected for ADMSC isolation, and differing administration methods could explain the discrepancies between the studies. However, all the *in vivo* experiments seem to suggest that ADMSC therapy could effectively alter body composition [34].

3.2. Diabetes

Obesity is associated with impaired glucose tolerance, often leading to type 2 diabetes mellitus (T2DM). T2DM, which constitutes 90% to 95% of all cases of diabetes, is characterized by decreased insulin sensitivity in peripheral tissues such as adipose tissue, skeletal muscles, or liver, as well as a progressive loss of proper insulin secretion [41]. T2DM reduces functional capacities and quality of life, dramatically increasing morbidity and premature mortality [42]. Therefore, novel therapeutic strategies can help to treat diabetes and reverse long-term complications effectively.

In this context, ADMSC-based therapy has emerged as a promising strategy. Several studies have proved its capacity to maintain glucose homeostasis and reduce insulin resistance in obesity models. For instance, Lee et al. showed that multiple administrations of ADMSCs upregulated the expression of GLUT4 in AT and skeletal muscle and reduced gluconeogenesis in the liver of HFD-fed mice, reducing insulin resistance [36]. Moreover, ADMSC-based treatments altered the adiponectin-to-leptin ratio and regulated the expression of *Ppara* and *Pparg*, which maintain energy homeostasis in major metabolic tissues. In line with these findings, other studies in similar models demonstrated that DIO mice receiving ADMSC injections improved glucose tolerance and insulin sensitivity, as indicated by a significant decrease in glucose levels [34,38,39,43]. Ishida et al. developed and transplanted ADMSC sheets subcutaneously in diabetic mice fed an HFD and high sucrose diet (HSD). ADMSC transplantation significantly increased adiponectin and decreased tumor necrosis factor- α (TNF- α) plasmatic levels, ultimately improving mice glucose tolerance [44].

Additionally, ADMSC has been reported to differentiate into insulin-producing cells (IPC). Timper K et al. reported for the first time the potential of ADMSCs to derive IPC, but initially, these cells did not secrete insulin [45]. Later, ex vivo experiments performed by Dave et al. showed that ADMSCs collected from scWAT and cultured in a specific differentiation medium began to express *Pdx1*, *Pax6*, and *Isl1*, all essential factors for the reprogramming of nonpancreatic cells to fully functional β -cells. They also reported that the stimulation of these cells led to the secretion of insulin [46]. In line with these findings, Karaoz et al. demonstrated that the ability of ADMSCs to differentiate into IPC was higher than MSCs isolated from BM, indicating AT as a better cell source for cell-based therapy to restore the metabolic complications of diabetes [24].

The potential of ADMSCs to produce insulin was also tested in vivo by Nam et al. [47]. They showed that the transplantation of IPC differentiated from ADMSCs underneath the kidney capsule of T2DM mice significantly increased circulating insulin and reduced hyperglycemia, as well as ameliorated triglycerides (TG), free fatty acids (FFA), and IL-6 serum levels. Similar outcomes were reported by Liang et al. who developed a chemical-based protocol that increased the efficiency of IPC generation, which, when transplanted, significantly mitigated hyperglycemia in diabetic rats [48]. In this context, Chandra et al. explored the potential of ADMSCs to generate pancreatic hormone-expressing islet-like cell aggregates (ICAs) from murine epididymal MSCs [49]. These cells expressed pancreatic hormones such as insulin, glucagon, or somatostatin and had secretory capacity. The transplantation of calcium alginate-encapsulated ICAs into diabetic mice restored normoglycemia within two weeks, demonstrating the feasibility of using ADMSCs as a source of autologous stem cells to differentiate into the pancreatic lineage.

The dual action of ADMSCs in treating diabetes, regulating insulin sensitivity in peripheral tissues, and restoring β -pancreatic cells' function was demonstrated by Tung-Quian et al. [35]. They showed that two episodes of systemic MSC administration in DIO mice effectively improved glucose homeostasis by targeting the pancreas and insulin-sensitive tissues via site-specific mechanisms. ADMSCs supported pancreatic islet growth by direct differentiation into IPC and by reducing the cytotoxicity of IL-1 and TNF- α secretion. At the same time, the localization of ADMSCs in peripheral tissues improved glucose tolerance, reducing serum levels of adipokines, restoring glycogen storage in hepatocytes, and increasing the expression of the IL-1 receptor antagonist and GLUT4 in skeletal muscles. Taken together, these results suggest that systemic ADMSCs administration ameliorates

HFD-induced obesity and restores metabolic balance through multisystemic regulations with some tissue-specific mechanism.

The efficiency of ADMSC therapy has been tested not only in obesity-induced IR mouse models but also in T2DM rat models. Xie et al. injected ADMSCs into streptozotocin (STZ)-induced diabetic rats and observed a decrease in glucose blood levels, an increase in glucose tolerance, and an enhancement in insulin sensitivity [50]. They examined the regulation of hepatic glucose metabolism to address the mechanism involved in this improvement. They observed that ADMSC administration stimulates the phosphorylation of hepatic AMP-activated protein kinase (AMPK) to restore hepatic glucose metabolism in T2DM. In another study, Wang et al. assessed the potential therapeutic effect of ADMSC isolated from HFD/STZ-induced T2DM and db/db mice [51]. Although less proliferative than cells from healthy controls, the intravenous injection of ADMSC from T2DM or db/db increased pancreatic β cell mass and insulin sensitivity while reducing inflammation up to 5 weeks post-infusion. This study offers evidence that ADMSCs from diabetic donors also have some potential for cell therapy in the treatment of insulin resistance and T2DM.

All the above studies prove the potential of ADMSCs for treating early phase T2DM. However, research on the late stages of diabetes is more scarce. For example, Hu et al. induced T2DM in a rat model that mimics the long-term complications of diabetes and administrated ADMSCs [52]. They observed that ADMSC infusion effectively reduced hyperglycemia, restoring pancreatic islet β -cells function and improving IR via the upregulation of GLUT4 in insulin-sensitive tissues. Similar results were reported by Yu et al. [53]. In this study, multiple intravenous infusions of ADMSCs efficiently restored glucose homeostasis, lowered serum lipid levels, and ameliorated the progression of metabolic complications such as chronic kidney disease (CKD), non-alcoholic steatohepatitis (NASH), lung fibrosis, and cataracts in rats with T2DM. Altogether, the results reported thus far demonstrated that ADMSC therapy has an anti-diabetic effect and alleviates not only the early stages but also the long-term complications of T2DM.

3.3. NAFLD

NAFLD is rapidly becoming one of the most common liver diseases, with a prevalence of 25% worldwide [54]. It is an umbrella term for a variety of conditions caused by excessive fat accumulation in the form of triglycerides in hepatocytes. Hepatosteatosis represents the first step of the disease. Steatosis can be benign and remain clinically silent. However, in many cases, complications can ultimately lead to steatohepatitis (NASH), fibrosis, cirrhosis, or even hepatocarcinoma [54]. NAFLD is often linked to the development of severe obesity and metabolic syndrome (MetS); it is estimated that more than 75% of patients with obesity are affected by NAFLD [55,56]. The underlying cause of NAFLD is complex and multifactorial. Some key inducers of this condition include the accumulation of lipids in hepatocytes, pro-inflammatory mediators, mitochondria dysfunction, and genetic and epigenetic factors [57]. Although the pathogenesis is well-studied, there is currently a lack of effective therapeutic options for this condition.

Self-renewal capacity, high multilineage potential, and anti-inflammatory and antioxidant properties make ADMSCs a promising alternative for treating NAFLD [23,58]. Several studies have demonstrated that the inflammatory factors secreted by injured liver tissue attract ADMSC to this organ [59,60]. ADMSCs engraft into the recipients' livers, enhancing hepatocyte proliferation and regeneration and acting as antioxidants. Pan et al. demonstrated that ADMSC transplantation into the liver of HFD-induced NAFLD rats restored the oxidative balance by reducing the content of malondialdehyde (MDA) and increasing the enzymatic activity of antioxidant defense such as superoxide dismutase (SOD), resulting in a reduction in lipid metabolism and an improvement of liver function, attenuating the disease progression of HFD-induced NAFLD [61]. These findings are in line with other investigations that showed that ADMSC therapy ameliorated hepatic oxidative stress through the upregulation of SOD and NADPH quinone oxidoreductase 1 (NQO1) activity and the downregulation of myeloperoxidase (MPO) after liver injury [62].

Furthermore, it has been shown that ADMSCs improve hepatic inflammation, which is a determinant in the progression of NAFLD. In this sense, Ezquer et al. demonstrated that ADMSC administration in obese mice with MetS reduced the levels of fibrosis markers and pro-inflammatory cytokines, although they still present steatosis [59]. In line with these findings, Yamato et al. showed that ADMSC treatment prevented the progression of NASH by suppressing IL-17-mediated inflammation, which was associated with hepatic stellate cell (HSC) activation [63]. In addition, Lee et al. showed that in severe liver fibrosis caused by persistent HFD-feeding, ADMSC transplantation downregulated the expression of pro-inflammatory cytokines as IL-4 or TNF- α while increasing the expression of anti-inflammatory cytokines [36].

Considering these positive results, the immunomodulatory activity of the extracellular vesicles (EV) released by ADMSCs have also been studied. Watanabe et al. used a melanocortin type-4 receptor knockout (Mc4r-KO), a mouse model of NASH with a rapid accumulation of fibrosis. They showed a similar improvement in fibrosis in the groups treated with MSCs and their EVs, as well as a significant increase in anti-inflammatory macrophages in the liver [64].

Another critical characteristic of ADMSCs that makes them interesting candidates to treat liver injury is their capacity to differentiate into hepatocyte-like cells (HLCs) and adopt the hepatocyte phenotype [65,66]. It has been reported that these ADMSC-derived HLCs are able to secret albumin, synthesize glycogen and urea, and have cytochrome P450 (CYP) enzyme activity [66]. In vivo experiments performed by Banas et al. showed that the transplantation of ADMSC-derived HLC restored liver function in a mouse model of acute liver failure [65]. These results concur with another study where the transplantation of HLCs increased the secretion of IL-10, IL-6, and TGF- β , and preserved liver function in a mouse model of liver injury induced by carbon tetrachloride (CCl₄) [67]. Of note, some studies showed that although HLCs could improve liver function, these cells lost several major properties and quickly progressed to cell death when transplanted in vivo [68]. In contrast, ADMSCs were not sensitive to the damaged environment and were preserved in the liver longer. Therefore, the autologous transplantation of ADMSCs in vivo seems more efficient than HLC for liver regeneration.

Taken together, the data reported so far indicate the therapeutic potential of ADMSCs to ameliorate the development of chronic liver disease, extending to NAFLD, liver fibrosis, and cirrhosis in animal models.

Table 1. The most relevant pre-clinical studies exploring the therapeutic efficiency of ADMSCs in the treatment of obesity and its metabolic complications.

ADMSC Source	Animal Model	Administration of ADMSC	Effects	Reference
Mouse	HFD mice	2×10^6 cells injected intravenously	<ul style="list-style-type: none"> Reduced body weight Reduced blood glucose levels and increased glucose tolerance Reduced fat cell deposition in the liver 	[34]
Mouse	HFD mice	1×10^6 cells injected intraperitoneally	<ul style="list-style-type: none"> Reduced adipocyte hypertrophy Improved insulin action and metabolic homeostasis Attenuated WAT inflammation 	[38]
Mouse	HFD mice	0.5×10^6 cells injected intravenously	<ul style="list-style-type: none"> Prevented the onset of NASH, alleviated the inflammatory process 	[59]

Table 1. Cont.

ADMSC Source	Animal Model	Administration of ADMSC	Effects	Reference
Mouse	HFD and HSD mice	ADMSC sheet transplantation into subcutaneous sites	<ul style="list-style-type: none"> Improved glucose intolerance Increased plasma adiponectin and decreased tumor necrosis factor-α levels 	[44]
Human	HFD mice	4.2×10^7 cells/kg injected intravenously	<ul style="list-style-type: none"> Decreased body weight Improved glucose tolerance and blood glucose homeostasis 	[35]
Human	HFD mice	1×10^6 cells/kg injected intraperitoneally every 2 weeks (5 injections)	<ul style="list-style-type: none"> Decreased body weight Reduced hyperlipidemia Improved obesity-associated metabolic syndromes 	[36]
Human	HFD mice	4.2×10^7 cells/kg injected intraperitoneally (second injection after 10 weeks)	<ul style="list-style-type: none"> Reduced blood glucose levels and improved glucose tolerance Reduced the levels of inflammatory mediators 	[39]
Human	HFD mice	Metformin preconditioned ADMSCs; 5×10^5 cells injected intramuscularly	<ul style="list-style-type: none"> Decreased body weight Decreased hyperglycemia and enhanced glucose uptake in muscle 	[40]
Human	HFD mice	5×10^5 cells injected intramuscularly	<ul style="list-style-type: none"> Decreased oxidized LDL and IL6 Decreased insulin resistance 	[43]
Human	HFD and db/db mice	2×10^6 cells injected intravenously	<ul style="list-style-type: none"> Suppressed an increase in body weight Improved dyslipidemia 	[37]
Rat	HFD rats	2×10^6 cells transplanted intrahepatic	<ul style="list-style-type: none"> Improved liver function, reducing lipid accumulation Reduced lipid metabolism and oxidative stress 	[61]
Human	T2DM mice (HFD + low-dose STZ)	ADMSCs differentiated into IPCs; 1.5×10^6 cells transplanted underneath the kidney capsule	<ul style="list-style-type: none"> Lowered blood glucose level by increasing the circulating insulin level and ameliorating metabolic parameters, including IL-6 	[47]
Mouse	T2DM mice (HFD + low-dose STZ)	Calcium alginate-encapsulated and transplanted	<ul style="list-style-type: none"> Restored normoglycemia 	[49]
Mouse	T2DM mice (HFD + low-dose STZ)	5×10^5 cells injected intravenously	<ul style="list-style-type: none"> Increased insulin sensitivity Reduced inflammation Decreased fat content in AT and liver Increased pancreatic β-cell mass 	[51]
Rat	T2DM rats (HFD + low-dose STZ)	ADMSCs differentiated into IPCs; 3×10^6 cells injected intravenously	<ul style="list-style-type: none"> Mitigated hyperglycemia 	[48]
Rat	T2DM rats (HFD + low-dose STZ)	3×10^6 cells injected intravenously	<ul style="list-style-type: none"> Lowered blood glucose level, increased glucose tolerance, and improved insulin sensitivity 	[50]

Table 1. Cont.

ADMSC Source	Animal Model	Administration of ADMSC	Effects	Reference
Rat	Long-term T2DM rats (HFD + low-dose STZ)	3×10^6 cells injected intravenously	<ul style="list-style-type: none"> Demonstrated significant protective effects against long-term T2DM complications by alleviating inflammation and promoting tissue repair 	[53]
Mouse	Ath+HFD mice	1×10^5 cells injected into the splenic subcapsule	<ul style="list-style-type: none"> Restored albumin expression in hepatic parenchymal cells and ameliorated fibrosis in liver 	[60]
Mouse	Ath+HFD or HFD mice	1×10^5 cells injected into spleen (second injection after 4 weeks)	<ul style="list-style-type: none"> Prevented the progression of NASH fibrosis by suppressing IL-17-mediated inflammation 	[63]
Human	Mc4r-KO NASH mice + LPS	1×10^6 cells injected intravenously	<ul style="list-style-type: none"> Decreased serum alanine transaminase levels and inflammatory markers Improved fibrosis and inflammation 	[64]
Human	Mice with liver injury (CCl4)	ADMSCs differentiated into HLCs; 1×10^6 cells injected intravenously	<ul style="list-style-type: none"> Restored liver function 	[65]
Rat	T2DM rats with liver fibrosis (HFD, low-dose STZ + CCl4)	2×10^3 cells injected intravenously (second injection after 2 weeks)	<ul style="list-style-type: none"> Reduced hyperglycemia and insulin resistance Alleviated liver injury by improving liver function 	[62]

4. Genetic Modifications of ADMSCs

Despite the positive results obtained in some pre-clinical studies, the actual clinical efficacy of ADMSCs still remains controversial [69–72]. Several investigations have shown that transplanted ADMSCs present a meager rate of survival and proliferation, possibly because of the damaged microenvironment of the affected tissues, which could lead to cell death [73]. Therefore, there is a need for novel approaches to generate more functional ADMSCs with enhanced therapeutic potential. In this context, genetic manipulation has emerged as a promising strategy.

The genetic engineering of ADMSCs has been studied in past years to enhance the therapeutic potential of these cells and improve the outcomes after transplantation. Several genetic engineering methods have been described to modify the ADMSC gene expression profile. These techniques can be broadly classified as viral- and non-viral-based transfection as well as Clustered Regularly Interspaced Short Palindromic Repeats (CRISPR)-Cas9 gene editing technology (Figure 2).

4.1. Viral-Based Transfection (Transduction)

Viral vectors are the most used gene transfer tool to modify the MSC genome due to their high efficiency in DNA transfer compared to non-viral methods. This gene-editing technique ensures the stable and long-term transcription of the target gene and, consequently, better efficiency than other methods [74]. In addition, the high efficiency of viral transduction does not modify the cell differentiation capacity or the immunophenotypic characteristics of ADMSCs [75].

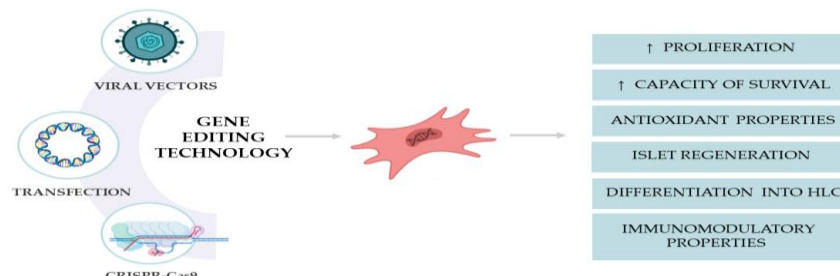


Figure 2. The genetic modification of ADMSCs increases their therapeutic potential by enhancing important characteristics such as proliferation or immunomodulation. Abbreviation: HLCs, hepatocyte-like cells.

Currently, lentivirus and adenovirus are the most predominant vectors used for ADMSC transduction. They have been used to enhance different properties of ADMSCs, such as proliferation or differentiation, thus improving their therapeutic capacity. For instance, Cho et al. overexpressed CXCR4 in ADMSCs using lentiviral vectors [76]. CXCR4 is a G-coupled transmembrane glycoprotein that mediates the stromal-derived factor-1 (SDF-1) signaling pathway and plays essential roles in the migration, engraftment, and proliferation of stem cells [77]. They reported that CXCR4 transduction into ADMSCs offered protection against induced cell death while increasing cellular growth and migration. These results suggest that the genetic modification improved ADMSC motility, retention, and proliferation, which could benefit *in vivo* migration, expansion, and therapeutic efficiency.

Other investigations focused on the enhancement of the antioxidant properties of ADMSCs by overexpressing key antioxidant enzymes. Baldari et al. demonstrated that the overexpression of SOD2 by lentiviral transduction significantly increased the survival rate of ADMSCs when exposed to hypoxic conditions [78]. Similar experiments were performed by Sen et al. but, in this case, using an adenoviral vector to overexpress SOD2. When these modified ADMSCs were exposed to high glucose, a reduction in superoxide generation and inflammation were observed compared with control cells, thus promoting ADMSC survival [79].

Another approach is to use viral vector-modified ADMSCs as a vehicle to deliver proteins that would otherwise be deficient in a specific condition. Sun et al. overexpressed betatrophin (BET), a hormone secreted by the liver and AT that stimulates pancreatic β -cell proliferation, in ADMSCs [80]. They reported that the overexpression of BET did not affect ADMSC proliferation or differentiation. However, the co-culture of human islets with modified ADMSCs did induce islet proliferation, β -cell specific transcription factor expression, and glucose-dependent insulin production. Thus, BET overexpression could be an innovative strategy for inducing β -cell regeneration and an alternative to insulin injections by increasing the number of endogenous insulin-producing cells in patients with diabetes.

The potential of lentiviral vectors to induce the transdifferentiation of ADMSCs has also been explored. Davoodian et al. overexpressed miR-122 and silenced let-7f, two key microRNAs in hepatic differentiation, in ADMSCs [81]. This modification resulted in the increased expression of hepatocyte markers, including ALB, AFP, CK18, CK19, and HNF4a, as well as urea, albumin, and glycogen production, confirming that the modified cells differentiated toward HLC. Therefore, these results demonstrate the possibility of using viral vectors to induce the transdifferentiation of ADMSCs.

The results so far propose viral vectors as an efficient tool to modify ADMSCs and increase their therapeutic potential. However, it has been reported that viral expression systems can cause immune and inflammatory responses in the host, and viral insertion in the host's genome poses a tumorigenic risk [82]. Accordingly, safety is the most significant barrier to future clinical therapeutic applications of modified ADMSCs.

4.2. Non-Viral Methods

To bypass the safety concerns associated with viral vectors, alternative, non-viral-based methods for transgene delivery have been established for ADMSCs. Currently, the non-viral genetic modification of ADMSCs can be performed by physical methods such as electroporation, nucleofection, and sonoporation, or chemical methods including lipidic agents, polymers, and inorganic nanoparticles [83].

Non-viral methods have been efficiently used to enhance the proliferation and differentiation capacity of ADMSCs. Sox2 and Oct4 are transcription factors that maintain pluripotency in embryonic stem cells, enhance proliferation, and prevent cell senescence in ADMSCs. Han et al. overexpressed Sox2 and Oct4 in ADMSCs by liposomal transfection [84] and showed that the modified cells exhibited enhanced proliferation and adipogenic differentiation capacity. Similar results were obtained by Kim et al. after over-expressing the proliferation regulator micro-RNA miR-302 [85]. They also observed an increase in the proliferation and cell survival of modified ADMSCs. In general, non-viral modification has shown benefits in the proliferation capability of ADMSCs, however, more research needs to be performed before clinical translation due to their lower efficiency.

4.3. CRISPR/Cas9 System

In recent years, new genetic modification tools have emerged in order to promote the insertion, deletion, or correction of genes at specific sites in the genome. Due to its high efficiency, specificity, simple design, and cost-effectiveness, CRISPR/Cas has become the most widely used genome editing technology [86,87]. The CRISPR/Cas9 system is based on the nucleolytic activity of the endonuclease protein Cas9, which is conducted to a specific site in the genome by a guide RNA (gRNA). The Cas9 protein binds to the target site determined by the gRNA and performs a double-strand break (DSB) followed by the introduction of mutations at the cleavage site by the non-homologous end-joining repair mechanism of the cell. Using a predesigned repair template, this system can not only knock out genes but also knock in (CRISPR/Cas9-SAM-System) or even insert specific mutations [86,88,89].

The efficiency of the CRISPR/Cas9 system has already been tested in MSCs by targeting critical genes involved in adipocyte differentiation and function. Lundh et al. introduced the CRISPR/Cas9-SAM system in MSCs through viral delivery and used gRNA targeting *Pparg2*, *Prdm16*, *Zfp423*, or *Ucp1* [90]. They demonstrated that this system could efficiently manipulate gene expression in pre- and mature adipocytes in vitro. This gene editing technology has also been optimized in ADMSCs obtained from human AT. Kamble et al. developed a method for gene knockout by introducing the CRISPR/Cas9 system through electroporation in ADMSCs. They knocked out *PPARG* genes with more than 90% efficiency, blocking the differentiation of ADMSCs into adipocytes [91].

Further exciting research using the CRISPR/Cas9 system on ADMSCs was performed by Claussnitzer et al. who targeted *ARID5B*, a gene essential for adipocyte development and normal lipid metabolism [92]. They identified a single nucleotide mutation in *ARID5B* that results in a reduction in mitochondrial thermogenesis and an increase in lipid storage in adipocytes. Using the CRISPR/Cas9 system, they repaired the *ARID5B* motif in ADMSCs from a patient with the risk allele, restoring thermogenesis and lipid metabolism [93].

Hence, CRISPR/Cas9 gene editing in ADMSCs seems to be a promising tool for therapeutic applications. However, all these investigations are still in an early stage, and more positive results are needed for their translation into the clinic.

5. Genetic Modification of ADMSCs as a Therapeutic Strategy

To successfully translate ADMSCs into clinical practice, it is essential to improve the functionality of these cells, enhancing their capacity for survival, homing to the inflammation site, and immunomodulatory properties. Gene editing tools are becoming one of the better ways to achieve this goal. To date, multiple results show the higher in vivo effi-

ciency of genetically modified ADMSCs compared to wild-type ADMSCs to treat metabolic disorders. These investigations are summarized in Table 2.

5.1. Genetically Modified ADMSCs in the Treatment of Metabolic Complications Associated with Obesity

Different approaches have been explored to enhance the antioxidant properties of ADMSCs to increase their survival. Briefly, Baldari et al. compared the administration efficiency of will-type ADMSCs versus ADMSCs overexpressing SOD2, an antioxidant enzyme [78]. They proved that modified ADMSCs showed higher cell engraftment and improved oxidative stress resistance, enhancing cell therapy potential. To evaluate the therapeutic capacity of this cytoprotective effect conferred by SOD2 overexpression, Sen et al. administrated these cells to an obese (*db/db*) diabetic mouse model [79]. They confirmed that mice receiving modified ADMSCs exhibited reduced adiposity and improved glucose tolerance, through anti-oxidative and anti-inflammatory mechanisms, compared to those receiving wild-type cells. Similar results were obtained by Domingues et al., who jointly upregulated the expression of SOD2 and catalase in ADMSC [94]. Taken together, these results suggest that overexpression of antioxidant enzymes using ADMSCs as gene delivery vehicles attenuates AT inflammation and improves glucose tolerance *in vivo*, proposing ADMSC-mediated gene therapy as a novel and safe therapeutic tool to combat the effects of hyperglycemia derived from obesity.

Another attractive target is neuregulin (Nrg4), a growth factor secreted by AT that regulates lipogenesis in the liver and is reduced in obesity. Wang et al. explored the therapeutic potential of this protein by overexpressing Nrg4 in ADMSCs and then transplanting the modified cells in HFD-fed mice [95]. Their results showed that Nrg4 upregulation could enhance the efficiency of ADMSCs in reducing IR and other obesity-related metabolic disorders, mainly by suppressing inflammation, enhancing glucose uptake in AT and muscle, and attenuating hepatic lipogenesis. It would provide a new therapeutic strategy for treating obesity, IR, and T2D.

5.2. Genetically Modified ADMSCs in Diabetes

ADMSCs have immense potency in curing T2DM due to their easy isolation, multiple differentiation potential, and immunomodulatory property. However, despite the promising efficacy in pre-clinical animal models, the administration of ADMSCs does not show clinically satisfactory therapeutic results, varying significantly between people with T2DM [96]. After transplantation in people with diabetes, ADMSCs are faced with an inflammatory and hyperglycemic environment that severely reduces cell viability [96,97], leading to the unsatisfactory efficiency of ADMSCs in diabetic models. However, many gene editing strategies have been adopted to maximize ADMSC therapeutic efficiency.

One interesting approach is using ADMSCs as a vehicle to deliver deficient proteins in diabetic individuals. In this sense, Sun et al. engineered ADMSCs to overexpress BET, a hormone that can increase the production and expansion of insulin-secreting β -cells [80]. Those engineered ADMSCs were then administrated into STZ-induced diabetic mice. This innovative approach increased the ratio of β -cells per islet and improved insulin secretion, ameliorating the hyperglycemia associated with this condition. Another strategy to enhance the therapeutic efficiency of ADMSCs in diabetes treatment is via their differentiation into IPC before transplantation. Pancreatic and duodenal homeobox 1 (*Pdx1*) is an exciting target gene as it plays a crucial role in normal pancreas development and is required for maintaining the normal function of islets. With this in mind, Lin et al. proved that the overexpression of *Pdx1* led to the differentiation of ADMSCs to IPC [98]. Subsequent transplantation of these cells under the kidney capsule of STZ-induced diabetic rats resulted in lowered blood glucose and increased glucose tolerance. Kajiyama et al. performed similar studies, where they transplanted *Pdx1* transduced-ADMSC in a hyperglycemic mouse model with pancreatic damage [99]. They reported that modified cells engrafted properly in the pancreas, wherein they expressed insulin, decreased blood glucose levels,

and increased survival. Some years later, Lee et al. performed similar experiments and observed reduced blood glucose levels, although modified ADMSC administration did not restore normoglycemia [100].

A further option to treat diabetes is the xenotransplantation of porcine islets, but this is primarily limited because of immune rejection and the early loss of transplanted islet cells [101]. To overcome this problem, Lee et al. proposed to co-transplant islets with genetically modified ADMSCs overexpressing both heme oxygenase- 1 (HO-1) and the soluble fusion protein of TNF- α receptor (TNF- α R-Fc) [102,103]. HO-1 is a stress-activated inducible enzyme and TNF- α R-Fc suppresses TNF- α induced inflammatory reactions. Both have been described to reduce the deleterious effects of oxidative stress, apoptosis, and the inflammatory factor in many cell lines [104,105]. This double overexpression strategy confirmed that the modified ADMSCs reduced the inflammatory reaction and improved the viability of the transplanted islets, significantly reducing rejection and reversing hyperglycemia.

5.3. Genetically Modified ADMSCs in NAFLD

Multiple studies have demonstrated that modified-ADMSC administration in obesity mice models has systemic benefits, reducing lipid deposition in the liver which is the leading cause of the development of NAFLD. For instance, Nrg4 overexpressing-ADMSCs reduced the liver fat content by attenuating hepatocyte lipogenesis [95]. In addition, antioxidant-upregulated ADMSC delivery has been shown to reduce fat accumulation in the liver by reducing systemic inflammation [94]. Domingues et al. demonstrated that mice receiving SOD2 and catalase-overexpressing ADMSCs showed lower levels of steatosis than those transplanted with non-modified ADMSC.

Nevertheless, the therapeutic potential of modifying ADMSCs has been tested not only for early stages of NAFLD derived by obesity-like steatosis but also for more advanced phases such as fibrosis. For instance, Kang et al. generated FGF21-secreting ADMSC and administrated them to a liver fibrosis mice model. The transplantation of FGF21-ADMSC significantly improved liver fibrosis by decreasing serum hyaluronic acid and reducing fibrosis-related factors' expression [106]. Similarly, Lou et al. established ADMSC overexpressing miR-122, a key regulator of liver fibrosis. They observed that administering these cells to mice improved liver fibrosis by suppressing the activation of HSC and alleviating collagen deposition [107].

5.4. Genetically Modified ADMSCs in Metabolic Syndrome

In the last few years, activating brown adipocytes to increase energy expenditure has emerged as a promising treatment strategy for MetS. Several studies have proved that the implantation of brown fat into obese mice improves glucose tolerance. However, the translation to humans has been limited by the low abundance of primary human beige adipocytes [108,109]. To overcome this limitation, research has focused on the potential of ADMSCs obtained from scWAT, which is much more abundant, and its genetic modification to turn into brown-like adipocytes ("browning").

In this context, Wang et al. generated human brown-like cells from ADMSCs using CRISPR/Cas9-SAM-gRNA to activate the endogenous expression of uncoupling protein 1 (UCP1), the main thermogenesis regulator. Obese mice transplanted with these modified cells showed a significant improvement in glucose tolerance, insulin sensitivity, and increased energy expenditure [110]. With the same goal, Tsagkaraki et al. tried to target the nuclear receptor-interacting protein 1 (NRIP1), a transcriptional co-repressor that regulates energy metabolism and suppresses thermogenesis [111]. They also used CRISPR technology to disrupt NRIP1 in ADMSCs, notably increasing thermogenesis in these cells. The transplantation of these CRISPR-enhanced brown-like adipocytes into HFD-fed mice decreased adiposity and liver fat deposition while enhancing glucose tolerance compared to the implantation of unmodified adipocytes.

These results demonstrate the benefits of using CRISPR/Cas9 technology to engineer human white adipocytes to display phenotypes similar to brown fat and may open cell-based therapeutic opportunities to combat metabolic disorders caused by high-calorie diets. Furthermore, CRISPR-based therapy is a safe alternative, as ex vivo delivered Cas9 and sgRNA are entirely degraded by human cells after high-efficiency genomic modification without detectable off-target editing.

Table 2. Relevant genetic modifications of ADMSCs to increase their therapeutic potential.

Modification in ADMSC	Method of Modification	ADMSC Source	Model	Effects	References
SOD2 overexpression	Lentivirus	Human	7×10^5 cells injected subcutaneously into mice	<ul style="list-style-type: none"> Promoted the survival and engraftment of transplanted ADMSCs 	[78]
SOD2 overexpression	Adenovirus	Human	Intraperitoneal injection in db/db mice	<ul style="list-style-type: none"> Reduced body weight Improved glucose tolerance Reduced inflammation 	[79]
SOD2 and catalase overexpression	Adenovirus	Human	1.5×10^6 cells injected intraperitoneally in HFD mice	<ul style="list-style-type: none"> Reduction in liver fat content Reduced systemic inflammation 	[94]
NRG4 overexpression	Lentivirus	Mouse	2×10^6 cells injected intravenously into HFD mice	<ul style="list-style-type: none"> Reduced blood glucose levels and enhanced insulin sensitivity Decreased fat cell deposition and lowered TG and TC levels in the serum and liver 	[95]
UCP1 overexpression	CRISPR–Cas9	Human	Subcutaneous implantation into HFD mice	<ul style="list-style-type: none"> Improved glucose tolerance and insulin sensitivity and increased energy expenditure 	[110]
NRIP1 deletion	CRISPR–Cas9	Human and mice	Subcutaneous implantation into HFD mice	<ul style="list-style-type: none"> Decreased adiposity and levels of liver triglycerides Enhanced glucose tolerance Decreased liver triglycerides 	[111,112]
BET overexpression	Adenovirus	Human	1×10^6 cells injected intravenously into T2DM mice	<ul style="list-style-type: none"> Ameliorated hyperglycemia and weight loss Induced β-cell proliferation and insulin secretion 	[80]
PDX1 overexpression	Retrovirus	Mouse	5×10^5 cells injected intravenously into T2DM mice	<ul style="list-style-type: none"> Decreased blood glucose levels and increased survival 	[99]
PDX1 overexpression	Adenovirus	Human	2×10^6 cells transplanted under the renal capsule of T2DM mice	<ul style="list-style-type: none"> Reduced blood glucose levels, although they did not restore normoglycemia 	[100]
PDX1 overexpression	Lentivirus	Human and rat	2×10^6 cells transplanted under the renal capsule of T2DM rats	<ul style="list-style-type: none"> Reduced blood glucose levels and led to higher glucose tolerance, smoother fur, and fewer cataracts 	[98]

Table 2. Cont.

Modification in ADMSC	Method of Modification	ADMSC Source	Model	Effects	References
HO-1 and TNF- α R-Fc overexpression	Adenoviral	Human	Transplantation of porcine islets with ADMSC in T1DM mice	• Reversed hyperglycemia	[103]
FGF21 overexpression	Plasmid transfection	Not defined	1.5×10^6 cells injected intravenously into TAA-treated mice	• Improved liver fibrosis	[106]
MiR-122 overexpression	Lentiviral	Mouse	1×10^5 cells injected intravenously into CCL4-treated mice	• Decreased liver fibrosis	[107]

6. Clinical Trials with Modified ADMSCs

The promising pre-clinical results have encouraged researchers to test MSC therapy in human clinical trials. In the last decade, more than 400 clinical trials based on MSCs have been performed to treat various diseases, according to the US National Institute of Health–Clinical Trials database (<http://clinicaltrials.gov>, accessed on 1 March 2020). Regarding the metabolic complications of obesity, interesting results have been obtained with MSCs obtained from different sources to treat T2DM. Zhang et al. carried out a systemic review and meta-analysis of published clinical trials to evaluate the safety and efficacy of MSC therapy for T2DM [113]. They considered 11 T2DM studies including 386 patients, all treated with MSCs isolated from BM, placenta, or UC. This analysis showed that stem cell therapy improved insulin requirements and had favorable therapeutic effects, but it is unclear which source of MSCs is most suitable for treating the disease. However, clinical studies using ADMSCs to treat T2DM are scarcer [96,113]. One ongoing study using ADMSCs found that fasting plasma glucose and glycated hemoglobin (HbA1c) in ADMSC-treated diabetic individuals decreased more than the controls (NCT00703612 [ClinicalTrials.gov](https://clinicaltrials.gov)).

MSC therapy has also been used for liver disease therapy. Currently, MSCs applied for liver disease in the clinic are primarily obtained from UC and BM, and only in a few cases from AT [23]. For instance, Sakai et al. conducted a clinical trial using autologous ADMSCs to treat patients with liver cirrhosis derived from NASH or fatty liver [114,115]. They observed a significant improvement in serum albumin concentration and pro-thrombin activity in most of the treated patients. However, only seven patients were in the trial, so more extensive trials are warranted to confirm the therapeutic efficiency.

Most of the clinical trials based on MSC therapy conducted to date have used autologous MSCs to minimize the immune response [116,117]. However, ADMSCs isolated from patients that have a chronic inflammatory disease such as obesity have less therapeutic potential compared with metabolically healthy individuals [118]. Furthermore, after being transplanted into obese individuals, MSCs are faced with an inflammatory environment that impairs their survival, leading to non-ideal therapeutic effects [119]. This fact supports the need to increase the therapeutic potential of ADMSCs, and one of the more promising strategies to achieve that is genetic modification.

To date, genetically engineered MSCs are being tested in only a few clinical studies to treat different conditions [75,120,121]. Promising results have been obtained with modified MSCs to treat some oncological diseases. Thus, genetically modified MSCs have been used in clinical trials of advanced gastrointestinal cancer [122], ovarian cancer (NCT02530047 [ClinicalTrials.gov](https://clinicaltrials.gov)), lung cancer (NCT03298763 [ClinicalTrials.gov](https://clinicaltrials.gov)), or neck cancer (NCT02079324 [ClinicalTrials.gov](https://clinicaltrials.gov)). Regarding metabolic diseases, to the best of

our knowledge, there is only one phase 1 clinical trial started in 2022 based on CRISPR-modified-MSC for T1DM (NCT05210530 [ClinicalTrials.gov](#)).

7. Limitations and Side Effects of ADMSC Therapy

Although pre-clinical trials of ADMSC therapy are effective and have few side effects, many problems still need to be solved before ADMSCs can be efficiently applied in the clinic for metabolic disorders. First, a standardized protocol needs to be developed, including specifications such as the injection site, injection method, injection dose, and other variables. The different conditions used so far could explain the discrepancies between studies and makes it difficult to evaluate the efficiency of the treatment.

Second, it is critical to address whether autologous or allogeneic ADMSC therapy is safer and more efficient for metabolic complications. While autologous ADMSCs may be the better option to avoid the immune response, factors including donor comorbidities such as obesity or diabetes may compromise the therapeutic potential of these cells [123]. Conversely, allogeneic ADMSC therapy may be more efficient but may cause an immune response [124]. It has been described that allogeneic ADMSCs are recognized by both the innate and adaptative immune systems and that their viability may be decreased following immune recognition. Moreover, some studies have shown that an antibody response is generated after the treatment, which may inhibit ADMSCs' therapeutic efficacy upon repeat injections [125,126].

Regarding the immune response, it is also essential to consider the possible changes in the immunogenicity of ADMSCs during their differentiation to HLC or IPC [127]. For instance, Li et al. described the upregulation of HLA-DR on MSCs after hepatocyte differentiation, which induced significantly more CD3+ and CD45+ cells after transplantation compared to undifferentiated MSCs [128]. Similarly, Mohammadi et al. reported that IPC exhibited an increased expression of MHC-I and CD80 that induced the proliferation of splenocytes, activation of CD4+ T cells, and IFN γ response [129–131]. Therefore, strategies such as genetic modification to reduce this immunogenicity would be extremely important for the future development of such therapies.

In addition to the limitations already discussed, the genetic stability of ADMSCs after expansion and manipulation is another major issue. Multiple replications in vitro expose cells to the risk of accumulating genetic and epigenetic alterations, which may promote cell senescence or even cell transformation, thus possibly affecting treatment efficacy and patient safety [132]. Moreover, genetic modification may increase this risk, as gene therapy vectors can integrate into the host's genome outside the target sequences, promoting tumorigenesis [74]. Thus, there is a need to optimize this technology prior to its use in clinical routine, especially considering its effectiveness, safety, and specificity.

8. Conclusions

Considering the good results obtained in vitro and the positive outcomes in clinical trials with modified cells, it is rational to think that modified ADMSCs are a promising strategy for treating obesity and its comorbidities. However, as obesity is a multifactorial disorder that affects metabolic homeostasis globally, it is critical to identify the specific cells/tissues to target using gene therapy-based ADMSCs. Consequently, additional pre-clinical studies are needed to ensure the safety and demonstrate the therapeutic potential of engineered ADMSCs.

Funding: This research was partially supported by a grant [PI22/01366] from the Instituto de Salud Carlos III and by FEDER funds: “Una manera de hacer Europa”. J.M.A.-M. also has support from the regional government of Aragón [B03_20R], co-financed with the FEDER Aragón 2014–2020: “Construyendo Europa desde Aragón”.

Institutional Review Board Statement: Not applicable.

Informed Consent Statement: Not applicable.

Data Availability Statement: Not applicable.

Acknowledgments: We want to thank Carolina Durante for the inspiring comments.

Conflicts of Interest: The authors declare no conflict of interest. The funders had no role in the design of the study; in the collection, analyses, or interpretation of data; in the writing of the manuscript; or in the decision to publish the results.

References

1. Fitch, A.K.; Bays, H.E. Obesity Definition, Diagnosis, Bias, Standard Operating Procedures (SOPs), and Telehealth: An Obesity Medicine Association (OMA) Clinical Practice Statement (CPS) 2022. *Obes. Pillars* **2022**, *1*, 100004. [[CrossRef](#)]
2. Heymsfield, S.B.; Wadden, T.A. Mechanisms, Pathophysiology, and Management of Obesity. *N. Engl. J. Med.* **2017**, *376*, 254–266. [[CrossRef](#)] [[PubMed](#)]
3. GBD 2015 Obesity Collaborators; Afshin, A.; Forouzanfar, M.H.; Reitsma, M.B.; Sur, P.; Estep, K.; Lee, A.; Marczak, L.; Mokdad, A.H.; Moradi-Lakeh, M.; et al. Health Effects of Overweight and Obesity in 195 Countries over 25 Years. *N. Engl. J. Med.* **2017**, *377*, 13–27. [[CrossRef](#)]
4. Richmond, T.K.; Thurston, I.B.; Sonnevile, K.R. Weight-Focused Public Health Interventions—No Benefit, Some Harm. *JAMA Pediatr.* **2021**, *175*, 238–239. [[CrossRef](#)]
5. Xia, Q.; Campbell, J.A.; Ahmad, H.; Si, L.; de Graaff, B.; Palmer, A.J. Bariatric Surgery Is a Cost-Saving Treatment for Obesity—A Comprehensive Meta-Analysis and Updated Systematic Review of Health Economic Evaluations of Bariatric Surgery. *Obes. Rev.* **2020**, *21*, e12932. [[CrossRef](#)] [[PubMed](#)]
6. Wilding, J.P.H.; Batterham, R.L.; Calanna, S.; Davies, M.; van Gaal, L.F.; Lingvay, I.; McGowan, B.M.; Rosenstock, J.; Tran, M.T.D.; Wadden, T.A.; et al. Once-Weekly Semaglutide in Adults with Overweight or Obesity. *N. Engl. J. Med.* **2021**, *384*, 989–1002. [[CrossRef](#)] [[PubMed](#)]
7. Jastreboff, A.M.; Aronne, L.J.; Ahmad, N.N.; Wharton, S.; Connery, L.; Alves, B.; Kiyo, A.; Zhang, S.; Liu, B.; Bunck, M.C.; et al. Tirzepatide Once Weekly for the Treatment of Obesity. *N. Engl. J. Med.* **2022**, *387*, 205–216. [[CrossRef](#)] [[PubMed](#)]
8. Scherer, P.E. Adipose Tissue: From Lipid Storage Compartment to Endocrine Organ. *Proc. Diabetes* **2006**, *55*, 1537–1545. [[CrossRef](#)] [[PubMed](#)]
9. Virtue, S.; Vidal-Puig, A. Adipose Tissue Expandability, Lipotoxicity and the Metabolic Syndrome—An Allostatic Perspective. *Biochim. Biophys. Acta Mol. Cell Biol. Lipids* **2010**, *1801*, 338–349. [[CrossRef](#)]
10. Choe, S.S.; Huh, J.Y.; Hwang, I.J.; Kim, J.I.; Kim, J.B. Adipose Tissue Remodeling: Its Role in Energy Metabolism and Metabolic Disorders. *Front. Endocrinol.* **2016**, *7*, 30. [[CrossRef](#)]
11. Hammarstedt, A.; Gogg, S.; Hedjazifar, S.; Nerstedt, A.; Smith, U. Impaired Adipo-Genesis and Dysfunctional Adipose Tissue in Human Hypertrophic Obesity. *Physiol. Rev.* **2018**, *98*, 1911–1941. [[CrossRef](#)]
12. McQuaid, S.E.; Hodson, L.; Neville, M.J.; Dennis, A.L.; Cheeseman, J.; Humphreys, S.M.; Ruge, T.; Gilbert, M.; Fielding, B.A.; Frayn, K.N.; et al. Downregulation of Adipose Tissue Fatty Acid Trafficking in Obesity: A Driver for Ectopic Fat Deposition? *Diabetes* **2011**, *60*, 47–55. [[CrossRef](#)] [[PubMed](#)]
13. Pittenger, M.F.; Discher, D.E.; Péault, B.M.; Phinney, D.G.; Hare, J.M.; Caplan, A.I. Mesenchymal Stem Cell Perspective: Cell Biology to Clinical Progress. *NPJ Regen. Med.* **2019**, *4*, 22. [[CrossRef](#)]
14. Andrzejewska, A.; Lukomska, B.; Janowski, M. Concise Review: Mesenchymal Stem Cells: From Roots to Boost. *Stem Cells* **2019**, *37*, 855–864. [[CrossRef](#)] [[PubMed](#)]
15. Jovic, D.; Yu, Y.; Wang, D.; Wang, K.; Li, H.; Xu, F.; Liu, C.; Liu, J.; Luo, Y. A Brief Overview of Global Trends in MSC-Based Cell Therapy. *Stem Cell Rev. Rep.* **2022**, *18*, 1525–1545. [[CrossRef](#)]
16. Fan, X.L.; Zhang, Y.; Li, X.; Fu, Q.L. Mechanisms Underlying the Protective Effects of Mesenchymal Stem Cell-Based Therapy. *Cell. Mol. Life Sci.* **2020**, *77*, 2771–2794. [[CrossRef](#)] [[PubMed](#)]
17. Ullah, M.; Liu, D.D.; Thakor, A.S. Mesenchymal Stromal Cell Homing: Mechanisms and Strategies for Improvement. *iScience* **2019**, *15*, 421–438. [[CrossRef](#)] [[PubMed](#)]
18. Wang, M.; Yuan, Q.; Xie, L. Mesenchymal Stem Cell-Based Immunomodulation: Properties and Clinical Application. *Stem Cells Int.* **2018**, *2018*, 3057624. [[CrossRef](#)] [[PubMed](#)]
19. Wang, Y.; Chen, X.; Cao, W.; Shi, Y. Plasticity of Mesenchymal Stem Cells in Immunomodulation: Pathological and Therapeutic Implications. *Nat. Immunol.* **2014**, *15*, 1009–1016. [[CrossRef](#)]
20. Bernardo, M.E.; Fibbe, W.E. Mesenchymal Stromal Cells: Sensors and Switchers of Inflammation. *Cell Stem Cell* **2013**, *13*, 392–402. [[CrossRef](#)] [[PubMed](#)]
21. Zha, K.; Sun, Z.; Yang, Y.; Chen, M.; Gao, C.; Fu, L.; Li, H.; Sui, X.; Guo, Q.; Liu, S. Recent Developed Strategies for Enhancing Chondrogenic Differentiation of MSC: Impact on MSC-Based Therapy for Cartilage Regeneration. *Stem Cells Int.* **2021**, *2021*, 8830834. [[CrossRef](#)]
22. Guo, X.; Bai, Y.; Zhang, L.; Zhang, B.; Zagidullin, N.; Carvalho, K.; Du, Z.; Cai, B. Cardiomyocyte Differentiation of Mesenchymal Stem Cells from Bone Marrow: New Regulators and Its Implications. *Stem Cell Res. Ther.* **2018**, *9*, 44. [[CrossRef](#)] [[PubMed](#)]
23. Yang, X.; Meng, Y.; Han, Z.; Ye, F.; Wei, L.; Zong, C. Mesenchymal Stem Cell Therapy for Liver Disease: Full of Chances and Challenges. *Cell Biosci.* **2020**, *10*, 123. [[CrossRef](#)]

24. Karaoz, E.; Okcu, A.; Ünal, Z.S.; Subasi, C.; Saglam, O.; Duruksu, G. Adipose Tissue-Derived Mesenchymal Stromal Cells Efficiently Differentiate into Insulin-Producing Cells in Pancreatic Islet Microenvironment Both in Vitro and in Vivo. *Cytotherapy* **2013**, *15*, 557–570. [CrossRef] [PubMed]
25. Hass, R.; Kasper, C.; Böhm, S.; Jacobs, R. Different Populations and Sources of Human Mesenchymal Stem Cells (MSC): A Comparison of Adult and Neonatal Tissue-Derived MSC. *Cell Commun. Signal.* **2011**, *9*, 12. [CrossRef] [PubMed]
26. Melief, S.M.; Zwaginga, J.J.; Fibbe, W.E.; Roelofs, H. Adipose Tissue-Derived Multipotent Stromal Cells Have a Higher Immunomodulatory Capacity Than Their Bone Marrow-Derived Counterparts. *Stem Cells Transl. Med.* **2013**, *2*, 455–463. [CrossRef]
27. Valencia, J.; Blanco, B.; Yáñez, R.; Vázquez, M.; Herrero Sánchez, C.; Fernández-García, M.; Rodríguez Serrano, C.; Pescador, D.; Blanco, J.F.; Hernando-Rodríguez, M.; et al. Comparative Analysis of the Immunomodulatory Capacities of Human Bone Marrow- and Adipose Tissue-Derived Mesenchymal Stromal Cells from the Same Donor. *Cytotherapy* **2016**, *18*, 1297–1311. [CrossRef] [PubMed]
28. El-Badawy, A.; Amer, M.; Abdelbaset, R.; Sherif, S.N.; Abo-Elela, M.; Ghallab, Y.H.; Abdelhamid, H.; Ismail, Y.; El-Badri, N. Adipose Stem Cells Display Higher Regenerative Capacities and More Adaptable Electro-Kinetic Properties Compared to Bone Marrow-Derived Mesenchymal Stromal Cells. *Sci. Rep.* **2016**, *6*, 37801. [CrossRef] [PubMed]
29. Kocan, B.; Maziarz, A.; Tabarkiewicz, J.; Ochiya, T.; Banaś-Ząbczyk, A. Trophic Activity and Phenotype of Adipose Tissue-Derived Mesenchymal Stem Cells as a Background of Their Regenerative Potential. *Stem Cells Int.* **2017**, *2017*, 1653254. [CrossRef] [PubMed]
30. Li, X.; Bai, J.; Ji, X.; Li, R.; Xuan, Y.; Wang, Y. Comprehensive Characterization of Four Different Populations of Human Mesenchymal Stem Cells as Regards Their Immune Properties, Proliferation and Differentiation. *Int. J. Mol. Med.* **2014**, *34*, 695–704. [CrossRef] [PubMed]
31. Xu, L.; Liu, Y.; Sun, Y.; Wang, B.; Xiong, Y.; Lin, W.; Wei, Q.; Wang, H.; He, W.; Wang, B.; et al. Tissue Source Determines the Differentiation Potentials of Mesenchymal Stem Cells: A Comparative Study of Human Mesenchymal Stem Cells from Bone Marrow and Adipose Tissue. *Stem Cell Res. Ther.* **2017**, *8*, 275. [CrossRef] [PubMed]
32. Heo, J.S.; Choi, Y.; Kim, H.S.; Kim, H.O. Comparison of Molecular Profiles of Human Mesenchymal Stem Cells Derived from Bone Marrow, Umbilical Cord Blood, Placenta and Adipose Tissue. *Int. J. Mol. Med.* **2016**, *37*, 115–125. [CrossRef] [PubMed]
33. Lin, X.; Li, H. Obesity: Epidemiology, Pathophysiology, and Therapeutics. *Front. Endocrinol.* **2021**, *12*, 706978. [CrossRef] [PubMed]
34. Cao, M.; Pan, Q.; Dong, H.; Yuan, X.; Li, Y.; Sun, Z.; Dong, X.; Wang, H. Adipose-Derived Mesenchymal Stem Cells Improve Glucose Homeostasis in High-Fat Diet-Induced Obese Mice. *Stem Cell Res. Ther.* **2015**, *6*, 208. [CrossRef] [PubMed]
35. Tung-Qian Ji, A.; Chang, Y.C.; Fu, Y.J.; Lee, O.K.; Ho, J.H. Niche-Dependent Regulations of Metabolic Balance in High-Fat Diet-Induced Diabetic Mice by Mesenchymal Stromal Cells. *Diabetes* **2015**, *64*, 926–936. [CrossRef]
36. Lee, C.-W.; Hsiao, W.-T.; Lee, O.K.-S. Mesenchymal Stromal Cell-Based Therapies Reduce Obesity and Metabolic Syndromes Induced by a High-Fat Diet. *Transl. Res.* **2017**, *182*, 61–74.e8. [CrossRef]
37. Liu, G.-Y.; Liu, J.; Wang, Y.-L.; Liu, Y.; Shao, Y.; Han, Y.; Qin, Y.-R.; Xiao, F.-J.; Li, P.-F.; Zhao, L.-J.; et al. Adipose-Derived Mesenchymal Stem Cells Ameliorate Lipid Metabolic Disturbance in Mice. *Stem Cells Transl. Med.* **2016**, *5*, 1162–1170. [CrossRef] [PubMed]
38. Shang, Q.; Bai, Y.; Wang, G.; Song, Q.; Guo, C.; Zhang, L.; Wang, Q. Delivery of Adipose-Derived Stem Cells Attenuates Adipose Tissue Inflammation and Insulin Resistance in Obese Mice Through Remodeling Macrophage Phenotypes. *Stem Cells Dev.* **2015**, *24*, 2052–2064. [CrossRef]
39. Jaber, H.; Issa, K.; Eid, A.; Saleh, F.A. The Therapeutic Effects of Adipose-Derived Mesenchymal Stem Cells on Obesity and Its Associated Diseases in Diet-Induced Obese Mice. *Sci. Rep.* **2021**, *11*, 6291. [CrossRef] [PubMed]
40. Shree, N.; Bhonde, R.R. Metformin Preconditioned Adipose Derived Mesenchymal Stem Cells Is a Better Option for the Reversal of Diabetes upon Transplantation. *Biomed. Pharmacother.* **2016**, *84*, 1662–1667. [CrossRef] [PubMed]
41. Sakran, N.; Graham, Y.; Pintar, T.; Yang, W.; Kassir, R.; Willigendael, E.M.; Singhal, R.; Kooreman, Z.E.; Ramnarain, D.; Mahawar, K.; et al. The Many Faces of Diabetes. Is There a Need for Re-Classification? A Narrative Review. *BMC Endocr. Disord.* **2022**, *22*, 9. [CrossRef] [PubMed]
42. Khan, M.A.B.; Hashim, M.J.; King, J.K.; Govender, R.D.; Mustafa, H.; Kaabi, J. al Epidemiology of Type 2 Diabetes—Global Burden of Disease and Forecasted Trends. *J. Epidemiol. Glob. Health* **2020**, *10*, 107–111. [CrossRef]
43. Shree, N.; Venkategowda, S.; Venkatrangan, M.V.; Datta, I.; Bhonde, R.R. Human Adipose Tissue Mesenchymal Stem Cells as a Novel Treatment Modality for Correcting Obesity Induced Metabolic Dysregulation. *Int. J. Obes.* **2019**, *43*, 2107–2118. [CrossRef] [PubMed]
44. Ishida, M.; Tatsumi, K.; Okumoto, K.; Kaji, H. Adipose Tissue-Derived Stem Cell Sheet Improves Glucose Metabolism in Obese Mice. *Stem Cells Dev.* **2020**, *29*, 488–497. [CrossRef]
45. Timper, K.; Seboek, D.; Eberhardt, M.; Linscheid, P.; Christ-Crain, M.; Keller, U.; Müller, B.; Zulewski, H. Human Adipose Tissue-Derived Mesenchymal Stem Cells Differentiate into Insulin, Somatostatin, and Glucagon Expressing Cells. *Biochem. Biophys. Res. Commun.* **2006**, *341*, 1135–1140. [CrossRef] [PubMed]
46. Dave, S.; Vanikar, A.; Trivedi, H. Ex Vivo Generation of Glucose Sensitive Insulin Secreting Mesenchymal Stem Cells Derived from Human Adipose Tissue. *Indian J. Endocrinol. Metab.* **2012**, *16*, 65. [CrossRef] [PubMed]

47. Nam, J.S.; Kang, H.M.; Kim, J.; Park, S.; Kim, H.; Ahn, C.W.; Park, J.O.; Kim, K.R. Transplantation of Insulin-Secreting Cells Differentiated from Human Adipose Tissue-Derived Stem Cells into Type 2 Diabetes Mice. *Biochem. Biophys. Res. Commun.* **2014**, *443*, 775–781. [[CrossRef](#)]
48. Liang, R.Y.; Zhang, K.L.; Chuang, M.H.; Lin, F.H.; Chen, T.C.; Lin, J.N.; Liang, Y.J.; Li, Y.A.; Chen, C.H.; Wong, P.L.J.; et al. A One-Step, Monolayer Culture and Chemical-Based Approach to Generate Insulin-Producing Cells from Human Adipose-Derived Stem Cells to Mitigate Hyperglycemia in STZ-Induced Diabetic Rats. *Cell Transplant.* **2022**, *31*, 09636897221106995. [[CrossRef](#)] [[PubMed](#)]
49. Chandra, V.; Phadnis, S.; Nair, P.D.; Bhonde, R.R. Generation of Pancreatic Hormone-Expressing Islet-Like Cell Aggregates from Murine Adipose Tissue-Derived Stem Cells Tissue-Specific Stem Cells. *Stem Cells* **2009**, *27*, 1941–1953. [[CrossRef](#)]
50. Xie, M.; Hao, H.J.; Cheng, Y.; Xie, Z.Y.; Yin, Y.Q.; Zhang, Q.; Gao, J.Q.; Liu, H.Y.; Mu, Y.M.; Han, W.D. Adipose-Derived Mesenchymal Stem Cells Ameliorate Hyperglycemia through Regulating Hepatic Glucose Metabolism in Type 2 Diabetic Rats. *Biochem. Biophys. Res. Commun.* **2017**, *483*, 435–441. [[CrossRef](#)]
51. Wang, M.; Song, L.; Strange, C.; Dong, X.; Wang, H. Therapeutic Effects of Adipose Stem Cells from Diabetic Mice for the Treatment of Type 2 Diabetes. *Mol. Ther.* **2018**, *26*, 1921–1930. [[CrossRef](#)] [[PubMed](#)]
52. Hu, J.; Fu, Z.; Chen, Y.; Tang, N.; Wang, L.; Sun, R.; Yan, S. Effects of Autologous Adipose-Derived Stem Cell Infusion on Type 2 Diabetic Rats. *Endocr. J.* **2015**, *62*, 339–352. [[CrossRef](#)]
53. Yu, S.; Cheng, Y.; Zhang, L.; Yin, Y.; Xue, J.; Li, B.; Gong, Z.; Gao, J.; Mu, Y. Treatment with Adipose Tissue-Derived Mesenchymal Stem Cells Exerts Anti-Diabetic Effects, Improves Long-Term Complications, and Attenuates Inflammation in Type 2 Diabetic Rats. *Stem Cell Res. Ther.* **2019**, *10*, 333. [[CrossRef](#)] [[PubMed](#)]
54. Younossi, Z.; Anstee, Q.M.; Marietti, M.; Hardy, T.; Henry, L.; Eslam, M.; George, J.; Bugianesi, E. Global Burden of NAFLD and NASH: Trends, Predictions, Risk Factors and Prevention. *Nat. Rev. Gastroenterol. Hepatol.* **2018**, *15*, 11–20. [[CrossRef](#)] [[PubMed](#)]
55. Sarwar, R.; Pierce, N.; Koppe, S. Obesity and Nonalcoholic Fatty Liver Disease: Current Perspectives. *Diabetes Metab. Syndr. Obes.* **2018**, *11*, 533–542. [[CrossRef](#)] [[PubMed](#)]
56. Quek, J.; Chan, K.E.; Wong, Z.Y.; Tan, C.; Tan, B.; Lim, W.H.; Tan, D.J.H.; Tang, A.S.P.; Tay, P.; Xiao, J.; et al. Global Prevalence of Non-Alcoholic Fatty Liver Disease and Non-Alcoholic Steatohepatitis in the Overweight and Obese Population: A Systematic Review and Meta-Analysis. *Lancet Gastroenterol. Hepatol.* **2023**, *8*, 20–30. [[CrossRef](#)]
57. Loomba, R.; Friedman, S.L.; Shulman, G.I. Mechanisms and Disease Consequences of Nonalcoholic Fatty Liver Disease. *Cell* **2021**, *184*, 2537–2564. [[CrossRef](#)] [[PubMed](#)]
58. Hu, C.; Zhao, L.; Li, L. Current Understanding of Adipose-Derived Mesenchymal Stem Cell-Based Therapies in Liver Diseases. *Stem Cell Res. Ther.* **2019**, *10*, 199. [[CrossRef](#)]
59. Ezquer, M.; Ezquer, F.; Ricca, M.; Allers, C.; Conget, P. Intravenous Administration of Multipotent Stromal Cells Prevents the Onset of Non-Alcoholic Steatohepatitis in Obese Mice with Metabolic Syndrome. *J. Hepatol.* **2011**, *55*, 1112–1120. [[CrossRef](#)]
60. Seki, A.; Sakai, Y.; Komura, T.; Nasti, A.; Yoshida, K.; Higashimoto, M.; Honda, M.; Usui, S.; Takamura, M.; Takamura, T.; et al. Adipose Tissue-Derived Stem Cells as a Regenerative Therapy for a Mouse Steatohepatitis-Induced Cirrhosis Model. *Hepatology* **2013**, *58*, 1133–1142. [[CrossRef](#)]
61. Pan, F.; Liao, N.; Zheng, Y.; Wang, Y.; Gao, Y.; Wang, S.; Jiang, Y.; Liu, X. Intrahepatic Transplantation of Adipose-Derived Stem Cells Attenuates the Progression of Non-Alcoholic Fatty Liver Disease in Rats. *Mol. Med. Rep.* **2015**, *12*, 3725–3733. [[CrossRef](#)]
62. Liao, N.; Zheng, Y.; Xie, H.; Zhao, B.; Zeng, Y.; Liu, X.; Liu, J. Adipose Tissue-Derived Stem Cells Ameliorate Hyperglycemia, Insulin Resistance and Liver Fibrosis in the Type 2 Diabetic Rats. *Stem Cell Res. Ther.* **2017**, *8*, 286. [[CrossRef](#)] [[PubMed](#)]
63. Yamato, M.; Sakai, Y.; Mochida, H.; Kawaguchi, K.; Takamura, M.; Usui, S.; Seki, A.; Mizukoshi, E.; Yamashita, T.; Yamashita, T.; et al. Adipose Tissue-Derived Stem Cells Prevent Fibrosis in Murine Steatohepatitis by Suppressing IL-17-Mediated Inflammation. *J. Gastroenterol. Hepatol.* **2019**, *34*, 1432–1440. [[CrossRef](#)]
64. Watanabe, T.; Tsuchiya, A.; Takeuchi, S.; Nojiri, S.; Yoshida, T.; Ogawa, M.; Itoh, M.; Takamura, M.; Suganami, T.; Ogawa, Y.; et al. Development of a Non-Alcoholic Steatohepatitis Model with Rapid Accumulation of Fibrosis, and Its Treatment Using Mesenchymal Stem Cells and Their Small Extracellular Vesicles. *Regen. Ther.* **2020**, *14*, 252–261. [[CrossRef](#)] [[PubMed](#)]
65. Banas, A.; Teratani, T.; Yamamoto, Y.; Tokuhara, M.; Takeshita, F.; Osaki, M.; Kato, T.; Okochi, H.; Ochiya, T. Rapid Hepatic Fate Specification of Adipose-Derived Stem Cells and Their Therapeutic Potential for Liver Failure. *J. Gastroenterol. Hepatol.* **2009**, *24*, 70–77. [[CrossRef](#)] [[PubMed](#)]
66. Aurich, H.; Sgiodda, M.; Kaltwasser, P.; Vetter, M.; Weise, A.; Liehr, T.; Brulport, M.; Hengstler, J.G.; Dollinger, M.M.; Fleig, W.E.; et al. Hepatocyte Differentiation of Mesenchymal Stem Cells from Human Adipose Tissue in Vitro Promotes Hepatic Integration in Vivo. *Gut* **2009**, *58*, 570–581. [[CrossRef](#)] [[PubMed](#)]
67. Xu, F.; Liu, J.; Deng, J.; Chen, X.; Wang, Y.; Xu, P.; Cheng, L.; Fu, Y.; Cheng, F.; Yao, Y.; et al. Rapid and High-Efficiency Generation of Mature Functional Hepatocyte-like Cells from Adipose-Derived Stem Cells by a Three-Step Protocol. *Stem Cell Res. Ther.* **2015**, *6*, 193. [[CrossRef](#)] [[PubMed](#)]
68. Wang, H.; Zhao, T.; Xu, F.; Li, Y.; Wu, M.; Zhu, D.; Cong, X.; Liu, Y. How Important Is Differentiation in the Therapeutic Effect of Mesenchymal Stromal Cells in Liver Disease? *Cytotherapy* **2014**, *16*, 309–318. [[CrossRef](#)]
69. Hoang, D.M.; Pham, P.T.; Bach, T.Q.; Ngo, A.T.L.; Nguyen, Q.T.; Phan, T.T.K.; Nguyen, G.H.; Le, P.T.T.; Hoang, V.T.; Forsyth, N.R.; et al. Stem Cell-Based Therapy for Human Diseases. *Signal Transduct. Target. Ther.* **2022**, *7*, 272. [[CrossRef](#)] [[PubMed](#)]

70. Shamsuddin, S.A.; Chan, A.M.L.; Ng, M.H.; Dain Yazid, M.; Law, J.X.; Binti, R.; Idrus, H.; Fauzi, M.B.; Heikal, M.; Yunus, M.; et al. Stem Cells as a Potential Therapy in Managing Various Disorders of Metabolic Syndrome: A Systematic Review. *Am. J. Transl. Res.* **2021**, *13*, 12217–12227. [PubMed]
71. Nguyen, L.T.; Hoang, D.M.; Nguyen, K.T.; Bui, D.M.; Nguyen, H.T.; Le, H.T.A.; Hoang, V.T.; Bui, H.T.H.; Dam, P.T.M.; Hoang, X.T.A.; et al. Type 2 Diabetes Mellitus Duration and Obesity Alter the Efficacy of Autologously Transplanted Bone Marrow-Derived Mesenchymal Stem/Stromal Cells. *Stem Cells Transl. Med.* **2021**, *10*, 1266–1278. [CrossRef]
72. Seo, Y.; Shin, T.H.; Kim, H.S. Current Strategies to Enhance Adipose Stem Cell Function: An Update. *Int. J. Mol. Sci.* **2019**, *20*, 3827. [CrossRef]
73. Preda, M.B.; Neculachi, C.A.; Fenyo, I.M.; Vacaru, A.M.; Publik, M.A.; Simionescu, M.; Burlacu, A. Short Lifespan of Syngeneic Transplanted MSC Is a Consequence of in Vivo Apoptosis and Immune Cell Recruitment in Mice. *Cell Death Dis.* **2021**, *12*, 566. [CrossRef] [PubMed]
74. Wei, W.; Huang, Y.; Li, D.; Gou, H.F.; Wang, W. Improved Therapeutic Potential of MSCs by Genetic Modification. *Gene Ther.* **2018**, *25*, 538–547. [CrossRef]
75. Hodgkinson, C.P.; Gomez, J.A.; Mirotsou, M.; Dzau, V.J. Genetic Engineering of Mesenchymal Stem Cells and Its Application in Human Disease Therapy. *Hum. Gene Ther.* **2010**, *21*, 1513–1526. [CrossRef]
76. Cho, H.H.; Kyoung, K.M.; Seo, M.J.; Kim, Y.J.; Chan Bae, Y.; Jung, J.S. Overexpression of CXCR4 Increases Migration and Proliferation of Human Adipose Tissue Stromal Cells. *Stem Cells Dev.* **2006**, *15*, 853–864. [CrossRef]
77. Marquez-Curtis, L.A.; Janowska-Wieczorek, A. Enhancing the Migration Ability of Mesenchymal Stromal Cells by Targeting the SDF-1/CXCR4 Axis. *Biomed. Res. Int.* **2013**, *2013*, 561098. [CrossRef] [PubMed]
78. Baldari, S.; di Rocco, G.; Trivisonno, A.; Samengo, D.; Pani, G.; Toietta, G. Promotion of Survival and Engraftment of Transplanted Adipose Tissue-Derived Stromal and Vascular Cells by Overexpression of Manganese Superoxide Dismutase. *Int. J. Mol. Sci.* **2016**, *17*, 1082. [CrossRef] [PubMed]
79. Sen, S.; Domingues, C.C.; Roushanel, C.; Chou, C.; Kim, C.; Yadava, N. Genetic Modification of Human Mesenchymal Stem Cells Helps to Reduce Adiposity and Improve Glucose Tolerance in an Obese Diabetic Mouse Model. *Stem Cell Res. Ther.* **2015**, *6*, 242. [CrossRef] [PubMed]
80. Sun, L.L.; Liu, T.J.; Li, L.; Tang, W.; Zou, J.J.; Chen, X.F.; Zheng, J.Y.; Jiang, B.G.; Shi, Y.Q. Transplantation of Betatrophin-Expressing Adipose-Derived Mesenchymal Stem Cells Induces β -Cell Proliferation in Diabetic Mice. *Int. J. Mol. Med.* **2017**, *39*, 936–948. [CrossRef]
81. Davoodian, N.; Lotfi, A.S.; Soleimani, M.; Ghaneialvar, H. The Combination of MiR-122 Overexpression and Let-7f Silencing Induces Hepatic Differentiation of Adipose Tissue-Derived Stem Cells. *Cell Biol. Int.* **2017**, *41*, 1083–1092. [CrossRef] [PubMed]
82. Clément, F.; Grockowiak, E.; Zylbersztejn, F.; Fossard, G.; Gobert, S.; Maguer-Satta, V. Stem Cell Manipulation, Gene Therapy and the Risk of Cancer Stem Cell Emergence. *Stem Cell Investig.* **2017**, *4*, 67. [CrossRef] [PubMed]
83. Hamann, A.; Nguyen, A.; Pannier, A.K. Nucleic Acid Delivery to Mesenchymal Stem Cells: A Review of Nonviral Methods and Applications. *J. Biol. Eng.* **2019**, *13*, 7. [CrossRef] [PubMed]
84. Han, S.M.; Han, S.H.; Coh, Y.R.; Jang, G.; Ra, J.C.; Kang, S.K.; Lee, H.W.; Youn, H.Y. Enhanced Proliferation and Differentiation of Oct4- And Sox2-Overexpressing Human Adipose Tissue Mesenchymal Stem Cells. *Exp. Mol. Med.* **2014**, *46*, e101. [CrossRef] [PubMed]
85. Kim, J.Y.; Shin, K.K.; Lee, A.L.; Kim, Y.S.; Park, H.J.; Park, Y.K.; Bae, Y.C.; Jung, J.S. MicroRNA-302 Induces Proliferation and Inhibits Oxidant-Induced Cell Death in Human Adipose Tissue-Derived Mesenchymal Stem Cells. *Cell Death Dis.* **2014**, *5*, e1385. [CrossRef] [PubMed]
86. Shin, J.; Oh, J.W. Development of CRISPR/Cas9 System for Targeted DNA Modifications and Recent Improvements in Modification Efficiency and Specificity. *BMB Rep.* **2020**, *53*, 341–348. [CrossRef]
87. Kantor, A.; McClements, M.E.; Maclare, R.E. Crispr-Cas9 Dna Base-Editing and Prime-Editing. *Int. J. Mol. Sci.* **2020**, *21*, 6240. [CrossRef]
88. Nidhi, S.; Anand, U.; Oleksak, P.; Tripathi, P.; Lal, J.A.; Thomas, G.; Kuca, K.; Tripathi, V. Novel Crispr–Cas Systems: An Updated Review of the Current Achievements, Applications, and Future Research Perspectives. *Int. J. Mol. Sci.* **2021**, *22*, 3327. [CrossRef] [PubMed]
89. Doudna, J.A. The Promise and Challenge of Therapeutic Genome Editing. *Nature* **2020**, *578*, 229–236. [CrossRef] [PubMed]
90. Lundh, M.; Plucińska, K.; Isidor, M.S.; Petersen, P.S.S.; Emanuelli, B. Bidirectional Manipulation of Gene Expression in Adipocytes Using CRISPRa and SiRNA. *Mol. Metab.* **2017**, *6*, 1313–1320. [CrossRef]
91. Kamble, P.G.; Hetty, S.; Vranic, M.; Almby, K.; Castillejo-López, C.; Abalo, X.M.; Pereira, M.J.; Eriksson, J.W. Proof-of-Concept for CRISPR/Cas9 Gene Editing in Human Preadipocytes: Deletion of FKBP5 and PPARG and Effects on Adipocyte Differentiation and Metabolism. *Sci. Rep.* **2020**, *10*, 10565. [CrossRef] [PubMed]
92. Shukare, M.L.; Huang, R.U.I.; Ehsani, A.L.I.; Zhang, G.; Chalise, J.P.; Whitson, R.H.; Itakura, K. 34-OR: Role of Arid5b in Thermogenesis and Adipose Tissue Browning. *Diabetes* **2021**, *70*, 34-OR. [CrossRef]
93. Claussnitzer, M.; Dankel, S.N.; Kim, K.-H.; Quon, G.; Meuleman, W.; Haugen, C.; Glunk, V.; Sousa, I.S.; Beaudry, J.L.; Puviindran, V.; et al. FTO Obesity Variant Circuitry and Adipocyte Browning in Humans. *N. Engl. J. Med.* **2015**, *373*, 895–907. [CrossRef]
94. Domingues, C.C.; Kundu, N.; Kropotova, Y.; Ahmadi, N.; Sen, S. Antioxidant-Upregulated Mesenchymal Stem Cells Reduce Inflammation and Improve Fatty Liver Disease in Diet-Induced Obesity. *Stem Cell Res. Ther.* **2019**, *10*, 280. [CrossRef] [PubMed]

95. Wang, W.; Zhang, Y.; Yang, C.; Wang, Y.; Shen, J.; Shi, M.; Wang, B. Feature Article: Transplantation of Neuregulin 4-Overexpressing Adipose-Derived Mesenchymal Stem Cells Ameliorates Insulin Resistance by Attenuating Hepatic Steatosis. *Exp. Biol. Med.* **2019**, *244*, 565–578. [CrossRef] [PubMed]
96. Qi, Y.; Ma, J.; Li, S.; Liu, W. Applicability of Adipose-Derived Mesenchymal Stem Cells in Treatment of Patients with Type 2 Diabetes. *Stem Cell Res. Ther.* **2019**, *10*, 274. [CrossRef] [PubMed]
97. Grohová, A.; Daóvá, K.; Štísek, R.; Palova-Jelinkova, L. Cell Based Therapy for Type 1 Diabetes: Should We Take Hyperglycemia into Account? *Front. Immunol.* **2019**, *10*, 79. [CrossRef] [PubMed]
98. Lin, G.; Wang, G.; Liu, G.; Yang, L.J.; Chang, L.J.; Lue, T.F.; Lin, C.S. Treatment of Type 1 Diabetes with Adipose Tissue-Derived Stem Cells Expressing Pancreatic Duodenal Homeobox 1. *Stem Cells Dev.* **2009**, *18*, 1399–1406. [CrossRef] [PubMed]
99. Kajiyama, H.; Hamazaki, T.S.; Tokuhara, M.; Masui, S.; Okabayashi, K.; Ohnuma, K.; Yabe, S.; Yasuda, K.; Ishiura, S.; Okochi, H.; et al. Pdx1-Transfected Adipose Tissue-Derived Stem Cells Differentiate into Insulin-Producing Cells in Vivo and Reduce Hyperglycemia in Diabetic Mice. *Int. J. Dev. Biol.* **2010**, *54*, 699–705. [CrossRef]
100. Lee, J.; Cheol Kim, S.; Jin Kim, S.; Lee, H.; Jung Jung, E.; Hee Jung, S.; Jong Han, D. Differentiation of Human Adipose Tissue-Derived Stem Cells Into Aggregates of Insulin-Producing Cells Through the Overexpression of Pancreatic and Duodenal Homeobox Gene-1. *Cell Transpl.* **2013**, *22*, 1053–1060. [CrossRef] [PubMed]
101. Lindeborg, E.; Kumagai-Braesch, M.; Tibell, A.; Christensson, B.; Möller, E. Biological Activity of Pig Islet-Cell Reactive IgG Antibodies in Xenotransplanted Diabetic Patients. *Xenotransplantation* **2004**, *11*, 457–470. [CrossRef] [PubMed]
102. Lee, H.S.; Lee, J.G.; Yeom, H.J.; Chung, Y.S.; Kang, B.; Hurh, S.; Cho, B.; Park, H.; Hwang, J.I.; Park, J.B.; et al. The Introduction of Human Heme Oxygenase-1 and Soluble Tumor Necrosis Factor- α Receptor Type i with Human IgG1 Fc in Porcine Islets Prolongs Islet Xenograft Survival in Humanized Mice. *Am. J. Transplant.* **2016**, *16*, 44–57. [CrossRef]
103. Lee, H.S.; Song, S.; Shin, D.Y.; Kim, G.S.; Lee, J.H.; Cho, C.W.; Lee, K.W.; Park, H.; Ahn, C.; Yang, J.; et al. Enhanced Effect of Human Mesenchymal Stem Cells Expressing Human TNF-AR-Fc and HO-1 Gene on Porcine Islet Xenotransplantation in Humanized Mice. *Xenotransplantation* **2018**, *25*, e12342. [CrossRef]
104. Öllinger, R.; Pratschke, J. Role of Heme Oxygenase-1 in Transplantation. *Transpl. Int.* **2010**, *23*, 1071–1081. [CrossRef] [PubMed]
105. Machen, J.; Bertera, S.; Chang, Y.; Bottino, R.; Balamurugan, A.N.; Robbins, P.D.; Trucco, M.; Giannoukakis, N. Prolongation of Islet Allograft Survival Following Ex Vivo Transduction with Adenovirus Encoding a Soluble Type 1 TNF Receptor-Ig Fusion Decoy. *Gene Ther.* **2004**, *11*, 1506–1514. [CrossRef]
106. Kang, H.; Seo, E.; Park, J.M.; Han, N.Y.; Lee, H.; Jun, H.S. Effects of FGF21-Secreting Adipose-Derived Stem Cells in Thioacetamide-Induced Hepatic Fibrosis. *J. Cell. Mol. Med.* **2018**, *22*, 5165–5169. [CrossRef]
107. Lou, G.; Yang, Y.; Liu, F.; Ye, B.; Chen, Z.; Zheng, M.; Liu, Y. MiR-122 Modification Enhances the Therapeutic Efficacy of Adipose Tissue-Derived Mesenchymal Stem Cells against Liver Fibrosis. *J. Cell. Mol. Med.* **2017**, *21*, 2963–2973. [CrossRef] [PubMed]
108. White, J.D.; Dewal, R.S.; Stanford, K.I. The Beneficial Effects of Brown Adipose Tissue Transplantation. *Mol. Asp. Med.* **2019**, *68*, 74–81. [CrossRef] [PubMed]
109. McNeill, B.T.; Suchacki, K.J.; Stimson, R.H. Human Brown Adipose Tissue as a Therapeutic Target: Warming up or Cooling Down? *Eur. J. Endocrinol.* **2021**, *184*, R243–R259. [CrossRef] [PubMed]
110. Wang, C.H.; Lundh, M.; Fu, A.; Kriszt, R.; Huang, T.L.; Lynes, M.D.; Leiria, L.O.; Shamsi, F.; Darcy, J.; Greenwood, B.P.; et al. CRISPR-Engineered Human Brown-like Adipocytes Prevent Diet-Induced Obesity and Ameliorate Metabolic Syndrome in Mice. *Sci. Transl. Med.* **2020**, *12*, eaaz8664. [CrossRef] [PubMed]
111. Tsagkaraki, E.; Nicoloro, S.M.; DeSouza, T.; Solivan-Rivera, J.; Desai, A.; Lifshitz, L.M.; Shen, Y.; Kelly, M.; Guilherme, A.; Henriques, F.; et al. CRISPR-Enhanced Human Adipocyte Browning as Cell Therapy for Metabolic Disease. *Nat. Commun.* **2021**, *12*, 6931. [CrossRef] [PubMed]
112. Shen, Y.; Cohen, J.L.; Nicoloro, S.M.; Kelly, M.; Yenilmez, B.; Henriques, F.; Tsagkaraki, E.; Edwards, Y.J.K.; Hu, X.; Friedline, R.H.; et al. CRISPR-Delivery Particles Targeting Nuclear Receptor-Interacting Protein 1 (Nrip1) in Adipose Cells to Enhance Energy Expenditure. *J. Biol. Chem.* **2018**, *293*, 17291–17305. [CrossRef] [PubMed]
113. Zhang, Y.; Chen, W.; Feng, B.; Cao, H. The Clinical Efficacy and Safety of Stem Cell Therapy for Diabetes Mellitus: A Systematic Review and Meta-Analysis. *Aging Dis.* **2020**, *11*, 141–153.
114. Sakai, Y.; Takamura, M.; Seki, A.; Sunagozaka, H.; Terashima, T.; Komura, T.; Yamato, M.; Miyazawa, M.; Kawaguchi, K.; Nasti, A.; et al. Phase I Clinical Study of Liver Regenerative Therapy for Cirrhosis by Intrahepatic Arterial Infusion of Freshly Isolated Autologous Adipose Tissue-Derived Stromal/Stem (Regenerative) Cell. *Regen. Ther.* **2017**, *6*, 52–64. [CrossRef]
115. Sakai, Y.; Fukunishi, S.; Takamura, M.; Kawaguchi, K.; Inoue, O.; Usui, S.; Takashima, S.; Seki, A.; Asai, A.; Tsuchimoto, Y.; et al. Clinical Trial of Autologous Adipose Tissue-Derived Regenerative (Stem) Cells Therapy for Exploration of Its Safety and Efficacy. *Regen. Ther.* **2021**, *18*, 97–101. [CrossRef]
116. Li, C.; Zhao, H.; Cheng, L.; Wang, B. Allogeneic vs. Autologous Mesenchymal Stem/Stromal Cells in Their Medication Practice. *Cell Biosci.* **2021**, *11*, 187. [CrossRef] [PubMed]
117. Chen, J.M.; Huang, Q.Y.; Chen, W.H.; Lin, S.; Shi, Q.Y. Clinical Evaluation of Autologous and Allogeneic Stem Cell Therapy for Intrauterine Adhesions: A Systematic Review and Meta-Analysis. *Front. Immunol.* **2022**, *13*, 899666. [CrossRef]
118. Louwen, F.; Ritter, A.; Kreis, N.N.; Yuan, J. Insight into the Development of Obesity: Functional Alterations of Adipose-Derived Mesenchymal Stem Cells. *Obes. Rev.* **2018**, *19*, 888–904. [CrossRef] [PubMed]

119. Boland, L.; Bitterlich, L.M.; Hogan, A.E.; Ankrum, J.A.; English, K. Translating MSC Therapy in the Age of Obesity. *Front. Immunol.* **2022**, *13*, 94333. [[CrossRef](#)] [[PubMed](#)]
120. Zhou, T.; Yuan, Z.; Weng, J.; Pei, D.; Du, X.; He, C.; Lai, P. Challenges and Advances in Clinical Applications of Mesenchymal Stromal Cells. *J. Hematol. Oncol.* **2021**, *14*, 24. [[CrossRef](#)] [[PubMed](#)]
121. Damasceno, P.K.F.; de Santana, T.A.; Santos, G.C.; Orge, I.D.; Silva, D.N.; Albuquerque, J.F.; Golinelli, G.; Grisendi, G.; Pinelli, M.; Ribeiro dos Santos, R.; et al. Genetic Engineering as a Strategy to Improve the Therapeutic Efficacy of Mesenchymal Stem/Stromal Cells in Regenerative Medicine. *Front. Cell Dev. Biol.* **2020**, *8*, 737. [[CrossRef](#)] [[PubMed](#)]
122. Von Einem, J.C.; Guenther, C.; Volk, H.D.; Grütz, G.; Hirsch, D.; Salat, C.; Stoetzer, O.; Nelson, P.J.; Michl, M.; Modest, D.P.; et al. Treatment of Advanced Gastrointestinal Cancer with Genetically Modified Autologous Mesenchymal Stem Cells: Results from the Phase 1/2 TREAT-ME-1 Trial. *Int. J. Cancer* **2019**, *145*, 1538–1546. [[CrossRef](#)]
123. Kornicka, K.; Houston, J.; Marycz, K. Dysfunction of Mesenchymal Stem Cells Isolated from Metabolic Syndrome and Type 2 Diabetic Patients as Result of Oxidative Stress and Autophagy May Limit Their Potential Therapeutic Use. *Stem Cell Rev. Rep.* **2018**, *14*, 337–345. [[CrossRef](#)]
124. Lohan, P.; Treacy, O.; Griffin, M.D.; Ritter, T.; Ryan, A.E. Anti-Donor Immune Responses Elicited by Allogeneic Mesenchymal Stem Cells and Their Extracellular Vesicles: Are We Still Learning? *Front. Immunol.* **2017**, *8*, 1626. [[CrossRef](#)] [[PubMed](#)]
125. Weiss, A.R.R.; Dahlke, M.H. Immunomodulation by Mesenchymal Stem Cells (MSCs): Mechanisms of Action of Living, Apoptotic, and Dead MSCs. *Front. Immunol.* **2019**, *10*, 1191. [[CrossRef](#)]
126. Kamm, J.L.; Riley, C.B.; Parlane, N.; Gee, E.K.; McIlwraith, C.W. Interactions Between Allogeneic Mesenchymal Stromal Cells and the Recipient Immune System: A Comparative Review with Relevance to Equine Outcomes. *Front. Vet. Sci.* **2021**, *7*, 617647. [[CrossRef](#)] [[PubMed](#)]
127. Lohan, P.; Coleman, C.M.; Murphy, J.M.; Griffin, M.D.; Ritter, T.; Ryan, A.E. Changes in Immunological Profile of Allogeneic Mesenchymal Stem Cells after Differentiation: Should We be Concerned? *Stem Cell Res. Ther.* **2014**, *5*, 99. [[CrossRef](#)] [[PubMed](#)]
128. Li, Y.; Wu, Q.; Wang, Y.; Li, L.; Chen, F.; Shi, Y.; Bu, H.; Bao, J. Immunogenicity of Hepatic Differentiated Human Umbilical Cord Mesenchymal Stem Cells Promoted by Porcine Decellularized Liver Scaffolds. *Xenotransplantation* **2017**, *24*, e12287. [[CrossRef](#)] [[PubMed](#)]
129. Yang, X.F.; Chen, T.; Ren, L.W.; Yang, L.; Qi, H.; Li, F.R. Immunogenicity of Insulin-Producing Cells Derived from Human Umbilical Cord Mesenchymal Stem Cells. *Exp. Ther. Med.* **2017**, *13*, 1456–1464. [[CrossRef](#)] [[PubMed](#)]
130. Mohammadi, N.; Mardomi, A.; Hasannia, H.; Enderami, S.E.; Ranjbaran, H.; Rafiei, A.; Abediankenari, S. Mouse Bone Marrow-Derived Mesenchymal Stem Cells Acquire Immunogenicity Concurrent with Differentiation to Insulin-Producing Cells. *Immunobiology* **2020**, *225*, 151994. [[CrossRef](#)]
131. Ghoneim, M.A.; Refaie, A.F.; Elbassiouny, B.L.; Gabr, M.M.; Zakaria, M.M. From Mesenchymal Stromal/Stem Cells to Insulin-Producing Cells: Progress and Challenges. *Stem Cell Rev. Rep.* **2020**, *16*, 1156–1172. [[CrossRef](#)] [[PubMed](#)]
132. Neri, S. Genetic Stability of Mesenchymal Stromal Cells for Regenerative Medicine Applications: A Fundamental Biosafety Aspect. *Int. J. Mol. Sci.* **2019**, *20*, 2046. [[CrossRef](#)] [[PubMed](#)]

Disclaimer/Publisher's Note: The statements, opinions and data contained in all publications are solely those of the individual author(s) and contributor(s) and not of MDPI and/or the editor(s). MDPI and/or the editor(s) disclaim responsibility for any injury to people or property resulting from any ideas, methods, instructions or products referred to in the content.

